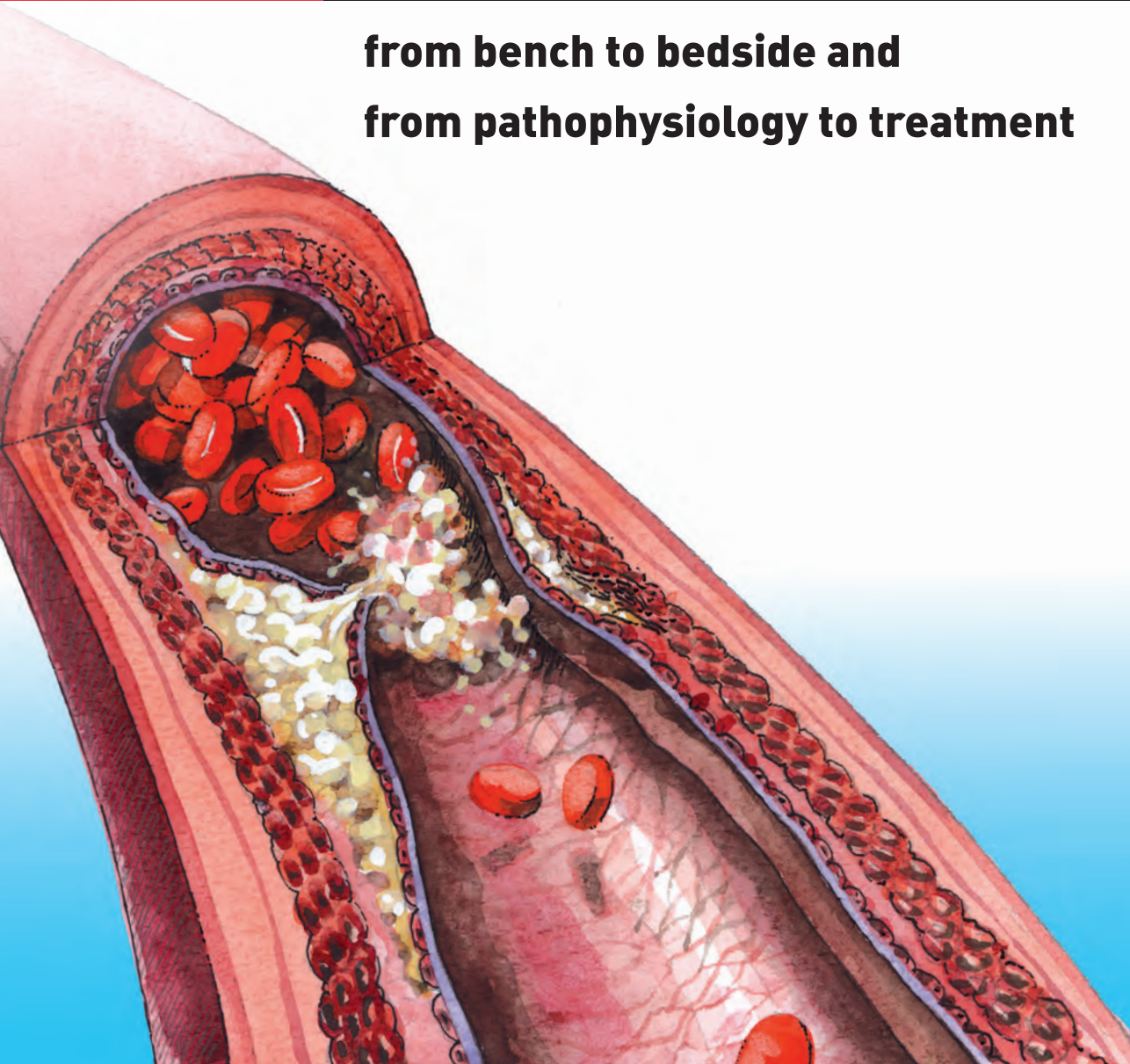


Wijnand K. den Dekker

ATHEROSCLEROSIS

**from bench to bedside and
from pathophysiology to treatment**



**Atherosclerosis;
From Bench to Bedside and
From Pathophysiology to Treatment**

Wijnand Khatulistono den Dekker

ISBN: 978-94-6169-487-4

© Wijnand K. den Dekker

Vormgeving omslag en uitnodiging: Bureau Het Bouwwerk, Dordrecht.

Atherosclerosis; From Bench to Bedside and From Pathophysiology to Treatment

Atherosclerose; van 'bench to bedside' en van diagnose tot behandeling

Proefschrift

ter verkrijging van de graad van doctor aan de
Erasmus Universiteit Rotterdam
op gezag van de
rector magnificus

prof.dr. H.A.P. Pols

en volgens besluit van het College voor Promoties.
De openbare verdediging zal plaatsvinden op

Vrijdag 11 April 2014 om 09.30 uur

Wijnand Khatulistono den Dekker
geboren te Pontianak, Indonesië



Promotiecommissie:

Promotor: Prof.dr. F.J. Zijlstra

Overige leden: Prof.dr. G. Pasterkamp
Prof.dr. J. D. Laman
Prof.dr. D.J.G.M. Duncker

Copromotoren: Dr. H.J. Duckers
Dr. C. Cheng

Financial support by the Dutch Heart Foundation for the publication of this thesis is gratefully acknowledged.

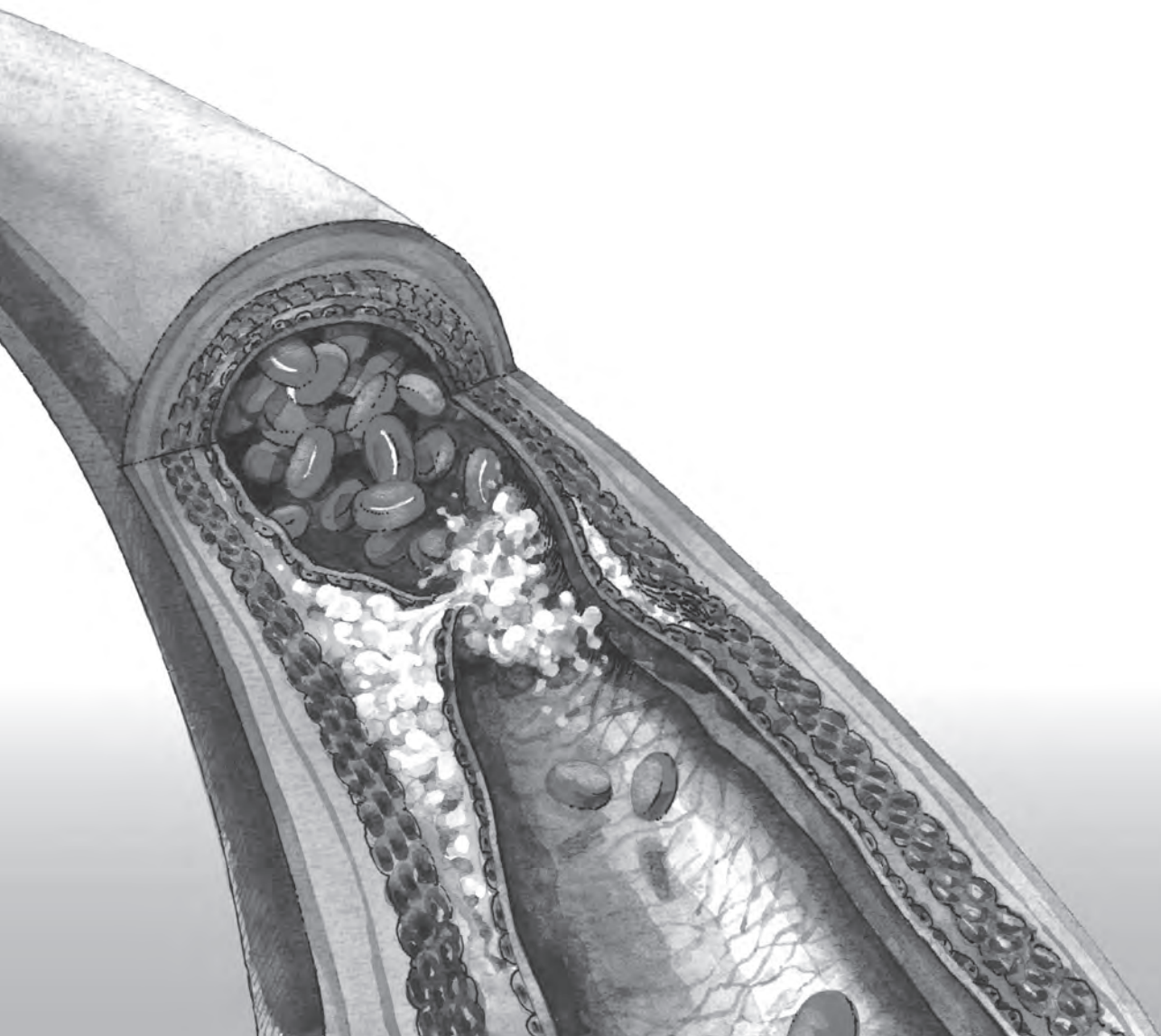
Financial support for the publication of this thesis was generously provided by OrbusNeich, Stichting 'de Kortinthiërs', Cardialyis, Erasmus University Rotterdam, Servier Nederland Farma B.V..

CONTENTS

Chapter 1	General introduction and outline of thesis	7
Chapter 2	Toll like receptor 4 in atherosclerosis and plaque destabilization	21
Chapter 3	Mast cells induce vascular smooth muscle cell apoptosis via a Toll like receptor 4 activation pathway	39
Chapter 4	Effect of shear stress alteration on atherosclerotic plaque vulnerability in cholesterol-fed rabbits	59
Chapter 5	Thsd-1: a new regulator of endothelial barrier function in vascular development and advanced atherosclerosis	75
Chapter 6	Final results of the HEALING IIB trial to evaluate a bio-engineered CD34 antibody coated stent (Genous™Stent) designed to promote vascular healing by capture of circulating endothelial progenitor cells in CAD patients	113
Chapter 7	Efficiency of statin treatment on EPC recruitment depends on baseline EPC titer, and does not improve angiographic outcome in coronary artery disease patients treated with the Genous™ stent	135
Chapter 8	Capture of circulatory endothelial progenitor cells and accelerated re-endothelialization of a bioengineered stent in human ex vivo shunt and rabbit denudation model	151
Chapter 9	Safety and feasibility of intracoronary infusion of adipose tissue-derived regenerative cells in patients with ST-elevation myocardial infarction	169
Chapter 10	Summarizing discussion	187
Chapter 11	Nederlandse samenvatting	201
	PhD portfolio	209
	List of publications	213
	Curriculum Vitae	217
	Dankwoord	219

Chapter 1

General introduction and outline of thesis



Despite continuous advances in therapeutic options, cardiovascular disease is still the leading cause of death worldwide¹. The WHO estimated that in 2008 17.3 million people died from cardiovascular disease, accounting for 30% of all deaths world-wide. Of these deaths, approximately 7.3 million were due to coronary heart disease while 6.2 million were due to stroke². The number of deaths due to cardiovascular disease will increase to 23.3 million by 2030. Coronary heart disease and stroke are the result of atherosclerotic plaque formation. Atherosclerosis, or stiffening of the artery (from the Greek *arteria* meaning artery and *sclerosis* meaning stiffening), is an ongoing process which already starts in childhood³⁻⁵. A healthy artery consists of three layers (see Figure 1). The outermost layer is called the *adventitia* (*tunica adventitia*) and consists of connective tissue. The middle layer is called the *media* (*tunica media*) and consists of multiple layers of smooth muscle cells. The innermost layer is called the *intima* (*tunica intima*) and consists of a single layer of endothelial cells. Normally, the endothelial lining of the intima regulates the vascular tone and is impermeable, so leucocytes can not adhere. However, different pro-atherogenic factors like smoking, dyslipidemia, hypertension or diabetes can cause endothelial dysfunction, one of the earliest signs of atherosclerosis⁶⁻⁸. Endothelial dysfunction is characterized by an imbalance between the bioavailability of vasodilating and vasoconstricting substances. This leads to a deterioration in endothelium dependent vasodilatation and a pro-inflammatory, and procoagulatory milieu. Endothelial dysfunction allows low-density lipoprotein (LDL) particles to enter the sub-endothelium. Once in the sub-endothelium, the LDL particles are prone to oxidation and form oxidized LDL. Furthermore, the damaged endothelium also expresses novel cell surface molecules like VCAM-1⁹, allowing monocytes and lymphocytes to adhere to the endothelium and migrate through the endothelium. Monocytes differentiate into macrophages and ingest the oxidized LDL, forming foam cells. The earliest form of atherosclerosis has developed, a so-called fatty streak. It contains oxidized LDL and lipid-loaded macrophages, but also T-lymphocytes, ag-

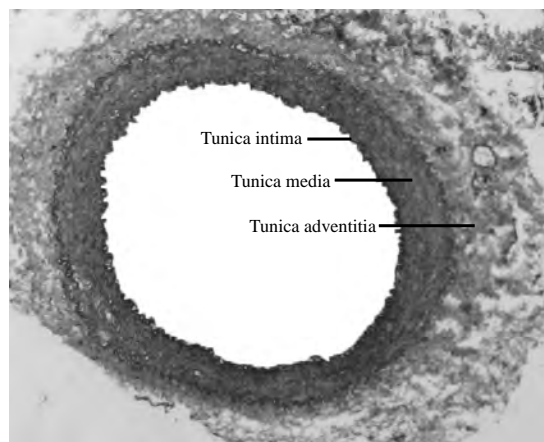


Figure 1: An example of a healthy rabbit artery, which shows the three layers

gregated platelets and vascular smooth muscle cells. The fatty streak continues to grow and the foam cells die releasing their contents. This attracts more immune competent cells and expands the lipid rich necrotic core. Vascular smooth muscle cells migrate from the media into the neo-intimal atheroma to form a fibrous cap. As the atheroma continues to expand, it can develop into a stable or unstable plaque¹⁰. Stable plaques are composed of a thick fibrous cap and contain only small amounts of lipids. In coronary arteries, these stable plaques are usually clinical silent or eventually may lead to stable angina pectoris. In contrast, an unstable or vulnerable plaque, has a thin fibrous cap (less than 65 μm), containing few vascular smooth muscle cells, a lipid rich necrotic core, and a high amount of macrophages¹¹⁻¹². Because of the thin fibrous cap, these plaques are prone to rupture. When a vulnerable plaque ruptures, the highly thrombogenic necrotic core comes into contact with blood, forming a thrombus¹³. This thrombus can (partially) occlude a coronary artery at the site of rupture or downstream, causing an acute coronary syndrome¹⁴⁻¹⁵ (see Figure 2).

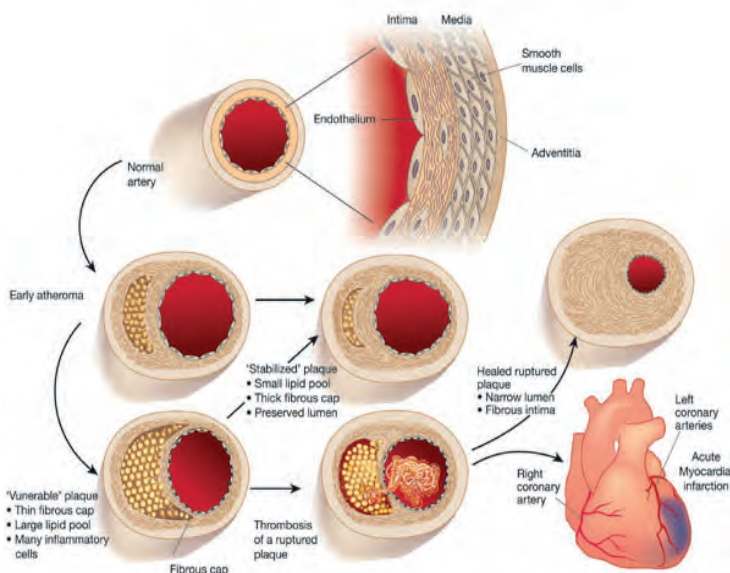


Figure 2: Schematic representation of the initiation and progression of an atherosclerotic plaque. Figure reprinted with permission from (8).

ANIMAL MODELS FOR ATHEROSCLEROSIS

Many different atherosclerosis models in various animal species exist with each its own advantages and limitations. The commonly used pig model provides a large laboratory animal, which is genetically, morphologically and physiologically relatively close to humans¹⁶, rendering it eminently suitable to image the cardiovascular system, both non-invasively as well as intravascular. However, major disadvantages of the porcine model are the costs

of animal housing and care, in combination with the prolonged period of time needed to induce advanced complex lesions (usually longer than six months). In contrast, mice are small animals which are easy to handle and far less costly to maintain. Two knock out mice, the apolipoprotein E (ApoE)^{-/-} and LDLr^{-/-} mice, are now widely used to investigate atherosclerosis, as they spontaneously develop atherosclerosis even on normal chow diet. Some groups claim that these knockout mice also spontaneously develop vulnerable plaques with plaque rupture in the brachiocephalic artery¹⁷. Vulnerable plaques do develop within three months when ApoE^{-/-} mice are fed on a high cholesterol diet, in combination with a tapered cast around the carotid artery¹⁸⁻²⁰. The main disadvantage of the mouse is the limited imaging possibility of the cardiovascular system; in particular intravascular imaging is not feasible. The rabbit is, like the mouse, easy to maintain and handle, less costly than the pig and also widely used to study atherosclerosis. Moreover, the size of the rabbit makes it suitable for cardiovascular imaging, both non-invasively as well as intravascular. New Zealand white rabbits develop early lesions with foam cells when fed a high-cholesterol diet²¹. High cholesterol diet in combination with balloon denudation leads to vascular smooth muscle cell rich plaques, resembling intimal hyperplasia. Aoyagi and coworkers showed that endothelial denudation caused intimal thickening mainly consisting of smooth muscle cells²². Constantinides and co-workers were the first to show that the rabbit can also be used to study plaque disruption and rupture, although the rupture described in their study was not spontaneous as it was induced with Russel's viper venom and histamine²³. The original protocol was a long-term experiment of more than one year, and since then some groups have attempted to shorten the protocol without losing the plaque rupture phenotype²⁴⁻²⁵. Previously, we have created an experimental murine model for induction of vulnerable plaque. In this model, a perivascular device, that induces shear stress alterations, is placed around the carotid artery of an ApoE^{-/-} mouse, fed on a high cholesterol diet. After nine weeks, lesions with a vulnerable plaque phenotype develop upstream, while downstream, stable lesions are induced by the alterations in shear stress. Although this murine model offers the opportunity to study different molecular biological pathways that regulate plaque destabilization, the small size of the animals severely limits the use of the model for in vivo diagnostics and percutaneous interventions. We therefore tried to create a vulnerable plaque model in the rabbit, based on our murine model.

THE IMMUNE SYSTEM AND ATHEROSCLEROSIS

Traditionally, atherosclerosis was thought to be a lipid driven disease, but this has changed in the late nineties when Russel Ross published a landmark paper in which he stated that atherosclerosis is a lipid-driven *inflammatory* disease²⁶. It is nowadays accepted that inflammation plays a pivotal role in the initiation and progression of atherosclerotic disease. The

immune system consists of two defense mechanisms, the adaptive and the innate immune arms. Adaptive immunity requires specific antigen recognition and targeting and consists of T lymphocytes and B lymphocytes. Different subsets of T lymphocytes exist with all specific effects on atherogenesis and atherosclerosis. T helper cells (Th) are divided in Th1 and Th2. Th1 are thought to be pro-atherogenic, as they produce pro-inflammatory cytokines, including IL-6 and interferon-gamma. The role of Th2 would be more anti-atherogenic, as they produce anti-inflammatory cytokines like IL-4. Another subset of T cells is the regulatory T cell, which would also be anti-atherogenic as it suppresses the immune response. So, Th1 on one side and Th2 and regulatory T cells on the other side influence progression of the atherosclerotic plaque into a stable or unstable plaque²⁷. The role of B lymphocytes is more limited than the T lymphocytes. It is thought that they produce neutralizing antibodies against oxidized LDL, thus attenuating atherosclerotic plaque formation²⁸⁻²⁹.

The innate immune system acts rapidly in a non-specific manner, and forms the first line of defense against invading pathogens. Examples of cell types of the innate immune system are monocytes, mast cells, dendritic cells and natural killer cells. Cells of the innate immune system can be activated via cell surface receptors, including Toll like receptors. The Toll like receptors belong to a family of pattern recognition receptors and are type I transmembrane receptors characterized by an extracellular domain with leucine-rich repeats and a carboxy terminal intracellular domain, similar to the intracellular domain of the interleukine-1 receptor. Activation of these receptors ultimately leads to nuclear translocation of NFκB and transcription of pro-inflammatory cytokines. Many different ligands for the Toll like receptors have been identified thus far, but it remains speculative what would serve as the endogenous ligand for the Toll like receptors in the process of atherosclerotic plaque formation and destabilization³⁰. Monocytes have been traditionally linked to the initiation of atherosclerosis, but there is also accumulative evidence that they can enter the plaque in more advanced plaques³¹. Dendritic cells are potent antigen presenting cells and only recently, Bobryshev and coworkers identified dendritic cells in the arterial wall³². Dendritic cells are thought to play a role in antigen presentation and priming in the development of atherosclerosis and have a distinct interaction with T lymphocytes. They might also play a role in plaque destabilization as their numbers increase in the rupture prone regions of plaques³³⁻³⁴. The limited literature on natural killer suggests that they play a role in the initiation of atherosclerosis, as absence of natural killer cells in LDLr -/- mice led to decreased early atherosclerosis but did not influence advanced lesions^{35,36}. Lastly, mast cells have also been recognized as important mediators in the progression of atherosclerosis³⁷. Activated mast cells can produce chymase, different pro-inflammatory cytokines (e.g. IL-6) and can activate matrix metalloproteinases, which can all lead to weakening of the cap of the atherosclerotic plaque³⁸⁻⁴⁰. Furthermore, Bot and colleagues showed that perivascular attracted and activated mast cells induced intraplaque haemorrhaging by increasing vascular permeability and enlarged the lipid rich necrotic core by inducing macrophage apoptosis⁴¹. We have looked at the role of Toll like

receptor 4 in plaque formation and progression. Furthermore, we specifically studied the role of Toll like receptor 4 on mast cells in plaque destabilization, using both *in vitro* techniques and our validated *in vivo* murine vulnerable plaque model.

NEOVASCULARISATION AND VULNERABLE PLAQUE DEVELOPMENT

Neovascularisation in atherosclerotic plaques is the result of intraplaque hypoxia and local inflammation. Hypoxia leads to stabilization and translocation of hypoxia inducible factor to the nucleus. Translocation of hypoxia inducible factor to the nucleus leads to transcription of different angiogenic factors including vascular endothelial growth factor-A (VEGF-A). Newly formed vessels arise from the vasa vasorum, a microvascular network originating in the adventitial layer. These neovessels are phenotypically immature, defined by lack of vascular integrity and increased fragility to rupture⁴². They are prone to extravasation of leucocytes and erythrocytes, which leads to intraplaque haemorrhaging within the atherosclerotic lesion. Accumulated red blood cells are phagocytosed by infiltrated macrophages, which ultimately leads to expansion of the necrotic core at the expense of the fibrous cap and thus atherosclerotic lesion stability⁴³. Pathological studies of human lesions have identified a remarkable correlation between intraplaque haemorrhaging and extensive necrotic core size with plaque rupture and clinical events⁴⁴⁻⁴⁶. These recent findings identify neovessels in advanced lesions as a potential mechanism of vulnerable plaque progression, and marks intimal neoangiogenesis as a potent target for pharmaceutical intervention to benefit treatment to stabilize culprit lesions in patients. In the light of this potential, our basic understanding of the underlying biological mechanism that governs this neoangiogenesis should be expanded, as current knowledge in context of atherosclerotic disease remains limited. In a recently performed genome-wide screen we identified Thrombospondin, type 1, domain containing 1 (Thsd-1) as a potential angiogenic factor. We have studied the role of Thsd-1 in vessel stabilization and evaluated its role in different experimental setups, including our murine vulnerable plaque model.

TREATMENT OF CORONARY ARTERY DISEASE

Treatment of coronary artery disease varies from lifestyle changes, to drug therapy. to revascularization procedures⁴⁷⁻⁴⁸. Patients should be encouraged to quit smoking, as smoking promotes free radical production, endothelial dysfunction and monocyte adhesion⁴⁹. Exercise, weight reduction and healthy food consumption can lead to a more favourable lipid profile and prevention of the metabolic syndrome⁵⁰.

Different drugs are used to treat coronary artery disease. Blood lowering drugs like ace-inhibitors and calcium channel blockers have also shown to improve outcome in the treatment of coronary artery disease. Beta blockers mainly reduce heart rate, reducing oxygen demand of the heart. Although recently there have been questions raised about the favourable effect of beta blockers on coronary artery disease, they still seem to reduce the risk of cardiac ischemia after a first myocardial infarction⁵¹. Aspirin is a platelet aggregation inhibitor and prevents the formation of a thrombus. Aspirins have been shown to be effective in acute myocardial infarction and secondary prevention of a myocardial infarction⁵²⁻⁵⁴. Statins are nowadays indispensable in the treatment of coronary artery disease. They not only lower the LDL levels⁵⁵, they also exert favourable pleiotropic effects ranging from prevention of reactive oxygen species formation to recruitment and differentiation of endothelial progenitor cells⁵⁶⁻⁵⁸.

In recent years there has been tremendous progress in the development of percutaneous treatment options of coronary artery disease, from balloon angioplasty to bare metal stent placement, to drug eluting stents, to bio-absorbable stents. The introduction of bare metal stents improved the outcome of percutaneous coronary intervention, but on the long-term, restenosis of the stent can occur due to vascular smooth muscle cell proliferation. Nowadays, more advanced stents bearing cytostatic compounds have been developed. These so-called drug eluting stents have largely overcome the problem of restenosis as they inhibit the proliferation of vascular smooth muscle cells. However, drug eluting stents have been associated with late stent thrombosis, as they also inhibit the regrowth of the endothelium⁵⁹. More recently, bio-absorbable stents have been developed and the first clinical studies have been completed⁶⁰. We have studied the efficacy of an endothelial progenitor cell capturing stent in combination with high dose Atorvastatin. Furthermore we showed that the endothelial progenitor cell capturing stent indeed captures endothelial progenitor cells, leading to accelerated re-endothelialization and reduced thrombogenicity.

Lately, stem cells have emerged as a new therapy in cardiovascular disease, mainly in the setting of an acute myocardial infarction but also in chronic ischemic heart failure and chronic myocardial ischemia⁶¹. The beneficial effects of the different stem cells are multifactorial, including promotion of neovascularisation, inhibition of apoptosis, reduction of negative remodelling, modulation of the immune system, stimulation of resident cardiac progenitor cells and attenuation of β adrenoreceptor down regulation. These effects should all lead to salvage of the cardiac myocyte and improvement of cardiac contractility. Many different types of stem cells exist and have been tested in pre-clinical and clinical settings, including first generation skeletal myoblasts and bone marrow derived mononuclear cells, second generation mesenchymal and mesenchymal-like stem cells and third generation embryonic stem cells and pluripotent stem cells. Although stem cell therapy seems very promising for the treatment of cardiovascular disease many questions still need to be answered to discover the best stem cell, optimal delivering period and optimal delivering method⁶¹. In this thesis

we describe the use of adipose tissue-derived regenerative cells in the treatment of ST segment elevation myocardial infarction.

AIM AND OUTLINE OF THIS THESIS

The general aim of this thesis was to twofold. Firstly, we investigated the pathophysiology of atherosclerotic plaque development and progression. Secondly, we studied novel therapies for coronary artery disease by using a novel stent and stem cell therapy. In order to do this we used basic science techniques, animal models and clinical studies.

As mentioned earlier, the immune system plays a pivotal role in the initiation and progression of atherosclerotic disease. In **chapter two** we provide a general overview of the role of a part of the innate immunity, namely Toll like receptor 4, in atherosclerosis and especially vulnerable plaque development.

In **chapter three** we investigated the role of Toll like receptor 4 in mast cells in a murine model for vulnerable plaque. The murine vulnerable plaque model is based upon shear stress alteration using a tapered perivascular cast. This cast is placed around the right common carotid artery creating low shear stress upstream and oscillatory shear stress downstream of the cast. Subsequently, upstream of the cast a vulnerable plaque develops while downstream of the cast a more stable plaque is formed.

In **chapter four** we up scaled the murine model to the rabbit in order to create a vulnerable plaque model in the rabbit. Rabbits were fed a high cholesterol diet and we also used a tapered perivascular cast around the right common carotid artery.

Neovascularization, driven by intraplaque hypoxia, results in the formation of immature and fragile vessels under influence of VEGF-A. These immature and fragile vessels have a greater vascular permeability resulting in the extravasation of leucocytes and erythrocytes, leading to expansion of the necrotic core and intraplaque haemorrhage. Stabilization of these so-called leaky vessels might prevent plaque destabilization and formation of a vulnerable plaque. In **chapter five** we studied the role of Thsd-1, which we recently identified as a possible regulator of vascular development, in different animal models for neovascularization, including a murine vulnerable plaque model.

In **Chapter six and seven** the results of the HEALING IIB trial are discussed, a study where we used an endothelial progenitor cell capturing stent (GENOUS stent) in combination with Atorvastatin for the treatment of coronary artery disease. In **chapter eight** we show in different experimental set-ups that use of the Genous stent indeed leads to increased re-endothelialization with reduced thrombogenicity.

In **chapter nine**, we discuss the results of the APOLLO trial in which we evaluated the safety and feasibility of adipose tissue-derived regenerative cells in the treatment of ST segment elevation myocardial infarction.

Finally, in **chapter ten**, a general overview and discussion of all results described in this thesis is given.

REFERENCES

1. Global status report on noncommunicable diseases 2010. Geneva, World Health Organization, 2011.
2. Global atlas on cardiovascular disease prevention and control. Geneva, World Health Organization, 2011.
3. Berenson GS, Srinivasan SR, Bao W, Newman WP, 3rd, Tracy RE, Wattigney WA. Association between multiple cardiovascular risk factors and atherosclerosis in children and young adults. The Bogalusa Heart Study. *N Engl J Med*. 1998 Jun 4;338(23):1650-6.
4. McGill HC, Jr., McMahan CA, Zieske AW, Malcom GT, Tracy RE, Strong JP. Effects of nonlipid risk factors on atherosclerosis in youth with a favorable lipoprotein profile. *Circulation*. 2001 Mar 20;103(11):1546-50.
5. McGill HC, Jr., McMahan CA, Malcom GT, Oalman MC, Strong JP. Effects of serum lipoproteins and smoking on atherosclerosis in young men and women. The PDAY Research Group. Pathobiological Determinants of Atherosclerosis in Youth. *Arterioscler Thromb Vasc Biol*. 1997 Jan;17(1):95-106.
6. Munzel T, Sinning C, Post F, Warnholtz A, Schulz E. Pathophysiology, diagnosis and prognostic implications of endothelial dysfunction. *Ann Med*. 2008;40(3):180-96.
7. Widlansky ME, Gokce N, Keaney JF, Jr., Vita JA. The clinical implications of endothelial dysfunction. *J Am Coll Cardiol*. 2003 Oct 1;42(7):1149-60.
8. Libby P. Inflammation in atherosclerosis. *Nature*. 2002 Dec 19-26;420(6917):868-74.
9. Cybulsky MI, Iiyama K, Li H, Zhu S, Chen M, Iiyama M, et al. A major role for VCAM-1, but not ICAM-1, in early atherosclerosis. *J Clin Invest*. 2001 May;107(10):1255-62.
10. Hansson GK, Hermansson A. The immune system in atherosclerosis. *Nat Immunol*. 2011 Mar;12(3):204-12.
11. Virmani R, Burke AP, Kolodgie FD, Farb A. Vulnerable plaque: the pathology of unstable coronary lesions. *J Interv Cardiol*. 2002 Dec;15(6):439-46.
12. Virmani R, Burke AP, Farb A, Kolodgie FD. Pathology of the vulnerable plaque. *J Am Coll Cardiol*. 2006 Apr 18;47(8 Suppl):C13-8.
13. Falk E, Shah PK, Fuster V. Coronary plaque disruption. *Circulation*. 1995 Aug 1;92(3):657-71.
14. Davies MJ, Thomas A. Thrombosis and acute coronary-artery lesions in sudden cardiac ischemic death. *N Engl J Med*. 1984 May 3;310(18):1137-40.
15. Davies MJ. Pathology of arterial thrombosis. *Br Med Bull*. 1994 Oct;50(4):789-802.
16. Wernersson R, Schierup MH, Jorgensen FG, Gorodkin J, Panitz F, Staerfeldt HH, et al. Pigs in sequence space: a 0.66X coverage pig genome survey based on shotgun sequencing. *BMC genomics*. 2005;6(1):70.

17. Williams H, Johnson JL, Carson KG, Jackson CL. Characteristics of intact and ruptured atherosclerotic plaques in brachiocephalic arteries of apolipoprotein E knockout mice. *Arteriosclerosis, thrombosis, and vascular biology*. 2002 May 1;22(5):788-92.
18. Cheng C, Tempel D, van Haperen R, de Boer HC, Segers D, Huisman M, et al. Shear stress-induced changes in atherosclerotic plaque composition are modulated by chemokines. *The Journal of clinical investigation*. 2007 Mar;117(3):616-26.
19. Cheng C, Tempel D, van Haperen R, van der Baan A, Grosveld F, Daemen MJ, et al. Atherosclerotic lesion size and vulnerability are determined by patterns of fluid shear stress. *Circulation*. 2006 Jun 13;113(23):2744-53.
20. Cheng C, van Haperen R, de Waard M, van Damme LC, Tempel D, Hanemaaijer L, et al. Shear stress affects the intracellular distribution of eNOS: direct demonstration by a novel in vivo technique. *Blood*. 2005 Dec 1;106(12):3691-8.
21. Kolodgie FD, Katocs AS, Jr., Largis EE, Wrenn SM, Cornhill JF, Herderick EE, et al. Hypercholesterolemia in the rabbit induced by feeding graded amounts of low-level cholesterol. Methodological considerations regarding individual variability in response to dietary cholesterol and development of lesion type. *Arterioscler Thromb Vasc Biol*. 1996 Dec;16(12):1454-64.
22. Aoyagi M, Yamamoto M, Azuma H, Nagashima G, Niimi Y, Tamaki M, et al. Immunolocalization of matrix metalloproteinases in rabbit carotid arteries after balloon denudation. *Histochemistry and cell biology*. 1998 Feb;109(2):97-102.
23. Constantinides P, Chakravarti RN. Rabbit arterial thrombosis production by systemic procedures. *Archives of pathology*. 1961 Aug;72:197-208.
24. Abela GS, Picon PD, Friedl SE, Gebara OC, Miyamoto A, Federman M, et al. Triggering of plaque disruption and arterial thrombosis in an atherosclerotic rabbit model. *Circulation*. 1995 Feb 1;91(3):776-84.
25. Phinikaridou A, Hallock KJ, Qiao Y, Hamilton JA. A robust rabbit model of human atherosclerosis and atherothrombosis. *Journal of lipid research*. 2009 May;50(5):787-97.
26. Ross R. Atherosclerosis—an inflammatory disease. *N Engl J Med*. 1999 Jan 14;340(2):115-26.
27. Wigren M, Nilsson J, Kolbus D. Lymphocytes in atherosclerosis. *Clin Chim Acta*. 2012 Oct 9;413(19-20):1562-8.
28. Ait-Oufella H, Herbin O, Bouaziz JD, Binder CJ, Uyttenhove C, Laurans L, et al. B cell depletion reduces the development of atherosclerosis in mice. *J Exp Med*. 2010 Aug 2;207(8):1579-87.
29. Kyaw T, Cui P, Tay C, Kanellakis P, Hosseini H, Liu E, et al. BAFF receptor mAb treatment ameliorates development and progression of atherosclerosis in hyperlipidemic ApoE(-/-) mice. *PLoS One*. 2013;8(4):e60430.
30. den Dekker WK, Cheng C, Pasterkamp G, Duckers HJ. Toll like receptor 4 in atherosclerosis and plaque destabilization. *Atherosclerosis*. 2010 Apr;209(2):314-20.
31. Swirski FK, Pittet MJ, Kircher MF, Aikawa E, Jaffer FA, Libby P, et al. Monocyte accumulation in mouse atherogenesis is progressive and proportional to extent of disease. *Proc Natl Acad Sci U S A*. 2006 Jul 5;103(27):10340-5.
32. Bobryshev YV, Lord RS. Ultrastructural recognition of cells with dendritic cell morphology in human aortic intima. Contacting interactions of Vascular Dendritic Cells in athero-resistant and athero-prone areas of the normal aorta. *Arch Histol Cytol*. 1995 Aug;58(3):307-22.

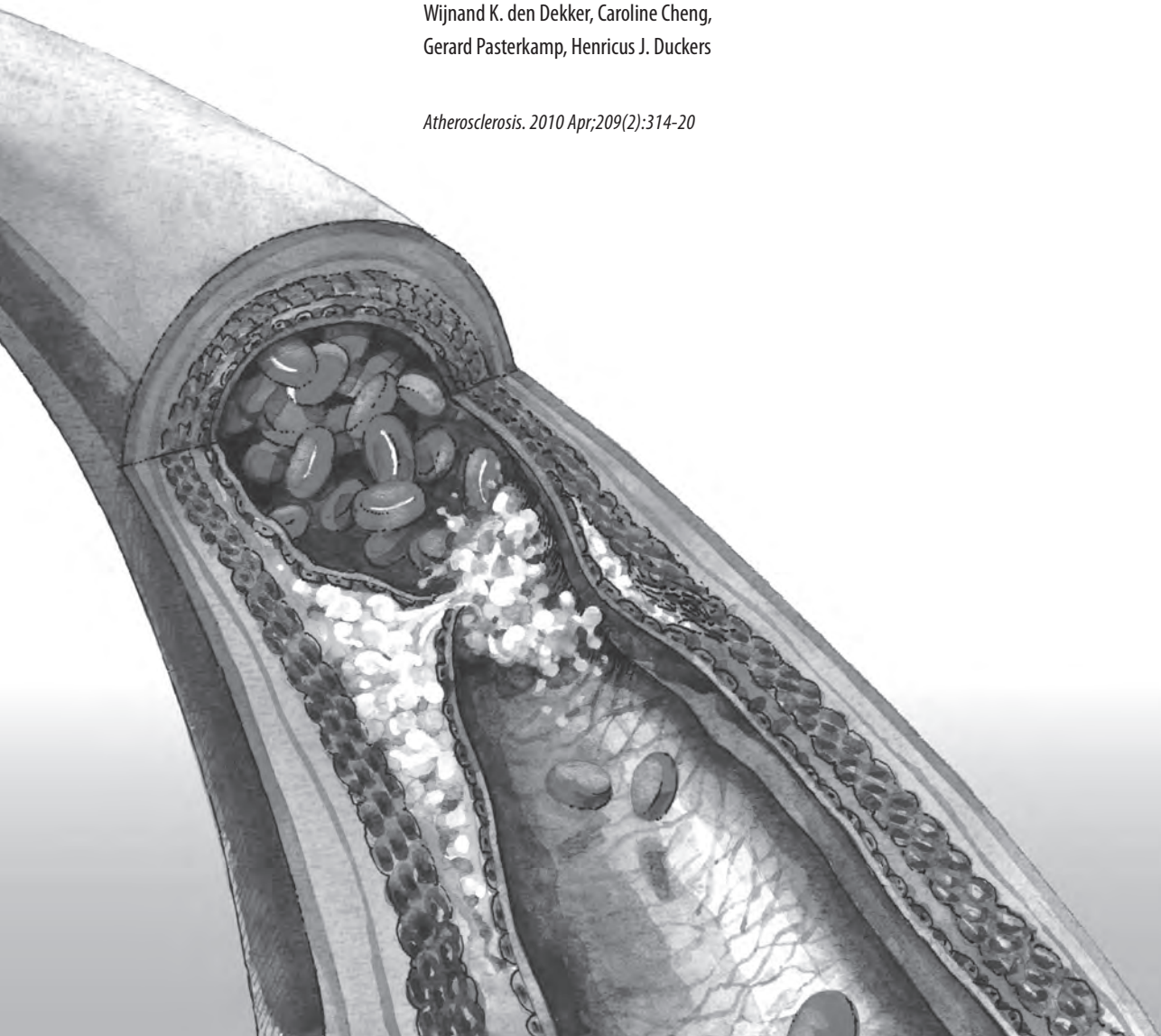
33. Bobryshev YV, Lord RS. Mapping of vascular dendritic cells in atherosclerotic arteries suggests their involvement in local immune-inflammatory reactions. *Cardiovasc Res*. 1998 Mar;37(3):799-810.
34. Yilmaz A, Lochno M, Traeg F, Cicha I, Reiss C, Stumpf C, et al. Emergence of dendritic cells in rupture-prone regions of vulnerable carotid plaques. *Atherosclerosis*. 2004 Sep;176(1):101-10.
35. Whitman SC, Rateri DL, Szilvassy SJ, Yokoyama W, Daugherty A. Depletion of natural killer cell function decreases atherosclerosis in low-density lipoprotein receptor null mice. *Arterioscler Thromb Vasc Biol*. 2004 Jun;24(6):1049-54.
36. Aslanian AM, Chapman HA, Charo IF. Transient role for CD1d-restricted natural killer T cells in the formation of atherosclerotic lesions. *Arterioscler Thromb Vasc Biol*. 2005 Mar;25(3):628-32.
37. Sun J, Sukhova GK, Wolters PJ, Yang M, Kitamoto S, Libby P, et al. Mast cells promote atherosclerosis by releasing proinflammatory cytokines. *Nat Med*. 2007 Jun;13(6):719-24.
38. Kovanen PT. Mast cells: multipotent local effector cells in atherothrombosis. *Immunol Rev*. 2007 Jun;217:105-22.
39. Lindstedt KA, Kovanen PT. Mast cells in vulnerable coronary plaques: potential mechanisms linking mast cell activation to plaque erosion and rupture. *Curr Opin Lipidol*. 2004 Oct;15(5):567-73.
40. Kovanen PT. Mast cells in atherogenesis: actions and reactions. *Curr Atheroscler Rep*. 2009 May;11(3):214-9.
41. Bot I, de Jager SC, Zerneck A, Lindstedt KA, van Berkel TJ, Weber C, et al. Perivascular mast cells promote atherogenesis and induce plaque destabilization in apolipoprotein E-deficient mice. *Circulation*. 2007 May 15;115(19):2516-25.
42. Sluimer JC, Daemen MJ. Novel concepts in atherogenesis: angiogenesis and hypoxia in atherosclerosis. *J Pathol*. 2009 May;218(1):7-29.
43. Kolodgie FD, Gold HK, Burke AP, Fowler DR, Kruth HS, Weber DK, et al. Intraplaque hemorrhage and progression of coronary atheroma. *N Engl J Med*. 2003 Dec 11;349(24):2316-25.
44. Altaf N, MacSweeney ST, Gladman J, Auer DP. Carotid intraplaque hemorrhage predicts recurrent symptoms in patients with high-grade carotid stenosis. *Stroke*. 2007 May;38(5):1633-5.
45. Hellings WE, Peeters W, Moll FL, Piers SR, van Setten J, Van der Spek PJ, et al. Composition of carotid atherosclerotic plaque is associated with cardiovascular outcome: a prognostic study. *Circulation*. 2010 May 4;121(17):1941-50.
46. Koole D, Heyligers J, Moll FL, Pasterkamp G. Intraplaque neovascularization and hemorrhage: markers for cardiovascular risk stratification and therapeutic monitoring. *J Cardiovasc Med (Hagerstown)*. 2012 Oct;13(10):635-9.
47. Pellicori P, Costanzo P, Joseph AC, Hoyer A, Atkin SL, Cleland JG. Medical management of stable coronary atherosclerosis. *Curr Atheroscler Rep*. 2013 Apr;15(4):313.
48. Task Force M, Montalescot G, Sechtem U, Achenbach S, Andreotti F, Arden C, et al. 2013 ESC guidelines on the management of stable coronary artery disease: The Task Force on the management of stable coronary artery disease of the European Society of Cardiology. *Eur Heart J*. 2013 Aug 30.
49. Grassi D, Desideri G, Ferri L, Aggio A, Tiberti S, Ferri C. Oxidative stress and endothelial dysfunction: say NO to cigarette smoking! *Curr Pharm Des*. 2010;16(23):2539-50.

50. Onat A. Metabolic syndrome: nature, therapeutic solutions and options. *Expert Opin Pharmacother*. 2011 Aug;12(12):1887-900.
51. Bangalore S, Steg G, Deedwania P, Crowley K, Eagle KA, Goto S, et al. beta-Blocker use and clinical outcomes in stable outpatients with and without coronary artery disease. *JAMA*. 2012 Oct 3;308(13):1340-9.
52. Lewis HD, Jr., Davis JW, Archibald DG, Steinke WE, Smitherman TC, Doherty JE, 3rd, et al. Protective effects of aspirin against acute myocardial infarction and death in men with unstable angina. Results of a Veterans Administration Cooperative Study. *N Engl J Med*. 1983 Aug 18;309(7):396-403.
53. Antithrombotic Trialists C. Collaborative meta-analysis of randomised trials of antiplatelet therapy for prevention of death, myocardial infarction, and stroke in high risk patients. *BMJ*. 2002 Jan 12;324(7329):71-86.
54. Randomised trial of intravenous streptokinase, oral aspirin, both, or neither among 17,187 cases of suspected acute myocardial infarction: ISIS-2. ISIS-2 (Second International Study of Infarct Survival) Collaborative Group. *Lancet*. 1988 Aug 13;2(8607):349-60.
55. Randomised trial of cholesterol lowering in 4444 patients with coronary heart disease: the Scandinavian Simvastatin Survival Study (4S). *Lancet*. 1994 Nov 19;344(8934):1383-9.
56. Libby P, Aikawa M. Mechanisms of plaque stabilization with statins. *Am J Cardiol*. 2003 Feb 20;91(4A):4B-8B.
57. Liu Y, Wei J, Hu S, Hu L. Beneficial effects of statins on endothelial progenitor cells. *Am J Med Sci*. 2012 Sep;344(3):220-6.
58. Rosenson RS. Pluripotential mechanisms of cardioprotection with HMG-CoA reductase inhibitor therapy. *Am J Cardiovasc Drugs*. 2001;1(6):411-20.
59. Nakazawa G, Finn AV, Joner M, Ladich E, Kutys R, Mont EK, et al. Delayed arterial healing and increased late stent thrombosis at culprit sites after drug-eluting stent placement for acute myocardial infarction patients: an autopsy study. *Circulation*. 2008 Sep 9;118(11):1138-45.
60. Patel N, Banning AP. Bioabsorbable scaffolds for the treatment of obstructive coronary artery disease: the next revolution in coronary intervention? *Heart*. 2013 Sep;99(17):1236-43.
61. Takashima SI, Tempel D, Duckers HJ. Current outlook of cardiac stem cell therapy towards a clinical application. *Heart*. 2013 Mar 22.

Chapter 2 Toll Like Receptor 4 in atherosclerosis and plaque destabilization

Wijnand K. den Dekker, Caroline Cheng,
Gerard Pasterkamp, Henricus J. Duckers

Atherosclerosis. 2010 Apr;209(2):314-20



ABSTRACT

The immune system plays a pivotal role in initiation and progression of atherosclerosis. Monocytes and T-lymphocytes are the first cells to enter the damaged endothelium. Differentiation of monocytes into macrophages and ingestion of lipids by these macrophages turning them into foam cells is a crucial step in the development of a fatty streak, the first sign of atherosclerosis. In recent years there has been accumulating evidence for the involvement of Toll Like Receptor 4, a pattern recognition receptor of the innate immune system, in the pathogenesis of atherosclerosis. Different cell types present in the atherosclerotic plaque express TLR4 and several pro-atherogenic ligands have been shown to activate TLR4.

The innate immune system and the TLR signaling cascade may play an important role not only in the pathogenesis of atherosclerosis, but also in plaque destabilization. In this review, we discuss the role of TLR4 in the pathogenesis of atherosclerosis and vulnerable plaque development

INTRODUCTION

Atherosclerosis is regarded as a lipid-induced inflammatory disease. Endothelial dysfunction leads to subendothelial accumulation of atherogenic lipoproteins and adhesion of leucocytes to the endothelium, including monocytes and T-lymphocytes. Subsequently, secreted cytokines can activate residing macrophages, endothelial cells and vascular smooth muscle cells, which actively participate in cellular immunity and contribute to local inflammation [1, 2]. The complex interplay between inflammatory cells, cytokines, and degrading enzymes may lead to progression of atherosclerotic lesion formation and eventually to unstable plaque formation or even plaque rupture [3].

Immune competent cells, including macrophages, mast cells and endothelial cells can recognize pathogen-associated molecular patterns (PAMPs), i.e. specific motifs shared by a variety of pathogens which are highly conserved through evolution. Lipopolysaccharide (LPS) from gram negative bacteria is one of the best known PAMP, whereas others include flagellin, peptidoglycan, double stranded RNA or unmethylated CpG motifs. PAMPs bind to pattern recognition receptors (PRRs), including Toll like receptors (TLRs) [4], which leads to activation of NF κ B and subsequent transcription of pro-inflammatory genes [5]. These TLRs are part of the innate immune system, which in contrast to the adaptive immune system is activated in a non-specific manner and forms the first line of defense against invading pathogens in mammals.

THE TOLL LIKE RECEPTOR FAMILY

The Toll receptor was initially described in the dorsoventral development of the *Drosophila* [6]. In 1996, Toll was described as a crucial receptor for the *Drosophila*'s defense against fungal infection, restricted to the innate immune response [7]. One year later, a mammalian homologue of the Toll receptor, Toll like receptor 4, was discovered [8]. This Toll like receptor 4 was likewise involved in the human innate immune response [9]. Since then, 13 different Toll like receptors have been identified in mammals (see table 1) and ten in the human species, with different endogenous and exogenous ligands (see table 1). Some TLRs (1,2,4,5,6,10,11) are found on the cell surface, whereas other TLRs (3,7,8,9) are intracellularly localized.

Toll like receptors are type I transmembrane receptors characterized by an extracellular domain with leucine-rich repeats and a carboxy terminal intracellular domain, similar to the intracellular domain of the interleukine-1 receptor. This domain, designated the Toll/II-1R (TIR) domain, contains about two hundred amino acids and consists of three conserved regions essential for the signaling cascade to downstream adapter molecules [10].

Table 1. *Different Toll like receptors, its ligands and its location*

Toll like receptor	Ligand	Location
TLR1	Tri-acyl peptides, i.e. Pam3CSK4 Mycobacterial lipoarabinomannan Soluble factors	Cell surface
TLR2	Peptidoglycan Lipoteichoic acid Zymosan HSP70 Glycolipids Lipopeptides/Lipoproteins, i.e. Pam3CSK4 Atypical LPS Phenol soluble modulin Mannuronic acid polymers Mycobacterial lipoarabinomannan Outer membrane proteins, i.e. porins	Cell surface
TLR3	Double stranded RNA Poly I:C	Cell compartment
TLR4	Lipopolysaccharide Heat Shock Proteins Fibronectin-EDA Heparan Sulfate Hyaluronic acid Fibrinogen MM-LDL Taxol Mannuronic acid polymers Envelope proteins Neutrophil elastase Chlamydia Pneumoniae HSP60	Cell surface
TLR5	Flagellin	Cell surface
TLR6	Di-acyl lipopeptides, i.e. MALP-2 Phenol soluble modulin Zymosan Lipoteichoic acid Soluble tuberculosis factor	Cell surface
TLR7	Imiquimod, resiquimod (imidazquinoline) Loxoribine (guanosine analogue) Bromopiridine (Pyrimidinone) Single-stranded RNA	Cell compartment
TLR8	Single-stranded RNA Small synthetic compounds Imiquimod, resiquimod (imidazquinoline)	Cell compartment
TLR9	Unmethylated CpG DNA	Cell compartment
TLR10	Unknown	Cell surface
TLR11	Profilin	Cell surface
TLR12	Unknown	?
TLR13	Unknown	?

TOLL LIKE RECEPTOR DOWNSTREAM SIGNALING CASCADE

Since the TLR signaling cascade is beyond the scope of this review, we will provide only a brief overview (for a review however, see Pállson-McDermott and O'Neill [11]). TLR4 signaling can be broadly divided in a Myeloid Differentiation factor 88 (MyD88)-dependent (early response) and MyD88-independent pathway (late response, see figure 1). In the MyD88-dependent pathway, activation of TLR leads to binding of the adaptor protein, MyD88, to the intracellular TIR domain. After binding of MyD88, IL-1R Associated Kinase 1 (IRAK1) will be activated due to IL-1R Associated Kinase 4 (IRAK4) facilitated phosphorylation of IRAK. Tumor Necrosis Factor Associated Receptor 6 (TRAF6) can now bind to the phosphorylated IRAK4-IRAK1 complex. Subsequently, IRAK1-TRAF6 dissociates from the TLR to activate another complex, comprising Transforming Growth Factor β Activated Kinase (TAK1), TAK1-Binding protein 1

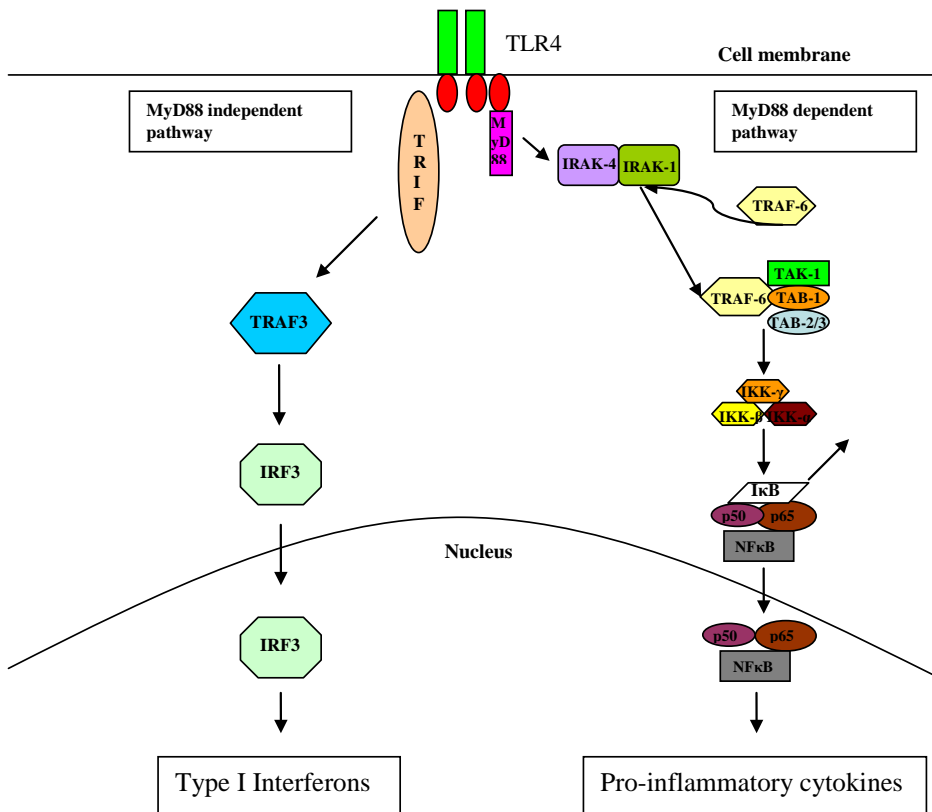


Figure 1: Schematic view of TLR signaling showing the MyD88 independent and MyD88 dependent pathway.

Abbreviations: TLR4, Toll Like Receptor 4; MyD88, Myeloid Differentiation Factor 88; IRAK, IL-1R Associated Kinase; TRAF, Tumor Necrosis Factor Receptor Associated Factor; TAK, Transforming Growth Factor β Associated Kinase; TAB, TAK-1 Binding Protein; IKK, IκB Kinase; IκB, Inhibitory Binding Protein κ B; NF κ B, Nuclear Factor κ B; TRIF, TIR Containing Adapter Molecule; IRF, Interferon Regulated Factor

(TAB1), and TAK1-Binding protein 2/3 (TAB2/3). TAK1 is then able to activate the inhibitor of nuclear factor- κ B (I κ B) Kinase complex (IKK complex), which will phosphorylate the I κ B proteins. I κ B proteins sequester the NF- κ B factors in the cytoplasm in an inactive form. Upon phosphorylation of the I κ Bs, the I κ Bs are degraded. Subsequent release and translocation of NF- κ B to the nucleus, activates transcription of different pro-inflammatory genes.

In the MyD88-independent pathway, activation of the TLR leads to binding of TIR-domain Containing Adapter Molecule (TRIF, also known as TICAM-1) to the intracellular TIR domain. TRIF activates Interferon (IFN)-Regulated Factor 3 (IRF3), which activates transcription of target genes, including type I interferons. This could be mediated via TRAF, as TRAF-deficient cells were not able to induce type I interferons.

ENDOGENOUS TOLL LIKE RECEPTOR 4 LIGANDS IN ATHEROSCLEROSIS

Various ligands for TLR4 have been identified (see table 1) and some have been proposed to function as the ligand for TLR4 in the process of atherosclerosis. Fibronectin is a high-molecular-weight extracellular matrix glycoprotein that acts as binding site for cell surface receptors, thereby regulating the extracellular matrix composition. In the neo-intima of atherosclerotic arteries a marked increase of fibronectin can be noticed together with the alternatively spliced fibronectin variant containing the Extra Domain A (fibronectin-EDA), which is normally absent in non-atherosclerotic arteries [12]. Tan and coworkers showed that deletion of fibronectin-EDA reduced atherosclerosis in mice on an atherogenic genetic background, possibly by decreased efficiency of LDL uptake by macrophages [13]. In arterial lesions of aging ApoE knockout mice, mRNA expression levels of fibronectin-EDA were increased as compared to younger animals. In addition, serum EDA levels were likewise significantly increased in aging ApoE knockout mice compared to age matched C57Bl/6 mice and young ApoE knockout mice [13, 14]. Fibronectin-EDA is able to activate TLR4 as well as to induce TLR4 expression as shown in primary cell cultures [15]. In addition, cultured mast cells can be activated via TLR4, as bone marrow derived-mast cells harvested from TLR4 deficient mice did not produce cytokines after fibronectin-EDA stimulation *in vitro* [16]. These studies indicate that fibronectin-EDA is a potential pro-atherogenic ligand for TLR4 signaling in macrophages and mast cells in the atherosclerotic plaque.

Lipids play an important role in the pathogenesis of atherosclerosis. Subendothelial lipid accumulation and ingestion by macrophages, leading to foam cell formation, is a key process in the development of fatty streaks. It is thought that lipids have to be oxidized before phagocytosis by macrophages can occur, as hypercholesterolemia has been shown to downregulate LDL receptors on the cell membranes of macrophages. Different roles for oxidized lipids have been reported in TLR4 expression and activation. Xu and coworkers showed that oxidized LDL (oxLDL) is able to increase TLR4 mRNA expression in cultured human monocytes-derived

macrophages, in contrast to native LDL [17]. However, whether oxLDL binds to and activates the TLR4 was not investigated. In contrast, pro-inflammatory cytokine production after TLR4 stimulation was inhibited in dendritic cells derived from hyperlipidemic mice, presumably by ox-LDL accumulation mediated inhibition of NF κ B translocation to the nucleus [18]. Likewise, oxidized 1-palmitoyl-2-arachidonoyl-sn-glycero-3-phosphorylcholine (Ox-PAPC), the major bioactive component of oxLDL is able to inhibit pro-inflammatory cytokine production and maturation of dendritic cells [19]. Minimally oxidized LDL (mmLDL), an early form of oxLDL, is able to induce actin polymerization and spreading of macrophages, which was shown to be dependent of the TLR4 pathway activation [20]. In addition, Miller and coworkers showed that cytokine production in macrophages induced by mmLDL is, in part, TLR4-dependent [21]. Ox-LDL is also capable of actin polymerization and macrophage spreading, but it remains unclear whether this is restricted to the TLR4 pathway. To date, the exact role of oxidized lipids in atherosclerosis via TLR4 signaling remains controversially.

Several heat shock proteins (HSPs) have been identified in the process of atherosclerosis. HSPs are molecular chaperones and play an important role in protein-protein interaction. HSPs are expressed on most cell types and expression is upregulated upon exposure to cellular stress, including inflammation, hyperthermia and hypoxia. Expression levels of HSP60 and HSP70 were increased in atherosclerotic plaques in the aortic arch of aging ApoE knockout mice [15], fed on a high cholesterol diet, in comparison to normocholesterolemic ApoE knockout mice. This up regulation of HSP mRNA attenuated when the atherosclerotic plaques stabilized [22]. Already in the early nineties, HSP60 and HSP70 have been described in the development of human atherosclerotic lesions [23, 24]. These recognized endogenous ligands for TLR4 [25, 26], might contribute to atherosclerosis via TLR4. However, to date no causal study for the role of HSP60 and HSP70 in the pathogenesis in atherosclerosis via TLR4 has been reported.

Although extensive research has been carried out to elucidate which endogenous ligand activates the TLR4 in the process of atherosclerosis, the molecular mechanism by which these candidate ligands activate TLR4 during atherogenesis and vulnerable plaque development remains to be elucidated.

TOLL LIKE RECEPTOR 4 REGULATION

Toll like receptor 4 is expressed in a number of different cell types present in the atherosclerotic plaque. TLR4 is expressed at low levels in endothelial cells in non-atherosclerotic arteries, but expression is upregulated in human atherosclerotic lesions [27]. Endothelial cells play a pivotal role in preserving the integrity of the arterial wall, whereas endothelial dysfunction is one of the earliest manifestation of atherosclerosis [1].

Monocytes are one of the first cells to enter the atherosclerotic plaque. It has been shown that TLR4 is already expressed on human and murine monocytes respectively, and that expression is increased in atherosclerotic disease [15]. TLR4 remains upregulated after differentiation into macrophages [17, 27]. Monocyte activation and differentiation into macrophages is followed by phagocytosis of oxLDL, which subsequently leads to foam cell formation. TLR4 has been shown to modify differentiation and activation of macrophages [20]. Statins, HMG-CoA reductase inhibitors and cholesterol-lowering medicines, are well known for their pleiotropic effects and it has been shown that they can inhibit NF- κ B activation in different cell types, including vascular smooth muscle cells and monocytes [28, 29]. Methe and co-workers showed that this NF- κ B inhibition in monocytes is dependent upon down regulation of TLR4 via inhibition of protein prenylation. This was independent of cholesterol levels as untreated hypercholesterolemic patients and normocholesterolemic controls showed the same level of reduction in TLR4 surface expression upon statin treatment [30]. Recently, it was shown that Candesartan, an angiotensin receptor blocker, and Pioglitazone, a peroxisome proliferators-activated receptor (PPAR)- γ agonist, are also able to block LPS induced TLR4 expression *in vivo* and *in vitro*, both on mRNA and protein levels [31, 32]. The precise mechanisms via which Candesartan and Pioglitazone exert this effect remain to be elucidated. However, this pleiotropic effect of statins, Candesartan and Pioglitazone might be used as treatment, to modulate the immune response/system in atherosclerosis.

Neutrophils are present in atherosclerotic plaques in low levels and for a long time it has been unclear what role neutrophils play in the pathogenesis of atherosclerosis. Only recently, Zerneck and co-workers showed that neutrophils are involved in atherosclerotic lesion development. CXCR4 blockade in ApoE^{-/-} mice on atherogenic diet, chemically or by bone marrow transplantation from CXCR4^{-/-} mice, induces an up regulation in the relative number of circulating neutrophils as well as an up regulation in the number of neutrophils present in atherosclerotic plaques. Treated mice showed an increase in atherosclerotic lesions, increased lipid deposition and increased number of apoptotic cells within the plaque, suggesting a more vulnerable phenotype. On the other hand, reducing the number of circulating neutrophils resulted in impaired plaque development [33]. Neutrophils express TLR4 [34] and TLR4 activation by LPS leads to increased neutrophil migration due to decreased chemokine receptor internalization [35]. The role of TLR4 signaling in neutrophils in cardiovascular disease is not yet fully understood. However, neutrophil elastase, a serine protease produced by neutrophils, is able to activate the NF- κ B pathway via TLR4 in different cell types, including macrophages and smooth muscle cells [36, 37]. Therefore, neutrophils might influence the phenotype of atherosclerotic lesions.

Beside monocytes and T-lymphocytes, mast cells have been suggested to be involved in the process of early and advanced atherosclerosis development. Mast cells are able to secrete a broad spectrum of bioactive components, including cytokines (e.g. IL-6 and TNF α , which attract monocytes and activate endothelium), chymase (remodeling and lipoprotein deg-

radation), tryptase (endothelial activation, fibrinogen cleavage) and histamine (endothelial activation). Therefore, they have been implicated as an important mediator of inflammation in atherosclerosis [38]. Bot and coworkers were able to show that mast cells, attracted and stimulated in the adventitial area, caused a significant increase in intraplaque hemorrhage in a murine model for atherosclerosis, characteristic for plaque instability [39]. In addition mast cells may promote plaque instability by induction of macrophage apoptosis, enhancement of microvascular leakage and stimulation of monocytes adhesion. Although TLR4 is expressed on murine mast cells [40], to date, no *in vivo* studies have described the involvement of mast cells in atherosclerosis via TLR4 signaling.

Dendritic cells (DCs) are antigen presenting cells that work in close proximity of monocytes, macrophages and T-lymphocytes. Although DCs are rarely found in healthy arteries, they accumulate in atherosclerotic lesions [41] and are known to express TLR4 [42]. Recently Wang and coworkers showed that the expression of TLR4 on DCs is increased in patients with acute coronary syndrome, compared to patients with stable angina and controls [43].

In a study performed by Stoll and coworkers, TLR4 expression was upregulated in medial smooth muscle cells of human atherosclerotic arteries [44]. Otsui and coworkers, hypothesize that TLR4 may be involved in early onset atherosclerosis rather than plaque instability, since there was no difference in TLR4 expression in smooth muscle cells between ACS and non-ACS patients [45]. This observation does not exclude the role of TLR4 in plaque instability as multiple cell types (DCs, monocytes/macrophages and endothelial cells) determine plaque stability as well. However, the data from Otsui may point to a limited role for TLR4 signaling in vascular smooth muscle cells during plaque destabilization.

Fibroblasts, abundantly present in the adventitial layer, have been shown to express TLR4 in human atherosclerotic arteries. LPS activation of local fibroblasts via TLR4 led to intimal hyperplasia in an *in vivo* murine model for atherosclerosis [46].

Taken together, TLR4 is abundantly expressed in a broad variety of cells in different stages of atherosclerosis formation. Currently it is still unclear via which cell type TLR4 would exert the most effect in atherosclerosis development and plaque destabilization.

TLR4 DURING EARLY ATHEROSCLEROSIS

Michelsen and coworkers were the first to suggest a direct link between TLR4 and atherosclerosis formation [47]. In this study TLR4/apolipoprotein E (ApoE) double knockout mice developed less atherosclerosis compared to ApoE knockout controls, although the intima reduction was less prominent as compared to MyD88/ApoE double knockout mice. In both TLR4/ApoE and MyD88/ApoE double knock-out mice this anti-atherogenic effect appeared to be independent of cholesterol levels. In addition, a significant reduction in lipid and macrophage content of the plaque was observed in both TLR4/ApoE and MyD88/ApoE double

knock-out mice, suggesting that TLR signaling may also be involved in advanced plaques and plaque vulnerability with characteristic lipid rich necrotic core and high macrophage content. Michelsen and coworkers did not specifically study progression into a vulnerable plaque, since these ApoE $-/-$ mice fail to develop plaques with a vulnerable phenotype without additional manipulation.

Vink and coworkers also pointed out the importance of TLR4 signaling in the early stages of atherosclerosis. In their model, BALB/c mice were implanted with a non-constrictive femoral artery cuff, loaded with LPS, in order to evaluate the involvement of TLR4 in the onset of atherosclerosis. Peri-adventitial LPS resulted in augmented neo-intima formation, but this effect was reduced in TLR4 null mice. They were also able to show that peri-adventitial fibroblasts expressed TLR4 and suggested that these fibroblasts mediated this neo-intima formation via TLR4 activation [46].

TLR4 IN ADVANCED LESIONS

Outward remodeling leads to an increase in vessel size and is a compensatory mechanism to the progression of atherosclerosis. In the process of outward remodeling, matrix metalloproteinases are produced which weaken the cap of a plaque, thus contributing to vulnerability of the plaque. Hollestelle and coworkers showed that peri-adventitial LPS stimulation in a non constrictive femoral cuff model with neo-intima formation, led to outward remodeling compared to non stimulated mice or TLR4 deficient mice [48]. In this model, TLR4 deficient mice did show neo-intima formation upon LPS stimulation and this may partially contribute to outward remodeling. Therefore, they investigated the importance of TLR4 in outward remodeling without neo-intima formation. For this purpose, they studied outward remodeling in a flow cessation model by examining the carotid artery contralateral to the ligated carotid artery. In this experiment outward remodeling was also dependent of TLR4, as TLR4 deficient mice did not show any outward remodeling compared to wild type mice. Taken together these data suggest that TLR4 signaling plays a role in the compensatory mechanism of outward remodeling and activation of matrix metalloproteinases underlying this process may also impede plaque stability, as they are involved in degradation of the extra cellular matrix.

A human vulnerable atherosclerotic plaque has a number of key features, including a thin fibrous cap of less than 65 μm with few vascular smooth muscle cells, a lipid rich necrotic core and high macrophage content. Rupture of such a vulnerable plaque leads to release of the highly thrombogenic necrotic core leading to acute thrombus formation and occlusion of the coronary artery. Rupture will most likely occur when the fibrous cap is thin, which is dependent on extra cellular matrix turnover. Infiltrating macrophages into the cap produce matrix metalloproteinases, including MMP-9, and other proteolytic enzymes which degrade local extracellular matrix [2]. LPS stimulation of human macrophages and murine mast cells

leads to increased production of MMP-9 and pro-MMP-9, a precursor molecule of MMP-9 [49, 50].

Vascular smooth muscle cells are the predominant matrix producing cells in the atherosclerotic plaque and therefore apoptosis of vascular smooth muscle cells leads to decrease of extracellular matrix production. TLR4 signaling may initiate vascular smooth muscle cell apoptosis through a Fas-associated death domain-dependent pathway [51]. Recently, Ishikawa and coworkers studied TLR4 expression at the site of ruptured plaques in patients with an acute myocardial infarction (AMI), stable angina (SA) and age-matched control patients [52]. Systemic TLR4 expression, mRNA and protein, on circulating monocytes was increased in patients with AMI and SA as compared to non-ischemic patients. These results are comparable to earlier results of Methe and coworkers, who showed that circulating monocytes in patients with unstable angina or AMI have up regulation of TLR4, mRNA and protein, as compared to healthy controls [53]. In AMI patients, local TLR4 levels at the site of plaque rupture were higher as compared to expression in circulating monocytes. Atherectomy specimens from the culprit lesion showed predominantly TLR4 expression in infiltrating macrophages. TLR4 on monocytes might not be the most suitable candidate as biomarker for AMI, however TLR4 expression on circulating monocytes have been associated with vulnerable plaque and plaque rupture.

TLR4 POLYMORPHISMS AND ATHEROSCLEROSIS

The Asp299Gly mutation in the TLR4 region on chromosome 9 is associated with an attenuated response to endotoxins due to impaired TLR4 signaling [54]. Kiechl and coworkers reported that the common Asp299Gly TLR4 polymorphism was associated with an increased risk of acute severe infection, but a decreased risk of carotid artery and femoral artery atherosclerosis and cardiovascular cause of death [55]. This might be due to lower levels of certain systemic pro-inflammatory cytokines, soluble adhesion molecules and acute phase reactants. Since this first observational study, conflicting reports have been published concerning the association between the Asp299Gly TLR4 polymorphism and cardiovascular disease. In a case-control study, the Asp299Gly TLR4 polymorphism was also associated with a decreased risk of acute coronary events, independent of standard coronary risk factors, together with reduced levels of plasma fibrinogen and soluble VCAM-1 [56]. Besides lowering pro-inflammatory status, the Asp299Gly polymorphism might also influence lipid metabolism as carriers of the Asp299Gly polymorphism had a lower risk of cardiovascular events upon statin treatment than non-carriers [57]. In contrast to these protecting effects of the Asp299Gly polymorphism, Edfeldt and coworkers showed that the Asp299Gly polymorphism was not associated with a decreased risk of myocardial infarction in men, but an increased risk. There was also no difference in serum Il-6, CRP and plasma fibrinogen concentrations [58].

and coworkers found no association between the Asp299Gly polymorphism and baseline carotid artery intima media thickness (IMT) or progression of IMT in a 3-year follow-up [59]. In the most recent report, published in this journal, Hernesniemi and coworkers also found no association between the Asp299Gly polymorphism and IMT. However, they did find an association between the Asp299Gly polymorphism and carotid artery compliance, which may be due to impaired TLR4 signaling [60]. Whether this also reflects a reduced risk for cardiovascular disease has to be awaited, as this study was conducted in young adults and the follow-up was not long to register any adverse cardiovascular events.

A large, prospective study is needed to establish a definitive effect of this polymorphism on cardiovascular events.

CONCLUSION

Atherosclerosis is regarded mainly an inflammation-driven disease, and there is accumulating evidence for the involvement of the Toll like receptor 4 in atherogenesis as an important mediator of the innate immune system. Toll like receptor 4 is widely expressed on different cell types known to be involved in the pathogenesis of atherosclerosis and has been shown to bind several known pro-atherogenic ligands. Stimulation of TLR4 leads to activation of NFκB transcription factor and pro-inflammatory proteins, which propels the inflammatory reaction and causes destabilization of atherosclerotic plaques. In the early phase of atherosclerosis, the role of TLR4 is established. Michelsen and coworkers showed a marked reduction of

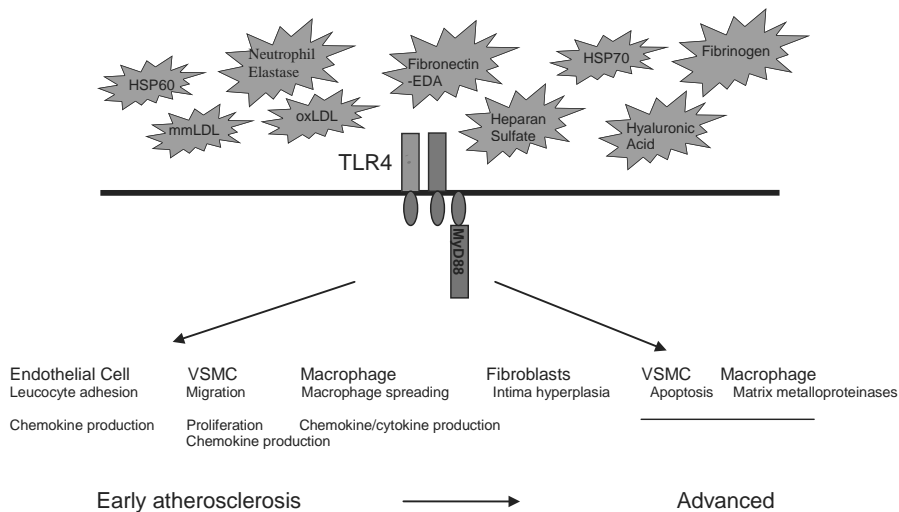


Figure 2: Different endogenous ligands can activate TLR4 in the pathogenesis of atherosclerosis. In early stages this will lead to plaque formation, while in advanced stages TLR4 activation might contribute to plaque destabilization by weakening of the fibrous cap.

atherosclerosis in TLR4/ApoE double knockout mice compared to ApoE knockout mice [47]. In contrast, the role of TLR4 signaling in advanced atherosclerosis, plaque destabilization and rupture is not yet fully assessed and only a few studies have reported a possible association between TLR4 signaling and plaque rupture. TLR4 expression was indeed upregulated at sites of plaque rupture, as well as in circulating monocytes, of patients with an AMI or unstable angina compared to healthy individuals or patients with stable angina. Hollestelle and co-workers were able to show that TLR4 is also involved in arterial outward remodeling, one of the characteristics of plaque instability, using TLR4 deficient mice [48]. Arterial remodeling is governed by the release of matrix metalloproteinases and may provide a link between TLR4 signaling and plaque vulnerability. We hypothesize that TLR4 signaling is involved in the early initiation of atherogenesis, as well as advanced atherosclerosis, plaque destabilization and plaque rupture (see figure 2).

Macrophages in the atherosclerotic plaque produce matrix metalloproteinases upon stimulation of TLR4, which degrade the extra cellular matrix and hence weaken the fibrous cap. Secondly, TLR4 stimulation can lead to vascular smooth muscle cell apoptosis leading to less extra cellular matrix production and subsequently weakening of the fibrous cap. Apoptosis of vascular smooth muscle cells by itself might also lead to cap weakening but the pathogenesis is not yet fully understood. In the process of atherosclerosis and plaque destabilization, the endogenous ligand for TLR4 remains to be elucidated as well as the main cell type, which would be responsible for these processes. Notwithstanding, TLR4 could provide a potent therapeutic target in the prevention of vulnerable plaque development.

REFERENCES

1. Ross, R., *Atherosclerosis—an inflammatory disease*. N Engl J Med, 1999. **340**(2): p. 115-26.
2. Libby, P., *Inflammation in atherosclerosis*. Nature, 2002. **420**(6917): p. 868-74.
3. Davies, M.J. and A.C. Thomas, *Plaque fissuring—the cause of acute myocardial infarction, sudden ischaemic death, and crescendo angina*. Br Heart J, 1985. **53**(4): p. 363-73.
4. Janeway, C.A., Jr. and R. Medzhitov, *Innate immune recognition*. Annu Rev Immunol, 2002. **20**: p. 197-216.
5. Lu, Y.C., W.C. Yeh, and P.S. Ohashi, *LPS/TLR4 signal transduction pathway*. Cytokine, 2008. **42**(2): p. 145-51.
6. Hashimoto, C., K.L. Hudson, and K.V. Anderson, *The Toll gene of Drosophila, required for dorsal-ventral embryonic polarity, appears to encode a transmembrane protein*. Cell, 1988. **52**(2): p. 269-79.
7. Lemaitre, B., et al., *The dorsoventral regulatory gene cassette spatzle/Toll/cactus controls the potent antifungal response in Drosophila adults*. Cell, 1996. **86**(6): p. 973-83.
8. Medzhitov, R., P. Preston-Hurlburt, and C.A. Janeway, Jr., *A human homologue of the Drosophila Toll protein signals activation of adaptive immunity*. Nature, 1997. **388**(6640): p. 394-7.
9. Poltorak, A., et al., *Defective LPS signaling in C3H/HeJ and C57BL/10ScCr mice: mutations in Tlr4 gene*. Science, 1998. **282**(5396): p. 2085-8.
10. Rock, F.L., et al., *A family of human receptors structurally related to Drosophila Toll*. Proc Natl Acad Sci U S A, 1998. **95**(2): p. 588-93.
11. Palsson-McDermott, E.M. and L.A. O'Neill, *Signal transduction by the lipopolysaccharide receptor, Toll-like receptor-4*. Immunology, 2004. **113**(2): p. 153-62.
12. Magnusson, M.K. and D.F. Mosher, *Fibronectin: structure, assembly, and cardiovascular implications*. Arterioscler Thromb Vasc Biol, 1998. **18**(9): p. 1363-70.
13. Tan, M.H., et al., *Deletion of the alternatively spliced fibronectin EIIIA domain in mice reduces atherosclerosis*. Blood, 2004. **104**(1): p. 11-8.
14. Babaev, V.R., et al., *Absence of regulated splicing of fibronectin EDA exon reduces atherosclerosis in mice*. Atherosclerosis, 2008. **197**(2): p. 534-40.
15. Schoneveld, A.H., et al., *Atherosclerotic lesion development and Toll like receptor 2 and 4 responsiveness*. Atherosclerosis, 2008. **197**(1): p. 95-104.
16. Gondokaryono, S.P., et al., *The extra domain A of fibronectin stimulates murine mast cells via toll-like receptor 4*. J Leukoc Biol, 2007. **82**(3): p. 657-65.
17. Xu, X.H., et al., *Toll-like receptor-4 is expressed by macrophages in murine and human lipid-rich atherosclerotic plaques and upregulated by oxidized LDL*. Circulation, 2001. **104**(25): p. 3103-8.
18. Shamshiev, A.T., et al., *Dyslipidemia inhibits Toll-like receptor-induced activation of CD8alpha-negative dendritic cells and protective Th1 type immunity*. J Exp Med, 2007. **204**(2): p. 441-52.
19. Bluml, S., et al., *Oxidized phospholipids negatively regulate dendritic cell maturation induced by TLRs and CD40*. J Immunol, 2005. **175**(1): p. 501-8.
20. Miller, Y.I., et al., *Minimally modified LDL binds to CD14, induces macrophage spreading via TLR4/MD-2, and inhibits phagocytosis of apoptotic cells*. J Biol Chem, 2003. **278**(3): p. 1561-8.

21. Miller, Y.I., et al., *Toll-like receptor 4-dependent and -independent cytokine secretion induced by minimally oxidized low-density lipoprotein in macrophages*. *Arterioscler Thromb Vasc Biol*, 2005. **25**(6): p. 1213-9.
22. Kanwar, R.K., et al., *Temporal expression of heat shock proteins 60 and 70 at lesion-prone sites during atherogenesis in ApoE-deficient mice*. *Arterioscler Thromb Vasc Biol*, 2001. **21**(12): p. 1991-7.
23. Kleindienst, R., et al., *Immunology of atherosclerosis. Demonstration of heat shock protein 60 expression and T lymphocytes bearing alpha/beta or gamma/delta receptor in human atherosclerotic lesions*. *Am J Pathol*, 1993. **142**(6): p. 1927-37.
24. Berberian, P.A., et al., *Immunohistochemical localization of heat shock protein-70 in normal-appearing and atherosclerotic specimens of human arteries*. *Am J Pathol*, 1990. **136**(1): p. 71-80.
25. Ohashi, K., et al., *Cutting edge: heat shock protein 60 is a putative endogenous ligand of the toll-like receptor-4 complex*. *J Immunol*, 2000. **164**(2): p. 558-61.
26. Vabulas, R.M., et al., *HSP70 as endogenous stimulus of the Toll/interleukin-1 receptor signal pathway*. *J Biol Chem*, 2002. **277**(17): p. 15107-12.
27. Edfeldt, K., et al., *Expression of toll-like receptors in human atherosclerotic lesions: a possible pathway for plaque activation*. *Circulation*, 2002. **105**(10): p. 1158-61.
28. Ortego, M., et al., *Atorvastatin reduces NF-kappaB activation and chemokine expression in vascular smooth muscle cells and mononuclear cells*. *Atherosclerosis*, 1999. **147**(2): p. 253-61.
29. Zelvyte, I., et al., *Modulation of inflammatory mediators and PPARgamma and NFkappaB expression by pravastatin in response to lipoproteins in human monocytes in vitro*. *Pharmacol Res*, 2002. **45**(2): p. 147-54.
30. Methe, H., et al., *Statins decrease Toll-like receptor 4 expression and downstream signaling in human CD14+ monocytes*. *Arterioscler Thromb Vasc Biol*, 2005. **25**(7): p. 1439-45.
31. Dasu, M.R., A.C. Riosvelasco, and I. Jialal, *Candesartan inhibits Toll-like receptor expression and activity both in vitro and in vivo*. *Atherosclerosis*, 2009. **202**(1): p. 76-83.
32. Dasu, M.R., et al., *Pioglitazone inhibits Toll-like receptor expression and activity in human monocytes and db/db mice*. *Endocrinology*, 2009. **150**(8): p. 3457-64.
33. Zernecke, A., et al., *Protective role of CXC receptor 4/CXC ligand 12 unveils the importance of neutrophils in atherosclerosis*. *Circ Res*, 2008. **102**(2): p. 209-17.
34. Hayashi, F., T.K. Means, and A.D. Luster, *Toll-like receptors stimulate human neutrophil function*. *Blood*, 2003. **102**(7): p. 2660-9.
35. Fan, J. and A.B. Malik, *Toll-like receptor-4 (TLR4) signaling augments chemokine-induced neutrophil migration by modulating cell surface expression of chemokine receptors*. *Nat Med*, 2003. **9**(3): p. 315-21.
36. Ribeiro-Gomes, F.L., et al., *Neutrophils activate macrophages for intracellular killing of Leishmania major through recruitment of TLR4 by neutrophil elastase*. *J Immunol*, 2007. **179**(6): p. 3988-94.
37. Lee, K.Y., et al., *Neutrophil-derived elastase induces TGF-beta1 secretion in human airway smooth muscle via NF-kappaB pathway*. *Am J Respir Cell Mol Biol*, 2006. **35**(4): p. 407-14.
38. Kovanen, P.T., *Mast cells: multipotent local effector cells in atherothrombosis*. *Immunol Rev*, 2007. **217**: p. 105-22.
39. Bot, I., et al., *Perivascular mast cells promote atherogenesis and induce plaque destabilization in apolipoprotein E-deficient mice*. *Circulation*, 2007. **115**(19): p. 2516-25.

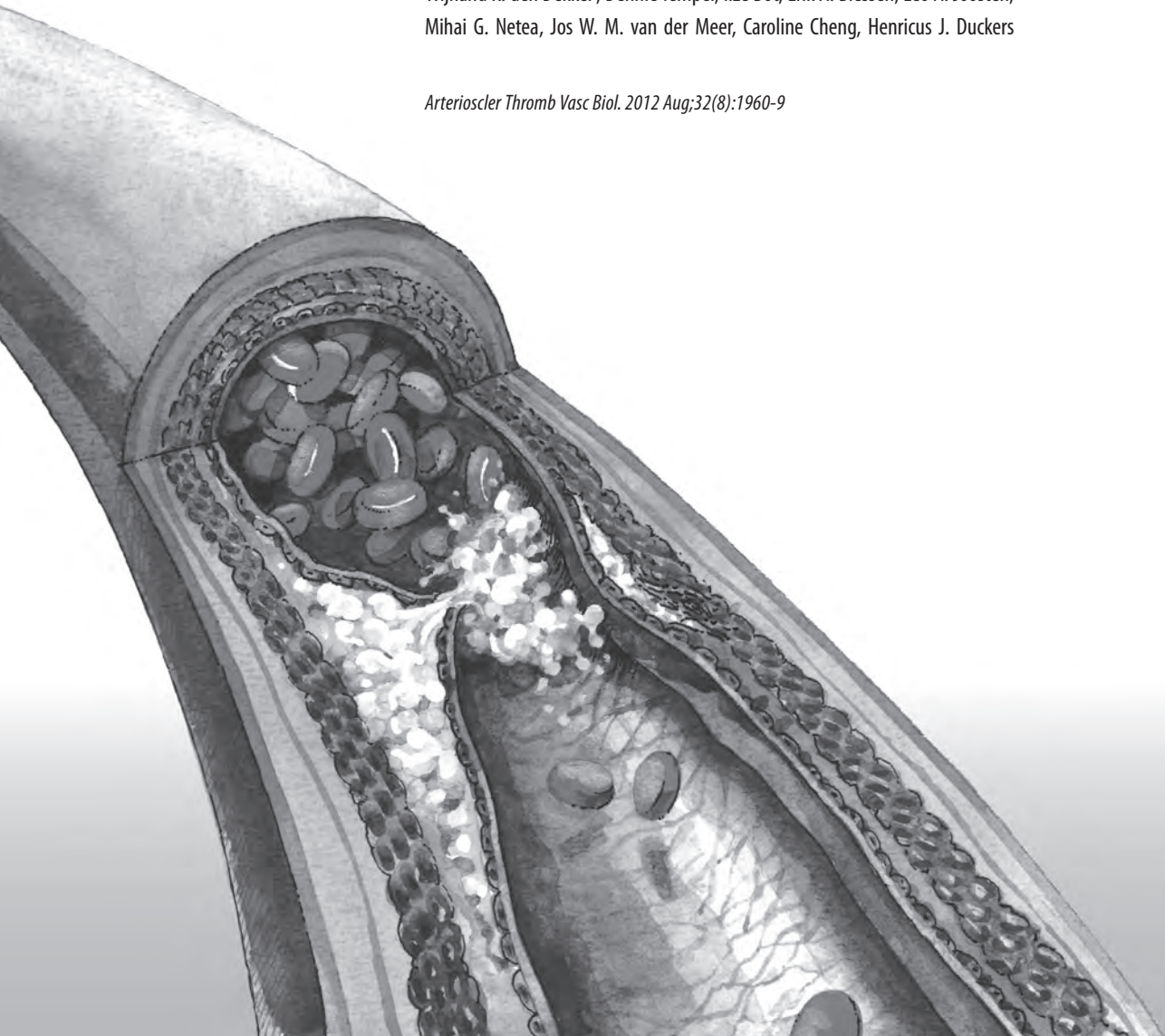
40. McCurdy, J.D., T.J. Lin, and J.S. Marshall, *Toll-like receptor 4-mediated activation of murine mast cells*. *J Leukoc Biol*, 2001. **70**(6): p. 977-84.
41. Bobryshev, Y.V. and R.S. Lord, *S-100 positive cells in human arterial intima and in atherosclerotic lesions*. *Cardiovasc Res*, 1995. **29**(5): p. 689-96.
42. Akira, S., K. Takeda, and T. Kaisho, *Toll-like receptors: critical proteins linking innate and acquired immunity*. *Nat Immunol*, 2001. **2**(8): p. 675-80.
43. Wang, L., et al., *Toll-like receptor-4 and mitogen-activated protein kinase signal system are involved in activation of dendritic cells in patients with acute coronary syndrome*. *Immunology*, 2008.
44. Stoll, L.L., et al., *Regulation of endotoxin-induced proinflammatory activation in human coronary artery cells: expression of functional membrane-bound CD14 by human coronary artery smooth muscle cells*. *J Immunol*, 2004. **173**(2): p. 1336-43.
45. Otsui, K., et al., *Enhanced expression of TLR4 in smooth muscle cells in human atherosclerotic coronary arteries*. *Heart Vessels*, 2007. **22**(6): p. 416-22.
46. Vink, A., et al., *In vivo evidence for a role of toll-like receptor 4 in the development of intimal lesions*. *Circulation*, 2002. **106**(15): p. 1985-90.
47. Michelsen, K.S., et al., *Lack of Toll-like receptor 4 or myeloid differentiation factor 88 reduces atherosclerosis and alters plaque phenotype in mice deficient in apolipoprotein E*. *Proc Natl Acad Sci U S A*, 2004. **101**(29): p. 10679-84.
48. Hollestelle, S.C., et al., *Toll-like receptor 4 is involved in outward arterial remodeling*. *Circulation*, 2004. **109**(3): p. 393-8.
49. Ikeda, T. and M. Funaba, *Altered function of murine mast cells in response to lipopolysaccharide and peptidoglycan*. *Immunol Lett*, 2003. **88**(1): p. 21-6.
50. Grenier, D. and L. Grignon, *Response of human macrophage-like cells to stimulation by *Fusobacterium nucleatum* ssp. *nucleatum* lipopolysaccharide*. *Oral Microbiol Immunol*, 2006. **21**(3): p. 190-6.
51. Haase, R., et al., *A dominant role of Toll-like receptor 4 in the signaling of apoptosis in bacteria-faced macrophages*. *J Immunol*, 2003. **171**(8): p. 4294-303.
52. Ishikawa, Y., et al., *Local expression of Toll-like receptor 4 at the site of ruptured plaques in patients with acute myocardial infarction*. *Clin Sci (Lond)*, 2008. **115**(4): p. 133-40.
53. Methe, H., et al., *Expansion of circulating Toll-like receptor 4-positive monocytes in patients with acute coronary syndrome*. *Circulation*, 2005. **111**(20): p. 2654-61.
54. Arbour, N.C., et al., *TLR4 mutations are associated with endotoxin hyporesponsiveness in humans*. *Nat Genet*, 2000. **25**(2): p. 187-91.
55. Kiechl, S., et al., *Toll-like receptor 4 polymorphisms and atherogenesis*. *N Engl J Med*, 2002. **347**(3): p. 185-92.
56. Ameziane, N., et al., *Association of the Toll-like receptor 4 gene Asp299Gly polymorphism with acute coronary events*. *Arterioscler Thromb Vasc Biol*, 2003. **23**(12): p. e61-4.
57. Boekholdt, S.M., et al., *Variants of toll-like receptor 4 modify the efficacy of statin therapy and the risk of cardiovascular events*. *Circulation*, 2003. **107**(19): p. 2416-21.
58. Edfeldt, K., et al., *Association of hypo-responsive toll-like receptor 4 variants with risk of myocardial infarction*. *Eur Heart J*, 2004. **25**(16): p. 1447-53.
59. Labrum, R., et al., *Toll receptor polymorphisms and carotid artery intima-media thickness*. *Stroke*, 2007. **38**(4): p. 1179-84.

60. Hernesniemi, J.A., et al., *Toll-like receptor 4 gene (Asp299Gly) polymorphism associates with carotid artery elasticity. The cardiovascular risk in young Finns study.* *Atherosclerosis*, 2008. **198**(1): p. 152-9.

Chapter 3 Mast Cells Induce Vascular Smooth Muscle Cell Apoptosis via a Toll-Like Receptor 4 Activation Pathway

Wijnand K. den Dekker, Dennie Tempel, Ilze Bot, Erik A. Biessen, Leo A. Joosten, Mihai G. Netea, Jos W. M. van der Meer, Caroline Cheng, Henricus J. Duckers

Arterioscler Thromb Vasc Biol. 2012 Aug;32(8):1960-9



ABSTRACT

Objective: Activated mast cells (MCs) release chymase, which can induce vascular smooth muscle cell (VSMC) apoptosis leading to plaque destabilization. Because the mechanism whereby MCs release chymase in atherosclerosis is unknown, we studied whether MC-associated VSMC apoptosis is regulated by Toll-like receptor 4 (TLR4) signaling.

Methods and results: Local recruitment and activation of MCs reduced VSMC content specifically in the cap region of vulnerable plaques in ApoE^{-/-} mice. Co-treatment with the TLR4 antagonist *Bartonella quintana* lipopolysaccharide prevented this VSMC loss, suggesting an important role for TLR4 signaling in MC-induced VSMC apoptosis. Co-culture of VSMCs with MCs activated by the TLR4 agonist *E. coli* LPS increased VSMC apoptosis. Apoptosis was inhibited by TLR4 and chymase blockers, indicating that TLR4 signaling is involved in chymase release in MCs. This pathway was mediated via IL-6, as IL-6 promoted MC-associated VSMC apoptosis, which was inhibited by blocking chymase release. In addition, TLR4 activation in MCs induced IL-6 production which was reduced by pre-incubation with either *B. quintana* lipopolysaccharide or an anti-TLR4 antibody.

Conclusion: We show that MCs promote VSMC apoptosis *in vivo*. In addition, TLR4 signaling is important in chymase release in MCs, and therefore in plaque destabilization by regulating VSMC apoptosis.

INTRODUCTION

Atherosclerosis is regarded as an inflammatory-driven disease in which macrophages and T-lymphocytes are well-known players and abundantly present in the diseased vascular wall¹⁻³. Macrophages ingesting oxidized lipids, thus forming foam cells, are one of the first steps in forming a fatty streak, the earliest form of atherosclerosis. A complex interplay between inflammatory cells, cytokines and degrading enzymes may lead to progression of an advanced atherosclerotic plaque into a rupture prone, unstable plaque. Rupture of this vulnerable plaque, characterized by a lipid rich necrotic core, high macrophage, low vascular smooth muscle cell (VSMC) content and a thin fibrous cap (<65 μm)⁴, is considered to be the major cause of an acute myocardial infarction (AMI)⁵. Besides macrophages and T-lymphocytes, there is accumulating evidence that mast cells are also important mediators in determining the phenotype of an atherosclerotic plaque^{6,7}. Activated mast cells may contribute to vulnerable plaque formation via different mechanisms. Bot and co-workers showed that mast cells can induce plaque destabilization in a murine model for atherosclerosis, associated with an increase in intraplaque haemorrhaging, due to enhanced vascular permeability, and enlargement of the lipid rich necrotic core, due to macrophage apoptosis⁸. Furthermore, mast cells produce a wide pallet of pro-inflammatory cytokines (e.g. IL-6)⁹, can induce vascular smooth muscle cell (VSMC) apoptosis¹⁰ and activate matrix metalloproteinases¹¹⁻¹³. All these processes might lead to weakening of the fibrous cap and subsequently a higher risk of plaque rupture. Indeed, it has been shown that activated mast cells are mainly located in the shoulder region of coronary plaques, which is the region with the highest chance of rupture¹⁴. Increased risk of plaque rupture in vulnerable plaque is associated with VSMC apoptosis^{10,15,16}, which weakens the VSMC-rich fibrous cap¹⁷. *In vitro* and *in vivo*, mast cells are capable of inducing VSMC apoptosis by chymase release^{10,18}. The effect of chymase release and the mechanism through which mast cells are activated to release chymase in the vulnerable plaque remains to be elucidated. Toll-like receptor 4 (TLR4) is an important pattern-recognition receptor of the innate immune system¹⁹. Activation of TLR4 activates a downstream signaling pathway that induces nuclear translocation of NF κ B and subsequent transcription of pro-inflammatory cytokines, including IL-6²⁰. It has previously been shown that mast cells express TLR4 and more recently, Avila and coworkers reviewed the importance of TLR4 on mast cells in the immune reaction against Gram-negative bacteria²¹. As it has been shown that IL-6 can up-regulate chymase protein expression in human mast cells²², we hypothesized that TLR4 signaling is involved in chymase release in mast cells. We investigated the role of TLR4 signaling on mast cell activation, and describe the subsequent effect on mast cell-induced VSMC apoptosis, both in a validated murine vulnerable plaque model and *in vitro* using co-culture experiments.

MATERIAL AND METHODS

Animal model

All animal work was performed in compliance with the guidelines issued by the Dutch government and was approved by our local animal welfare committee. We used twelve weeks old female ApoE knockout (ApoE^{-/-}/C57Bl6) mice (Jackson Laboratory, UK). Vulnerable plaque formation was induced as described earlier^{23, 24}. In short, after two weeks of acclimatization, mice were fed a Western Diet (WD, containing 15% (w/w) cacao and 0.25% (w/w) cholesterol (Arie Blok, the Netherlands). Two weeks after initiation of WD, a tapered flow-altering cast was surgically implanted around the right common carotid artery. Eight and nine weeks after cast placement, Pluronic F-127 gel (Sigma, the Netherlands), containing different pharmacological compounds or PBS placebo, was applied peri-adventitially, upstream of the cast. These compounds included the natural TLR4 antagonist *Bartonella quintana* lipopolysaccharide (LPS), isolated as previously described²⁵, the functional grade purified TLR4 antibody (TLR4a, eBioscience, USA) or 2,4Dinitrophenyl-Human Serum Albumin (DNP-HSA, Sigma, the Netherlands), which attracts and activates specifically mast cells⁸. The mice were randomly assigned to the treatment groups (N=8 per group, see table I). Three days after the second application of Pluronic F-127 gel, mice were sacrificed and the carotid artery was dissected and embedded in OCT compound (Sakura Finetek, the Netherlands), snap-frozen in liquid nitrogen, and stored in -80 °C until further processing. The findings of this first experiment were further validated in two additional *in vivo* studies. In the first study, one group of mice (N=6) was treated with lentivirus coding for a shRNA sequence that targets murine TLR4 to achieve local silencing of the gene, while the second group of mice (N=6) was treated with sham lentivirus. Both lentiviruses were applied around the carotid artery eight weeks after cast placement. One week later, we applied Pluronic F-127 gel containing DNP-HSA around the carotid artery in all animals. Three days after application of the gel we sacrificed the animals and took out the carotid artery. In the second study, we used cromolyn as an alternative strategy to stabilize the mast cells. Two groups of mice (N=4 per group) received an intravenous injection of cromolyn (25mg/kg) or

Table 1 Pharmacological treatment for the five different groups

	1 st time Pluronic F127 containing:	2 nd time Pluronic F127 containing:	Group referred to as:
Group 1	PBS	PBS	Gel
Group 2	PBS	DNP-HSA	DNP-HSA
Group 3	TLR4a (TLR4 antibody)	TLR4a (TLR4 antibody)	TLR4a
Group 4	<i>B. quintana</i> LPS	<i>B. quintana</i> LPS	BartLPS
Group 5	<i>B. quintana</i> LPS	<i>B. quintana</i> LPS-DNP-HSA	BartLPS/DNP-HSA

PBS thirty minutes before local DNP-HSA challenge. During the challenge the mice received twice daily an intraperitoneal injection of cromolyn (50mg/kg) or PBS. Three days after start of the challenge mice were sacrificed and the carotid arteries were again taken out and processed.

Histology and immunohistochemistry

The carotid artery region upstream of the cast was serially sectioned in 6 μm sections. Histological and immunohistochemical analysis was performed on 72 μm intervals, covering the whole vulnerable plaque. Mast cells were stained by Toluidine Blue (Sigma, the Netherlands). Non-activated and activated mast cells were distinguished by bright-field assessment of cell morphology after Toluidine Blue staining. Activated mast cells show degranulation and release of Toluidine Blue positive remnants, whereas inactive mast cells show intracellular and intravesicular accumulation of Toluidine Blue. In addition to Toluidine Blue staining and routine HE staining, different immunohistochemical stainings were performed to evaluate plaque stability. Sections were stained for VSMCs (anti- α -actin, Sigma, the Netherlands), apoptotic cells (TUNEL assay, Roche, the Netherlands) macrophages (anti-CD68 antibody, AbD Serotec, USA), endothelial cells (anti-PECAM1 antibody, BD Biosciences, the Netherlands) and erythrocytes (anti-TER119 antibody, BD Pharmingen, the Netherlands). The signal was visualized by immunofluorescence-labeled secondary antibody and recorded with a ZEISS LSM510LNO inverted laser scanning confocal microscope (Carl Zeiss). Lipid deposition was analyzed using Oil-Red-O staining (Sigma, Zwijndrecht, the Netherlands) and visualized by bright field microscopy.

Mast cell culture conditions

MC/9 cells (Lonza, the Netherlands, catalog number CRL-8306) were grown in modified Dulbecco's modified Eagle's medium (DMEM, supplemented with 4.5 g/L glucose, 584 mg/L L-Glutamine, 1.5 g/L NaBic, 5 mM mercapto-ethanol, Lonza, the Netherlands) and supplemented with 10% Rat T-stim (BD Biosciences, the Netherlands), 10% FCS and 1 % penicillin/streptomycin. Cells were plated in a 24-well plate (1×10^6 cells/ml/well). Cells were activated with 100 ng *E. coli* LPS with or without pre-incubation with either *B. quintana* LPS or an anti-TLR4 antibody. Cells were pre-incubated for thirty minutes before adding *E. coli* LPS. We harvested medium and cells after 24 hours of stimulation, centrifuged medium and cells, collected supernatant and stored supernatant until further use. Every experiment was conducted three times with triplicate samples.

IL-6 and IL-1 β enzyme linked immunosorbent assays (ELISA)

Murine IL-6 and IL-1 β levels were measured by commercially available ELISAs (BD Biosciences, the Netherlands). 96-Wells plates were coated with anti-mouse IL-6 capture antibody and

incubated overnight at 4°C. The wells were washed three times (PBS with 0.05% Tween-20) and blocked for one hour at room temperature with 200 µl assay diluent (PBS with 10 % FBS). Wells were washed three times and 100 µl standard or sample was added to each well and incubated for two hours. Wells were washed five times and 100 µl biotinylated anti mouse IL-6 was added and incubated for one hour. Wells were washed seven times and 100 µl streptavidin-horseradish peroxidase conjugate was added and incubated for thirty minutes. 50 µl Stop solution was added to each well (1M H₃PO₄) and colored product was read at 450nm within 30 minutes with λ correction 570 nm. IL-1β was measured with a similar protocol.

VSMC co-culture with MC/9 cells

Murine VSMCs were isolated from the aorta²⁶ and grown in DMEM (Lonza, the Netherlands, catalog number CRL8306), supplemented with 10% Fetal Calf Serum (FCS) and 1% penicillin/streptomycin. MC/9 cells were grown as described previously. After one week VSMCs (1x10⁵ cells/ml/well) were plated in a transwell 12 well plate with insert (Costar, the Netherlands). After 24 hours, the inserts were filled with respectively 1 ml medium with or without 100ng *E. coli* LPS (serotype O55:B5, Sigma, The Netherlands) or IL-6, MC/9 cells (1x10⁵ cells/ml, 1 ml), MC/9 cells with 100ng *E. coli* LPS, MC/9 cells with 100ng *E. coli* LPS and pre-incubation with TLR4 antibody (10 µg/ml), MC/9 cells with 100ng *E. coli* LPS and pre-incubation with *B. quintana* LPS (10 µg/ml), MC/9 cells treated with murine MCPT-4 siRNA and with 100ng *E. coli* LPS, and MC/9 cells treated with murine IL-6 siRNA and with 100ng *E. coli* LPS. After 48 hours of co-culture, VSMCs were harvested and analyzed for apoptosis using a commercially available Annexin V staining kit (BD Biosciences, the Netherlands). Every experiment was conducted three times with triplicate samples.

Annexin V staining of murine VSMCs

The insert of the transwell dish was discarded and the supernatant of the VSMCs was collected and transferred to 15ml tubes. Cells were washed with PBS and incubated with trypsin/EDTA (Lonza, Breda, the Netherlands) for five minutes. Medium was added and both medium and cells were transferred to the corresponding 15ml tubes. We centrifuged the tubes, 400G for five minutes, discarded the supernatant and incubated the cells with 100µl FACS buffer, 5µl Propidium Iodide (PI) and 5µl FITC Annexin V, for 15 minutes at room temperature. 400µl Binding buffer 1X was added and 100.000 cells were analyzed by flow cytometry (FACScanto, BD Biosciences, the Netherlands). Cells that stained positive for both FITC Annexin V and PI are identified as late apoptotic cells and were used for analysis. Data were analyzed using Flowjo (Tree Star, Inc., USA).

Quantification and statistical analysis

Data analysis was performed using an automated commercial image analysis system (Impak C, Clemex technologies, Canada) to evaluate differences in plaque phenotype upstream of the cast between the different treatment groups. HE staining was used to measure intima/media ratio and evaluate cap thickness and necrotic core size, α -actin staining to evaluate VSMC content, TUNEL staining to measure apoptotic cell percentage, CD31 staining to evaluate neovascularization, CD68 staining to evaluate macrophage content and TER119 staining to assess intraplaque haemorrhaging. To compare apoptotic cell percentage in cap and core region, we made an overlay of anti- α -actin staining and corresponding TUNEL staining. TUNEL positive cells in the α -actin positive area were regarded as apoptotic cells in the cap region, while TUNEL positive cells outside the actin positive region were considered as apoptotic cells in the core region. Multiple groups were compared with one-way ANOVA and a subsequent Student-Newman-Keuls multiple comparisons test. Two-tailed Students' *t* tests were used to compare individual groups. Data are presented as mean \pm SEM. P-values less than 0.05 were considered significantly different.

RESULTS

TLR4 inhibition reduces mast cell activation, but does not affect the absolute number of recruited mast cells *in vivo*

To examine the effect of local DNP-HSA treatment on mast cell recruitment and activation, we examined cryosections with Toluidine Blue staining to detect resting and activated adventitial mast cells. As expected, DNP-HSA treatment significantly increased the absolute number of adventitial mast cells by 115% (figure 1A,E), and the percentage of activated mast cells by 88% (figure 1F, F). Co-treatment of DNP-HSA with the natural TLR4 antagonist *B. quintana* LPS²⁵ did not influence the absolute number of adventitial mast cells (figure 1B, E), but significantly reduced the percentage of activated mast cells by 33% (figure 1B, F). Monotherapy with *B. quintana* LPS or an anti-TLR4 antibody (TLR4a) did not change mast cell recruitment and activation in the plaque (figure 1E, F). These data suggest that mast cell activation in our murine vulnerable plaque model is regulated via TLR4 signaling.

Mast cell recruitment and activation does not influence atherosclerotic lesion growth, but promotes atherosclerotic plaque destabilization

To assess the effect of mast cell recruitment and activation on atherosclerotic lesion development, we measured the intima/media ratio (I/M ratio). There was no difference in I/M ratio between control, DNP-HSA or combined DNP-HSA and *B. quintana* LPS treated mice (figure 1C, D,G). Moreover, monotherapy with *B. quintana* LPS or TLR4a did not influence the I/M ratio

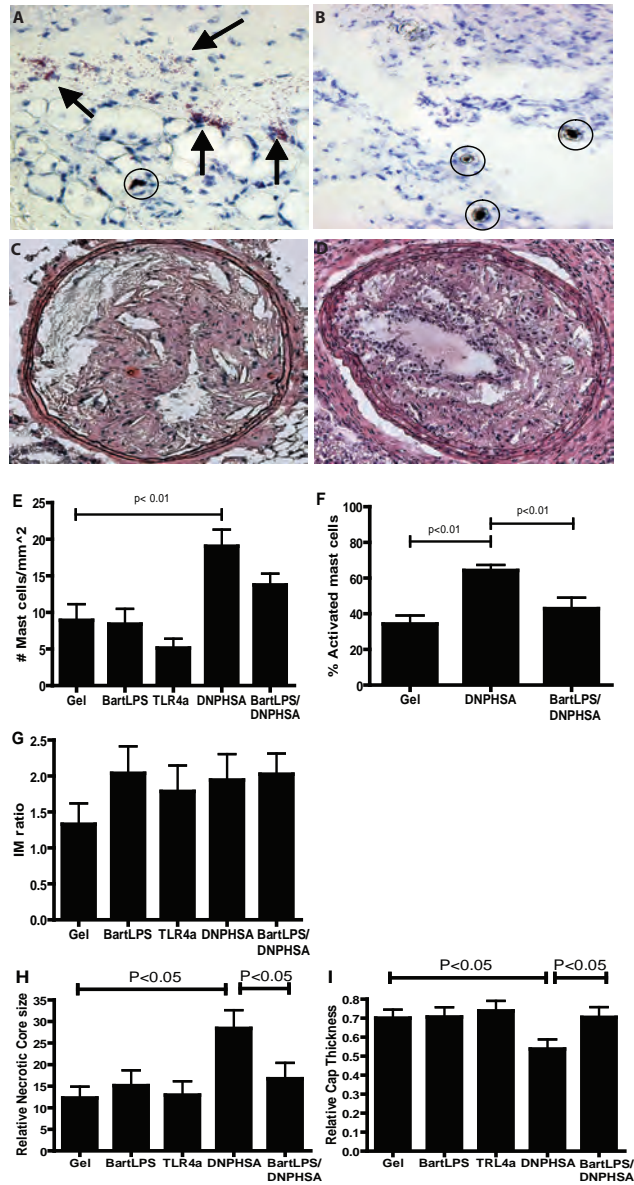


Figure 1

Representative sections stained for Toluidine Blue (upper panel) and Hematoxylin/Eosin (lower panel) of a DNP-HSA (A and C) and *B. quintana* LPS/DNP-HSA treated lesion (B and D). Arrows indicate activated, degranulated mast cells, while circles indicate resting, non-degranulated mast cells. (E) Quantification of adventitial mast cells mast cells. DNP-HSA treatment increased the absolute mast cell numbers ($P < 0.01$). (F) Quantification of the percentage activated mast cells. Local DNP-HSA increased the percentage activated mast cells ($P < 0.01$), which was inhibited by *B. quintana* LPS ($P < 0.01$). (G) The intima/media ratio was not affected. (H) Relative necrotic core size was increased upon DNP-HSA, which could be prevented by co-treatment with *B. quintana* LPS. (I) Reversely, DNP-HSA decreased relative cap thickness and this again could be prevented by co-treatment with *B. quintana* LPS. Data are presented as mean \pm SEM ($N = 8$ per group).

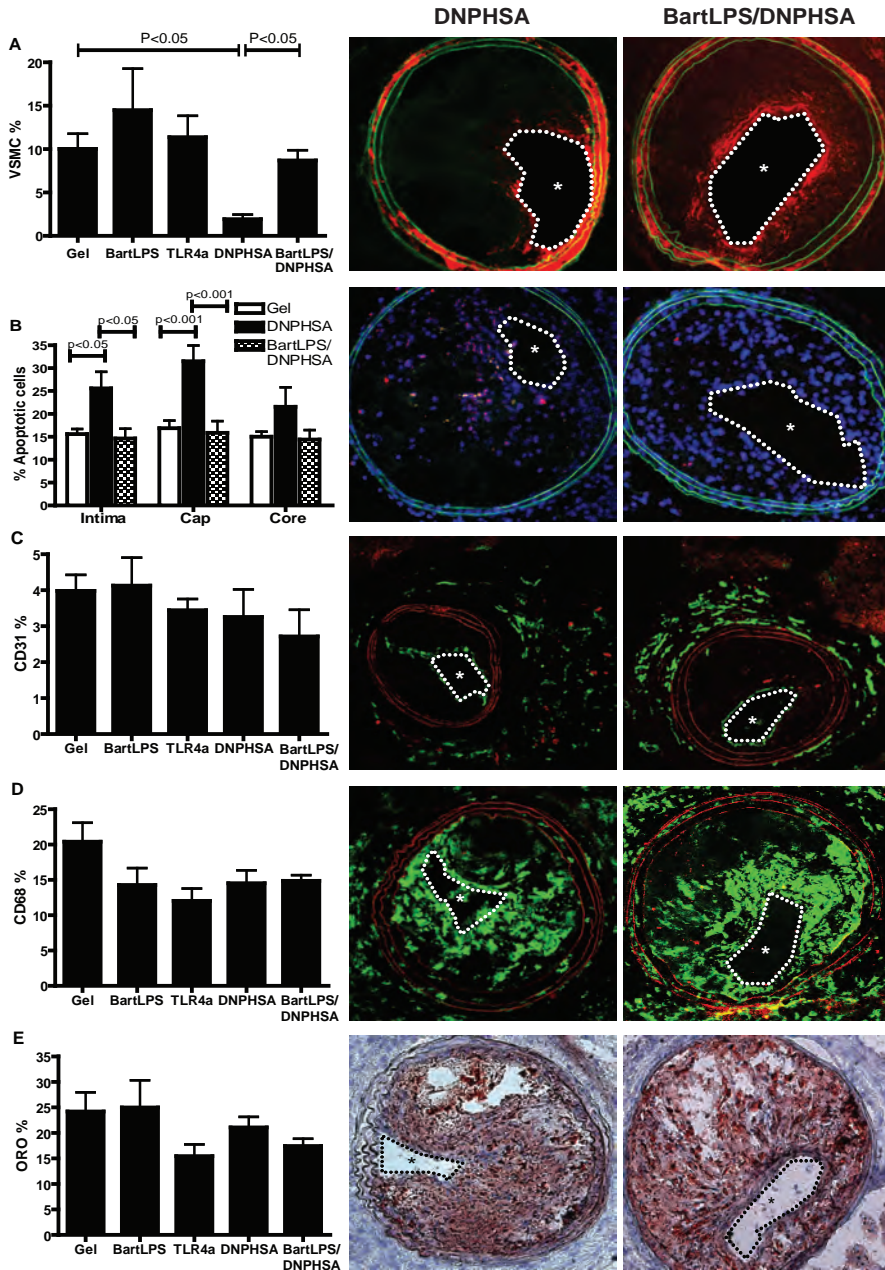


Figure 2

Effect of mast cell activation on plaque phenotype. (A) Adventitial recruitment and activation of mast cells reduced VSMC percentage in the plaque ($P < 0.05$), which was prevented by co-treatment with the TLR4 antagonist *B. quintana* LPS ($P < 0.05$). (B) TUNEL assay showed increased apoptotic cell percentage in DNP-HSA treated mice ($P < 0.05$), which was prevented by co-treatment with *B. quintana* LPS ($P < 0.05$). (E) DNP-HSA treatment was not associated with a change in (C) neovascularization, (D) % macrophages or (E) lipid deposition. * denotes the lumen. Data are presented as mean \pm SEM ($N = 8$ per group).

(figure 1G). Taken together, these data indicate that mast cell recruitment and activation by DNP-HSA does not affect lesion size.

The effect of mast cell recruitment and activation on plaque phenotype was further analyzed by immunohistochemistry. DNP-HSA treatment significantly reduced VSMC content by 87%. Remarkably, co-treatment with *B. quintana* LPS prevented mast cell-associated loss in VSMC content (figure 2A). As shown in figure 2A, VSMCs were mainly lost in the cap region, resulting in weakening of the fibrous cap. Apoptotic cell percentage in atherosclerotic plaques in DNP-HSA treated mice was significantly increased by 63%, as identified by TUNEL assay and mainly located in the cap region (Figure 2B) Co-treatment with *B. quintana* LPS again counteracted this increase in apoptotic cell percentage. Loss of VSMCs was also reflected in cap thickness and necrotic core size, as mast cell activation reduced cap thickness by 25% and increased necrotic core size with 120%, whereas TLR4 inhibition by *B. quintana* LPS normalized cap thickness and necrotic core size (figure 1H and 1I). Further analysis of plaque phenotype showed that mast cell recruitment and activation did not alter neovascularization, macrophage content or lipid deposition (Figure 2C-E). There was also no difference in intraplaque haemorrhaging detected (data not shown). These data indicate that mast cell recruitment and activation through TLR4 activation mediates VSMC apoptosis in the fibrous cap overlying the necrotic core.

Mast cells promote plaque destabilization *in vivo* in a TLR4-dependent manner

We further validated the involvement of TLR4 and mast cells in plaque destabilization with two additional experiments. In the first experiment, we validated the involvement of mast cells in the TLR4-mediated plaque destabilizing effect. The mast cell stabilizer cromolyn was used to test DNP-HSA induced mast cell recruitment and VSMC apoptosis. Cromolyn treatment significantly decreased the total number of peri-adventitial mast cells with 250% compared to PBS treatment (Figure 3A), but not percentage of activated mast cells (Figure 3B). This reduction in adventitial mast cells by cromolyn promoted VSMC numbers in the plaque (Figure 3C,E,F). Furthermore, there was a reduction in the number of apoptotic cells in the cap region as compared to PBS treated animals, while a significant reduction in the core-residing apoptotic cells was also observed (Figure 3D). These data clearly show that the effect of TLR4-mediated on plaque destabilization was indeed mediated by activated mast cells.

In a second control experiment, we used shRNA to target TLR4 and to induce gene silencing in mast cells to validate the importance of TLR4 activation. Lentiviral transfection of the TLR4 shRNA combined with DNP-HSA did not influence the number of peri-adventitial mast cells (Figure 4A) but led to a significant decrease in activated peri-adventitial mast cells (Figure 4B) as compared to sham treated controls, which was coincided with a decline in the number of apoptotic VSMCs in the cap region. A non-significant decrease of apoptotic cells in the core was also observed (Figure 4C-F). Based on these findings, we conclude that mast-cell mediated cap thinning in the advanced atherosclerotic lesion is dependent on TLR4 activation.

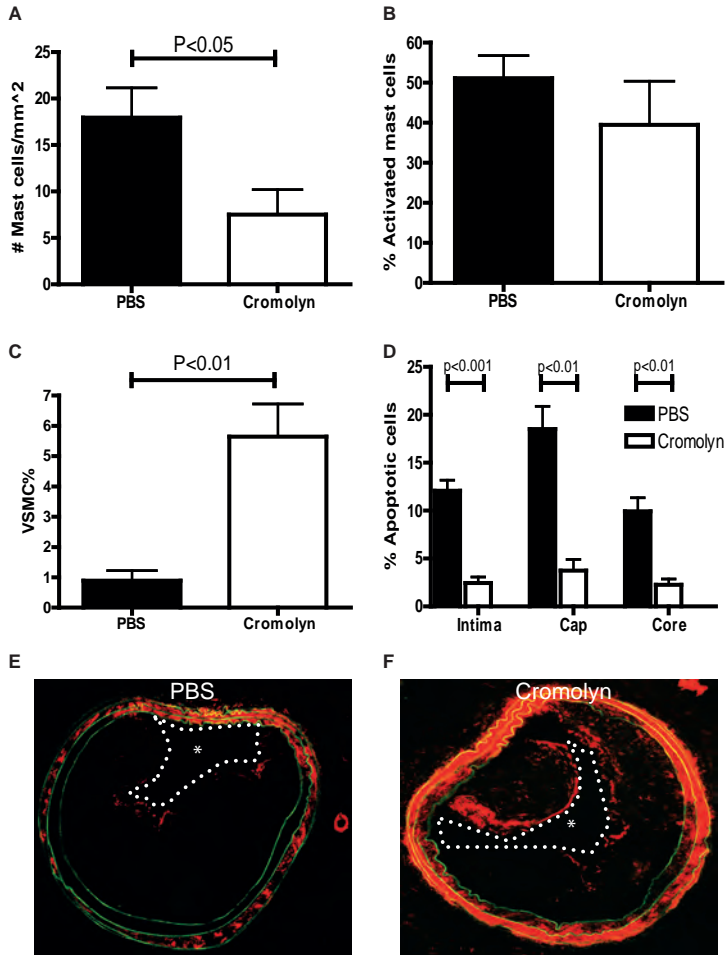


Figure 3

Effect of mast cell stabilizer cromolyn on mast cell recruitment and activation and subsequent VSMC apoptosis by DNP-HSA. Cromolyn treatment significantly decreased mast cell number (A) but not percentage activated (B). (C) This decrease in mast cell number was associated with an increase in VMC numbers. (D) There were less apoptotic cells in the cap region. (E) Representative picture of VSMC staining of DNP-HSA treated mouse. (F) Representative picture of VSMC staining of combined DNP-HSA/cromolyn treated mouse.

Mast cells induce VSMC apoptosis via TLR4 activation and subsequent chymase release *in vitro*

To further assess the role of mast cells in VSMC apoptosis, we co-cultured murine VSMCs with murine mast cells (MC/9 cells) in a 0.4µm trans-well culture dish. Mast cells were activated with 100ng *E. coli* LPS, a TLR4 agonist, with or without the natural TLR4 antagonist *B. quintana* LPS or a TLR4a. Mast cells activated by *E. coli* LPS increased VSMC apoptosis by 53% (figure 5A, B, E), whereas *E. coli* LPS did not have a direct apoptotic effect in a monoculture of VSMCs

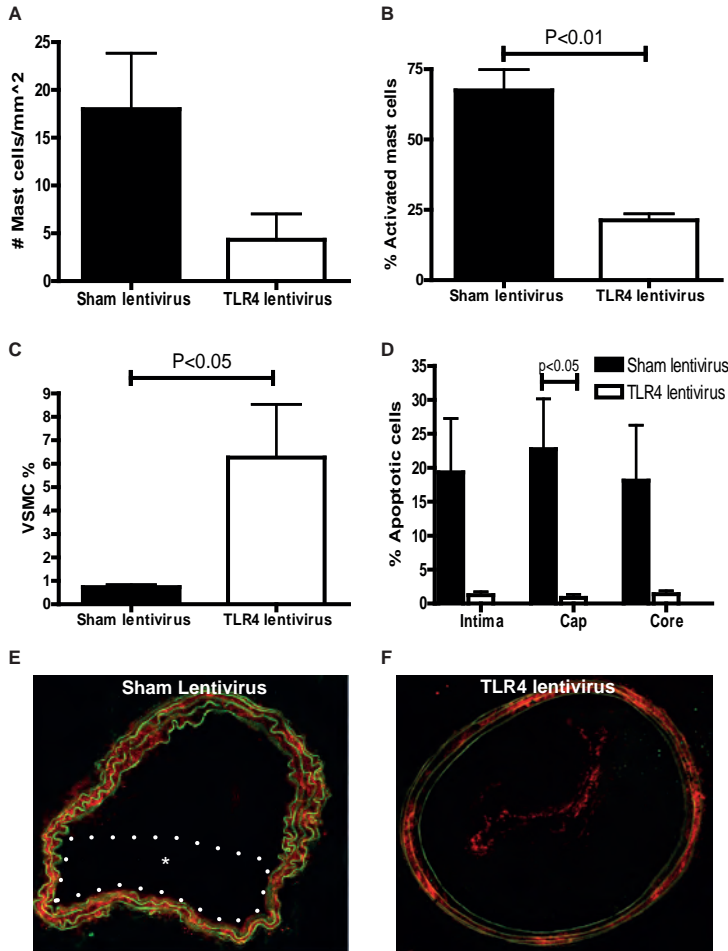


Figure 4

Effect of TLR4 knockdown in MC/9 cells with lentiviral shRNA on DNP-HSA induced mast cell recruitment and activation and subsequent VSMC apoptosis. (A) Knockdown of TLR4 did not influence mast cell number but did decrease percentage of activated mast cells (B). In addition, there were more VSMCs (C) and less apoptotic cells in the cap region (D). (E) Representative picture of VSMC staining of DNP-HSA treated mouse. (F) Representative picture of VSMC staining of combined DNP-HSA/shTLR4 treated mouse.

(figure 5D, E). Induction of VSMC apoptosis by activated mast cells was inhibited by pre-incubation with TLR4a, as well as *B. quintana* LPS (figure 5C, E).

As Bot and coworkers recently pointed out a potential role of chymase in determining plaque stability²⁷ and Leskinen and coworkers and Guo and coworkers showed that chymase may induce VSMC apoptosis *in vitro*¹⁰ and *in vivo*¹⁸ respectively, we co-cultured *E. coli* LPS-activated mast cells with VSMCs in the presence or absence of a chymase inhibitor (Soy Bean Trypsin Inhibitor [SBTI], 100µg/ml). SBTI inhibited VSMC apoptosis, induced by TLR4 activated mast cells (Figure 6A), indicating a role for TLR4 signaling in chymase-induced VSMC apoptosis. The role of

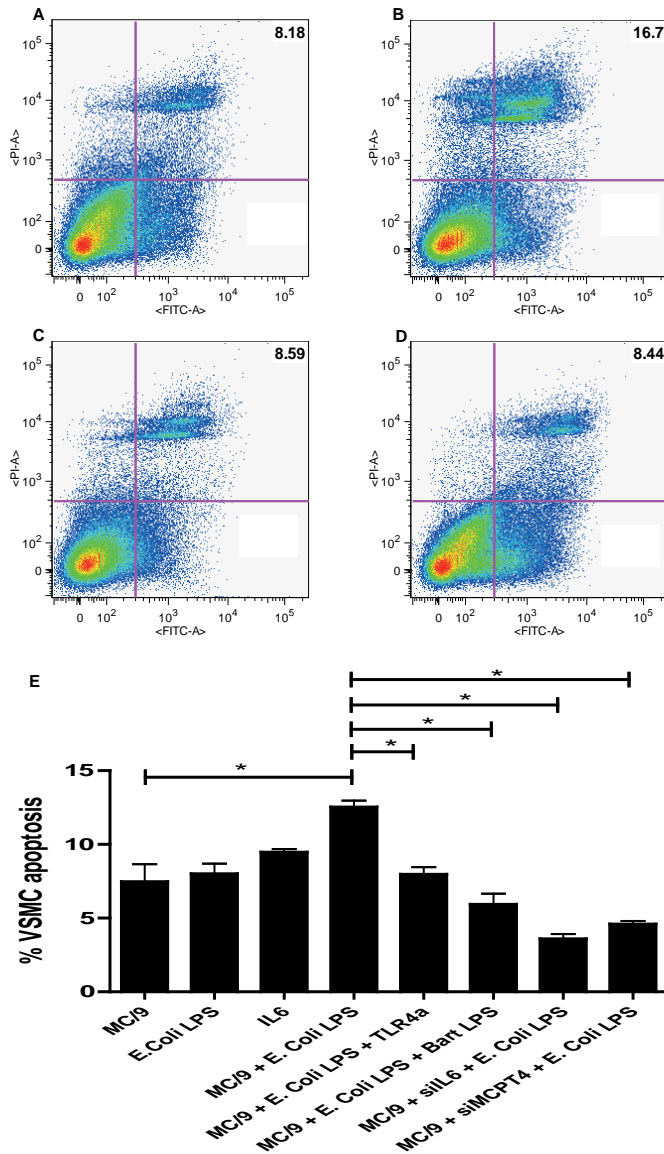


Figure 5

Flow cytometric assessment of Annexin V staining to detect apoptotic VSMCs after 48 hours of co-culture with MC/9 mast cells in different conditions. Vertical axis represents PI staining, and horizontal axis represents Annexin V staining. (A) Representative picture of VSMCs co-cultured with MC/9 cells. (B) Representative picture of VSMCs co-cultured with MC/9 cells activated with *E. Coli* LPS. (C) Representative picture of VSMCs co-cultured with MC/9 cells activated with *E. Coli* LPS after pre-treatment with *B. quintana* LPS. (D) Representative picture of VSMCs co-cultured with MC/9 cells activated with *E. Coli* LPS after pre-treatment with TLR4 antibody. (E) Quantification of FACS data, indicating the late apoptotic (Annexin V+/PI+) VSMC percentage in the different groups. The apoptotic VSMC percentage was significantly increased by *E. coli* LPS stimulation of co-cultured MC/9 ($P < 0.05$). This could be prevented by pre-incubation of MC/9 cells with *B. quintana* LPS ($P < 0.002$) or TLR4a ($P < 0.01$). Furthermore, pretreatment of MC/9 cells with siMCPT-4 or siIL-6 also prevented VSMC apoptosis. Data are presented as mean \pm SEM. Data represent 3 different experiments.

chymase in the TLR4 activation pathway in mast cells was further validated by the use of siRNA mediated silencing of MCPT-4, the murine equivalent of human chymase. VSMC apoptosis by *E. coli* LPS activated mast cells was prevented by pretreatment of mast cells with siMCPT-4 (figure 5E), indicating that chymase plays an important role in this process.

Kirshenbaum and co-workers showed that *E. coli* LPS can increase chymase expression in mature human mast cells via IL-1 β and IL-6 autocrine stimulation²². We therefore hypothesized that TLR4 signaling is involved in chymase-induced VSMC apoptosis via IL-1 β and IL-6 induction and examined cytokine production by mast cells activated with *E. coli* LPS. Stimulation of mast cells with 100ng *E. coli* LPS significantly increased IL-6 cytokine production from not detectable in control condition to 393.5 \pm 46.6 pg/ml (figure 6A), which was abolished by pre-incubation with 10 μ g *B. quintana* LPS or 10 μ g TLR4a (figure 6B). However, mast cells failed to produce IL-1 β upon stimulation with 100ng *E. coli* LPS (data not shown). To further validate the importance of IL-6 in the process of mast cell induced VSMC apoptosis, MC/9

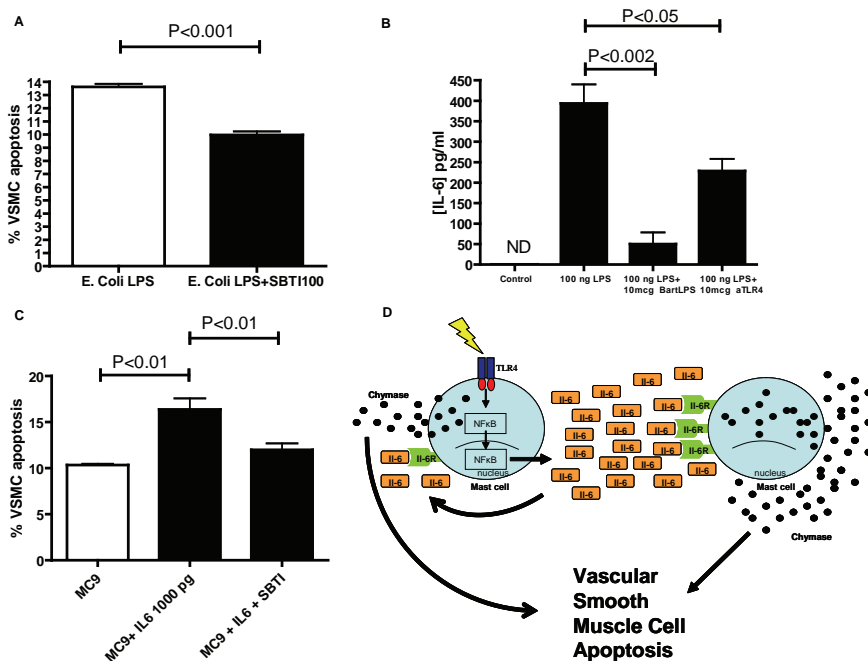


Figure 6

Mast cell-induced VSMC apoptosis via TLR4 signaling. (A) Pre-incubation with chymase inhibitor SBT1 normalized mast cell-mediated VSMC apoptosis ($P < 0.001$). (B) Stimulation of MC/9 cells with 100ng *E. coli* LPS induced IL-6 production ($P < 0.001$), which was inhibited by pre-incubation with both *B. quintana* LPS ($P < 0.001$) and TLR4a ($P < 0.05$). (C) MC/9 cells stimulated with IL-6 significantly increased VSMC apoptosis ($P < 0.01$), whereas pre-incubation with SBT1 inhibited this effect ($P < 0.05$). Data are presented as mean \pm SEM. Data represent 3 different experiments. (D) Suggested mechanism of TLR4 activation on mast cells leading to VSMC apoptosis in atherosclerosis. Activation of TLR4 on mast cells leads to nuclear translocation of NF κ B and consequently transcription of pro-inflammatory cytokines, including IL-6. IL-6 triggers chymase release via autocrine and paracrine stimulation and subsequent VSMC apoptosis.

cells were pre-treated with siIL-6. Silencing of IL-6 significantly diminished VSMC apoptosis induced by *E. coli* activated MC/9 cells (Figure 5E).

Next, we tested whether IL-6 induce VSMC apoptosis by either directly affecting VSMC survival or by autostimulation and activation of mast cells. Monoculture of VSMC with IL-6 stimulation did not affect VSMC death, whereas a similar dose of IL-6 (1000 pg) administered to mast cells in cocultures significantly increased VSMC apoptosis (Figure 6C). We further assessed whether this VSMC apoptosis was due to stimulation of chymase release by IL-6. Chymase inhibition by SBTI was able to block mast cell-mediated VSMC apoptosis in response to IL-6 (Figure 6C). Thus combined, these data clearly indicate that mast cell activation by TLR4 induced VSMC apoptosis by IL-6 regulated chymase production.

DISCUSSION

Our study shows for the first time that TLR4 activation on mast cells is involved in mast cell-induced atherosclerotic plaque destabilization by VSMC apoptosis, *in vivo* and *in vitro*. This apoptosis is dependent on mast cell IL-6 production and subsequent chymase release in an autocrine fashion. To test our hypothesis, we combined a well-established model for mast cell recruitment and activation in murine atherosclerosis with our vulnerable plaque model in ApoE^{-/-} mice^{8,24}. Local recruitment and activation of mast cells specifically induced VSMC apoptosis without affecting other vulnerable plaque parameters, such as lipid and macrophage content or neovascularization. Inhibition of TLR4 signaling, using the natural TLR4 antagonist *B. quintana* LPS²⁵, reduced the number of activated mast cells and was able to prevent mast cell-induced VSMC apoptosis. These results were subsequently validated in two control experiments using (A) shRNA mediated silencing of TLR4, and (B) the mast cell stabilizer cromolyn. This suggests a role for TLR4 in mast cell-induced VSMC apoptosis, and therefore, cap thinning-related destabilization of vulnerable plaque. The lack of effect on the percentage of VSMCs in the vulnerable lesion in the *B. quintana* LPS and TLR4a monotherapy treated-groups, points towards a specific role for TLR4 in mast cell-related vulnerable plaque destabilization. In addition, TLR4 inhibition did not alter intimal accumulation of other cell types, including macrophages and endothelial cells. Mast cells have been suggested to be involved in initiation and progression of atherosclerotic disease, and could potentially influence plaque phenotype by producing a broad variety of bioactive components, including cytokines (e.g. IL-6 and TNF)²⁸, chymase, tryptase and histamine and activating matrix metalloproteinases^{12,17}. In relation to vulnerable plaque, it has been shown that mast cells accumulate predominantly in the shoulder region of the advanced human atherosclerotic lesions, the region most prone to rupture¹⁴. However, studies that describe the role of mast cells in atherosclerosis *in vivo* and clearly demonstrate a causative role for this type of cells in vulnerable plaque are very limited. It was already shown that mast cells could induce VSMC

apoptosis¹⁰ *in vitro*, and that mast cell chymase is responsible for this phenomenon. Since this first observation, different groups have studied the pathway downstream of chymase, leading to VSMC apoptosis. Leskinen and co-workers showed that chymase induces degradation of fibronectin, which causes disruption of focal adhesion interaction with the extracellular matrix, leading to loss of FAK activation and inhibition of the outside-in signaling, which ultimately leads to apoptosis of cells¹⁵. The exact mechanism of mast cell activation and subsequent release of chymase in atherosclerosis is not yet known. Kirshenbaum and co-workers showed, *in vitro*, that *E. coli* LPS up-regulates chymase expression on human mast cells via IL-1 β and IL-6 production, as those cytokines by themselves or in combination were also able to upregulate chymase expression²². Our *in vitro* data clearly indicate that TLR4 activation on mast cells is involved in chymase release and thus VSMC apoptosis. First, we established that the TLR4 is present on MC/9 cells (data not shown, for primers see McCurdy et al.²⁸). Then, we investigated whether we could replicate our *in vivo* data by co-culturing MC/9 cells with VSMCs in the presence of *E. coli* LPS with or without pre-incubation with *B. quintana* LPS or TLR4a. We co-cultured VSMCs and MC/9 cells in a transwell 12 well plate with 0.4 μ m pore size inserts. In this setup there was no mixing of VSMCs and MC/9 cells as the MC/9 cells seeded in the upper insert chamber remained separated from the VSMCs in the bottom chamber. However, bio-active compounds, e.g. chymase, released by mast cells upon stimulation can diffuse to the lower chamber and exert their biological activity on the VSMCs. Conform the findings in our vulnerable plaque model, co-culture of *E. coli* LPS-activated MC/9 cells with VSMCs increased VSMC apoptosis and this could indeed be prevented by pre-incubation with two different TLR4 inhibitors, *B. quintana* LPS and TLR4a. This indicated that mast cells induced apoptosis of VSMCs by release of a paracrine factor. Pre-incubation of mast cells with the chymase inhibitor SBTI reduced VSMC apoptosis significantly, suggesting that indeed chymase is involved in mast cell induced VSMC apoptosis. Likewise, pretreatment of MC/9 cells with siMCPT-4 also prevented VSMC apoptosis.

Based on the study of Kirshenbaum²² and the fact that TLR4 activation leads to nuclear translocation of NF κ B and subsequently transcription of pro-inflammatory cytokines, including IL-6²⁰, we suggested that IL-6 can auto-stimulate the mast cell to release chymase. TLR4 activation on MC/9 mast cells indeed led to IL-6 production and this was blocked by *B. quintana* LPS and in lesser extent by TLR4a. Furthermore, knockdown of IL-6 in MC/9 cells led to less VSMC apoptosis. We also could demonstrate that TLR4 activation on mast cells could lead to VSMC apoptosis via IL-6 induced chymase release. Together, these data clearly indicate that mast cell-induced apoptosis of VSMCs is controlled by TLR4 signaling, via autocrine IL-6/chymase release mechanism and points towards a plaque destabilizing role of mast cells by chymase release. In line with our findings, Bot and coworkers have recently demonstrated that chymase inhibition by RO5066852 could indeed help to stabilize advanced atherosclerotic lesions²⁷. Our findings further strengthen the notion that mast cells play an important role in determining plaque stability via different pathways.

A limitation of the study is that we used an artificial model to create a vulnerable plaque in the mouse. We are aware that the brachiocephalic artery can be used as a natural model to study the vulnerable plaque. However, this site is not accessible for perivascular intervention.

In conclusion, we demonstrate that TLR4 signaling is important for mast cell-induced VSMC apoptosis. TLR4 activation leads to IL-6 production, which in turn auto-stimulates the mast cell to release chymase. Finally, chymase induces VSMC apoptosis, thus destabilizing the atherosclerotic plaque by thinning of the fibrous cap (figure 6D).

REFERENCES

1. Hansson GK. Inflammation, atherosclerosis, and coronary artery disease. *N Engl J Med*. 2005;352:1685-1695.
2. Libby P. Inflammation in atherosclerosis. *Nature*. 2002;420:868-874.
3. Ross R. Atherosclerosis—an inflammatory disease. *N Engl J Med*. 1999;340:115-126.
4. Virmani R, Burke AP, Farb A, Kolodgie FD. Pathology of the vulnerable plaque. *J Am Coll Cardiol*. 2006;47:C13-18.
5. Davies MJ, Thomas AC. Plaque fissuring—the cause of acute myocardial infarction, sudden ischaemic death, and crescendo angina. *Br Heart J*. 1985;53:363-373.
6. Lindstedt KA, Kovanen PT. Mast cells in vulnerable coronary plaques: potential mechanisms linking mast cell activation to plaque erosion and rupture. *Curr Opin Lipidol*. 2004;15:567-573.
7. Lindstedt KA, Mayranpaa MI, Kovanen PT. Mast cells in vulnerable atherosclerotic plaques—a view to a kill. *J Cell Mol Med*. 2007;11:739-758.
8. Bot I, de Jager SC, Zerneck A, Lindstedt KA, van Berkel TJ, Weber C, Biessen EA. Perivascular mast cells promote atherogenesis and induce plaque destabilization in apolipoprotein E-deficient mice. *Circulation*. 2007;115:2516-2525.
9. Sun J, Sukhova GK, Wolters PJ, Yang M, Kitamoto S, Libby P, MacFarlane LA, Mallen-St Clair J, Shi GP. Mast cells promote atherosclerosis by releasing proinflammatory cytokines. *Nat Med*. 2007;13:719-724.
10. Leskinen M, Wang Y, Leszczynski D, Lindstedt KA, Kovanen PT. Mast cell chymase induces apoptosis of vascular smooth muscle cells. *Arterioscler Thromb Vasc Biol*. 2001;21:516-522.
11. Gruber BL, Marchese MJ, Suzuki K, Schwartz LB, Okada Y, Nagase H, Ramamurthy NS. Synovial procollagenase activation by human mast cell tryptase dependence upon matrix metalloproteinase 3 activation. *J Clin Invest*. 1989;84:1657-1662.
12. Johnson JL, Jackson CL, Angelini GD, George SJ. Activation of matrix-degrading metalloproteinases by mast cell proteases in atherosclerotic plaques. *Arterioscler Thromb Vasc Biol*. 1998;18:1707-1715.
13. Saarinen J, Kalkkinen N, Welgus HG, Kovanen PT. Activation of human interstitial procollagenase through direct cleavage of the Leu83-Thr84 bond by mast cell chymase. *J Biol Chem*. 1994;269:18134-18140.
14. Kaartinen M, Penttila A, Kovanen PT. Accumulation of activated mast cells in the shoulder region of human coronary atheroma, the predilection site of atheromatous rupture. *Circulation*. 1994;90:1669-1678.
15. Leskinen MJ, Lindstedt KA, Wang Y, Kovanen PT. Mast cell chymase induces smooth muscle cell apoptosis by a mechanism involving fibronectin degradation and disruption of focal adhesions. *Arterioscler Thromb Vasc Biol*. 2003;23:238-243.
16. Leskinen MJ, Heikkila HM, Speer MY, Hakala JK, Laine M, Kovanen PT, Lindstedt KA. Mast cell chymase induces smooth muscle cell apoptosis by disrupting NF-kappaB-mediated survival signaling. *Exp Cell Res*. 2006;312:1289-1298.

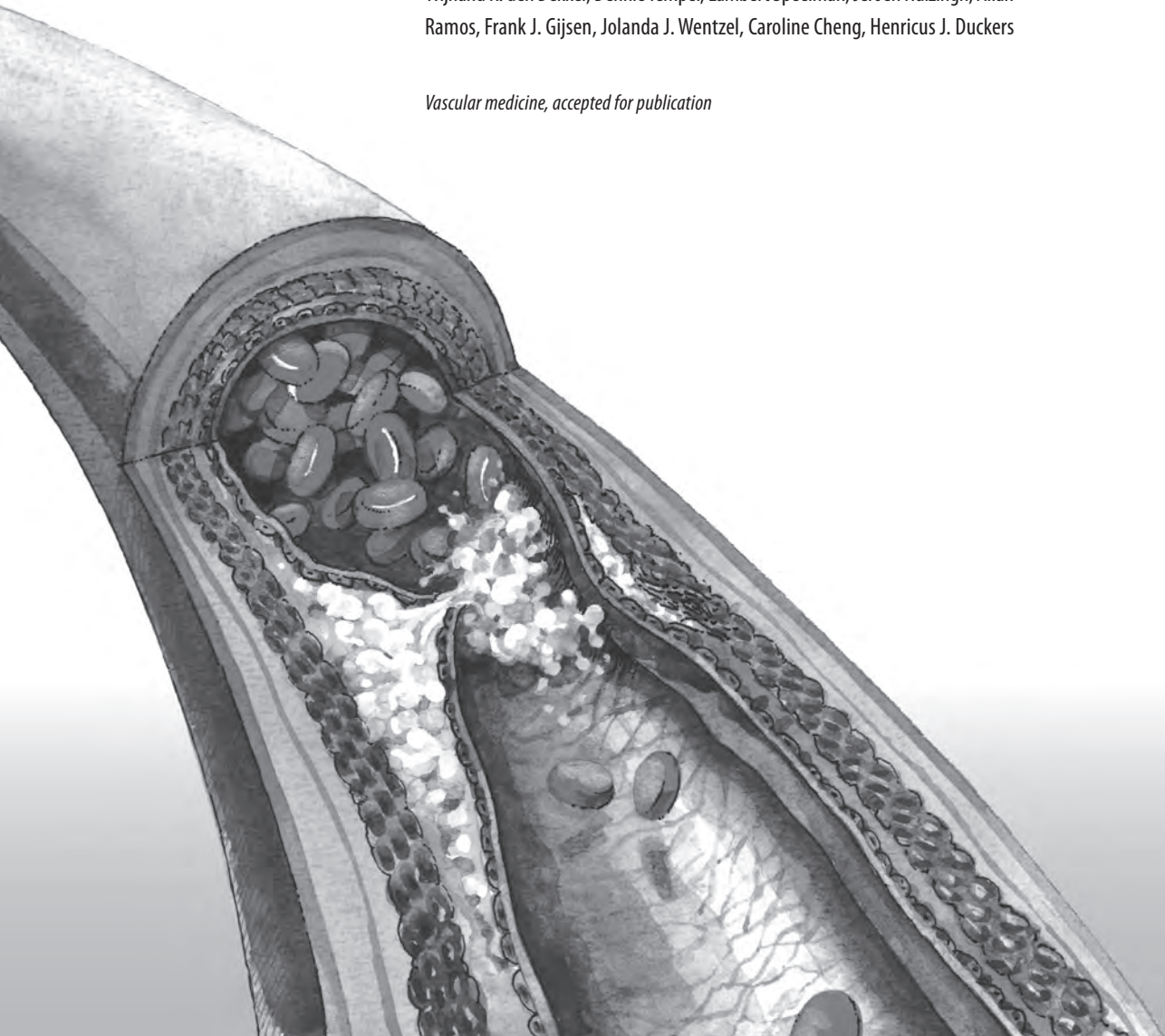
17. Kovanen PT. Mast cells and degradation of pericellular and extracellular matrices: potential contributions to erosion, rupture and intraplaque haemorrhage of atherosclerotic plaques. *Biochem Soc Trans.* 2007;35:857-861.
18. Guo T, Chen WQ, Zhang C, Zhao YX, Zhang Y. Chymase activity is closely related with plaque vulnerability in a hamster model of atherosclerosis. *Atherosclerosis.* 2009;207:59-67.
19. Poltorak A, He X, Smirnova I, Liu MY, Van Huffel C, Du X, Birdwell D, Alejos E, Silva M, Galanos C, Freudenberg M, Ricciardi-Castagnoli P, Layton B, Beutler B. Defective LPS signaling in C3H/HeJ and C57BL/10ScCr mice: mutations in Tlr4 gene. *Science.* 1998;282:2085-2088.
20. Palsson-McDermott EM, O'Neill LA. Signal transduction by the lipopolysaccharide receptor, Toll-like receptor-4. *Immunology.* 2004;113:153-162.
21. Avila M, Gonzalez-Espinosa C. Signaling through Toll-like receptor 4 and mast cell-dependent innate immunity responses. *IUBMB Life*;63:922-929.
22. Kirshenbaum AS, Swindle E, Kulka M, Wu Y, Metcalfe DD. Effect of lipopolysaccharide (LPS) and peptidoglycan (PGN) on human mast cell numbers, cytokine production, and protease composition. *BMC Immunol.* 2008;9:45.
23. Cheng C, van Haperen R, de Waard M, van Damme LC, Tempel D, Hanemaaijer L, van Cappellen GW, Bos J, Slager CJ, Duncker DJ, van der Steen AF, de Crom R, Krams R. Shear stress affects the intracellular distribution of eNOS: direct demonstration by a novel in vivo technique. *Blood.* 2005;106:3691-3698.
24. Cheng C, Tempel D, van Haperen R, van der Baan A, Grosveld F, Daemen MJ, Krams R, de Crom R. Atherosclerotic lesion size and vulnerability are determined by patterns of fluid shear stress. *Circulation.* 2006;113:2744-2753.
25. Popa C, Abdollahi-Roodsaz S, Joosten LA, Takahashi N, Sprong T, Matera G, Liberto MC, Foca A, van Deuren M, Kullberg BJ, van den Berg WB, van der Meer JW, Netea MG. Bartonella quintana lipopolysaccharide is a natural antagonist of Toll-like receptor 4. *Infect Immun.* 2007;75:4831-4837.
26. Ray JL, Leach R, Herbert JM, Benson M. Isolation of vascular smooth muscle cells from a single murine aorta. *Methods Cell Sci.* 2001;23:185-188.
27. Bot I, Bot M, van Heiningen SH, van Santbrink PJ, Lankhuizen IM, Hartman P, Gruener S, Hilpert H, van Berkel TJ, Fingerle J, Biessen EA. Mast Cell Chymase Inhibition Reduces Atherosclerotic Plaque Progression and Improves Plaque Stability in ApoE^{-/-} Mice. *Cardiovasc Res.*
28. McCurdy JD, Lin TJ, Marshall JS. Toll-like receptor 4-mediated activation of murine mast cells. *J Leukoc Biol.* 2001;70:977-984.

Chapter 4

Effect of shear stress alteration on atherosclerotic plaque vulnerability in cholesterol-fed rabbits

Wijnand K. den Dekker, Dennie Tempel, Lambert Speelman, Jeroen Huizingh, Allan Ramos, Frank J. Gijsen, Jolanda J. Wentzel, Caroline Cheng, Henricus J. Duckers

Vascular medicine, accepted for publication



ABSTRACT

Background: Previously, we have created an experimental murine model for induction of vulnerable plaque (VP). Although this murine model offers the opportunity to study the different molecular biological pathways that regulate plaque destabilization, the size of the animals severely limits the use of the model for in vivo diagnostics and percutaneous interventions. This study aimed to create a VP model in the rabbit, based on the murine model, to aid the assessment and development of novel diagnostic and interventional tools.

Methods and results: New Zealand white rabbits were fed on a 2% cholesterol diet. After one week, a shear stress altering device was implanted around the right carotid artery. Twelve weeks after cast placement the carotid artery was isolated and processed for (immuno-)histological analysis to evaluate the presence of a VP phenotype. Atherosclerotic plaques with high lipid and macrophage content, low vascular smooth muscle cell content and intimal neovascularization were located upstream and downstream of the cast. The plaques lacked a significant necrotic core.

Conclusion: We were able to create atherosclerotic plaques with a phenotype beyond that of a fatty streak, with a high percentage of lipids and macrophages, a thick cap with some vascular smooth muscle cells and neovascularization. However, as there was only a small necrotic core, the overall phenotype seems less vulnerable as compared to the thin fibrous cap atheroma in patients.

INTRODUCTION

Wall shear stress is a hemodynamic force that plays an important role in the induction and preservation of endothelial cell homeostasis during vascular development and in the mature vascular system. In straight arterial segments where unidirectional laminar flow prevails, average shear stress levels are actively maintained to trigger an athero-protective expression profile in endothelial cells. In contrast, initial areas of atherosclerosis development correlate strongly with specific sites in the vascular structure where the endothelium is constantly exposed to relatively low and oscillatory shear stress¹⁻⁴. Previously, we have shown in an *in vivo* study that lowering shear stress by placement of a tapered perivascular cast around the common carotid artery of an apolipoprotein E-deficient (ApoE^{-/-}) mouse promotes atherosclerotic plaque development in the upstream and downstream vessel segment⁵. Upstream, these lesions showed characteristics of a human vulnerable plaque, the culprit atherosclerotic lesions that are associated with rupture in patients and are defined by a distinct morphology, which include the presence of a thin fibrous cap, large necrotic core and high inflammatory state. In contrast, in the downstream vessel region where oscillatory shear stress was induced, atherosclerotic lesions with a more stable phenotype were formed with a thick fibrous cap, neglectable necrotic core, and low infiltration of inflammatory cells. This murine cast model offered the ideal setting to study different molecular biological pathways that regulate plaque formation and destabilization, as the effect of interventions on the two specific types of plaques could be compared within one single carotid artery. Subsequent studies indeed provided important insights in the pathogenesis of the disease⁶⁻⁹. However, the small size of the animals severely limits the use of this model for *in vivo* diagnostics and percutaneous interventions. Currently, rabbits are widely used to study atherosclerosis, as they are sensitive to a high cholesterol diet, leading up to accumulation of high levels of total plasma cholesterol and subsequent development of atherosclerotic lesions^{10,11}. Furthermore, it has been shown that rabbits can be used for *in vivo* intravascular evaluation of atherosclerotic plaques, for example by IVUS or optical coherence tomography¹². However, the type of atherosclerotic lesions that these rabbits develop are usually early fatty-streak-like plaques, containing high levels of macrophage-derived foam cells, but with no clear definition of a fibrous cap or necrotic core, thus not resembling the complex vulnerable lesions found in humans¹³. This makes it very difficult to extrapolate the findings obtained in rabbits to the human condition. Low shear stress could provide the crucial pro atherogenic trigger to initiate and promote the growth of an advanced lesion in the rabbit animal model, which in morphology and complexity would better represent advanced human lesions.

Here we aim to induce complex atherosclerotic lesion development in the New Zealand white rabbit by local shear stress reduction using our cast device in combination with a high cholesterol diet. This advanced plaque model in rabbits could provide a useful platform for preclinical validation of new intravascular diagnostic applications and interventional therapies for vulnerable plaque.

MATERIAL AND METHODS

Animal operations

All animal experiments were performed according to institutional and national regulations and approved by the Institutional Review Board on Animal Experiments of the Erasmus University Medical Center. We used sixteen male New Zealand white rabbits (3-3.5 kg, Charles River, United Kingdom), divided into two groups of eight rabbits. In the first group, the effect of shear stress alteration on atherosclerotic plaque development was evaluated, while in the second group the effect of combined shear stress alteration and endothelial damage on atherosclerotic plaque development was studied. After arrival, the rabbits were individually housed and fed a normal chow diet (Arie Blok, the Netherlands) ad libitum with free access to water. After two weeks of acclimatization, rabbits were fed a Western diet, containing 2% (w,w) cholesterol (Arie Blok, the Netherlands). Two weeks after the start of Western diet, a flow altering cast (see figure 1) was surgically implanted around the right common carotid artery. Before surgery, animals were anaesthetized with an intramuscular injection of ketamine hydrochloride (25 mg/kg, 100 mg/ml) and a subcutaneous injection of domitor (0.5 mg/kg, 1 mg/ml). The right common carotid artery was exposed and both halves of the cast were placed around the vessel and fixed with two sutures. In the second group, we inflicted endothelial damage by external manipulation and stretching of the carotid artery before cast placement. The wound was closed and the rabbits were allowed to recover. Rabbits were given 10 ml Ringers Lactate, 10 ml 10% Glucose solution and Temgesic® (0.05 mg/kg) subcu-

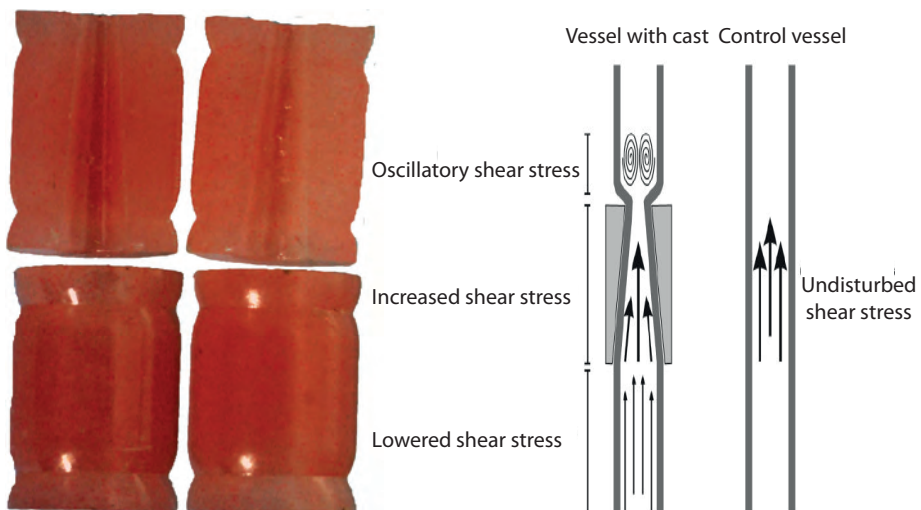


Figure 1
Example of cast and its schematic influence on shear stress

taneously, for postoperative rehydration and analgetic. Twelve weeks after cast placement, rabbits were euthanized using an overdose of pentobarbital and the right common carotid artery was flushed and taken out, snap-frozen in liquid nitrogen and stored in -80 °C until further analysis.

Shear stress altering cast device

To induce standardized alterations in shear stress, we up-scaled the existing murine cast to fit the rabbit carotid artery. Casts with different inner diameters were used, based on the initial diameter of the carotid artery as measured with ultrasound. The upstream inner diameter is 2.5, 2, or 1.5 mm (non-constrictive) and gradually declines to 1.25, 1, and 0.75 mm at the downstream side of the cast (constrictive), respectively, creating a fifty percent tapering. It has been shown that this tapering induces alterations in shear stress in the mouse with a region of low shear stress upstream of the cast, high shear stress in the cast and oscillatory shear stress downstream of the cast ⁵.

Doppler measurement

In order to validate that the rabbit cast could induce shear stress alterations, pulsed-wave Doppler velocities and M-mode luminal diameter were measured in naive carotid arteries and after cast placement in sixteen different New Zealand white rabbits. The ultrasound measurements were performed with the Vevo2100 system (Visualsonics Inc., Toronto, Canada), using a 40-Mhz center frequency linear interfaced array transducer (MS550D). Briefly, the carotid artery was dissected and the pulsed-wave Doppler assessment was measured at an angle of max 65°. Luminal diameter was measured using M-mode (see Figure 1B). After cast placement, Doppler velocity measurements and M-mode were repeated upstream and downstream of the cast to determine whether cast placement induced shear stress alterations upstream and/or downstream of the cast. Flow through the artery was estimated using a Poiseuille profile and computed as:

$$Q = \frac{\pi R^2}{2} \overline{V_{\max}}$$

with Q the flow, R the time-average vessel diameter and $\overline{V_{\max}}$ the time-average peak velocity, measured in the center of the lumen. Consequently, shear stress was calculated as:

$$\tau = \frac{2\eta}{R} \overline{V_{\max}}$$

with τ the wall shear stress and η the blood viscosity, set as 3.10^{-3} Pa.s. Both Q and τ are determined prior to cast placement and proximal to the cast after cast placement.

Cholesterol measurement

Blood samples were collected from the middle ear artery at baseline, cast placement and at sacrifice. Serum samples were stored at -80 °C until further use. Total cholesterol, LDL, VLDL and HDL were measured using Cobas® determination kits and measured using a Roche/Hitachi analyzer (Roche diagnostics, Indianapolis, USA).

Histology and immunohistochemistry

The carotid artery region was serially sectioned in 6 µm cryosections. Histological and immunohistochemical analysis was performed on 72 µm intervals, covering the whole region upstream and downstream of the cast. In addition to routine haematoxylin-eosin (HE) staining, different immunohistochemical stainings were performed to evaluate plaque stability. Sections were stained for vascular smooth muscle cells (VSMCs, anti- α -actin, DAKO, the Netherlands), macrophages (anti-RAM11 antibody, DAKO), endothelial cells (anti-PECAM1 antibody, DAKO, the Netherlands) followed by a biotinylated secondary antibody. We used 3, 3'-diamino-benzidine as enzyme substrate for horse radish peroxidase and the signal was visualized using bright field microscopy. Lipid deposition was analyzed using Oil-Red-O staining (Sigma, Zwijndrecht, the Netherlands) and visualized by bright field microscopy.

Quantification and statistical analysis

Data analysis was performed using an automated commercial image analysis system (Impak C, Clemex technologies, Canada) to evaluate differences in plaque phenotype upstream and downstream of the cast and between the two groups. HE staining was used to measure intima/media ratio and percentage of luminal stenosis, α -actin staining to evaluate VSMC content, CD31 staining to evaluate neovascularization and RAM11 staining to evaluate macrophage content. Multiple groups were compared with one-way ANOVA and a subsequent Student-Newman-Keuls multiple comparisons test. Two-tailed Students' *t*-tests were used to compare individual groups. Data are presented as mean \pm SD. P-values less than 0.05 were considered significantly different.

RESULTS

Low shear stress and shear stress oscillations both induce plaque formation in cholesterol-fed New Zealand white rabbits.

We first investigated the effect of Western diet on the plasma lipid profile of the rabbits. The results are summarized in table 1. After two weeks of Western diet, total plasma cholesterol, LDL-cholesterol and VLDL cholesterol levels showed a significant increase that was maintained until the time point of sacrifice at twelve weeks. There was also a significant increase in HDL-cholesterol after two and twelve weeks of Western diet.

Doppler velocity measurements of the blood flow assessed the effect of the perivascular cast on shear stress in the straight rabbit carotid artery. Before cast-placement, the time-averaged peak blood velocity was 527 ± 215 mm/s. Doppler velocity measurements close to the vessel wall showed a symmetric profile, while the center velocity was 30-40% higher than at the vessel wall.

Table 1. Rabbit lipid profile

Group	Cast (n=8)	Cast plus endothelial damage (n=8)
Total cholesterol (mmol/L)		
Week 0	0.9 ± 0.1	1.0 ± 0.1
Week 2	20.4 ± 2.5 ^a	16.3 ± 3.9 ^b
Week 12	32.2 ± 2.5 ^a	40.6 ± 5.7 ^b
HDL cholesterol (mmol/L)		
Week 0	0.5 ± 0.1	0.4 ± 0.1
Week 2	1.7 ± 0.3 ^c	1.7 ± 0.1 ^a
Week 12	2.4 ± 0.3 ^c	4.1 ± 0.8 ^c
LDL cholesterol (mmol/L)		
Week 0	0.3 ± 0.1	0.3 ± 0.1
Week 2	16.4 ± 1.7 ^a	11.5 ± 2.4 ^b
Week 12	23.1 ± 2.0 ^a	32.2 ± 5.6 ^b
VLDL cholesterol (mmol/L)		
Week 0	0.2 ± 0.0	0.2 ± 0.0
Week 2	0.4 ± 0.1 ^c	0.3 ± 0.0
Week 12	0.4 ± 0.1 ^c	1.0 ± 0.3

^a $P < 0.0001$ as compared with baseline

^b $P < 0.005$ as compared with baseline

^c $P < 0.05$ as compared with baseline

As the velocity at the wall cannot be accurately measured, a parabolic profile is assumed for flow computation. The average (\pm SD) flow before cast placement was 29.4 ± 9.0 ml/min and the shear stress at the wall 4.3 ± 2.3 Pa. After cast placement, the downstream segment registered flow-reversal near the vessel wall consistent with the occurrence of oscillatory shear stress (figure 2). Upstream of the cast, the time-average peak blood velocity at the center was significantly reduced to 320 ± 176 mm/s ($p=0.02$). The flow reduced to 19.7 ± 13.7 ml/min ($p=0.02$) and the shear stress reduced to 2.4 ± 1.2 Pa ($p=0.03$). The lumen radius before cast placement and proximal to the cast after cast placement remained unchanged (0.8 ± 0.1 mm for both cases). Combined, these data indicate that shear stress levels in the upstream region from the cast were significantly reduced, while oscillatory shear stress was successfully induced in the downstream region.

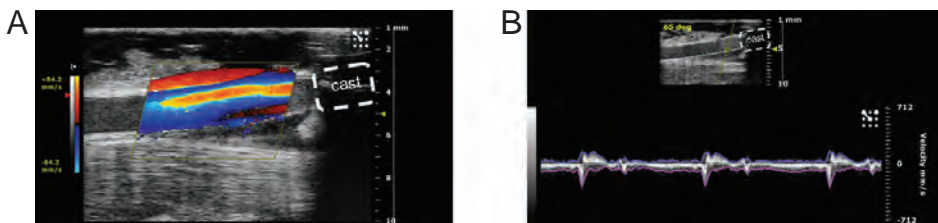


Figure 2

Doppler measurements of the rabbit carotid artery

A. Color flow in the carotid artery after cast placement, downstream of the cast. B. Pulse wave velocity measurement downstream of the cast, near the vessel wall, showing flow reversal.

To examine the effect of cast placement on atherosclerotic lesion size in hypercholesterolemic rabbits, we sacrificed the animals after they had been exposed to shear stress alteration for 12 weeks. The upstream and downstream carotid regions with low and oscillatory shear stress were assessed by histological evaluation for atherosclerotic lesion growth. Low and oscillatory shear stress both triggered atherogenesis in the upstream and downstream vessel regions in 50% (4/8) of the rabbits. In 12.5% (1/8) of the rabbits, atherosclerotic plaque developed only upstream of the cast, while in 25% (2/8) of the rabbits no significant lesions were detected (results summarized in table 2). These results were independent of cholesterol levels. Figure 3 shows the intima/media ratio upstream and downstream and representative pictures of HE staining. The lesion size between the upstream and downstream regions was not significantly different (0.25 ± 0.09 and 0.24 ± 0.11 respectively, $p>0.05$).

Table 2. Effect of cast placement on atherosclerotic plaque development

Group	Plaque upstream	Plaque downstream	Plaque upstream + downstream	No atherosclerotic plaque
Cast	12.5% (1/8)	12.5% (1/8)	50% (4/8)	25% (2/8)
Cast plus endothelial damage	12.5% (1/8)	12.5% (1/8)	75% (6/8)	0% (0/8)

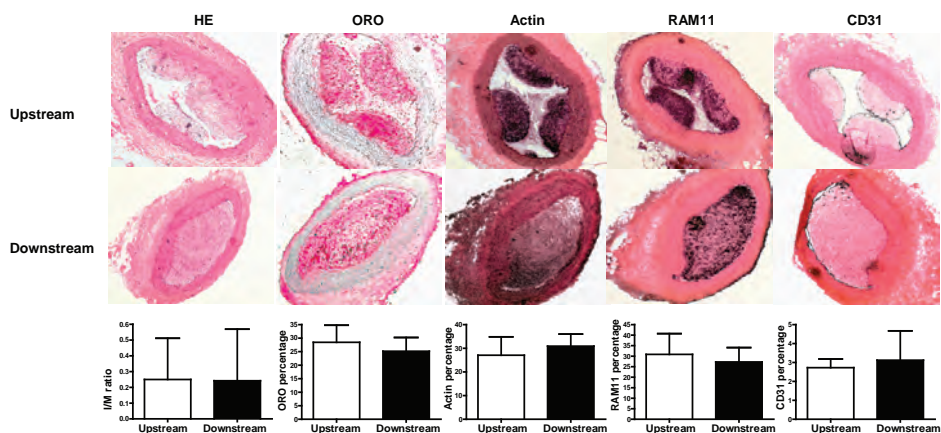


Figure 3

Analysis of plaque phenotype upstream and downstream of the cast in the cast only group.

Representative pictures of Haematoxylin/Eosin staining (HE), lipid staining (ORO), vascular smooth muscle cell (Actin), macrophages (CD68) and endothelial cells (CD31) upstream and downstream of the cast. Quantification of the different stainings revealed no significant difference between upstream and downstream of the cast. Graphs show mean per group \pm SD, n=8 per group.

Shear stress alteration promotes atherogenic growth beyond the fatty streak phenotype.

After initial assessment of lesion size, we performed immunohistochemical analysis of the plaques for lipid, VSMC, macrophage and endothelial cell content in order to analyze plaque phenotype. No clear difference in lesion phenotype was observed between the plaques found in the low or the oscillatory shear stress region. As shown in figure 2, both upstream and downstream atherosclerotic plaques contained abundantly foam cells as we observed a high percentage of lipids ($23.0 \pm 10.0\%$ vs. $25.2 \pm 5.1\%$) and high macrophage content ($30.8 \pm 9.9\%$ vs. $27.3 \pm 11.2\%$). This was accompanied by the accumulation of VSMCs ($27.1 \pm 7.7\%$ vs. $30.9 \pm 5.1\%$) and CD31 positive endothelial cells ($2.2 \pm 0.8\%$ vs. $3.1 \pm 1.0\%$) in the plaque, suggesting the presence of a fibrous cap and intimal neovascularization. However no necrotic core could be detected and intraplaque hemorrhaging was absent in the lesions.

The combination of low shear stress and endothelial damage significantly increases the size of atherosclerotic plaque in the upstream region.

Although shear stress alteration alone was capable to induce atherosclerotic lesions beyond the fatty streak state as indicated by the presence of intimal VSMCs in the fibrous cap, these lesions still lacked a distinct necrotic core and showed a relative thick fibrous cap. We aimed to further increase lesion vulnerability by combining shear stress alteration with mechanical endothelial damage. Combined treatment increased the number of rabbits that developed atherosclerotic plaque both upstream and downstream of the cast to 75% (6/8). In the

remaining two rabbits we found atherosclerotic plaque either upstream or downstream of the cast (the data are summarized in table 2). Quantification of lesion size by intima/media measurement showed that there was a significant increase in the low shear stress, upstream region of the cast, as compared to the group that only received cast placement without endothelial damage (from 0.25 ± 0.09 to 0.66 ± 0.12 , $p < 0.05$; see figure 4). Endothelial damage did not significantly affect the intima/media ratio in the downstream region (0.24 ± 0.11 vs. 0.45 ± 0.10 , combined versus single treatment respectively, $p > 0.05$; see figure 4). Within the group that received combined endothelial damage and cast placement there was a trend towards a difference in lesion size in the upstream and downstream vascular segment (0.66 ± 0.12 vs. 0.45 ± 0.10 , $p = 0.07$; see figure 4). These findings were confirmed when we measured lesion size by percentage of luminal stenosis (see figure 4).

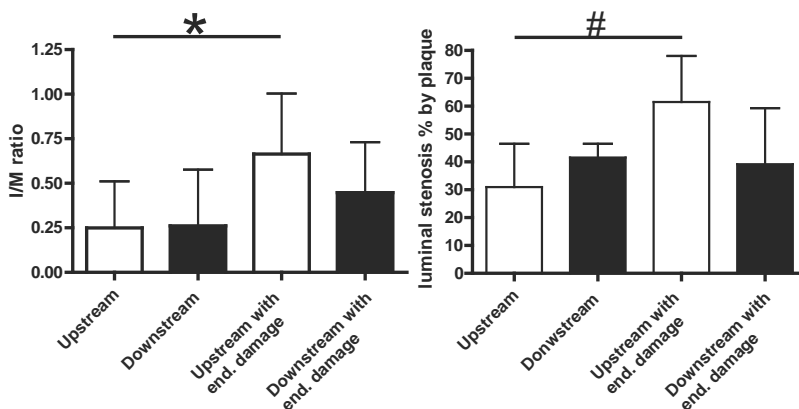


Figure 4

Analysis of plaque size by I/M ratio and percentage of luminal stenosis

*Combination of cast placement and endothelial damage significantly increases plaque size upstream of the cast, as measured by I/M ratio and percentage of luminal stenosis. Graphs show mean per group \pm SD, $n=8$ per group. * $p < 0.05$, 0.66 ± 0.12 vs. 0.25 ± 0.09 # $p < 0.05$, 61.5 ± 16.6 vs. 30.9 ± 15.6*

Combined treatment of shear stress alteration and endothelial damage increases plaque vulnerability.

We compared lipid, macrophage, endothelial cell and VSMC content between the cast placement with endothelial damage and the cast placement without endothelial damage group to see whether endothelial damage increased plaque vulnerability (see figure 5). There was a significant decrease in VSMCs upstream of the cast as demonstrated by VSMC-actin staining (from $27.1 \pm 7.7\%$ to $15.6 \pm 4.8\%$, cast versus cast with endothelial damage respectively, $p < 0.05$). Downstream of the cast there was also a decrease in VSMC content, but this reached no statistical significance (from $30.9 \pm 5.1\%$ to $21.1 \pm 7.0\%$, cast versus cast with endothelial damage respectively, $p > 0.05$).

These data indicate that endothelial damage aggravated plaque vulnerability by a decrease in plaque stabilizing VSMCs. In addition, we demonstrated the presence of CD31 positive endothelial cells in the intimal area, pointing towards neovascularization in the plaque (see figure 5).

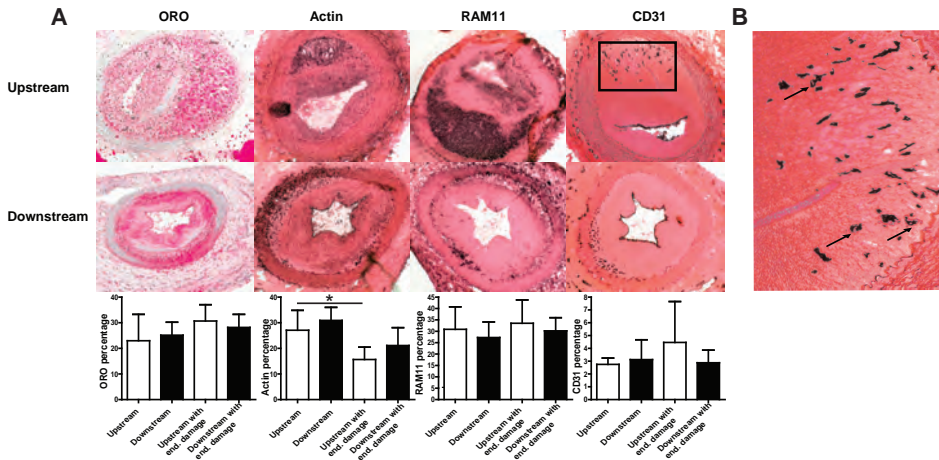


Figure 5

Analysis of plaque phenotype upstream and downstream of the cast in the combined cast and endothelial damage group.

*A. Representative pictures of lipid staining (ORO), vascular smooth muscle cell (Actin), macrophages (CD68) and endothelial cells (CD31) upstream and downstream of the cast of the combined cast and endothelial damage group. There was a significant decrease in vascular smooth muscle cell content upstream of the cast, compared with upstream of the cast only group. Graphs show mean per group \pm SD, $n=8$ per group. * $p<0.05$, $15.7 \pm 4.8\%$ vs. $27.1 \pm 7.7\%$*

B. Magnification of CD31 staining showing newly formed vessels with lumen formation (arrows) in the plaque.

DISCUSSION

Many animal models to study the vulnerable plaque are long term experiments and the plaques often do not fulfill the criteria for advanced human atherosclerotic plaque. The rabbit is widely used as it is easy to keep and handle, suitable for cardiovascular imaging, both non-invasively as well as intravascular, and not as costly as the pig. Different models to develop atherosclerosis in rabbits exist and most models are based on a high cholesterol diet, with the percentage of cholesterol usually ranging from 0.5 to 4%. A high cholesterol diet in rabbits typically leads to early atherosclerotic lesions with foam cells¹⁴⁻¹⁶. This high cholesterol diet has been combined with a number of other methods causing endothelial dysfunction or injury, such as balloon denudation, hollow cuff implantation, hypertension, and induction of diabetes or infection¹⁷⁻²¹. However, none of these methods have shown to specifically create a human-like vulnerable plaque model in rabbits. Low shear stress is a known atherogenic stimulus and we have previously shown that induction of low shear

stress with a flow tapering cast induces vulnerable plaque formation in the carotid artery in mice ⁵. Although Marano and co-workers showed that increased shear stress protected rabbits from collar induced neo-intima hyperplasia ²², induction of low shear stress to induce atherosclerosis has never been described in rabbits. Therefore, the aim of the current study was to develop a low shear stress based vulnerable plaque model in the rabbit that would allow advanced lesions to develop in a large animal model with resemblance to human vulnerable plaque. We hypothesized that we could induce vulnerable plaques by flow alteration in New Zealand white rabbits within twelve weeks after cast placement using a scaled up model of the flow-altering murine cast device. Furthermore, we investigated whether endothelial damage could accelerate this process.

In the murine model, the tapered cast is known to induce low shear stress upstream and oscillatory shear stress down stream of the device. To validate that we could also induce shear stress alterations in the carotid artery of the rabbit, we measured Doppler blood flow velocities in the naive carotid artery and upstream and downstream of the cast after cast placement. In the mouse model, a reversal of flow downstream of the cast, and a reduction of approximately 33% of flow (15N/m^2 to 10N/m^2) in the upstream region is induced by cast placement ⁸. Comparable with the murine model, we measured a reduction in flow of 33% upstream of the cast (30ml/min to 20ml/min), while downstream of the cast, oscillatory shear stress was observed, indicating that we were able to recreate the same hemodynamic conditions as in our murine model.

In our rabbit model, we were able to create atherosclerotic plaques with high amount of lipids, high macrophage and VSMC content, and intimal neovascularization as indicated by CD31 positive endothelial cells in the plaque. There were no signs of intraplaque hemorrhaging or plaque rupture. Combination of cast placement with endothelial damage increased lesion size and decreased VSMC content, but did not affect other VP parameters. VSMCs are crucial in determining the thickness and integrity of the fibrous cap as they constitute a major part of this fibrous cap and also produce the extracellular matrix which further stabilizes and thickens the cap. On the other hand, macrophages produce matrix metalloproteinases which breakdown extracellular matrix, thus weakening the fibrous cap. In our combined group we also found a high amount of macrophages but fewer VSMCs, indeed indicating thinning of the fibrous cap. In addition, it is known that intimal neovascularization promotes plaque progression towards a vulnerable plaque as those newly formed vessels are often leaky and form the basis of intraplaque haemorrhaging ²³. Recently, Hellings and coworkers also showed that intimal neovascularization not only promotes intraplaque haemorrhaging but also predicts clinical outcome, as patients with increased vessel density in a single excised carotid plaque were at higher risk for future cardiovascular events ²⁴. In both our cast and combined groups, neovascularization was also observed indicating progression towards a more advanced lesion. Moreover, our model could be used to develop and validate new tools to study intraplaque neovascularization. As mentioned earlier, different rabbit models

exist to create atherosclerotic lesions in rabbits. None of them have fulfilled all the criteria for human-like vulnerable plaques. One may postulate whether our model could be further improved by combining it with a different existing rabbit-atherosclerosis method. For example, it has become clear that the immune system plays an important role in atherosclerotic plaque formation and it has been postulated that activation of inflammatory cells could trigger atherosclerosis. Indeed, Lehr and coworkers showed that repeated intravenous endotoxin injection in hypercholesterolemic rabbits accelerated atherosclerosis formation²⁰. Combination of our rabbit model with injection of endotoxin might enhance plaque vulnerability by stimulation of the immune system, thus stimulating necrotic core formation. Constantinides and co-workers showed that the rabbit can also be used to study plaque disruption and rupture, although the rupture described in their study was not spontaneous as it was induced with Russel's viper venom and histamine²⁵. Their original protocol was a long-term experiment (more than one year), so it would be interesting to see whether we could induce the same amount of plaque rupture in our shorter protocol.

Although we created the same conditions as in our murine vulnerable plaque model, hypercholesterolemia in combination with altered shear stress, the plaques in the rabbit were not as vulnerable as those observed in the murine model. We did find abundant intimal neovascularization, high macrophage and lipid content, but these advanced lesions lacked a prominent necrotic core or intraplaque haemorrhage. This lack of a vulnerable phenotype in the altered shear stress-induced lesions in the New Zealand white rabbit model could be explained by a number of arguments. Wildtype mice are normally protected against atherosclerosis, as their lipoprotein profile is enriched in HDL versus LDL, whereas in humans, this profile is reversed. LDL oxidation and deposition in the vessel wall promotes atherogenesis. In the atherosclerosis-prone ApoE^{-/-} mouse, a functional ApoE gene is lacking, causing a shift in the lipoprotein profile, mainly towards VLDL and in lesser extent to LDL. Furthermore, the absence of ApoE causes a pro-inflammatory state due to T-lymphocyte activation and proliferation and promotes VSMC proliferation that is present from birth and favors atherosclerotic plaque development²⁶. Similar to mice, the lipoprotein profile of wildtype rabbits is larger in the HDL fraction, thus rendering the species protected against atherosclerosis. We were able to induce a state of hypercholesterolemia via a high cholesterol diet. However, the main mass of plasma cholesterol in diet-induced hypercholesterolemia in rabbits is found in LDL, in contrast to VLDL in the ApoE^{-/-} mice. The use of transgenic rabbits, such as the Wattanabe Heritable Hyperlipidemic rabbit (WHHL), which, like the ApoE^{-/-} mice, are born with lipoprotein profiles with high LDL/HDL ratios due to a defect in the LDL receptor, could provide a more suitable experimentation model for the induction of vulnerable plaque development by shear stress alteration. We are currently conducting a study in WHHL rabbits to test this hypothesis.

Our study has several limitations. Firstly, the animals were already sacrificed at twelve weeks after cast placement. It is possible that we would be able to create a more human-like

vulnerable plaque when the duration of the protocol was prolonged. The 12 weeks duration for the experiments was chosen, because we wanted to create a rapid model for vulnerable plaque development. Moreover, the duration that New Zealand white rabbits can be fed a cholesterol-rich diet is limited as they develop hepatic failure when they are fed a cholesterol-rich diet for a longer period²⁷. Secondly, we did not perform the Doppler wave measurement in the same group of rabbits in which we induced the immunohistological analysis of the atherosclerotic plaques. As a result we cannot correlate the degree of shear stress change with morphological changes in the carotid artery, ie plaque formation and phenotype, per animal. Thirdly, we decided to injure the endothelium by external stretch which is an easy and quick procedure. However, this is not as controlled as balloon denudation and we do not know if any additional damage was done to the vessel. For example, we might have injured the vasa vasorum surrounding the carotid artery, leading to impaired oxygen supply of the vessel.

In summary, here we present a novel method to induce atherosclerosis in NZW rabbits using a flow altering device. Both low and oscillatory shear stresses are capable to induce atherosclerosis in a large animal model. The phenotype of the lesion induced by low shear stress is beyond that of the fatty streak, with infiltration of VSMCs into a thick cap and macrophages, abundant lipid deposition and neovascularization, but a prominent necrotic core is still lacking, rendering the overall phenotype of the lesions less vulnerable of those induced with the similar device in ApoE^{-/-} mice.

REFERENCES

1. Chatzizisis YS, Coskun AU, Jonas M, Edelman ER, Feldman CL, Stone PH. Role of endothelial shear stress in the natural history of coronary atherosclerosis and vascular remodeling: molecular, cellular, and vascular behavior. *J Am Coll Cardiol*. 2007 Jun 26;49(25):2379-93.
2. Dhawan SS, Avati Nanjundappa RP, Branch JR, Taylor WR, Quyyumi AA, Jo H, et al. Shear stress and plaque development. *Expert Rev Cardiovasc Ther*. 2010 Apr;8(4):545-56.
3. Helderma F, Segers D, de Crom R, Hierck BP, Poelmann RE, Evans PC, et al. Effect of shear stress on vascular inflammation and plaque development. *Curr Opin Lipidol*. 2007 Oct;18(5):527-33.
4. Koskinas KC, Chatzizisis YS, Baker AB, Edelman ER, Stone PH, Feldman CL. The role of low endothelial shear stress in the conversion of atherosclerotic lesions from stable to unstable plaque. *Curr Opin Cardiol*. 2009 Nov;24(6):580-90.
5. Cheng C, van Haperen R, de Waard M, van Damme LC, Tempel D, Hanemaaijer L, et al. Shear stress affects the intracellular distribution of eNOS: direct demonstration by a novel in vivo technique. *Blood*. 2005 Dec 1;106(12):3691-8.
6. Cheng C, Noordeloos AM, Jeney V, Soares MP, Moll F, Pasterkamp G, et al. Heme oxygenase 1 determines atherosclerotic lesion progression into a vulnerable plaque. *Circulation*. 2009 Jun 16;119(23):3017-27.
7. Cheng C, Tempel D, van Haperen R, de Boer HC, Segers D, Huisman M, et al. Shear stress-induced changes in atherosclerotic plaque composition are modulated by chemokines. *The Journal of clinical investigation*. 2007 Mar;117(3):616-26.
8. Cheng C, Tempel D, van Haperen R, van der Baan A, Grosveld F, Daemen MJ, et al. Atherosclerotic lesion size and vulnerability are determined by patterns of fluid shear stress. *Circulation*. 2006 Jun 13;113(23):2744-53.
9. Van der Heiden K, Hierck BP, Krams R, de Crom R, Cheng C, Baiker M, et al. Endothelial primary cilia in areas of disturbed flow are at the base of atherosclerosis. *Atherosclerosis*. 2008 Feb;196(2):542-50.
10. Clarkson S, Newburgh LH. The Relation between Atherosclerosis and Ingested Cholesterol in the Rabbit. *The Journal of experimental medicine*. 1926 Apr 30;43(5):595-612.
11. Bocan TM, Mueller SB, Mazur MJ, Uhlendorf PD, Brown EQ, Kieft KA. The relationship between the degree of dietary-induced hypercholesterolemia in the rabbit and atherosclerotic lesion formation. *Atherosclerosis*. 1993 Aug;102(1):9-22.
12. Tian J, Hu S, Sun Y, Ban X, Yu H, Dong N, et al. A novel model of atherosclerosis in rabbits using injury to arterial walls induced by ferric chloride as evaluated by optical coherence tomography as well as intravascular ultrasound and histology. *J Biomed Biotechnol*. 2012;2012:121867.
13. Kolodgie FD, Katocs AS, Jr., Largis EE, Wrenn SM, Cornhill JF, Herderick EE, et al. Hypercholesterolemia in the rabbit induced by feeding graded amounts of low-level cholesterol. Methodological considerations regarding individual variability in response to dietary cholesterol and development of lesion type. *Arteriosclerosis, thrombosis, and vascular biology*. 1996 Dec;16(12):1454-64.
14. Finking G, Hanke H. Nikolaj Nikolajewitsch Anitschkow (1885-1964) established the cholesterol-fed rabbit as a model for atherosclerosis research. *Atherosclerosis*. 1997 Nov;135(1):1-7.
15. Jokinen MP, Clarkson TB, Prichard RW. Animal models in atherosclerosis research. *Exp Mol Pathol*. 1985 Feb;42(1):1-28.

16. Stehbens WE. An appraisal of cholesterol feeding in experimental atherogenesis. *Prog Cardiovasc Dis.* 1986 Sep-Oct;29(2):107-28.
17. Booth RF, Martin JF, Honey AC, Hassall DG, Beesley JE, Moncada S. Rapid development of atherosclerotic lesions in the rabbit carotid artery induced by perivascular manipulation. *Atherosclerosis.* 1989 Apr;76(2-3):257-68.
18. Campbell DJ, Day AJ, Skinner SL, Tume RK. The effect of hypertension on the accumulation of lipids and the uptake of (3H)cholesterol by the aorta of normal-fed and cholesterol-fed rabbits. *Atherosclerosis.* 1973 Sep-Oct;18(2):301-19.
19. Friedman M, Byers SO. Aortic Atherosclerosis Intensification in Rabbits by Prior Endothelial Denudation. *Arch Pathol.* 1965 Apr;79:345-56.
20. Lehr HA, Sagban TA, Ihling C, Zahringer U, Hungerer KD, Blumrich M, et al. Immunopathogenesis of atherosclerosis: endotoxin accelerates atherosclerosis in rabbits on hypercholesterolemic diet. *Circulation.* 2001 Aug 21;104(8):914-20.
21. Yin W, Yuan Z, Wang Z, Yang B, Yang Y. A diet high in saturated fat and sucrose alters gluco-regulation and induces aortic fatty streaks in New Zealand White rabbits. *Int J Exp Diabetes Res.* 2002 Jul-Sep;3(3):179-84.
22. Marano G, Palazzesi S, Vergari A, Ferrari AU. Protection by shear stress from collar-induced intimal thickening: role of nitric oxide. *Arterioscler Thromb Vasc Biol.* 1999 Nov;19(11):2609-14.
23. Michel JB, Virmani R, Arbustini E, Pasterkamp G. Intraplaque haemorrhages as the trigger of plaque vulnerability. *European heart journal.* Mar 12.
24. Hellings WE, Peeters W, Moll FL, Piers SR, van Setten J, Van der Spek PJ, et al. Composition of carotid atherosclerotic plaque is associated with cardiovascular outcome: a prognostic study. *Circulation.* May 4;121(17):1941-50.
25. Constantinides P, Chakravarti RN. Rabbit arterial thrombosis production by systemic procedures. *Arch Pathol.* 1961 Aug;72:197-208.
26. Greenow K, Pearce NJ, Ramji DP. The key role of apolipoprotein E in atherosclerosis. *Journal of molecular medicine (Berlin, Germany).* 2005 May;83(5):329-42.
27. Prior JT, Kurtz DM, Ziegler DD. The hypercholesteremic rabbit. An aid to understanding arteriosclerosis in man? *Arch Pathol.* 1961 Jun;71:672-84.

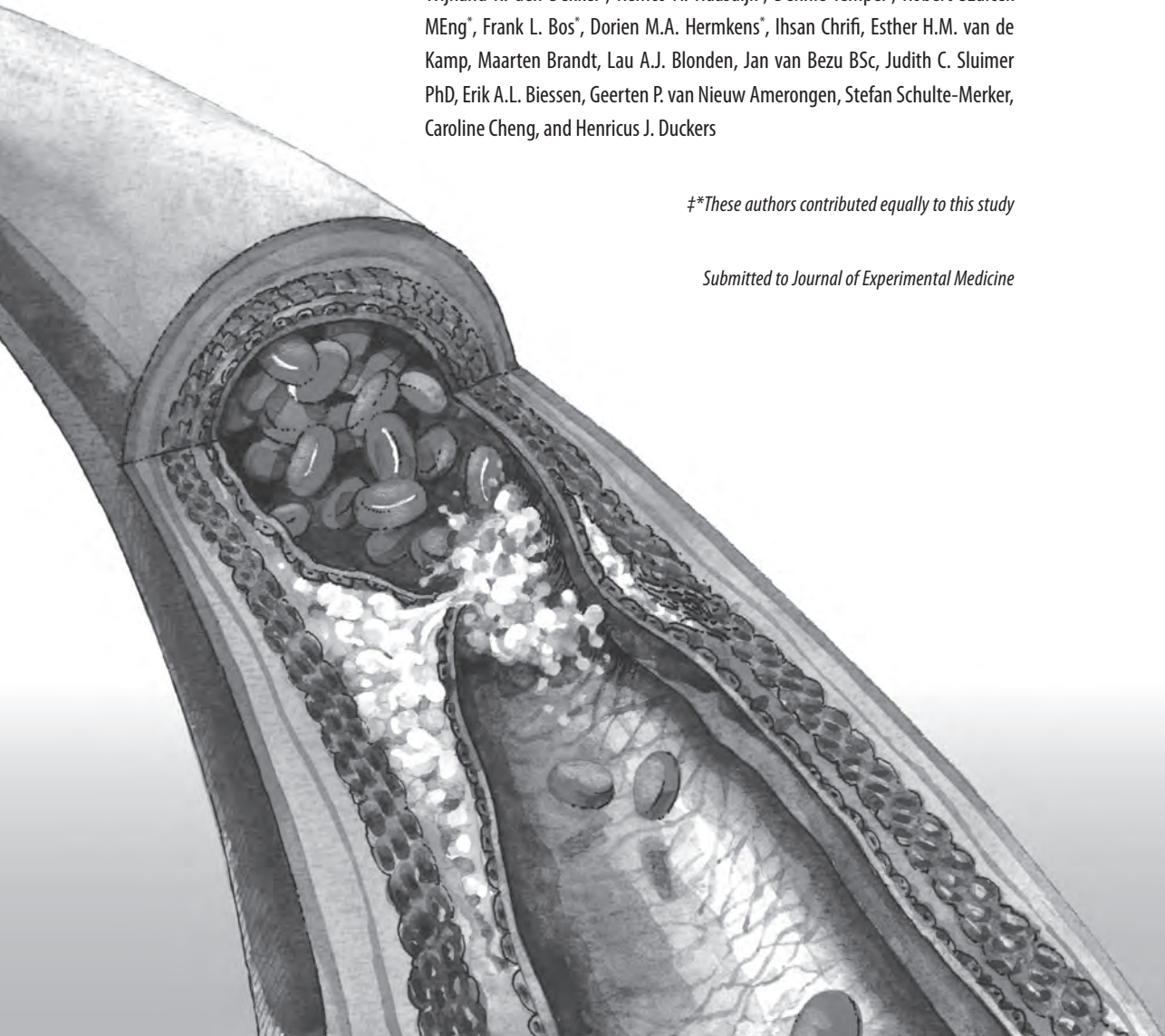
Chapter 5

Thsd-1: a new regulator of endothelial barrier function in vascular development and advanced atherosclerosis.

Wijnand K. den Dekker[‡], Remco A. Haasdijk[‡], Dennie Tempel^{*}, Robert Szulcek MEng^{*}, Frank L. Bos^{*}, Dorien M.A. Hermkens^{*}, Ihsan Chrifi, Esther H.M. van de Kamp, Maarten Brandt, Lau A.J. Blonden, Jan van Bezu BSc, Judith C. Sluimer PhD, Erik A.L. Biessen, Geerten P. van Nieuw Amerongen, Stefan Schulte-Merker, Caroline Cheng, and Henricus J. Duckers

*‡*These authors contributed equally to this study*

Submitted to Journal of Experimental Medicine



ABSTRACT

Background: Impairment of the endothelial barrier leads to haemorrhaging and is involved in vascular-related disease, including atherosclerosis. The mechanism that regulates vascular integrity is complex and requires further definition. Using a microarray screen for angiogenesis-associated genes during embryogenesis, we identified Thrombospondin type I domain 1 (Thsd-1) as a new angiopotent factor with an undefined biological function. Here we investigate the contribution of Thsd-1 to vascular integrity.

Methods and Results: Verification by *in situ* hybridization in zebrafish demonstrates that Thsd-1 is predominantly expressed in endothelial cells (ECs). Knockdown of Thsd-1 in zebrafish embryos and in a murine retina model induced severe haemorrhaging. Vascular growth remained unaffected, despite a decline in vascular integrity. Studies in human ECs verified the deleterious effect of Thsd-1 silencing on endothelial barrier function and identified Thsd-1 as a new binding partner of the CRT-LRP1 complex. Thsd-1 activates downstream signalling of LRP1 via FAK-PI3K, leading to Rac1-mediated actin cytoskeleton interaction with cell-cell junctions. In human carotid endarterectomy specimens, Thsd-1 expression in ECs increases in advanced atherosclerotic lesions with intraplaque haemorrhaging as compared to stable lesions, implying involvement of Thsd-1 in neovascular bleeding. In a murine atherosclerosis model, Thsd-1 overexpression decreased plaque vulnerability by attenuating vascular leakage, while Thsd-1 knockdown aggravated haemorrhaging, again independent of vascular growth. Pro-atherogenic factors (including low oxygen and TNF α) decrease Thsd-1 expression, whereas anti-atherogenic IL-10 increases mRNA expression of protective Thsd-1.

Conclusions: Thsd-1 is a crucial regulator of endothelial barrier function during vascular development and in the pathobiology of haemorrhaging-prone neovascular growth in atherosclerosis.

NON-STANDARD ABBREVIATIONS AND ACRONYMS

CRT	=	calreticulin
CV	=	caudal vein
DMEM	=	Dulbecco's modified Eagle's medium
dpf	=	days post-fertilization
EC	=	endothelial cell
ELL	=	eleven-nineteen lysine-rich leukemia
FAK	=	focal adhesion kinase
FAK-P	=	phosphorylated focal adhesion kinase
FCS	=	foetal calf serum
hpf	=	hours post-fertilization
HRP	=	horse radish peroxidase
HUVEC	=	human umbilical vein endothelial cell
KD	=	knockdown
LRP1	=	low density lipoprotein receptor-related protein 1
MCeV	=	midcerebral vein
MO	=	morpholino
N-DAB	=	nickel-3,3'-diaminobenzidine
OE	=	overexpression
PI3K	=	phosphatidylinositol 3-kinase
PI3K-P	=	phosphorylated phosphatidylinositol 3-kinase
SEM	=	standard error of the mean
si-sham	=	scrambled non-targeting siRNA
si-Thsd-1	=	Thsd-1 targeting siRNA
Thsd-1	=	Thrombospondin type I domain 1
TSP1	=	thrombospondin type I domain
UIC	=	uninjected control
VSMC	=	vascular smooth muscle cell
WD	=	Western diet
ECIS	=	Electric cell-substrate impedance sensing

INTRODUCTION

The vascular endothelium functions as a selective barrier for protein and fluid exchange between the blood stream and the surrounding tissues. The integrity of the vascular endothelium is actively controlled by dynamic interaction between the endothelial cytoskeleton, cell-cell junctions and cell-matrix focal adhesions¹. During vascular development, although physical contacts between endothelial cells (ECs) are present during the earliest phases of vasculogenesis and angiogenesis, a functional vascular barrier is only established after the neovessels have undergone critical rearrangements at the molecular level of the actin cytoskeleton and cell-cell junction sites. This maturation of the endothelial barrier is stringently controlled by members of the Rho family of GTPases²⁻⁵. In particular, Rac1 plays a vital role in maintaining vascular barrier function: Rac1-mediated adaptation of the actin cytoskeleton strengthens the VE-cadherin/actin cytoskeleton bonds, which are crucial for the formation of stable endothelial cell-cell junctions⁶⁻⁹. Disruption of this Rac1-regulatory pathway leads to endothelial barrier dysfunction and loss of vascular integrity, and is implicated to be an important contributing factor to the onset and progression of vascular-related diseases such as diabetic retinopathy and atherosclerosis^{1,10}. In atherosclerosis, dysfunction of the endothelium on top of the fibrous cap triggers extravasation of inflammatory cells that contribute to lesion growth. As atherosclerosis progresses, plaques become characterized by neovascular growth of vessels which are phenotypically immature, defined by lack of endothelial barrier function and increased susceptibility to rupture¹¹. Although previous studies have demonstrated the importance of endothelial barrier function in vascular development and disease, our knowledge of the molecular mechanisms that orchestrate the basic (Rac1-mediated) principles of regulation remains limited, in particular in the light of vascular related pathologies. In this study, we have identified a new gene with a high level of endothelial expression that is a potent regulator of endothelial barrier integrity.

Recently, we have carried out a genome-wide microarray analysis in search for genes involved in the regulation of new vessel formation. Gene expression profiles of isolated Flk1-positive angioblasts during murine embryonic development were compared with the profiles of Flk1-negative cells. One of the genes that was identified as a new potential regulator of vascular development was Thrombospondin type I domain 1 (Thsd-1). Although Thsd-1 was previously described as a marker of hematopoietic stem cells and ECs¹², the basic biological function of Thsd-1 in angiogenesis *in vitro* and *in vivo* remains fully unknown.

Here, we sought to characterize the function of Thsd-1 in ECs during blood vessel formation *in vitro* using primary cell cultures and *in vivo* in zebrafish and murine vascular development. Our data show that Thsd-1 plays an important role in establishing and preserving the endothelial barrier function during angiogenesis *in vivo*, as loss of Thsd-1 led to vessel disruption and severe haemorrhaging. Silencing of Thsd-1 led to vessel rupture of the cranial vasculature in developing zebrafish, whereas extensive haemorrhaging was detected during postnatal

vascular retinal development in mice. This loss of endothelial integrity was unrelated to the angiogenic potential of the ECs, for no difference in vascular growth was observed. Further *in vitro* studies demonstrate that Thsd-1 activates the calreticulin (CRT) - low density lipoprotein receptor-related protein 1 (LRP1) signalling pathway by complex formation with CRT. Loss of this complex interferes with actin cytoskeleton modulation - a process shown to be regulated by Rac1 - leading to loss of endothelial barrier function by limiting VE-cadherin/actin cytoskeleton interaction. These findings point towards an important role for Thsd-1 in the basic regulation of vascular barrier function. In addition, a strong increase in Thsd-1 endothelial expression was observed in the neovasculature of advanced human atherosclerotic lesions, suggesting a possible Thsd-1-mediated feed-back mechanism to counteract loss of vascular integrity of intimal neovessels. Evaluation of Thsd-1 function in a well-validated flow-based murine vulnerable plaque model, clearly demonstrated that siRNA-mediated silencing of endogenous Thsd-1 further compromised neovascular integrity and worsened intraplaque haemorrhaging, whereas overexpression of Thsd-1 improved endothelial barrier function and significantly reduced vascular bleeding. These *in vivo* studies identify Thsd-1 as a vital factor in the formation and conservation of intimal neovessel integrity in advanced atherosclerosis. Loss of Thsd-1 function results in extensive intraplaque haemorrhaging and amplifies the inflamed state of the plaque lesion, leading to a further decline of vulnerable plaque stability. Considering the potent vascular stabilising function of the gene, Thsd-1 might be an interesting target for the development of therapeutics in the treatment of vascular pathologies in which endothelial barrier function is affected.

MATERIAL AND METHODS

This study was carried out in accordance with the Council of Europe Convention (ETS123)/Directive (86/609/EEC) for the protection of vertebrate animals used for experimental and other scientific purposes and with the approval of the National and Local Animal Care Committee.

Zebrafish

Zebrafish (*Danio rerio*) were maintained under standard laboratory conditions. The transgenic zebrafish lines used were Tg(Fli1:eGFP)^{y1} and Tg(Kdrl:eGFP x Gata1:dsRed)^{y1}.

Whole-mount in situ hybridization

As template for *in vitro* transcription, a Thsd-1 cDNA fragment of at least 250 bp was used to ensure probe specificity. Antisense RNA probes of Thsd-1 were generated by *in vitro* tran-

scription using the digoxigenin RNA Labeling Mix from Roche (Woerden, The Netherlands). *In situ* hybridization was carried out as previously described ¹³.

o-Dianisidine staining

Erythrocytes were stained by incubating embryos in a solution containing *o*-Dianisidine (Sigma-Aldrich, Zwijndrecht, The Netherlands) as previously described ¹³.

Mice

Plugged FVB/N mice (*Mus musculus*) were ordered at Harlan (Indianapolis, USA). ApoE^{-/-}/C57Bl/6J mice were obtained at Jackson Laboratory (bar Harbor, USA). C57BL/6J mice were obtained from laboratory stock. They were maintained under standard husbandry conditions.

Mouse model of retinal vascularisation

Two-day old C57BL/6J mice pups were anesthetized by placement on ice. Thsd-1 targeting siRNA (si-Thsd-1) was injected into the left eye. As a control, scrambled non-targeting siRNA (si-sham) was injected into the right eye. Mice pups were killed five days after intra-ocular injection. The retinas were stained with Alexa Fluor[®] 488 conjugated isolectin GS-IB₄ (Invitrogen, Bleiswijk, The Netherlands) before assessment under a fluorescence microscope (Axiovert S100; Carl Zeiss, Sliedrecht, The Netherlands). To rescue the phenotype caused by Thsd-1 knockdown, another group of two-day old C57BL/6J mice pups were treated by intra-ocular injection of si-Thsd-1 in both eyes as described combined with or without Rac1 activator (CN02-A, 0.25 U/ml; Cytoskeleton, Denver, USA).

TER-119 staining

Retinas were incubated with TER-119 antibody (Novus Biologicals, Cambridge, UK) to stain erythrocytes.

Murine vulnerable plaque model

All animal work was carried out in compliance with the guidelines issued by the Dutch government and was approved by our local animal welfare committee. We used twelve week old female ApoE knockout mice (ApoE^{-/-}/C57BL/6J) mice (Jackson Laboratory, UK). All *in vivo* studies were done with our in-house developed murine vulnerable plaque model. Two weeks after arrival, mice were put on a Western Diet (WD, containing 15% (w/w) cacao and 0.25% (w/w) cholesterol (Arie Blok, the Netherlands)). Two weeks after start of WD, mice were oper-

ated and a tapered cast was surgically inserted around the right common carotid artery. Nine weeks after cast placement, mice were re-operated and adenovirus overexpressing Thsd-1 (adThsd-1) or sham (adsham) virus were placed around the right common carotid artery (n=8 per group). We sacrificed the mice three days later. One hour before sacrifice, FITC-labelled Dextran was intravenously injected. After sacrifice the carotid artery was flushed, taken out, and snap frozen in liquid nitrogen. The carotid artery was maintained in an -80°C freezer until further use. In a subsequent experiment, we applied siThsd-1 or siSham to study the effect of Thsd-1 knock down. Like in the over expression experiment, the mice were sacrificed three days later, after injection on Dextran-FITC.

The effect of Thsd-1 over expression or knock down on Thsd-1 mRNA expression was analyzed using qPCR. Thsd-1 expression was normalized for the murine household gene HPRT. We used the following primers: For Thsd-1; 5'-AGA GCC AGC AAA AGG ACA AA-3' (forward) and 5'-CAA GGA GGT GGC AGT ACC AT-3' (reverse) and for HPRT; 5'-TCA GGA GAG AGA AAA GAT GTG ATT GA-3' (forward) and 5'-ACG CCA ACA CTGCTG AAA CA-3'(reverse) (Biolegio, Nijmegen, The Netherlands).

Thsd-1 and CD31 expression in human carotid endarterectomy specimens

Human carotid endarterectomy specimens were kindly provided by professor Biessen from the University of Maastricht. From all samples, we randomly took three regions and studied the Thsd-1 and CD31 expression, as marker for endothelial cells, for every region and determined the Thsd-1/CD31 ratio. The average of these three regions was used as final Thsd-1/CD31 ratio for that sample. Thsd-1 was stained using a rabbit anti-human Thsd-1 polyclonal antibody (Sigma, Zwijndrecht, the Netherlands) and CD31 using a mouse anti-human monoclonal antibody (Dako Cytomation). A horseradish peroxidase (HRP) labeled secondary antibody, anti-human for Thsd-1 and anti-mouse for CD31, in combination with nickel-3, 3'-diaminobenzidine (N-DAB, Sigma) was used to visualize the signal.

Cell cultures

Primary cultures of human umbilical vein endothelial cells (HUVEC) were cultured in EBM⁺-2 medium supplemented with a commercial BulletKit. Primary aorta-derived human vascular smooth muscle cells (vSMC) were cultured in SmGM⁺-2 medium supplemented with a commercial BulletKit, 10% foetal calf serum (FCS) and 1% penicillin/streptomycin (Lonza, Breda, The Netherlands). HeLa and sarcoma cells were cultured in Dulbecco's modified Eagle's medium (DMEM) supplemented with 10% FCS (Cambrex, Wiesbaden, Germany). Cells were cultured at 37°C in 5% CO₂. Passages three to six were used throughout the study.

2D matrigel assay

To induce network-formation, HUVECs - transfected with si-sham or si-Thsd-1 - were cultured on a 2D Matrigel™ matrix (BD, Breda, The Netherlands). The tubules were stained by Calcein-AM (BD, Breda, The Netherlands) after 24 hours of network-formation. Each condition was assessed by fluorescence microscopy (Axiovert S100; Carl Zeiss, Sliedrecht, The Netherlands). Image analysis of the number of junctions, tubules and total tubule length was carried out using Angiosys Image Analysis Software 1.0 (TCS CellWorks, Buckingham, UK).

Transwell permeability and ECIS assay

Endothelial barrier function *in vitro* was evaluated by culturing HUVECs on porous filters and measuring the passage of horse radish peroxidase (HRP) as previously described^{14, 15}. For electric cell-substrate impedance sensing (ECIS) measurements, cells were seeded on gelatin-coated electric cell-substrate impedance sensing arrays, each with 8 wells with 10 gold electrodes per well (Applied Biophysics, Troy, NY), experiments were conducted following standard protocols as previously described¹⁶.

Co-immunoprecipitation

Protein complexes were immunoprecipitated using Dynabeads® magnetic beads from Invitrogen (Bleiswijk, The Netherlands) according to the instruction manual and analyzed using a 12.5% SDS-PAGE gel, followed by immunoblotting using Thsd-1 antibody (Sigma-Aldrich, Zwijndrecht, The Netherlands), CD36 antibody (Hycult Biotech, Uden, The Netherlands), CRT antibody (Thermo Fisher Scientific, Breda, The Netherlands) and LRP1 antibody that recognizes the heavy chain of the protein (Abcam, Cambridge, UK).

Western blot analysis

To determine whether knockdown of Thsd-1 interfered with cellular processes, Western blot analysis was carried out using HUVEC protein lysates. At 72 hours post-transfection, HUVECs were serum starved for four hours and replenished with EBM⁻² medium supplemented with commercial BulletKit, with or without Rac1 activator (CN02-A, 0.05 U/ml; Cytoskeleton, Denver, USA) for 30 minutes. Cells were lysed in NP40 Cell Lysis Buffer (Invitrogen, Bleiswijk, The Netherlands) and analysed on a 12.5% SDS-PAGE gel, followed by immunoblotting using antibodies against focal adhesion kinase (FAK), phosphorylated-FAK (Y397) (FAK-P) (Abcam, Cambridge, UK), phosphatidylinositol 3-kinase p85 α (PI3K) (Cell Signaling Technology, Leiden, The Netherlands), phosphorylated-PI3K p85 α (Y508) (PI3K-P) (Santa Cruz Biotechnology, Heidelberg, Germany), and Rac1 (Abcam, Cambridge, UK). Beta-actin antibody (Abcam,

Cambridge, UK) was used as a loading control. Protein bands were visualized by the Odyssey® Infrared Imaging System and analyzed by Odyssey 3.0 software (LI-COR Biotechnology, Cambridge, UK).

Rac1 activation assay

Rac1 activity was measured using the G-LISA® Rac Activation Assay Biochem Kit™ from Cytoskeleton (Denver, USA) according to the instruction manual.

Statistical analysis

Data were reported as mean ± standard error of the mean (SEM). Statistical significance was evaluated using a Student's *t*-test and was accepted at $P < 0.05$ (* $P < 0.05$, ** $P < 0.01$ in the figures).

RESULTS

Vascular specific expression of Thsd-1 during mouse and zebrafish embryogenesis.

To identify new genes involved in angiogenesis, a genome-wide microarray analysis was carried out followed by validation of the results by qPCR. Gene expression profiles of Flk1-positive angioblasts at various stages of murine embryonic development were compared with the profiles of Flk1-negative cells. Thsd-1 was upregulated in Flk1-positive angioblasts from 8 to 16 days post-fertilization (dpf). Expression levels were highest upregulated around 8 to 11 dpf, which coincides with the period of early angiogenesis in murine development and suggests a potential role of Thsd-1 in blood vessel formation (Figure 1A).

Further evidence of a vascular-related expression profile for Thsd-1 was provided by examining the gene in developing zebrafish larvae by whole-mount *in situ* hybridization: expression of the Thsd-1 zebrafish orthologue was detected in the main axial vessels - dorsal aorta and posterior cardinal vein - and head vessels at 26 hours post-fertilization (hpf). In addition, Thsd-1 expression was also detected in the caudal and midcerebral veins (MCeV) and in the somites (Figure 1B).

Knockdown of Thsd-1 in zebrafish induces haemorrhaging of cerebral vessels.

For functional evaluation of Thsd-1 *in vivo*, the gene was silenced in developing zebrafish of the Tg(Fli1:eGFP)^{y1} and the Tg(Kdrl:eGFP x Gata1:dsRed)^{y1} line, using morpholino (MO)-knockdown technology. Adequate targeting of Thsd-1 was verified using qPCR analysis.

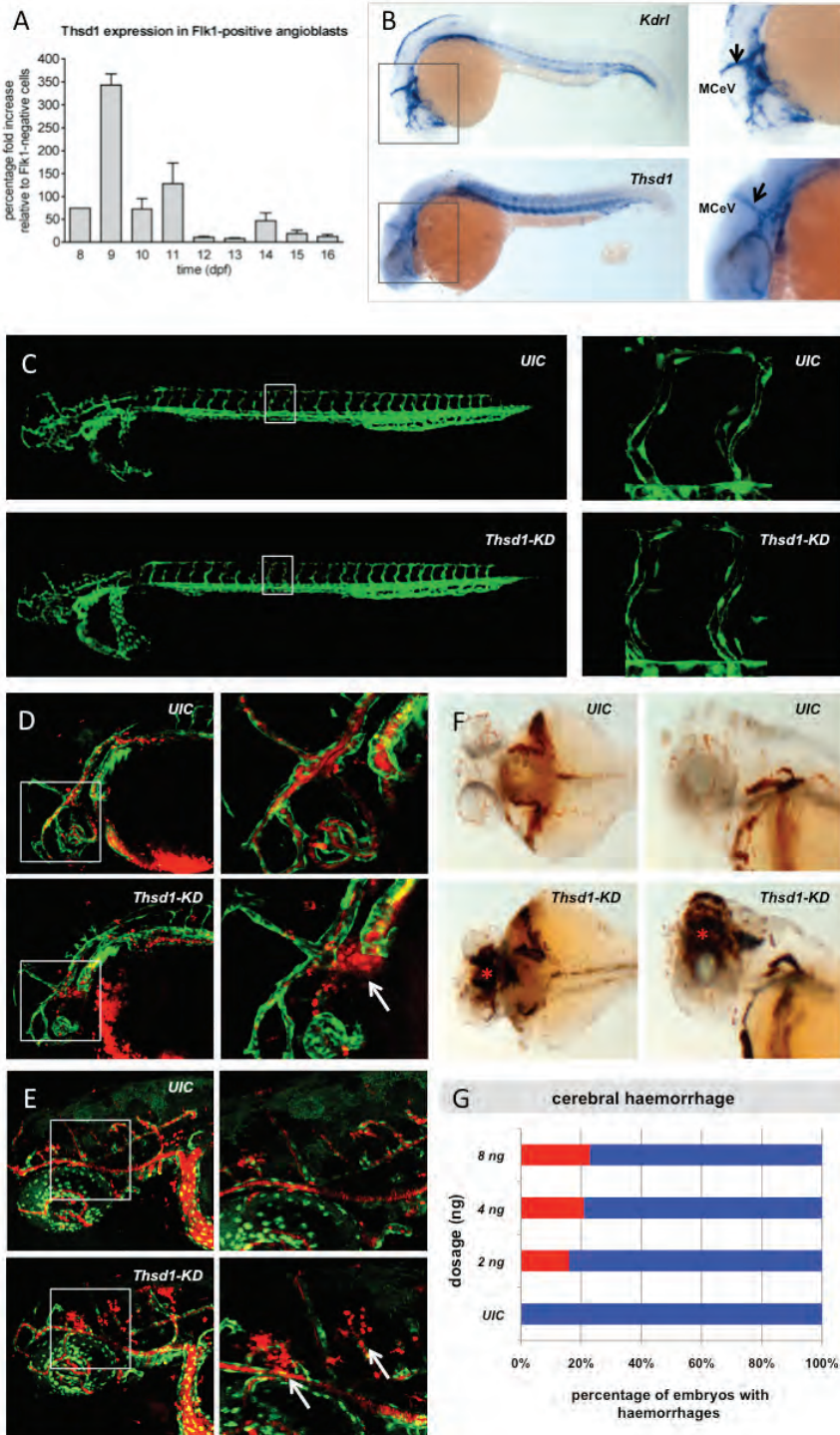


Figure 1

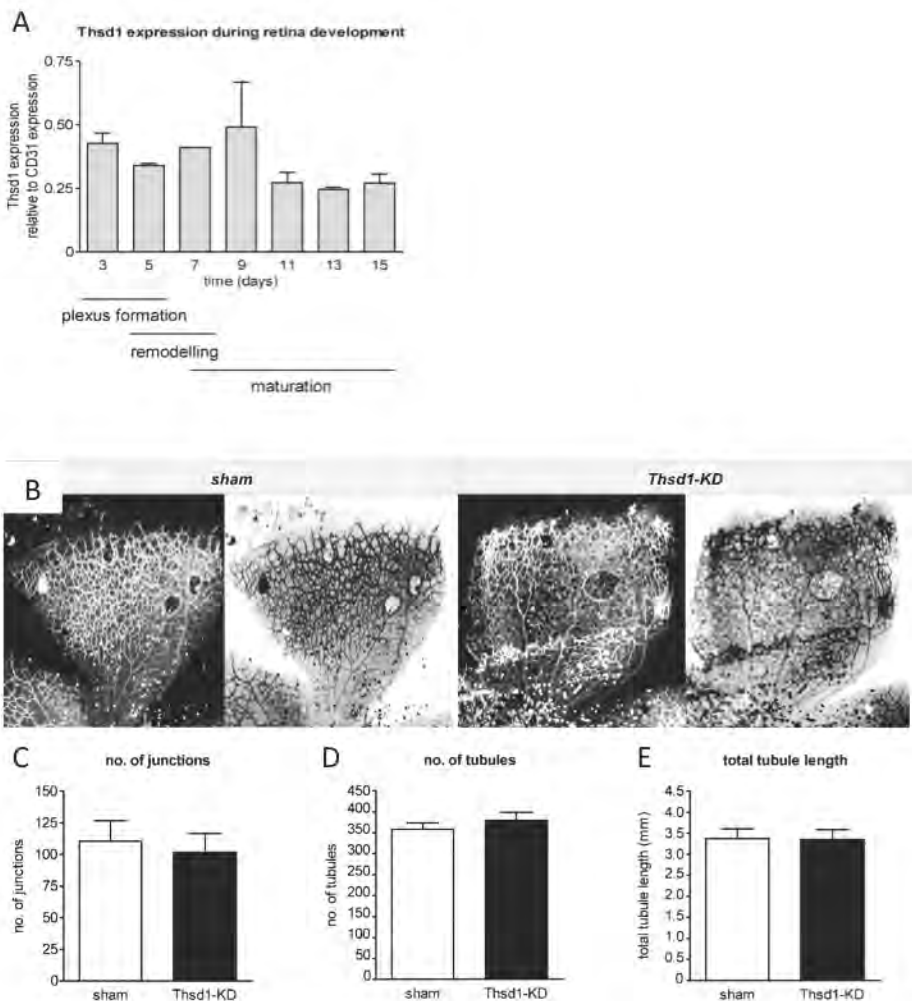
Thsd-1 is upregulated in vascular endothelial cells during mouse and zebrafish development. (A) Endogenous expression level of Thsd-1 in Flk1-positive angioblasts during murine embryonic development from 8 to 16 days post-fertilization (dpf) compared with Flk1-negative cells as analyzed by qPCR. The expression level of Thsd-1 in Flk1-negative cells was arbitrarily set to one (n=4; mean±SEM). The highest upregulation was detected around day 8 to 11, which coincides with the period of early angiogenesis in murine development. (B) Whole-mount in situ hybridization comparison of endothelial cell marker gene Kdr1 (upper panel) with Thsd-1 (lower panel) in zebrafish at 26 hours post-fertilization (hpf), lateral view, cranial is to the left. Like Kdr1, Thsd-1 transcripts were localized in the developing vascular network, including intersomite vessels, main axial vessels - dorsal aorta and posterior cardinal vein - and cerebral vasculature (black arrow), as well as in the caudal vein and midcerebral vein (MCeV). In addition, expression of Thsd-1 in the somites was observed. Right hand panel shows high magnification images of the cranial region. Morpholino-induced knockdown of Thsd-1 in zebrafish results in acute cerebral haemorrhages without affecting vascular growth. (C) Tg(Fli1:eGFP)¹ embryos at 26 hpf, lateral view, cranial is to the left. No apparent morphological abnormalities in the trunk or cerebral vasculature were observed in the Thsd-1 morpholino injected (Thsd-1-KD) and the uninjected control (UIC) embryos. Right hand panel shows high magnification images of intersegmental outgrowth in the trunk region. Tg(Kdr1:eGFP x Gata1:dsRed)¹ Thsd-1-KD embryos around (D) 28 hpf and (E) 2 days post-fertilization (dpf), lateral view, cranial is to the left. Endothelial cells (Kdr1-GFP+ green) and erythrocytes (Gata1:dsRed+ red). Right hand panel shows high magnification images of the cranial region. Extensive and frequent haemorrhages were detected in the head region (white arrow). (F) o-Dianisidine stained embryos around 26-28 hpf, top view (left) lateral view (right), cranial is to the left. Areas of accumulated blood (red asterisk symbol) in the head region were observed in Thsd-1-KD embryos. (G) Morpholino dose-response increase in the percentage of zebrafish with the cerebral haemorrhage phenotype (red bar) versus wildtype phenotype (no cerebral haemorrhaging, blue bar).

Silencing of Thsd-1 had no effect on vascular growth and macroscopic evaluation showed no obvious defects in the general vasculature (Figure 1C). However, time-lapse studies carried out during the first 48 hours post-fertilization identified severe and frequent haemorrhaging in the cranial region (a known predilection site for vascular haemorrhaging in zebrafish^{13, 17-21}) that was observed in 24% of the injected embryos (n=195). Haemorrhaging occurred as a sudden rupture of blood vessels, implying intrinsic weakness and lack of integrity of the neovascular barrier (Figure 1D, E). Cerebral haemorrhaging was further confirmed by an o-Dianisidine staining of iron/haem in red blood cells in Thsd-1-silenced wildtype zebrafish. Thsd-1 silencing resulted in large areas of accumulated blood in the head-area of the larvae as compared to uninjected controls (Figure 1F). This phenotype was consistently observed in the Thsd-1-silenced zebrafish after injections of different MO concentrations (Figure 1G).

Thsd-1 knockdown in the developing retinal vasculature of neonatal mice promotes vascular haemorrhages.

To further validate the findings in the zebrafish, Thsd-1 function was studied during the development of the retinal vasculature of neonatal mice. To determine the optimal moment of Thsd-1 knockdown, Thsd-1 mRNA expression in the murine retinas was evaluated during postnatal development by qPCR. Thsd-1 mRNA levels were adjusted to CD31 mRNA levels to compensate for changes in percentage of ECs. High expression levels of Thsd-1 were observed from 3 to 9 days post-partum, which corresponds with the period of plexus formation and vascular remodelling (Figure 2A). Based on these findings, Thsd-1 knockdown was induced in the first week of retinal vascular development by intra-ocular injection of a siRNA

pool composed of four different *Thsd-1* targeting siRNA sequences in two-day-old wild type C57BL/6J mouse pups, and compared to controls injected with a non-targeting siRNA pool (si-sham). Efficient knockdown of *Thsd-1* was observed two days after intra-ocular injection. Assessment and quantification of the number of vascular branches, the total number of vessels and the total tubule length after visualization of the vasculature by isolectin GS-IB₄ staining, identified no difference between si-*Thsd-1* and si-sham injected eyes five days after intra-ocular injection (Figure 2B-E). However, double-staining of retinas with isolectin GS-IB₄ (ECs, green) and TER-119 antibody (erythrocytes, red) identified a significant higher frequency



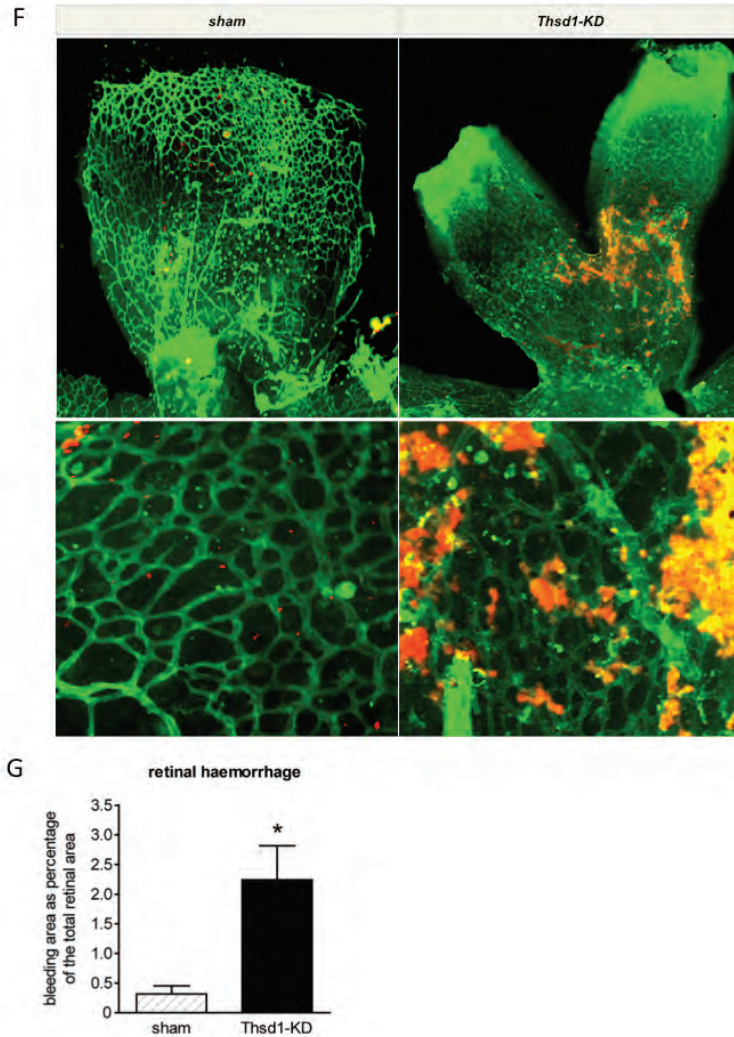


Figure 2

Thsd-1 silencing during murine retinal vascular development results in vascular haemorrhaging without affecting vascular growth. (A) Endogenous expression level of *Thsd-1* in the developing retinal vasculature of neonatal mice from 3 to 15 days after birth reflected to CD31 expression in the retina ($n=3$; mean \pm SEM). *Thsd-1* is highly expressed from day 3 to 9, which corresponds with the period of plexus formation and remodelling. (B) Whole mount en-face staining of *Thsd-1* targeting siRNA (*Thsd-1*-KD) versus scrambled non-targeting siRNA (sham) injected retinas. Isolectin GS-IB₄ Fitc was used to visualize the retinal vasculature. Left hand image shows black-and white micrograph, right hand image shows the inverse image. (C-E) Quantification by means of the dimensions of the vascular network showed no morphological defects after *Thsd-1* knockdown (*Thsd-1*-KD) as parameters including (C) number of junctions, (D) number of tubules and (E) total tubule length remain unaffected. In contrast double-staining of retinas with isolectin GS-IB₄ (endothelial cells, green) and TER-119 (erythrocytes, red) demonstrated severe and frequent vascular haemorrhaging in the *Thsd-1*-KD group: (F) *Thsd-1* silencing induced significantly larger areas of extra-vascular TER-119 erythrocytes accumulation. Upper panel shows low magnification and lower panel shows high magnification micrographs. (G) Quantification of retinal haemorrhage with the bleeding area expressed as percentage of the total retinal area showed a 600% increase in *Thsd-1*-KD versus sham retinas ($n=10$; mean \pm SEM, * $P<0.05$).

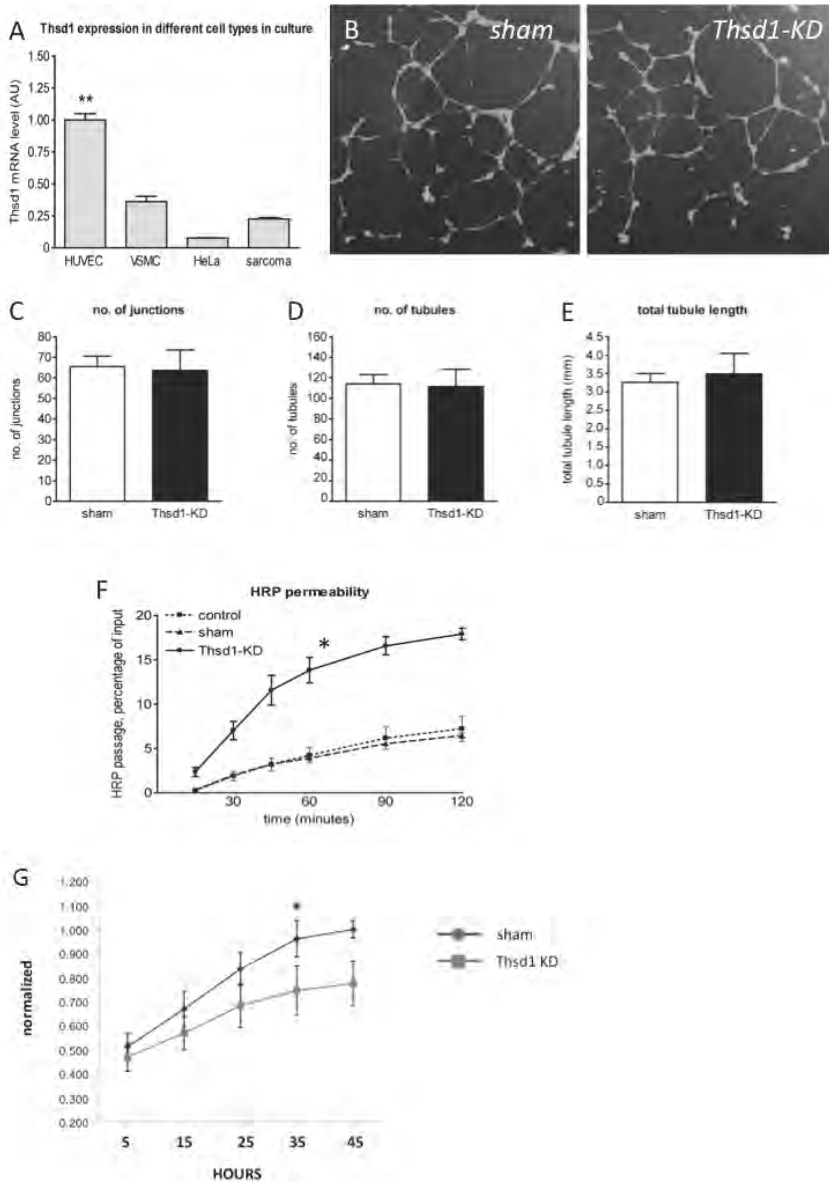


Figure 3

Thsd-1 knockdown in cultured endothelial cells impairs endothelial integrity. (A) *Thsd-1* was highly expressed in HUVEC compared to VSMC, HeLa and sarcoma cells, as demonstrated by qPCR analysis. (B) Assessment of network-formation capacity for *Thsd-1*-silenced ECs (*Thsd-1*-KD) in a 2D matrigel experiment. Tubules were stained by Calcein-AM uptake. (C-E) quantification of the vascular network showed no morphological changes in *Thsd-1*-KD HUVECs: (C) number of junctions, (D) number of tubules and (E) total tubule length remained unaffected. ($n=3$; mean \pm SEM, $**P<0.01$) (F) Measurement of endothelial barrier function *in vitro*. Macromolecule passage (horseradish peroxidase, HRP) over a confluent monolayer of HUVECs during thrombin (1U/ml) stimulation for the different conditions show significant increased HRP permeability after *Thsd-1* silencing ($n=3$; mean \pm SEM, $*P<0.05$). (G) ECIS measurement of sham or *Thsd-1*-silenced HUVEC monolayers show delay in electric resistance build-up as a result of *Thsd-1* inhibition. ($n=3$; mean \pm SEM, $*P<0.05$).

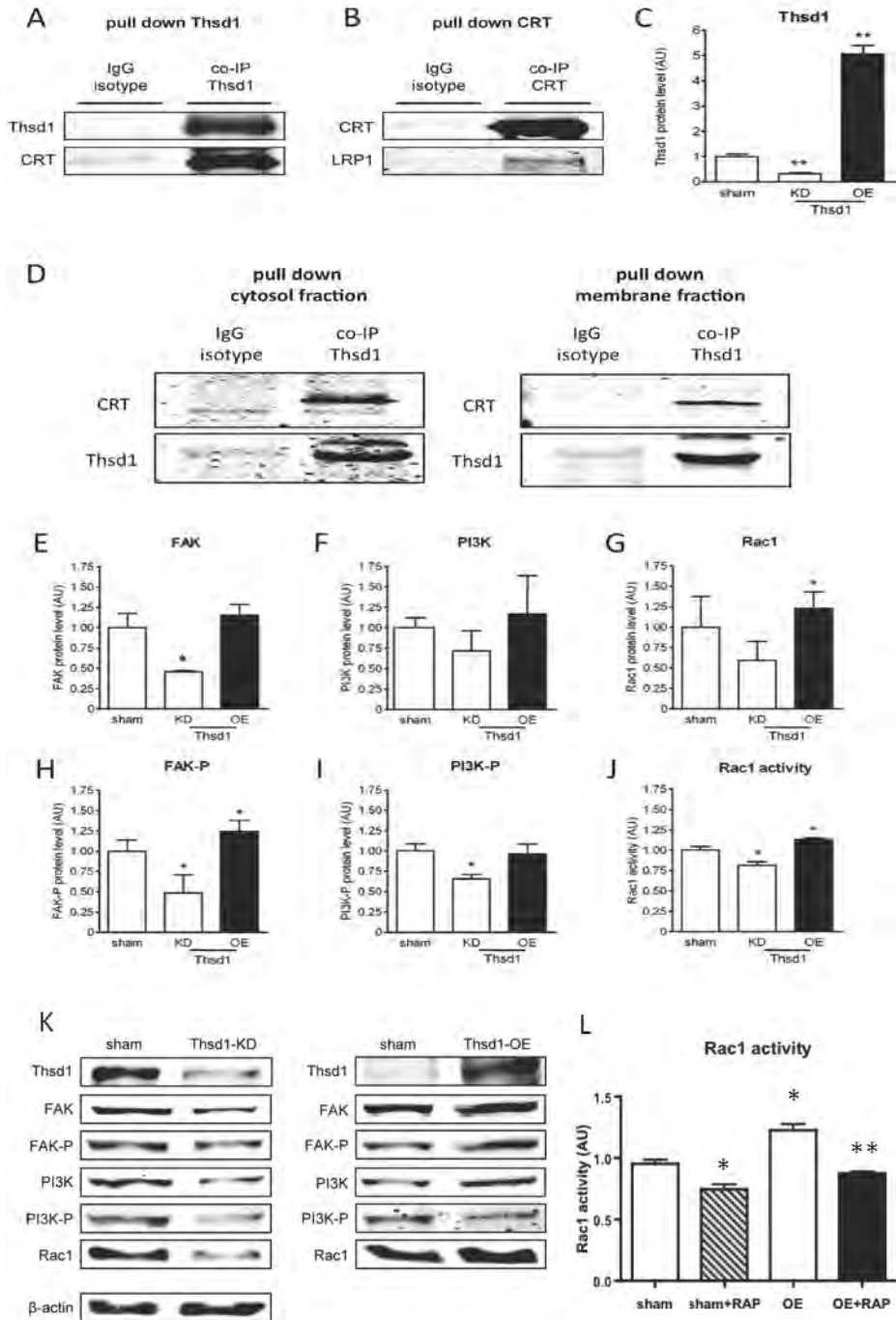
of haemorrhaging and larger areas of bleeding in the si-Thsd-1 injected eyes, whereas retinal haemorrhaging was hardly observed in si-sham injected controls (Figure 2F, G). Thus, like in the developing zebrafish, loss of Thsd-1 expression had no effect on vascular growth, but had resulted in a vasculature highly susceptible to vascular haemorrhaging. Combined, these data has identified a role for Thsd-1 in establishing vascular integrity during blood vessel development.

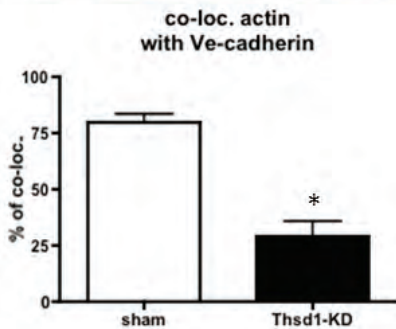
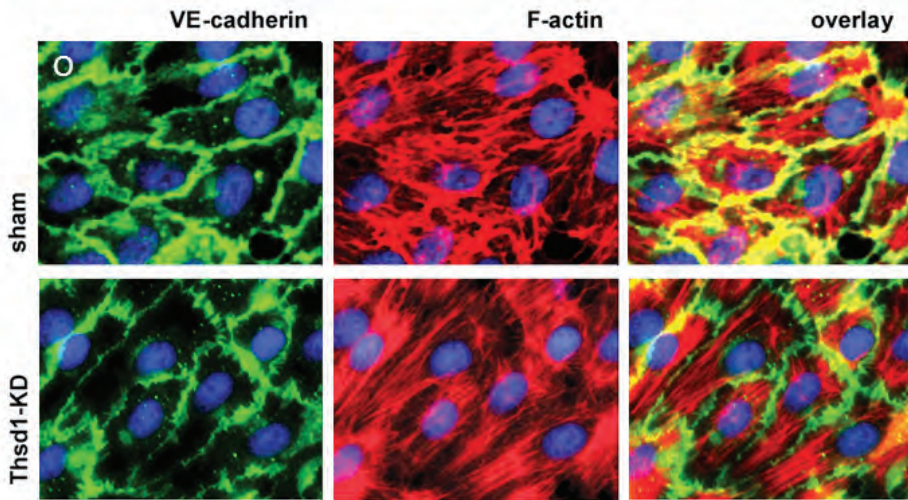
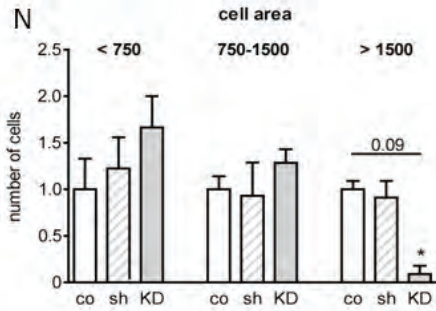
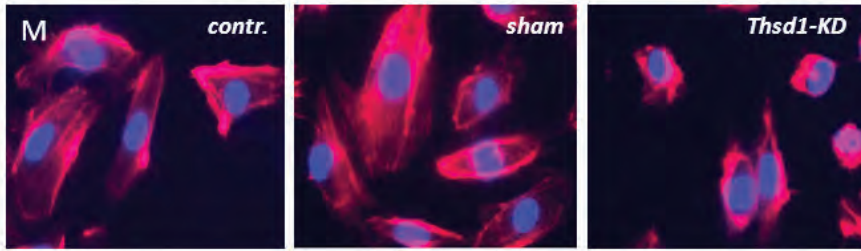
Thsd-1 controls endothelial barrier function *in vitro*

To clarify the molecular mechanism underlying the impaired endothelial integrity, we moved to *in vitro* assays to define Thsd-1 function in vascular cells. Expression level of Thsd-1 was evaluated in different cell types. In a comparison between HUVECs, VSMCs, HeLa and sarcoma cells, the highest mRNA expression level of Thsd-1 was observed in HUVECs (Figure 3A). In line with previous *in vivo* findings, siRNA-mediated knockdown of Thsd-1 in HUVECs did not affect sprouting capacity in a standard 2D matrigel analysis (as indicated by the number of junctions, capillary tubules or total tubule length) when compared to cultures transfected with equimolar of non-targeting siRNA (si-sham) and untransfected controls (Figure 3B-E). Adequate knockdown of the target gene was validated on both mRNA and protein assessment, and did not affect the expression of family member Thrombospondin 1. A Transwell permeability assay that measures macromolecule (HRP) passage was carried out to determine the effect of Thsd-1 on endothelial barrier function in HUVECs. Like in the *in vivo* findings, endothelial barrier function was significantly decreased in Thsd-1-depleted HUVECs as suggested by increased permeability for HRP (Figure 3F). Further evaluation of endothelial barrier function by conducting ECIS experiments showed that Thsd-1 silencing in HUVEC monolayers severely impeded the build-up of endothelial electric resistance as compared to sham treated groups, thus verifying a decline in effective cell junction formation (Figure 3G).

Thsd-1 mediates cell-cell interaction via CRT-LRP1 downstream signalling regulation of Rac1

Previous reports indicated that Thrombospondin 1 mediates EC apoptosis via CD36 binding and signalling²²⁻²⁴. To evaluate if Thsd-1, like its family member, may mediate vascular barrier function via this apoptosis pathway, co-immunoprecipitation analysis was carried out to identify the binding partners of Thsd-1. No binding between Thsd-1 and CD36 was detected in HUVECs. In addition, no effect was observed on early or late apoptosis in si-Thsd-1 transfected cells compared to si-sham transfected and untransfected controls. Thus, these data indicate that Thsd-1 operates via a separate, CD36 independent pathway. Based on the homology in protein domains between Thsd-1 and Thrombospondin 1, the CRT-LRP1 complex may provide a potential binding target for Thsd-1. Co-immunoprecipitation analysis confirmed that Thsd-1 and CRT could indeed form a protein complex. Likewise, CRT binding





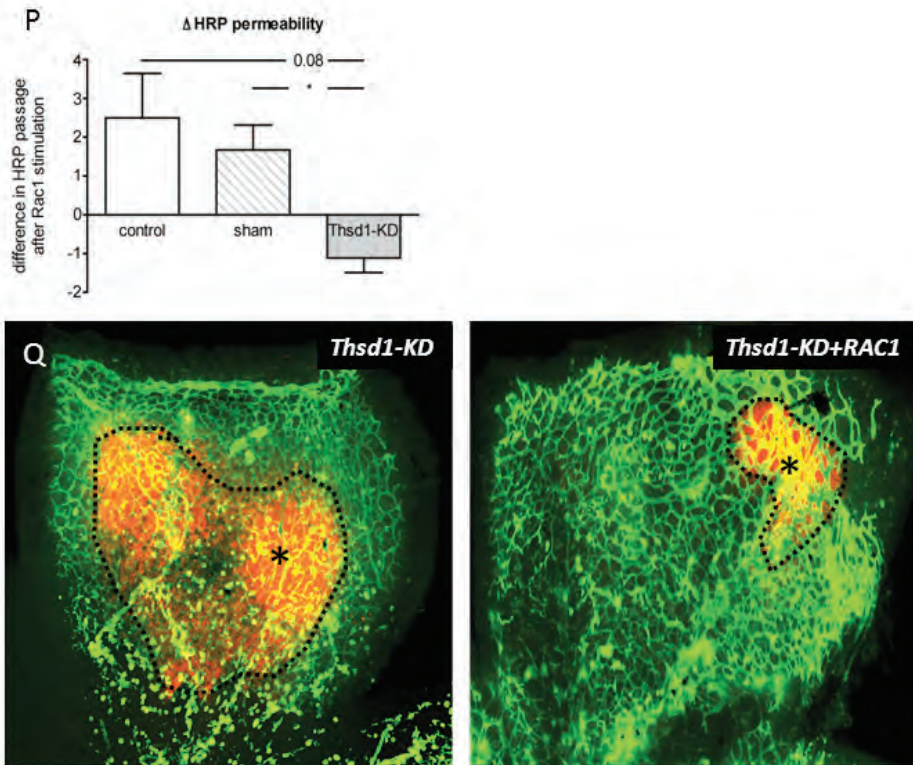


Figure 4

Thsd-1 binds CRT-LRP1 complex and induces actin cytoskeleton modulation via Rac1 activation. (A) Immunoprecipitation of *Thsd-1* in HUVECs showed an effective pull down of *Thsd-1* (upper panel) and co-immunoprecipitation of CRT (lower panel). Immunoprecipitation using a mouse IgG isotype control showed no effective pull down of *Thsd-1* or CRT. (B) Immunoprecipitation of CRT in HUVECs showed an effective pull down of CRT (upper panel) and co-immunoprecipitation of LRP1 (lower panel). Immunoprecipitation using a mouse IgG isotype control showed no effective pull down of CRT or LRP1. (C) Westernblot analysis of *Thsd-1* level in HUVECs transfected with *Thsd-1* targeting siRNA (*Thsd-1*-KD) or In HUVECs with adenovirus transfection mediated *Thsd-1* overexpression. (D) Co-immunoprecipitation of *Thsd-1* using IgG capture antibody directed against *Thsd-1* compared to IgG isotype control on the isolation beads in the membrane and cytosol fraction show that *Thsd-1* binding to CRT takes place in cell membrane fraction and cytosol fraction (shown are representative results of $n=2$). (E-K) Westernblot analysis of CRT-LRP1 downstream targets in *Thsd-1* silenced or overexpression conditions: *Thsd-1* silencing downregulated (E) FAK, (H) FAK-P and (I) PI3K-P, whereas (F) PI3K and (G) Rac1 were not affected. Overexpression of *Thsd-1* (*Thsd-1*-OE) enhanced (H) FAK-P, and (G) Rac1, whereas (E) FAK, (F) PI3K, and (I) PI3K-P remained unaffected. (J) *Thsd-1*-KD in HUVECs showed a decline in Rac1-GTP levels measured by GEF-assays, while *Thsd-1*-OE resulted in an increase in Rac1-GTP levels. ($n=4$; mean \pm SEM, * $P<0.05$, ** $P<0.01$) (L) Preincubation with 50 μ g/ml RAP before Rac1 activation with high serum medium limited the effect of *Thsd-1* overexpression on Rac1 activation. ($n=4$; mean \pm SEM, * $P<0.05$ versus sham, ** $P<0.05$ versus *Thsd-1*-OE).

Rac1 activity affects actin cytoskeleton dynamics during cell spreading. Actin mobility was assessed in a cell spreading assay. (M) 30 minutes post seeding, HUVECs transfected with si*Thsd-1* showed a delay in actin cytoskeleton spreading as compared to non-targeting siRNA sham transfected and untransfected and controls (sham and contr.). F-actin fibres are shown by phalloidin-rhodamin staining (red), nuclei are visualized with DAPI. (N) Quantification of the cell/actin surface area showed a decrease in the number of large cells (>1500 nm²) in *Thsd-1*-KD HUVECs (KD) as compared to non-transfected controls (co) and sham siRNA transfected cultures (sh) ($n=3$; mean \pm SEM, * $P<0.05$). (O) *Thsd-1*-KD reduced co-localization of VE-cadherin with the actin cytoskeleton at the cell-cell junctions, as demonstrated by intracellular immunofluorescent staining. VE-cadherin (green), F-actin (red), co-localized area (yellow) and nuclei (blue). Quantification of the % of actin filaments that are co-localized with VE-cadherin are shown in the lower graph. ($n=3$; mean \pm SEM, * $P<0.05$).

*Rac1 stimulation rescues impaired endothelial integrity in Thsd-1-depleted cells. (P) Measurement of endothelial barrier function in vitro. Differences in HRP passage in Rac1-stimulated HUVEC monolayers compared to no Rac1 activation after 120 minutes of thrombin activation are shown. Control, sham and Thsd-1-KD conditions without Rac1 activation were set to 0. Graphs indicate changes in HRP passage in response to Rac1 activation in the different groups (n=3; mean±SEM, *P<0.05). (Q) Representative pictures of double-stained retinas with isolectin GS-IB₄ (endothelial cells, green) and TER-119 (erythrocytes, red). Rac1 stimulation reduced area size of TER-119 erythrocytes accumulation (dotted area marked by asterisk symbol) after Thsd-1 knockdown (Thsd-1-KD) (n=5).*

to LRP1 was verified (Figure 4A, B). In addition, separation of the cytosolic and cell-membrane fraction demonstrated that Thsd-1 was present in both compartments (Figure 4D). Co-immunoprecipitation of the different fractions clearly showed that cell-membrane bound Thsd-1 could directly bind to CRT located in the same compartment, although Thsd-1 binding to CRT in the cytosol also takes place (Figure 4D). Western blot studies further demonstrated that the downstream signalling cascade of CRT-LRP1 was regulated by Thsd-1 (Figure 4C-K): knockdown of Thsd-1 (Figure 4C) decreased signal transduction via FAK by downregulation of FAK protein and phosphorylation levels (Figure 4E, H), while PI3K phosphorylation was diminished (Figure 4F, I). Further downstream, Thsd-1 silencing inhibited PI3K mediated Rac1 activation, demonstrated by a decline in Rac1-GTP levels, while total Rac1 protein levels remained unaffected (Figure 4G, J). These findings are further strengthened by the effect of Thsd-1 overexpression: HUVECs transfected with an Adenoviral plasmid expressing human Thsd-1 cDNA showed opposite effects with increased FAK phosphorylation and Rac1 activation as compared to sham adenovirus treated controls (Figure 4C-K). A LRP1 blocking study with RAP (Receptor Associated Protein) was conducted to verify direct Thsd-1 involvement in CRT-LRP1 signaling. Indeed, RAP treatment blocked Rac1 activation in Thsd-1 overexpressing HUVECs, indicating that LRP1 activation via Thsd-1-CRT complex formation is relevant for Thsd-1 signaling via Rac1 (Figure 4L).

Rac1 is an important mediator of endothelial barrier function as it enforces cell-cell and cell-matrix interaction via regulation of the actin cytoskeleton⁷⁻⁹. To study the Rac1-mediated function of Thsd-1 in actin dynamics, si-Thsd-1, si-sham and control ECs were evaluated in an adhesion assay in which cells were seeded on a collagen-coated surface. Cell spreading and actin filaments distribution was evaluated at different timepoints post-seeding (Figure 4M). Quantification and stratification of cell size showed that Thsd-1 knockdown induced a trend towards decrease in the number of large cells (>1500 nm²) compared to si-sham transfected controls (Figure 4N). This decline in cell size and thus spreading efficiency was associated with a defect in cell-extracellular matrix interaction: Paxillin and vinculin visualization of focal adhesion (FA) sites showed a significant decline of FA capping at stress fiber ends in Thsd-1-silenced cells versus control conditions at different time points post-cell seeding.

Loss of association between VE-cadherin and the actin cytoskeleton at cell-cell junction sites promotes endothelial and vascular permeability⁶. Therefore, the effect of Thsd-1 knock-

down was assessed on VE-cadherin/actin cytoskeleton association in a confluent HUVEC monolayer. Knockdown of Thsd-1 in HUVECs reduced co-localization of VE-cadherin with the actin cytoskeleton compared with sham transfected and untransfected controls (Figure 4O).

Taken together these data indicate that Thsd-1 modulates cell-cell interaction via a signalling mechanism that involves CRT-LRP1, FAK, PI3K and Rac1-mediated regulation of the endothelial cytoskeleton.

Rac1 activation prevents loss of endothelial barrier function induced by Thsd-1 knockdown

Our experiments point towards a Rac1-mediated loss of endothelial integrity in response to Thsd-1 silencing. To validate whether this Thsd-1-induced modulation of Rac1 activity is crucial for this process, si-Thsd-1 transfected HUVECs were treated with a pharmaceutical activator for Rac1 in the transwell permeability assay *in vitro*. Rac1 stimulation rescued endothelial permeability after Thsd-1 knockdown (Figure 4P), thus confirming that Thsd-1-induced loss of endothelial permeability in cultured cells was indeed mediated via Rac1 inhibition. To further validate these *in vitro* findings, a phenotype rescue experiment was carried out in the murine retina vascularisation model: Thsd-1 was silenced in combination with treatment with the Rac1 activator and compared to controls that had been treated with intra-ocular injection of si-Thsd-1 only. In line with our *in vitro* findings, Rac1 activation reversed the effects of Thsd-1 silencing with a significant reduction in the extend of vascular haemorrhaging (Figure 4Q). Combined, these data provide evidence that Thsd-1 regulates endothelial permeability via Rac1 activation.

Thsd-1 correlates with neovascular intraplaque haemorrhaging and increased plaque vulnerability.

Intimal neovascular growth of highly permeable vessels with compromised vascular integrity is an important contributor to atherosclerotic lesion progression and plaque destabilization. Previous reports demonstrated an association between changes in expression levels of VE-cadherin and loss of endothelial cell-cell contacts in plaque neovessels with intimal extravasation of blood-derived cells²⁵, while increased Rac1 activation was correlated to lesion advancement²⁶, suggesting an involvement of these molecular regulators of cell-cell barrier function. Next, we investigated the possible role of Tsdh1 in the patho-biology of the compromised neovasculature in advanced atherosclerotic lesions. A correlation study was carried out in human atherosclerotic plaques that were obtained from patients with symptomatic carotid artery disease. Plaques were divided into stable plaques and advanced plaques vulnerable to rupture with pathological evidence of intraplaque haemorrhage. Thsd-1 and CD31 expression was determined by immunohistochemistry (Figure 5A, B). The ratio of CD31+ endothelial cells expressing Thsd-1 was significantly increased in vulnerable plaques with intraplaque haemorrhage compared to stable plaques, $0.34 \pm 0.04\%$ vs. $0.20 \pm 0.03\%$ of

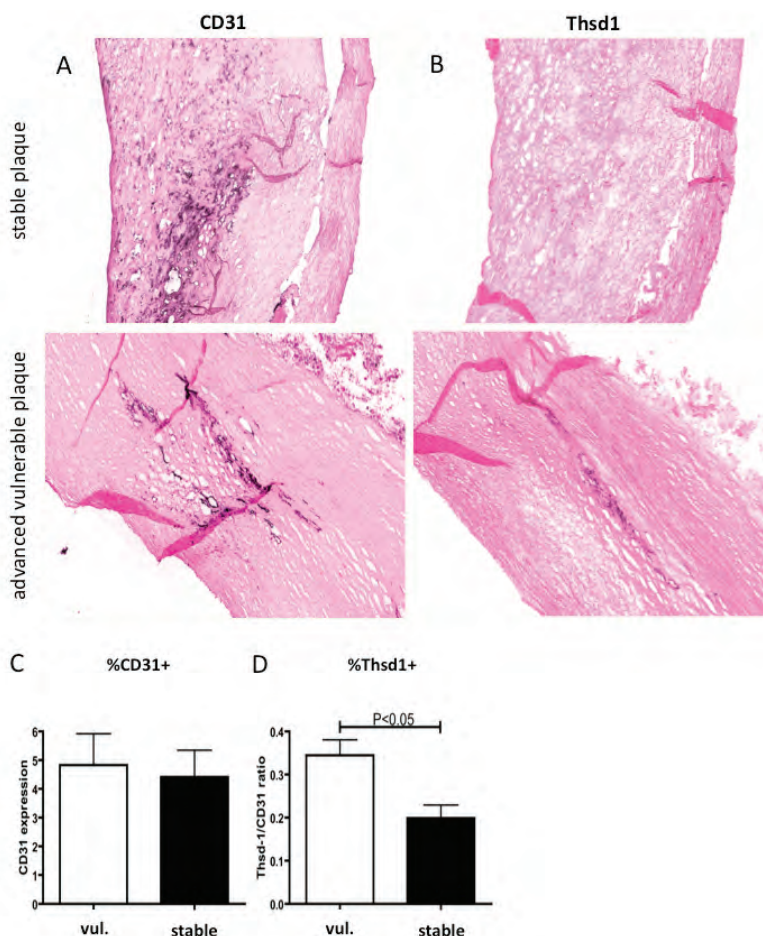
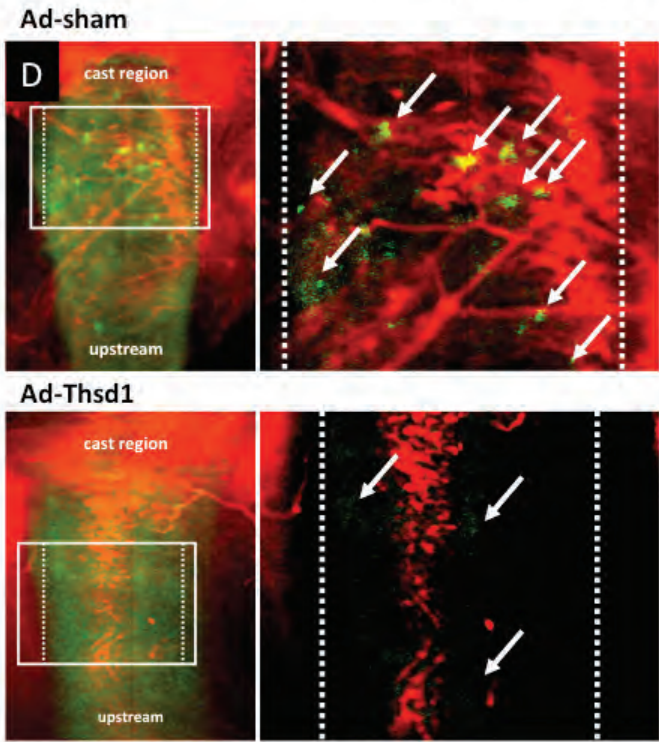
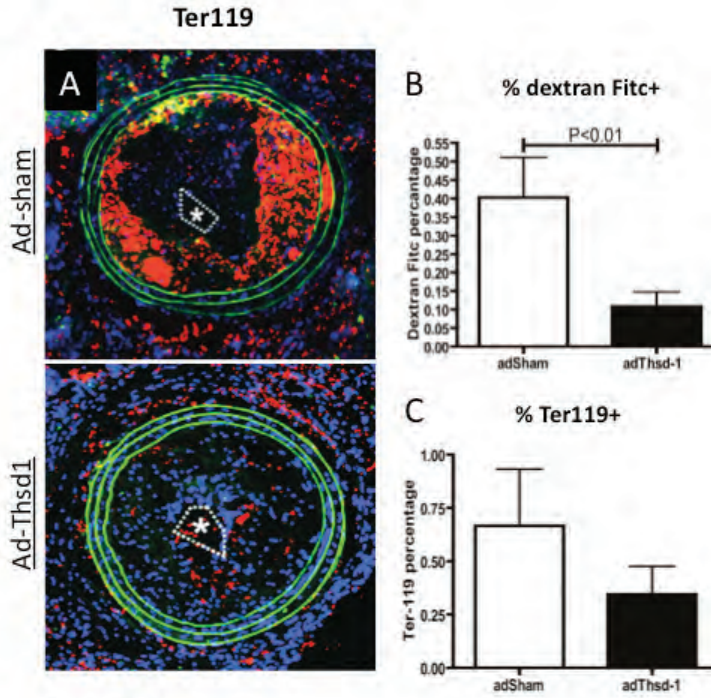
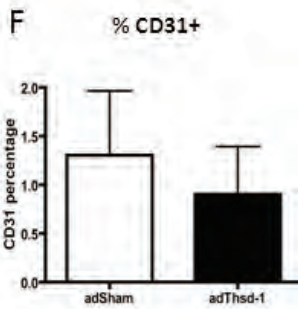
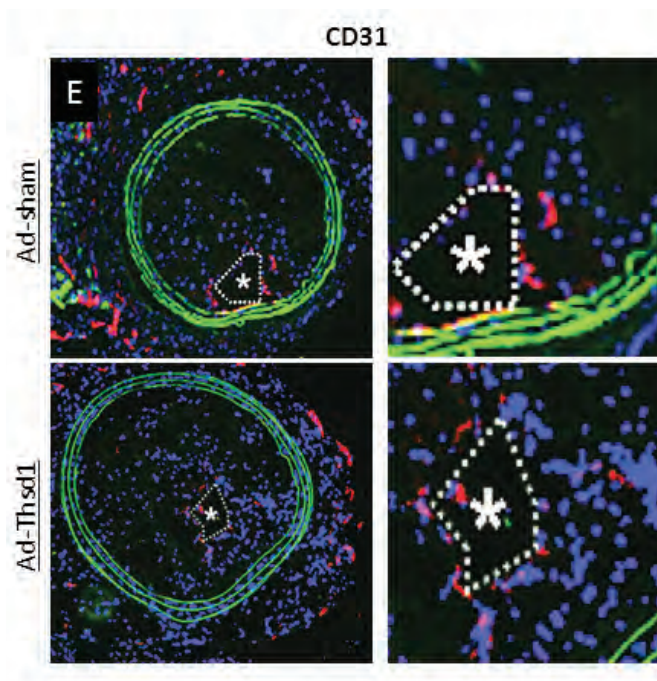


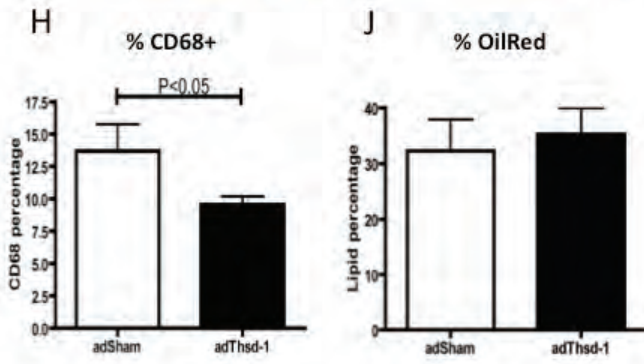
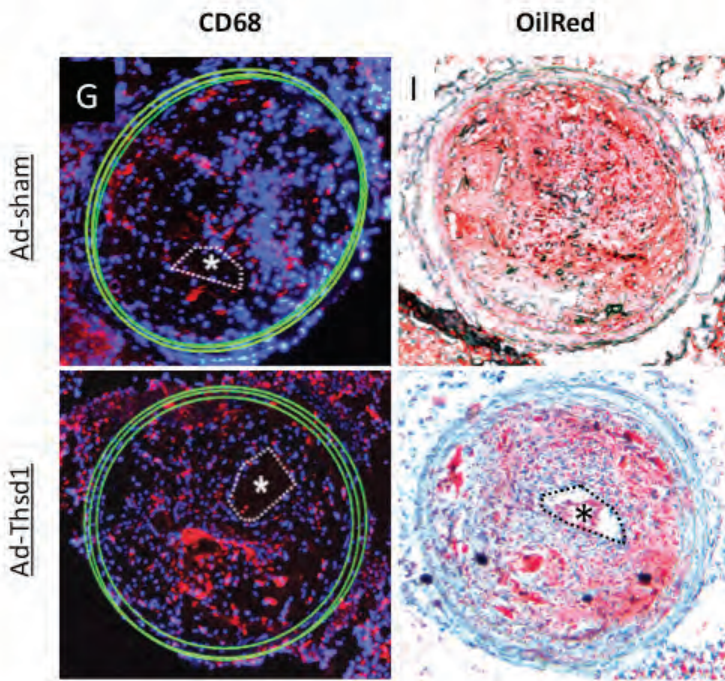
Figure 5

Thsd-1 expression correlates with vascular haemorrhaging in advanced atherosclerotic plaque vulnerable to rupture. Representative sections of carotid endarterectomy specimens stained for (A) CD31 and (B) Thsd-1. Specimens were divided in stable plaque (upper row) and advanced vulnerable plaque lesions with intraplaque haemorrhage (lower row). (C) Quantification of CD31 expression in stable plaque (stable) and vulnerable plaque (vul.) with intraplaque haemorrhage. No significant difference in CD31 expression between the two groups was observed. (D) Quantification of Thsd-1/CD31 ratio in stable plaque and vulnerable plaque with intraplaque haemorrhage. Thsd-1/CD31 ratio was significantly increased in vulnerable plaque specimens with intraplaque haemorrhage (n=5; mean±SEM, $P < 0.05$)

total intimal area (Figure 5D). This was independent of the degree of vascularisation, as there was no difference in CD31 expression between stable plaques and vulnerable plaques with intraplaque haemorrhage, $4.8 \pm 1.1\%$ vs. $4.4 \pm 0.9\%$ of total intimal area (Figure 5C). These results point towards a possible role for Thsd-1 in endothelial barrier dysfunction in advanced atherosclerotic lesions that are vulnerable to rupture.







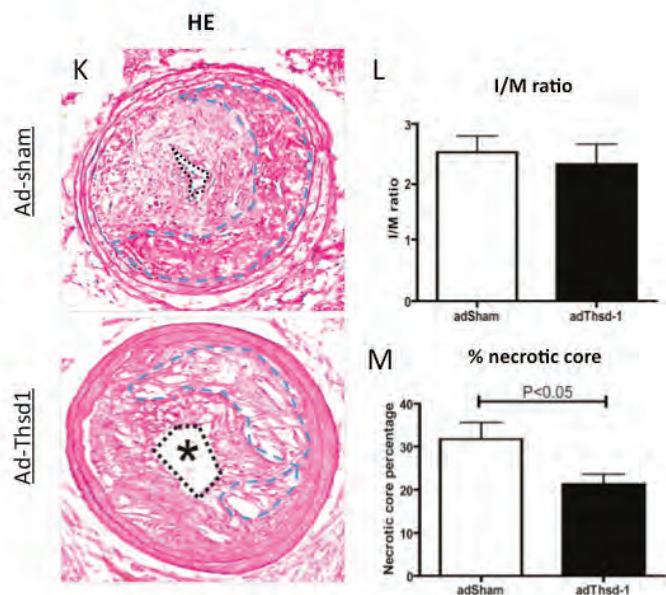


Figure 6

Overexpression of Thsd-1 attenuates intraplaque haemorrhaging and stabilizes plaque phenotype in a murine model for vulnerable plaque. (A) Representative sections stained for Ter119 of ad-sham and ad-Thsd-1 treated advanced murine lesions. (B) Quantification of % Dextran Fitc+ area, and (C) % Ter119+ area. (D) Whole mount immunostaining of the adventitial vasculature with isolectin GS-IB₄ (endothelial cells, red) with detection of Dextran Fitc perivascular leakage (green, indicated by arrows) in the upstream (atherosclerotic) carotid region from the flow device. Dotted lines indicate vessel boundaries (n=6). (E) Representative sections stained for CD31 of ad-sham and ad-Thsd-1 treated advanced murine lesions. (F) Quantification of % CD31+ area. (G) Representative sections stained for CD68 of ad-sham and ad-Thsd-1 treated advanced murine lesions. (H) Quantification of % CD68+ area. (I) Representative sections stained for lipids of ad-sham and ad-Thsd-1 treated advanced murine lesions. (J) Quantification of % Oilred O+ area. (K) Representative hematoxylin-eosin staining of ad-sham and ad-Thsd-1 treated advanced murine lesions. (L) Quantification of intima/media (I/M) ratio and (M) % necrotic core area. For all micrographs, lumen areas are indicated by dotted lines (white) marked by an asterisk symbol. Necrotic core areas are indicated by dotted lines in blue. For A, E, and G: green is autofluorescence of elastin fibres, blue is DAPI, red is Ter119, CD31, and CD68 respectively. (n=10; mean±SEM, P<0.05)

Thsd-1 attenuates intraplaque haemorrhage and plaque destabilization, without affecting neovascular growth.

Our previous *in vivo* and *in vitro* findings indicate that Thsd-1 is a beneficial factor for maintaining endothelial barrier function. Here we hypothesized that Thsd-1 overexpression may reduce vascular bleeding in vulnerable plaque. The effect of Thsd-1 overexpression was assessed in our ApoE^{-/-} vulnerable plaque model. Peri-adventitial adenoviral transfection of an expression plasmid encoding for murine Thsd-1 cDNA in the carotid artery resulted in a significant increase in Thsd-1 mRNA expression compared to transfection with a control adenoviral vector (ad-Thsd-1 and ad-sham respectively, P < 0.05). Endogenous Thsd-1 expression in the carotid arteries of non-treated ApoE^{-/-} mice was significantly increased in response to 1 week of feeding of a high cholesterol high fat diet. Overexpression of Thsd-1 induced clear attenuation of the plaque phenotype at 9 weeks post flow-alteration and

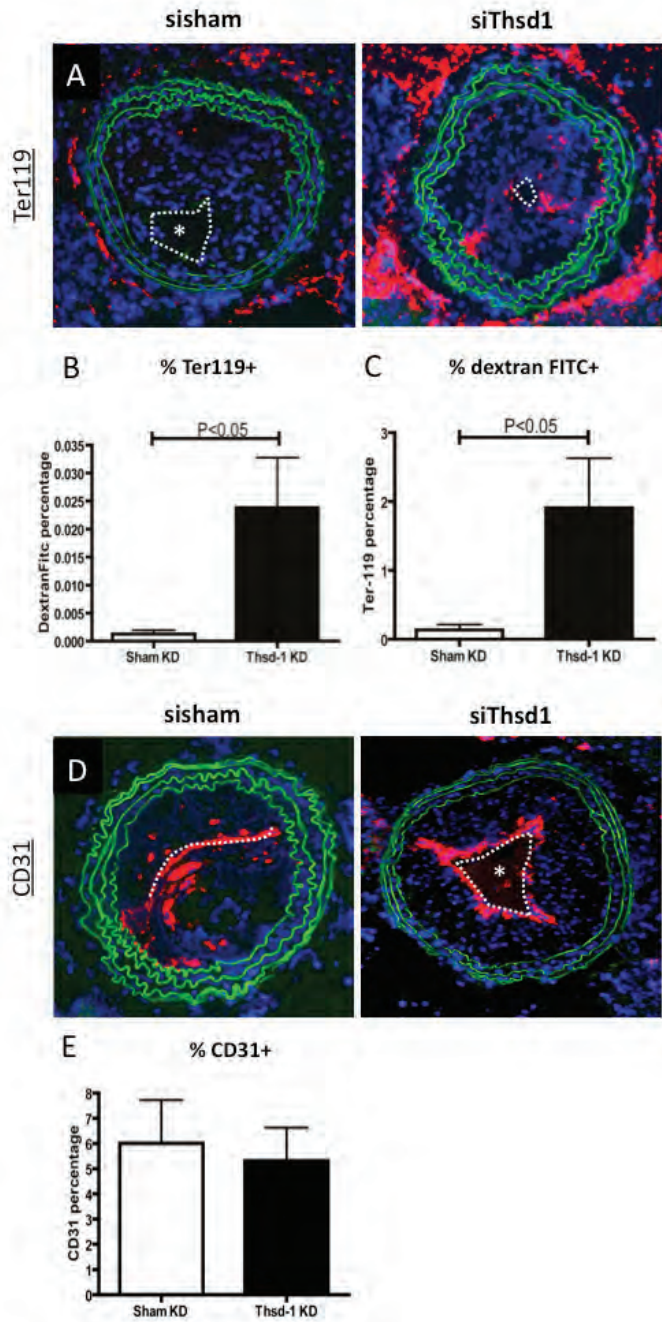
atherosclerosis induction, indicated by a significant 75% decrease in neovascular leakage, as measured by Dextran-FITC extravasation in ad-Thsd-1 treated murine carotid arteries compared to ad-sham treated controls ($P < 0.01$, Figure 6A, B). This observation was also validated by Ter-119 immunohistological detection of perivascular accumulation of erythrocytes (Figure 6A, C). A reduction in vascular leakage was also detected in the plaque adventitial area, where Thsd-1 reduced Dextran-Fitc leakage with 75% ($P < 0.05$) as observed by whole mount visualization by confocal microscopy (Figure 6D). These effects were independent of intimal neovascular growth, as no changes in numbers of CD31+ endothelial structures were observed (Figure 6E, F). Coincided with improved neovascular integrity, a 40% reduction in intraplaque macrophages accumulation in the Thsd-1 overexpression group was observed (Figure 6G, H), whereas intraplaque lipid accumulation remained unaffected ($P < 0.05$, Figure 6I, J). This reduction in percentage of intraplaque macrophages did not affect lesion size as measured by intima/media ratio (figure 6K, L). However necrotic core area was significantly decreased (Figure 6M). Together, these data clearly demonstrate that Thsd-1 overexpression is capable to restore compromised endothelial barrier function in vulnerable plaque.

siRNA mediated silencing of Thsd-1 aggravates vascular leakage in murine vulnerable plaque.

The protective function of Thsd-1 in the vasculature of vulnerable plaque is also validated by a Thsd-1 knockdown experiment in the same murine vulnerable plaque model: Thsd-1 knockdown of the atherosclerotic carotid arteries was achieved by siRNA mediated silencing, as shown by qPCR validation. In line with previous results, Thsd-1 knockdown in the murine vulnerable plaque model severely aggravated vascular leakage, shown by a 2000% increase in Dextran-Fitc perivascular leakage (Figure 7A, B) and a 500% increase in intimal extravascular accumulation of Ter-119+ erythrocytes ($P < 0.05$, Figure 7C). Like in the Thsd-1 overexpression condition, no effect of Thsd-1 knockdown on intimal neovascular growth was observed, as no difference in CD31+ endothelial structures was detected (Figure 7D, E). However, Thsd-1 knockdown did not affect intraplaque macrophage or lipid accumulation (Figure 7F, G). Lesion and necrotic core size also remained unaffected (Figure 7H, I).

Pro-atherogenic and anti-atherogenic stimuli determine Thsd-1 mRNA expression in HUVECs.

Combined, these results of our murine disease model for vulnerable plaque clearly demonstrate that Thsd-1 attenuates vascular haemorrhaging and plaque destabilization by enhancing intimal neovascular integrity. To further characterize the influence of atherogenic triggers on Thsd-1 expression in atherosclerosis, we assessed the effect of two well-known pro-atherogenic stimuli (low oxygen and the pro-inflammatory cytokine TNF α) and one anti-atherogenic stimulus (the anti-inflammatory cytokine IL-10) on Thsd-1 expression in HUVECS.



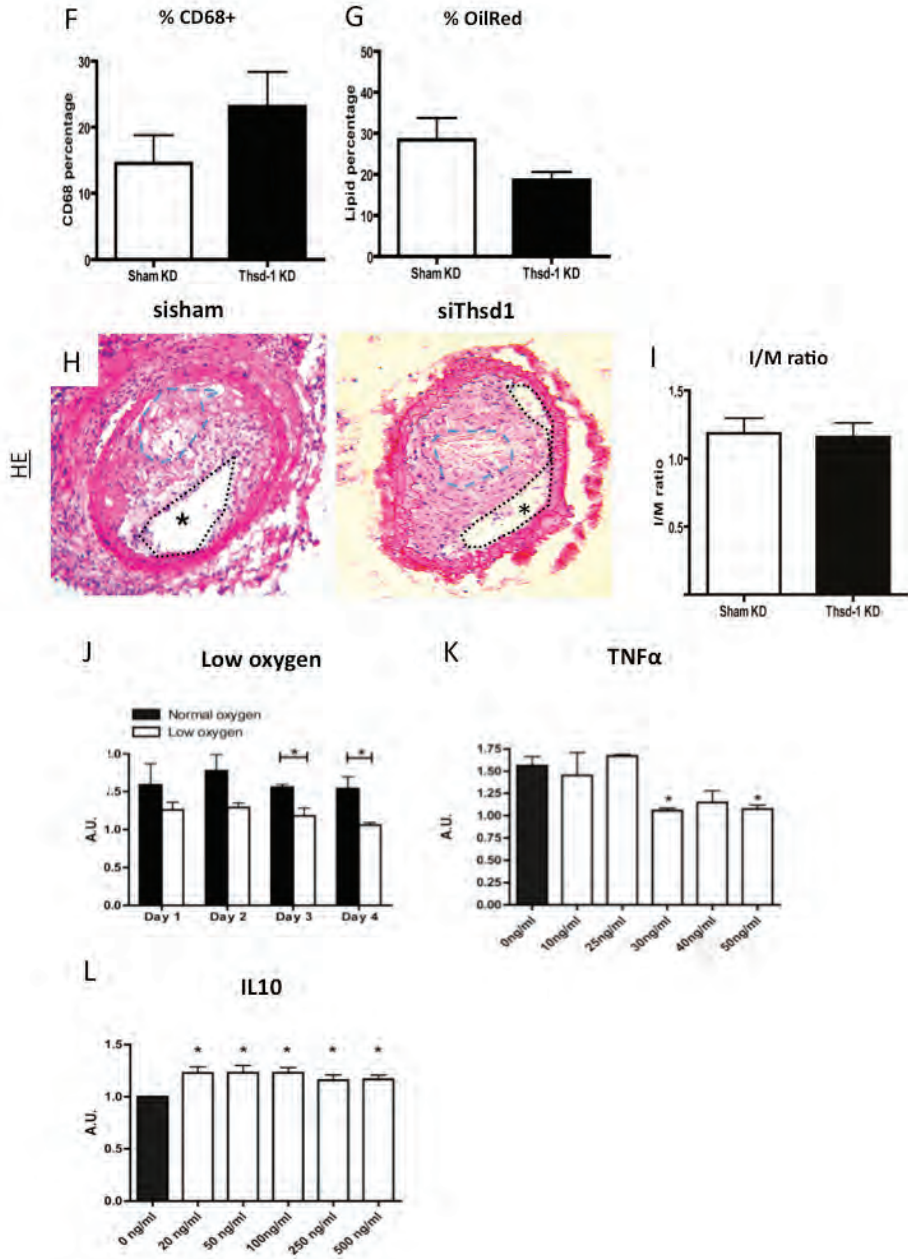


Figure 7

Thsd-1 knockdown severely aggravates intraplaque haemorrhaging in murine vulnerable plaque. (A) Representative sections stained for Ter119 of sisham and siThsd-1 treated advanced murine lesions. (B) Quantification of % Dextran Fitc+ area, and (C) % Ter119+ area. (D) Representative sections stained for CD31 of ad-sham and ad-Thsd-1 treated advanced murine lesions. (E) Quantification of % CD31+ area. (F) Quantification of % CD68+ area. (G) Quantification of % Oilred O+ area. (H) Representative hematoxylin-eosin staining of ad-sham and ad-Thsd-1 treated advanced murine lesions. (I) Quantification of intima/media (I/M) ratio. For all micrographs, lumen areas are indicated by dotted lines (white) marked by an asterisk symbol. Necrotic core areas are indicated by dotted lines in blue. For A, and D: green is autofluorescence of elastin fibres, blue is DAPI, red is Ter119, and CD31 respectively. (n=10; mean±SEM), P<0.05.

*Pro-atherogenic and anti-atherogenic stimuli determine Thsd-1 mRNA expression. Response of endogenous Thsd-1 expression levels in HUVECs to pro-atherogenic stimuli, including (J) low (3%) and normal (20%) oxygen conditions over time, and (K) different concentrations of TNFα. (L) Response of endogenous Thsd-1 expression to anti-atherogenic stimulus IL-10. Thsd-1 expression in endothelial cells was diminished by pro-atherogenic stimuli, while anti-atherogenic stimulus IL-10 increased Thsd-1 mRNA expression. (n=4; mean±SEM, *P<0.05)*

HUVECS were exposed to low oxygen (3%) conditions for four days and compared to normal oxygen (20%) cultures. From day 1, a steady decrease in Thsd-1 mRNA levels was observed compared to normal oxygen controls. On day 3 and 4, Thsd-1 mRNA expression was significantly decreased in HUVECS exposed to low oxygen (Figure 7J). Likewise, stimulation with different concentrations of the pro-atherogenic cytokine TNFα also decreased Thsd-1 mRNA expression in HUVECs (Figure 7K). In contrast, the anti-atherogenic cytokine IL-10 triggered a rise in Thsd-1 expression levels (Figure 7L). Thus the anti-atherogenic and pro-atherogenic factors that are abundant in the micro-environment of advanced atherosclerotic lesions determine the expression level of cell-cell barrier function protective Thsd-1.

DISCUSSION

In this study we have for the first time identified Thsd-1 as a potent angiogenic regulator during embryonic and post-natal vascular development. We showed that Thsd-1 was upregulated in the developing murine embryo in Flk1 positive angioblasts compared to Flk1 negative cells, while whole mount *in situ* hybridization in developing zebrafish larvae validated the predominant vascular expression of Thsd1. The thrombospondin type I domain (TSP1) in the Thsd-1 protein shares a high homology (98%) with the TSP1 domain of Thrombospondin 1, a gene known for its anti-angiogenic properties^{23, 27}. Reports indicate that upregulation of the zebrafish Thrombospondin 1 orthologue by mRNA injection of eleven-nineteen lysine-rich leukemia (ELL) - a transcription factor of Thrombospondin 1 - resulted in multiple vascular haemorrhaging²⁸. Unlike Thrombospondin 1, the basic function of Thsd-1 in vascular development was until now, still largely unknown. Based on the specific expression of Thsd-1 in the EC subset, we hypothesized that Thsd-1 may play a functional role in angiogenesis. Indeed, knockdown of Thsd-1 in the developing zebrafish with MO injections resulted in frequent and severe haemorrhaging in the head region.

Coinciding with this finding, the cranial region was also the location of high Thsd-1 expression in the cerebral vasculature during early development. In addition, multiple previous studies have suggested that the cranial vasculature may be a predilection site for vascular rupture in the zebrafish model^{13, 17, 21}. Several zebrafish mutants have been identified that display a very similar vascular haemorrhaging phenotype, including *heg1*, *ccm1*, *ccm2* and *ccm3*^{17, 29, 30}. Like Thsd-1, these genes appear to be involved directly or indirectly in Rac1 activation and RhoA degradation³¹. Little is known about the biochemical and physical properties of Thsd-1. Previously, it has been demonstrated that the Thsd-1 gene is located between FLJ11712 and C13orf9 within 13q14.3 and has three transcripts (splice variants) of which isoform 1 and 2 are single-pass type I membrane proteins, while isoform 3 is secreted extracellularly into the blood plasma. Thsd-1 is a glycoprotein of 852 amino acids (94584 Da) synthesised by many cells and contains a type 1 thrombospondin domain (TSP1), which has been found in a number of proteins involved in the complement pathway, as well as in ECM proteins³²⁻³⁴.

Our studies indicate that whereas the vascular integrity seemed to be affected by Thsd-1 silencing, the vascular cerebral network appeared to remain intact. This distinct phenotype was once again observed when Thsd-1 was silenced in a murine retinal model for angiogenesis³⁵, in which Thsd-1 knockdown with siRNA resulted in vascular haemorrhages, independent of changes in vascular macrostructures such as outgrowth of the vasculature towards the border and total number of vessels. To obtain more insight in the molecular mechanisms by which Thsd-1 affects vascular integrity without affecting vascular growth, we studied the function of Thsd-1 in HUVEC in a number of *in vitro* assays. Cultured monolayers of Thsd-1-silenced HUVECs reacted in line with the observed phenotype *in vivo*, demonstrating that cell-cell barrier function was diminished in a transwell permeability assay. On the other hand, sprouting capacity remained unaffected as shown by 2D matrigel assay. Further evaluation of the binding partners and downstream pathways of Thsd-1 identified CRT of the CRT-LRP1 complex as a direct downstream effector of Thsd-1, and clarified that Thsd-1 modulates cell-cell barrier function via a Rac1-actin cytoskeleton mediated pathway in which FAK-PI3K signalling is involved. It has to be noted that LRP1 immunoblotting of Thsd-1 pulldown lysates shows only a very weak LRP1 band (data not shown). As LRP1 can be detected as a clear band in CRT pulldown samples, these findings imply that LRP1 is not directly associated to Thsd-1, but forms a complex with Thsd-1 via the intermediate adaptor function of CRT.

Rac1 activity is crucial for the process of cell spreading, as it decreases cell contractility via actomyosin suppression and counteracts RhoA-induced actin stress fibre formation.³⁵ In addition, activation of Rac1 has been reported to preserve cell-cell junction formation and thereby endothelial barrier function^{36, 37}. Here our data clearly show that Thsd-1 is involved in Rac1 activation and that Thsd-1 knockdown diminished adaptation of the actin cytoskeleton of ECs during cell adhesion.

It was previously reported that cells with impaired interaction between the actin cytoskeleton and cell-cell junction sites were able to proceed through the early phase of *in vitro* network-formation, while in the later phases of angiogenesis increased rigidity of the actin cytoskeleton resulted in loss of endothelial barrier function³⁸. In the later phase of vascular development, the maturation of newly formed vessels in response to biological and biomechanical cues - such as pericyte stimulation and blood flow - are characterized by the transition of 'pro-angiogenic' ECs into the quiescent phalanx cell phenotype. Acquisition of this phalanx cell phenotype includes strengthening of the cell-cell junctions mediated by VE-cadherin, and involves modulation in junction complex assembly, restriction of VEGFR2 signalling and actin cytoskeleton reorganization³⁹. In the light of the findings reported in this study, Thsd-1 silencing may therefore compromise vascular integrity by inhibiting Rac1 modulation of the actin cytoskeleton in late angiogenesis during this transition into quiescent phalanx cell phase. Indeed, qPCR evaluation of cocultures of HUVECs with human brain-derived pericytes in a duochamber system that enables direct reciprocal contact, showed that Thsd-1 expression was significantly induced by pericyte stimulation (preliminary data, not shown). However, further evaluation of typical neovessel stabilizing or mural cell (VSMC or pericytes) recruitment factors, including Angtp1 and 2, Tie2, PDGFBB, PDGFR2, VEGFA and VEGFR2, showed no changes in response to Thsd-1 silencing (preliminary data, now shown). Additional studies are needed to clarify the potential role of Thsd-1 in neovessel stabilization. Rac1 activation is regulated by FAK⁴⁰. Previously, it has been demonstrated that Thrombospondin 1 binds to CRT, leading to stabilization of the CRT-LRP1 complex on the cell surface resulting in downstream activation of FAK⁴¹. As Thsd-1 shares a similar domain with Thrombospondin 1, we hypothesized that Thsd-1 could likewise bind to CRT. Our data confirmed complex formation of Thsd-1 and CRT. In addition, the downstream activation of the CRT-LRP1/FAK signalling cascade was verified *in vitro* and *in vivo*. We further demonstrated that PI3K activation, downstream of FAK, was inhibited by Thsd-1 knockdown. Previously, it was demonstrated that PI3K is involved in the regulation of vessel integrity during embryonic development and tumour neovascularisation. Loss of PI3K led to depolarization or junction disassembly, which resulted in weak cell-cell junctions, leakage and structural failure⁴². Over-expression of PI3K promotes Rac1 activity⁴³. In line with these findings, our data demonstrate that loss of Thsd-1 inhibited FAK-PI3K signalling, which was associated with a decrease in Rac1 activity. These findings provide further proof that Thsd-1 regulates vessel integrity by a Rac1-mediated pathway (Figure 8).

As endothelial cell-cell barrier function and neovascular integrity play important roles in progression and destabilization of rupture prone atherosclerotic lesions, we aimed to evaluate the function of Thsd-1 in this widespread vascular-related disease. Advanced atherosclerotic lesions in humans are characterized by intimal growth of a neovasculature with apparent compromised integrity. Immunopathological assessment of human carotid endarterectomy

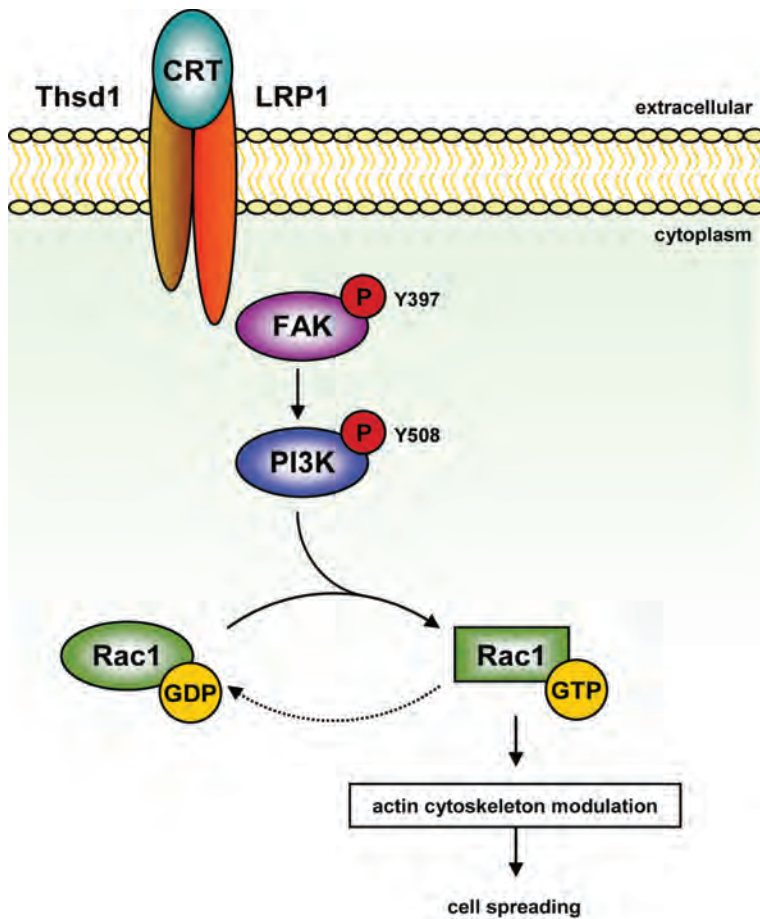


Figure 8

Molecular pathway of Thsd-1 during angiogenesis. Thsd-1 maintains vascular integrity by its interaction with CRT on the cell surface, stabilising the CRT-LRP1 complex. Complex stabilisation results in downstream activation of FAK and PI3K, which increases Rac1-GTP levels. Rac1 regulates cell spreading by actin cytoskeleton modulation and maintains endothelial integrity by strengthening VE-cadherin/actin bonds.

specimens demonstrated that Thsd-1 expression was significantly increased in advanced vulnerable lesions with intraplaque haemorrhaging compared to stable plaques, suggesting a compensatory upregulation of Thsd-1 to maintain vascular integrity in the intimal neovascular endothelium. This idea of a Thsd-1-involved feedback mechanism in order to preserve cell-cell barrier function was validated by our Thsd-1 gain and loss of function studies in the murine vulnerable plaque model: Thsd-1 overexpression led to less intraplaque haemor-

rhaging as measured by a lower percentage of intraplaque erythrocytes and a decrease in intraplaque Dextran-Fitc leakage.

Methia and co-workers previously showed that ApoE^{-/-} mice on a high cholesterol diet exhibited dramatic blood-brain-barrier defects. ApoE consists of three isoforms, ApoE2, ApoE3 and ApoE4. It was further demonstrated that ApoE4 is a major risk factor for Alzheimer disease (Gene dose of apolipoprotein E type 4 allele and the risk of Alzheimer's disease in late onset families⁴³). Interestingly, Nishitsuji and co-workers could prove that the effect of ApoE on blood brain barrier leakage was isoform dependent as ApoE4 knock-in mice showed a more severely compromised blood brain barrier function than ApoE3 knock-in mice⁴⁴. Later, Bell and coworkers showed that ApoE, ApoE3 and ApoE4 regulate blood brain barrier permeability via the CypA-NFκB-MMP 9 pathway. ApoE and ApoE3 are both known to suppress CypA-NFκB-MMP 9 activation via LRP1⁴⁵. In contrast, the working mechanism of ApoE4 is LRP1 independent of MMP9.

Potentially, the LRP1-mediated inhibition of CypA-NFκB-MMP 9 signalling could represent a second mechanism via which Thsd-1 regulates vascular permeability; Thsd-1 may activate LRP1 leading to decreased CypA levels and subsequently less nuclear NFκB translocation and MMP 9 activation, thus contributing to endothelial integrity. Although it has been shown that Thrombospondin influences MMP 9 activity, it has not yet been shown that this pathway also acts via LRP1. Additional studies are needed to further elucidate the contribution of Thsd-1 function to vascular integrity via MMP9 activation.

There is emerging evidence that intraplaque haemorrhaging plays an important role in plaque progression towards a vulnerable plaque^{46,47}. Furthermore, intraplaque haemorrhaging is correlated with plaque rupture and predicted future cardiovascular events and outcome in cardiovascular patients^{48,49}. Intraplaque haemorrhage is the result from extravasation of erythrocytes from newly formed vessels. Neovascularisation, driven by intraplaque hypoxia⁵⁰, results in the formation of immature and fragile vessels under influence of VEGF-A. These immature and fragile vessels have a greater vascular permeability resulting in the extravasation of leucocytes and erythrocytes, leading to an increase in inflammatory response, expansion of the necrotic core and intraplaque haemorrhaging. Stabilization of these so-called leaky vessels might prevent plaque destabilization and formation of a vulnerable plaque¹⁰. Remarkably, macrophage accumulation and necrotic core size were in decline after Thsd-1 was overexpressed in our vulnerable plaque animal model. This indicates that as Thsd-1 attenuates endothelial dysfunction in atherosclerosis, the beneficial effects of improved neovascular integrity in the lesion also slow down plaque progression. Overall, Thsd-1 overexpression led to a more stable plaque phenotype compared to sham treated animals, an effect that was independent of neovascular growth as there was no difference in percentage of adventitial or intimal endothelial structures. A limitation of these overexpression studies is that adThsd-1 virus transfection could not be achieved selectively, and overexpression of Thsd-1 in non-endothelial cells may contribute to the observed findings. However, by con-

ducting Thsd-1 loss of function studies in the same animal model, the essential role of Thsd-1 in the regulation of vascular integrity and attenuation of atherosclerosis progression could be confirmed: in contrast to Thsd-1 overexpression, Thsd-1 knockdown led to a significant increase in intraplaque erythrocyte and Dextran-Fitc perivascular leakage without affecting neovascular growth.

In conclusion, here we have identified Thsd-1 as a new regulator of vascular integrity in vascular development and advanced vascular disease. To our knowledge, this study is the first report of the biological function of Thsd-1 in ECs during normal embryonic and postnatal blood vessel formation. In advanced atherosclerotic lesions, Thsd-1 is involved in maintaining cell-cell barrier function in the intraplaque neovasculature and protects the plaque from extensive haemorrhaging and further disease progression. In the light of our findings of the basic and pathobiological function of Thsd-1, the gene may be considered an interesting research target for the development of novel diagnostics and therapeutics in the treatment of atherosclerosis and other vascular-related diseases in which the pathophysiology entails loss of bloodvessel integrity.

Sources of Funding

This work was supported by grants from the Dutch Heart Foundation (grant nr. 2011T072) (G.P.v.N.A.) and the Dutch Organisation for Scientific Research (grant nr. 91776325 and 91696061) (H.J.D. and C.C respectively).

Disclosures

None.

REFERENCES

1. Klaassen I, Van Noorden CJ, Schlingemann RO. Molecular basis of the inner blood-retinal barrier and its breakdown in diabetic macular edema and other pathological conditions. *Prog Retin Eye Res.*
2. Vandembroucke E, Mehta D, Minshall R, Malik AB. Regulation of endothelial junctional permeability. *Ann N Y Acad Sci.* 2008;1123:134-145
3. Tian X, Tian Y, Sarich N, Wu T, Birukova AA. Novel role of stathmin in microtubule-dependent control of endothelial permeability. *FASEB J.*26:3862-3874
4. Spindler V, Schlegel N, Waschke J. Role of gtpases in control of microvascular permeability. *Cardiovasc Res.*87:243-253
5. Broman MT, Mehta D, Malik AB. Cdc42 regulates the restoration of endothelial adherens junctions and permeability. *Trends Cardiovasc Med.* 2007;17:151-156
6. Kim SH, Cho YR, Kim HJ, Oh JS, Ahn EK, Ko HJ, Hwang BJ, Lee SJ, Cho Y, Kim YK, Stetler-Stevenson WG, Seo DW. Antagonism of vegf-a-induced increase in vascular permeability by an integrin alpha3beta1-shp-1-camp/pka pathway. *Blood.*120:4892-4902
7. Huvencers S, Oldenburg J, Spanjaard E, van der Krogt G, Grigoriev I, Akhmanova A, Rehmann H, de Rooij J. Vinculin associates with endothelial ve-cadherin junctions to control force-dependent remodeling. *J Cell Biol.*196:641-652
8. Hoang MV, Nagy JA, Senger DR. Active rac1 improves pathologic vegf neovessel architecture and reduces vascular leak: Mechanistic similarities with angiopoietin-1. *Blood.*117:1751-1760
9. Kraemer A, Goodwin M, Verma S, Yap AS, Ali RG. Rac is a dominant regulator of cadherin-directed actin assembly that is activated by adhesive ligation independently of tiam1. *Am J Physiol Cell Physiol.* 2007;292:C1061-1069
10. Jain RK, Finn AV, Kolodgie FD, Gold HK, Virmani R. Antiangiogenic therapy for normalization of atherosclerotic plaque vasculature: A potential strategy for plaque stabilization. *Nat Clin Pract Cardiovasc Med.* 2007;4:491-502
11. Sluimer JC, Daemen MJ. Novel concepts in atherogenesis: Angiogenesis and hypoxia in atherosclerosis. *J Pathol.* 2009;218:7-29
12. Takayanagi S, Hiroyama T, Yamazaki S, Nakajima T, Morita Y, Usui J, Eto K, Motohashi T, Shiomi K, Keino-Masu K, Masu M, Oike Y, Mori S, Yoshida N, Iwama A, Nakauchi H. Genetic marking of hematopoietic stem and endothelial cells: Identification of the tmtsp gene encoding a novel cell surface protein with the thrombospondin-1 domain. *Blood.* 2006;107:4317-4325
13. Gjini E, Hekking LH, Kuchler A, Saharinen P, Wienholds E, Post JA, Alitalo K, Schulte-Merker S. Zebrafish tie-2 shares a redundant role with tie-1 in heart development and regulates vessel integrity. *Dis Model Mech.*4:57-66
14. van der Heijden M, van Nieuw Amerongen GP, van Bezu J, Paul MA, Groeneveld AB, van Hinsbergh VW. Opposing effects of the angiopoietins on the thrombin-induced permeability of human pulmonary microvascular endothelial cells. *PLoS One.*6:e23448
15. van Nieuw Amerongen GP, Vermeer MA, Negre-Aminou P, Lankelma J, Emeis JJ, van Hinsbergh VW. Simvastatin improves disturbed endothelial barrier function. *Circulation.* 2000;102:2803-2809

16. Aman J, van Bezu J, Damanafshan A, Huveneers S, Eringa EC, Vogel SM, Groeneveld AB, Vonk Noordegraaf A, van Hinsbergh VW, van Nieuw Amerongen GP. Effective treatment of edema and endothelial barrier dysfunction with imatinib. *Circulation*. 2012;126:2728-2738
17. Kleaveland B, Zheng X, Liu JJ, Blum Y, Tung JJ, Zou Z, Sweeney SM, Chen M, Guo L, Lu MM, Zhou D, Kitajewski J, Affolter M, Ginsberg MH, Kahn ML. Regulation of cardiovascular development and integrity by the heart of glass-cerebral cavernous malformation protein pathway. *Nat Med*. 2009;15:169-176
18. Montero-Balaguer M, Swirsding K, Orsenigo F, Cotelli F, Mione M, Dejana E. Stable vascular connections and remodeling require full expression of ve-cadherin in zebrafish embryos. *PLoS One*. 2009;4:e5772
19. Gore AV, Lampugnani MG, Dye L, Dejana E, Weinstein BM. Combinatorial interaction between ccm pathway genes precipitates hemorrhagic stroke. *Dis Model Mech*. 2008;1:275-281
20. Liu J, Fraser SD, Faloon PW, Rollins EL, Vom Berg J, Starovic-Subota O, Laliberte AL, Chen JN, Serluca FC, Childs SJ. A betapix pak2a signaling pathway regulates cerebral vascular stability in zebrafish. *Proc Natl Acad Sci U S A*. 2007;104:13990-13995
21. Buchner DA, Su F, Yamaoka JS, Kamei M, Shavit JA, Barthel LK, McGee B, Amigo JD, Kim S, Hanosh AW, Jagadeeswaran P, Goldman D, Lawson ND, Raymond PA, Weinstein BM, Ginsburg D, Lyons SE. Pak2a mutations cause cerebral hemorrhage in redhead zebrafish. *Proc Natl Acad Sci U S A*. 2007;104:13996-14001
22. Kwon HB, Choi YK, Lim JJ, Kwon SH, Her S, Kim HJ, Lim KJ, Ahn JC, Kim YM, Bae MK, Park JA, Jeong CH, Mochizuki N, Kim KW. Akap12 regulates vascular integrity in zebrafish. *Exp Mol Med*. 44:225-235
23. Armstrong LC, Bornstein P. Thrombospondins 1 and 2 function as inhibitors of angiogenesis. *Matrix Biol*. 2003;22:63-71
24. Dawson DW, Pearce SF, Zhong R, Silverstein RL, Frazier WA, Bouck NP. Cd36 mediates the in vitro inhibitory effects of thrombospondin-1 on endothelial cells. *J Cell Biol*. 1997;138:707-717
25. Bobryshev YV, Cherian SM, Inder SJ, Lord RS. Neovascular expression of ve-cadherin in human atherosclerotic arteries and its relation to intimal inflammation. *Cardiovasc Res*. 1999;43:1003-1017
26. Ohkawara H, Ishibashi T, Shiomi M, Sugimoto K, Uekita H, Kamioka M, Takuwa Y, Teramoto T, Maruyama Y, Takeishi Y. Rhoa and rac1 changes in the atherosclerotic lesions of whhlmi rabbits. *J Atheroscler Thromb*. 2009;16:846-856
27. Good DJ, Polverini PJ, Rastinejad F, Le Beau MM, Lemons RS, Frazier WA, Bouck NP. A tumor suppressor-dependent inhibitor of angiogenesis is immunologically and functionally indistinguishable from a fragment of thrombospondin. *Proc Natl Acad Sci U S A*. 1990;87:6624-6628
28. Zhou J, Feng X, Ban B, Liu J, Wang Z, Xiao W. Elongation factor ell (eleven-nineteen lysine-rich leukemia) acts as a transcription factor for direct thrombospondin-1 regulation. *J Biol Chem*. 2009;284:19142-19152
29. Voss K, Stahl S, Hogan BM, Reinders J, Schleider E, Schulte-Merker S, Felbor U. Functional analyses of human and zebrafish 18-amino acid in-frame deletion pave the way for domain mapping of the cerebral cavernous malformation 3 protein. *Hum Mutat*. 2009;30:1003-1011
30. Stainier DY, Fouquet B, Chen JN, Warren KS, Weinstein BM, Meiler SE, Mohideen MA, Neuhaus SC, Solnica-Krezel L, Schier AF, Zwartkruis F, Stemple DL, Malicki J, Driever W, Fishman MC. Muta-

- tions affecting the formation and function of the cardiovascular system in the zebrafish embryo. *Development*. 1996;123:285-292
31. Faurobert E, Albiges-Rizo C. Recent insights into cerebral cavernous malformations: A complex jigsaw puzzle under construction. *FEBS J*.277:1084-1096
 32. Ko JM, Chan PL, Yau WL, Chan HK, Chan KC, Yu ZY, Kwong FM, Miller LD, Liu ET, Yang LC, Lo PH, Stanbridge EJ, Tang JC, Srivastava G, Tsao SW, Law S, Lung ML. Monochromosome transfer and microarray analysis identify a critical tumor-suppressive region mapping to chromosome 13q14 and Thsd-1 in esophageal carcinoma. *Molecular cancer research : MCR*. 2008;6:592-603
 33. Dunham A, Matthews LH, Burton J, Ashurst JL, Howe KL, Ashcroft KJ, Beare DM, Burford DC, Hunt SE, Griffiths-Jones S, Jones MC, Keenan SJ, Oliver K, Scott CE, Ainscough R, Almeida JP, Ambrose KD, Andrews DT, Ashwell RI, Babbage AK, Bagguley CL, Bailey J, Bannerjee R, Barlow KF, Bates K, Beasley H, Bird CP, Bray-Allen S, Brown AJ, Brown JY, Burrill W, Carder C, Carter NP, Chapman JC, Clamp ME, Clark SY, Clarke G, Clee CM, Clegg SC, Cobley V, Collins JE, Corby N, Coville GJ, Deloukas P, Dhami P, Dunham I, Dunn M, Earthrowl ME, Ellington AG, Faulkner L, Frankish AG, Frankland J, French L, Garner P, Garnett J, Gilbert JG, Gilson CJ, Ghori J, Grafham DV, Gribble SM, Griffiths C, Hall RE, Hammond S, Harley JL, Hart EA, Heath PD, Howden PJ, Huckle EJ, Hunt PJ, Hunt AR, Johnson C, Johnson D, Kay M, Kimberley AM, King A, Laird GK, Langford CJ, Lawlor S, Leongamornlert DA, Lloyd DM, Lloyd C, Loveland JE, Lovell J, Martin S, Mashreghi-Mohammadi M, McLaren SJ, McMurray A, Milne S, Moore MJ, Nickerson T, Palmer SA, Pearce AV, Peck AI, Pelan S, Phillimore B, Porter KM, Rice CM, Searle S, Sehra HK, Shownkeen R, Skuce CD, Smith M, Steward CA, Sycamore N, Tester J, Thomas DW, Tracey A, Tromans A, Tubby B, Wall M, Wallis JM, West AP, Whitehead SL, Willey DL, Wilming L, Wray PW, Wright MW, Young L, Coulson A, Durbin R, Hubbard T, Sulston JE, Beck S, Bentley DR, Rogers J, Ross MT. The DNA sequence and analysis of human chromosome 13. *Nature*. 2004;428:522-528
 34. Ota T, Suzuki Y, Nishikawa T, Otsuki T, Sugiyama T, Irie R, Wakamatsu A, Hayashi K, Sato H, Nagai K, Kimura K, Makita H, Sekine M, Obayashi M, Nishi T, Shibahara T, Tanaka T, Ishii S, Yamamoto J, Saito K, Kawai Y, Isono Y, Nakamura Y, Nagahari K, Murakami K, Yasuda T, Iwayanagi T, Wagatsuma M, Shiratori A, Sudo H, Hosoiri T, Kaku Y, Kodaira H, Kondo H, Sugawara M, Takahashi M, Kanda K, Yokoi T, Furuya T, Kikkawa E, Omura Y, Abe K, Kamihara K, Katsuta N, Sato K, Tanikawa M, Yamazaki M, Ninomiya K, Ishibashi T, Yamashita H, Murakawa K, Fujimori K, Tanai H, Kimata M, Watanabe M, Hiraoka S, Chiba Y, Ishida S, Ono Y, Takiguchi S, Watanabe S, Yosida M, Hotuta T, Kusano J, Kanehori K, Takahashi-Fujii A, Hara H, Tanase TO, Nomura Y, Togiya S, Komai F, Hara R, Takeuchi K, Arita M, Imose N, Musashino K, Yuuki H, Oshima A, Sasaki N, Aotsuka S, Yoshikawa Y, Matsunawa H, Ichihara T, Shiohata N, Sano S, Moriya S, Momiyama H, Satoh N, Takami S, Terashima Y, Suzuki O, Nakagawa S, Senoh A, Mizoguchi H, Goto Y, Shimizu F, Wakebe H, Hishigaki H, Watanabe T, Sugiyama A, Takemoto M, Kawakami B, Watanabe K, Kumagai A, Itakura S, Fukuzumi Y, Fujimori Y, Komiyama M, Tashiro H, Tanigami A, Fujiwara T, Ono T, Yamada K, Fujii Y, Ozaki K, Hiraio M, Ohmori Y, Kawabata A, Hikiji T, Kobatake N, Inagaki H, Ikema Y, Okamoto S, Okitani R, Kawakami T, Noguchi S, Itoh T, Shigeta K, Senba T, Matsumura K, Nakajima Y, Mizuno T, Morinaga M, Sasaki M, Togashi T, Oyama M, Hata H, Komatsu T, Mizushima-Sugano J, Satoh T, Shirai Y, Takahashi Y, Nakagawa K, Okumura K, Nagase T, Nomura N, Kikuchi H, Masuho Y, Yamashita R, Nakai K, Yada T, Ohara O, Isogai T, Sugano S. Complete sequencing and characterization of 21,243 full-length human cdnas. *Nature genetics*. 2004;36:40-45

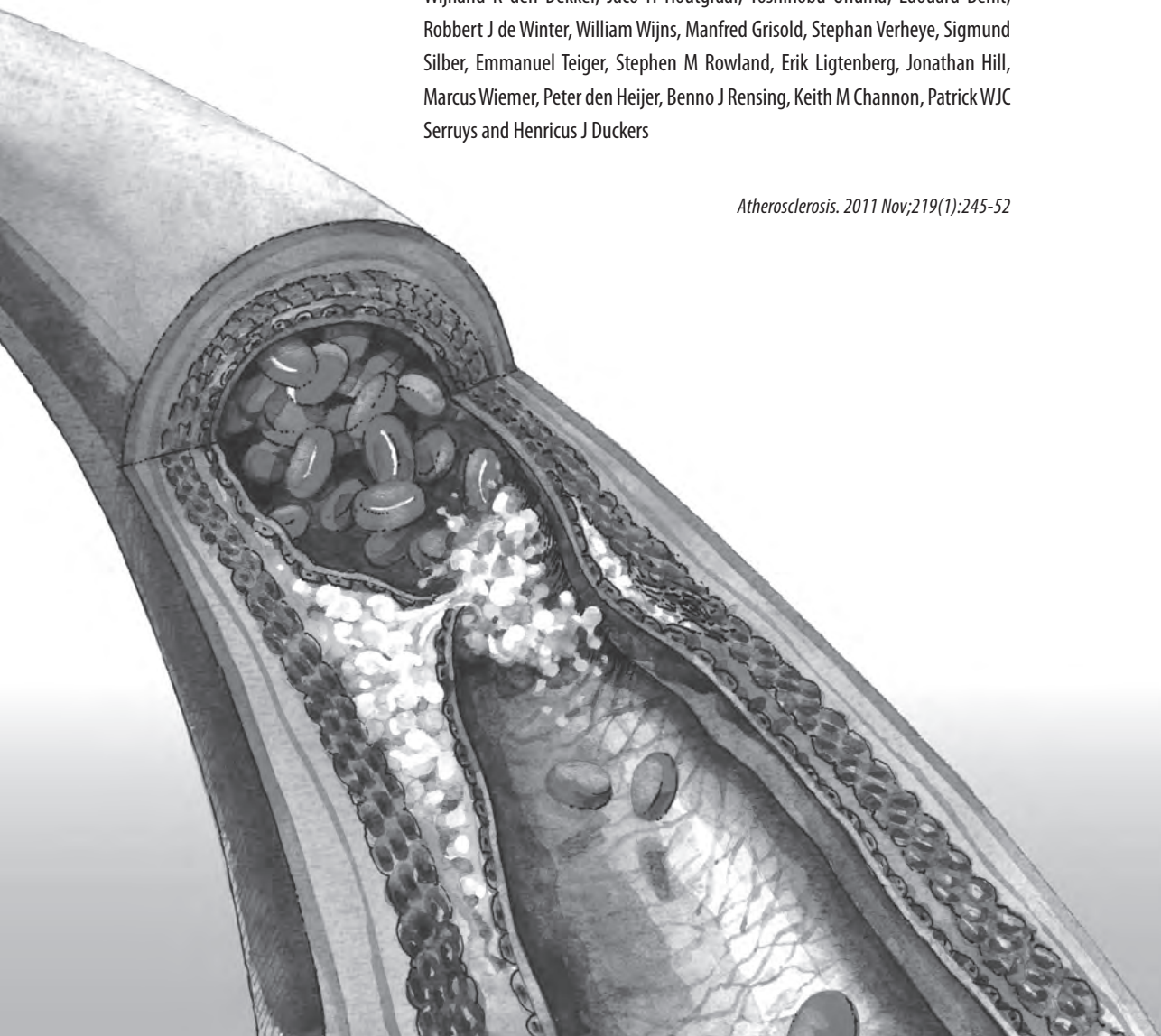
35. Stahl A, Connor KM, Sapieha P, Chen J, Dennison RJ, Krah NM, Seaward MR, Willett KL, Aderman CM, Guerin KI, Hua J, Lofqvist C, Hellstrom A, Smith LE. The mouse retina as an angiogenesis model. *Invest Ophthalmol Vis Sci.* 2010;51:2813-2826
36. Waschke J, Burger S, Curry FR, Drenckhahn D, Adamson RH. Activation of rac-1 and cdc42 stabilizes the microvascular endothelial barrier. *Histochem Cell Biol.* 2006;125:397-406
37. Wojciak-Stothard B, Potempa S, Eichholtz T, Ridley AJ. Rho and rac but not cdc42 regulate endothelial cell permeability. *J Cell Sci.* 2001;114:1343-1355
38. Chervin-Petiot A, Courcon M, Almagro S, Nicolas A, Grichine A, Grunwald D, Prandini MH, Huber P, Gulino-Debrac D. Epithelial protein lost in neoplasm (eplin) interacts with alpha-catenin and actin filaments in endothelial cells and stabilizes vascular capillary network in vitro. *J Biol Chem.* 2007;282:7556-7572
39. Potente M, Gerhardt H, Carmeliet P. Basic and therapeutic aspects of angiogenesis. *Cell.* 2006;146:873-887
40. Tomar A, Schlaepfer DD. Focal adhesion kinase: Switching between gaps and gefs in the regulation of cell motility. *Curr Opin Cell Biol.* 2009;21:676-683
41. Orr AW, Pallero MA, Xiong WC, Murphy-Ullrich JE. Thrombospondin induces rhoa inactivation through fak-dependent signaling to stimulate focal adhesion disassembly. *J Biol Chem.* 2004;279:48983-48992
42. Yuan TL, Choi HS, Matsui A, Benes C, Lifshits E, Luo J, Frangioni JV, Cantley LC. Class 1a pi3k regulates vessel integrity during development and tumorigenesis. *Proc Natl Acad Sci U S A.* 2008;105:9739-9744
43. Corder EH, Saunders AM, Strittmatter WJ, Schmechel DE, Gaskell PC, Small GW, Roses AD, Haines JL, Pericak-Vance MA. Gene dose of apolipoprotein e type 4 allele and the risk of alzheimer's disease in late onset families. *Science.* 1993;261:921-923
44. Nishitsuji K, Hosono T, Nakamura T, Bu G, Michikawa M. Apolipoprotein e regulates the integrity of tight junctions in an isoform-dependent manner in an in vitro blood-brain barrier model. *J Biol Chem.* 2011;286:17536-17542
45. Bell RD, Winkler EA, Singh I, Sagare AP, Deane R, Wu Z, Holtzman DM, Betsholtz C, Armulik A, Sallstrom J, Berk BC, Zlokovic BV. Apolipoprotein e controls cerebrovascular integrity via cyclophilin a. *Nature.* 2012;485:512-516
46. Kolodgie FD, Gold HK, Burke AP, Fowler DR, Kruth HS, Weber DK, Farb A, Guerrero I, Hayase M, Kutys R, Narula J, Finn AV, Virmani R. Intraplaque hemorrhage and progression of coronary atheroma. *N Engl J Med.* 2003;349:2316-2325
47. Michel JB, Virmani R, Arbustini E, Pasterkamp G. Intraplaque haemorrhages as the trigger of plaque vulnerability. *Eur Heart J.* 2011;32:1977-1985, 1985a, 1985b, 1985c
48. Altaf N, MacSweeney ST, Gladman J, Auer DP. Carotid intraplaque hemorrhage predicts recurrent symptoms in patients with high-grade carotid stenosis. *Stroke.* 2007;38:1633-1635
49. Hellings WE, Peeters W, Moll FL, Piers SR, van Setten J, Van der Spek PJ, de Vries JP, Seldenrijk KA, De Bruin PC, Vink A, Velema E, de Kleijn DP, Pasterkamp G. Composition of carotid atherosclerotic plaque is associated with cardiovascular outcome: A prognostic study. *Circulation.* 2010;121:1941-1950
50. Moreno PR, Purushothaman KR, Sirol M, Levy AP, Fuster V. Neovascularization in human atherosclerosis. *Circulation.* 2006;113:2245-2252

Chapter 6

Final Results of the HEALING IIB Trial to Evaluate a Bio-engineered CD34 Antibody Coated Stent (Genous™ Stent) Designed to Promote Vascular Healing by Capture of Circulating Endothelial Progenitor Cells in CAD Patients.

Wijnand K den Dekker, Jaco H Houtgraaf, Yoshinobu Onuma, Edouard Benit, Robbert J de Winter, William Wijns, Manfred Grisold, Stephan Verheye, Sigmund Silber, Emmanuel Teiger, Stephen M Rowland, Erik Ligtenberg, Jonathan Hill, Marcus Wiemer, Peter den Heijer, Benno J Rensing, Keith M Channon, Patrick WJC Serruys and Henricus J Duckers

Atherosclerosis. 2011 Nov;219(1):245-52



ABSTRACT

Objective: to assess the safety and efficacy of the Genous™ endothelial progenitor cell (EPC) capturing stent in conjunction with HmG-CoA-reductase inhibitors (statins) to stimulate EPC recruitment, in the treatment of patients with de novo coronary artery lesions.

Methods and results: The HEALING IIB study was a multi-center, prospective trial, including 100 patients. The primary efficacy endpoint was late luminal loss by QCA at 6 month follow-up (FU). Although statin therapy increased relative EPC levels by 5.6-fold, the angiographic outcome at 6 month FU was not improved in patients with an overall in-stent late luminal loss of 0.76 ± 0.50 mm. The composite major adverse cardiac events (MACE) rate was 9.4%, whereas 6.3% clinically justified target lesion revascularizations (TLRs) were observed. 2 Patients died within the first 30 days after stent implantation due to angiographically verified in-stent thrombosis. At 12 month FU, MACE and TLR increased to 15.6% and 11.5% respectively and stabilized until 24 month FU. 18 Month angiographic FU showed a significant decrease in late luminal loss (0.67 ± 0.54 , 11.8% reduction or 10% by matched serial analysis, $P=0.001$)

Conclusion: the HEALING IIB study suggests that statin therapy in combination with the EPC capture stent does not contribute to a reduction of in-stent restenosis formation for the treatment of de novo coronary artery disease. Although concomitant statin therapy was able to stimulate EPC recruitment, it did not improve the angiographic outcome of the bio-engineered EPC capture stent. Remarkably, angiographic late loss was significantly reduced between 6 and 18 months. (ClinicalTrial.gov number, NCT00349895.)

INTRODUCTION

Drug eluting stents (DES) have emerged as an effective means of attenuating stent-related restenosis formation and has enabled the field of percutaneous coronary intervention to move forward to complex coronary angioplasty, with an efficacy equivalent to surgical intervention in the short and long term ¹. The mainstay of drugs eluted from the stent polymer comprise cytostatic or cytotoxic compounds to impede neo-intimal formation that arise from vascular smooth muscle cell (VSMC) activation and proliferation. Lately, DES have been associated with late in-stent thrombosis, presumably based on a concomitant impeded arterial repair response characterized by incomplete endothelial coverage of the stent struts, persistent fibrin deposition and inflammation beyond 24-month post implantation ². Therefore, prolonged (6-12 months) dual anti-platelet therapy has been recommended in conjunction with DES in order to mitigate the risk of stent thrombosis that is associated with incomplete healing. In addition, the polymer coating of the DES, which ensures prolonged release of the anti-proliferative compounds, inherently invokes inflammation and cytotoxicity with delayed stent coverage. Furthermore, non-erodable polymers were associated with granulomatous and hypersensitivity reactions in relevant animal models. Finally, DES have been shown to interfere with proper endothelial function in arterial segments adjacent to the implanted stent, as suggested by an impaired or paradoxical vasomotor response, which could pose the segment at risk for ischemia and coronary occlusion ³.

Alternatively, therapeutic interventions aimed to facilitate the vascular repair response following coronary intervention could reinstate endothelial integrity and maintain vascular senescence to prevent VSMC proliferation, local inflammation and vascular platelet activation, while maintaining local vasomotor function to ensure short and long-term success of the treated arterial segment. The underlying strategy of accelerated endothelialization aims to provide a non-thrombogenic coating of exposed stent surfaces to reduce in-stent thrombosis and potentially decrease neo-intimal hyperplasia. Reinstatement of the endothelial integrity can be augmented by local delivery of endothelial mitogenic compounds, including VEGF ⁴, or facilitation of attachment of circulating endothelial progenitor cells (EPCs) to the strut surface.

In 2003, development was begun of a bio-engineered stent with a proprietary coating containing an anti-human CD34 antibody (Genous™ Bio-engineered R stent, OrbusNeich) that sequesters circulating CD34+ haematopoietic cells to the stent strut surface, facilitates strut coverage and initiates the arterial repair response. Moreover, the combination of this CD34 antibody-coating with conventional sirolimus-eluting stents appeared to overcome the delayed endothelial coverage in stented porcine coronary arteries ⁵.

The first clinical experience with the EPC capturing Genous Stent was obtained in 16 patients in the HEALING-FIM study. The healing technology approach was deemed safe and feasible with an in-stent late luminal loss of 0.63 ± 0.21 mm at the 6 month angiographic follow-up (FU) ⁶. The original design of this stent platform was adapted before proceeding to the phase I/II study, including modification of monoclonal antibody with a higher affinity and transfer from a wet to a dry lyophilized preparation CD34-antibody coated stent premounted on an Evolution2™ PTCA balloon catheter. In the HEALING II study, treatment with the Genous Stent of 63 elective patients with a de-novo lesion resulted in a 6-month angiographic late loss of 0.78 ± 0.39 mm and percent in-stent volume obstruction of $22.9\pm 13.7\%$ ^{7,8}. A sub-analysis of the individual patients suggested that specifically patients with a lower EPC titer responded relatively poorly to the EPC capture technology compared to patients with a normal EPC titer, with more prominent late loss and higher incidence of revascularization events. Low EPC titer concurred with a lack of HMG-CoA-reductase inhibitors (statins) in the pharmacotherapy of these CAD patients.

As statins have been shown to augment EPC titer, survival, and activity in vitro and in vivo, we hypothesized that concomitant treatment of CAD with statin therapy could stimulate the EPC titer and efficacy in these patients and therefore the overall response to the EPC capture technology. This led to the design of the HEALING IIB study that aimed to assess the safety and efficacy of the Genous Stent in conjunction with optimal statin therapy to stimulate EPC recruitment in the treatment of stent-related restenosis formation in 100 elective patients with de novo native coronary artery lesions.

METHODS

Patient selection enrollment

The Healing IIB study was a multi-center, open-label, prospective trial that enrolled 100 patients from 13 sites in 7 European countries. Patients were eligible for enrollment if they met the following inclusion criteria: age between 18 and 85 years old, diagnosis of de novo stable or unstable angina or silent ischemia based on up to two de novo lesions in two independent native coronary arteries eligible for coronary stenting. Target lesions should be less than 12 mm in length and should be able to be covered by a single trial stent of 13 mm or 18 mm length, with a reference artery of 2.5 to 3.5 mm diameter by visual estimation. Exclusion criteria for study participation included an acute coronary syndrome with positive cardiac markers within 72 hours preceding the index procedure; renal dysfunction or suspected liver disease; thrombocytopenia or leucopenia; unprotected left main coronary artery disease; ostial target lesions; severely calcified lesions; totally occluded vessels, excessive tortuosity

of the target vessel and target lesions involving a bifurcation with a side branch that would require stenting; intervention of another lesion within 6 months before or anticipated within the scheduled FU of the index procedure; or left ventricular ejection fraction of less than 30 percent. The trial was reviewed and approved by the local Medical Ethics Review Committees, and written informed consent was obtained from all patients.

Genous™ R stent - Endothelial progenitor cell capture technology

The Genous™ Bio-engineered R stent is based on a 316L stainless steel stent platform with study devices available in diameters of 2.5, 3.0, and 3.5mm and lengths of 9, 18, 23, and 33mm (OrbusNeich Medical, Fort Lauderdale, FL) with a polysaccharide matrix coating covalently coupled with murine anti-human CD34 antibodies which specifically target the CD34-positive circulating endothelial cell progenitor population.

Study Procedure

Elective patients that met all angiographic in- and exclusion criteria were approached for enrollment in the study. After written informed consent, patients were started on 80mg atorvastatin qd, at least two weeks before index procedure. Patients already on statin therapy were switched to 80 mg atorvastatin qd. Pre-dilatation of the target lesion was left at the investigator's discretion, whereas post-dilatation was performed as required to achieve less than 20% residual stenosis by visual assessment, with TIMI grade III flow. The stent was deployed at nominal pressure at a stent-to-vessel ratio of 1.1: 1.

Aspirin treatment was initiated 12 hours before the procedure (75 mg qd), whereas a loading dose of 300 mg of clopidogrel was administered prior to the procedure, proceeded by 75 mg qd for the period of 4 weeks. Administration of GPIIb/IIIa was left at the investigator's discretion.

Angiographic success was defined as the percentage of patients with a residual diameter stenosis within the stent of less than 20%, as measured by on-line QCA and grade III TIMI flow. Procedural success was defined as the percentage of patients with an angiographic successful stent placement and the absence of cardiac death, MI, CABG or a Target Lesion Revascularization (TLR) event during the index hospitalization.

Clinical and angiographical follow-up

Anginal status (according to the Canadian Cardiovascular Society Classification of Angina and the Braunwald Classification for Unstable Angina) and the documentation of Major Adverse Cardiac Events (MACE) were assessed at 1, 6, 12, 18 and 24 month FU. Circulating CD34+ EPC

titers were quantified by flow cytometric analysis at screening, at baseline (2 weeks after initiation of high dose Atorvastatin) and at 30 days FU of the index procedure.

Quantitative angiographic analysis was performed at 6- and 18-month FU. Coronary angiograms were obtained in perpendicular views following an intracoronary injection of nitrates. Off-line quantitative analyses of pre-procedural, post-procedural, 6- and 18-month FU angiographic data were performed at an independent imaging core laboratory (Cardi-alysis, Rotterdam, the Netherlands). Restenosis was defined as a reduction of at least 50% of the luminal diameter. Late luminal loss was defined as the difference between the minimal luminal diameter after procedure and at six months FU. The target lesion was defined as the stented segment including 5 mm proximal and distal to the stented segment.

Study End Points

The primary efficacy endpoint was in-stent late luminal loss at 6 months as assessed by quantitative coronary angiography. The secondary safety endpoints included MACE rate and device-related serious adverse events at 1, 6, 12 and 24 months FU and the incidence of in-stent thrombosis as documented by coronary angiography. MACE was defined as the incidence of cardiac death, Q-wave or non-Q-wave myocardial infarction, emergent cardiac surgery and clinically justified TLR. A TLR/target vessel revascularization (TVR) event was considered clinically justified when the diameter stenosis was more than 50% (by QCA) and the occurrence of either, (1) clinical symptoms suspect of recurrent angina pectoris, or (2) ischemia-related ECG changes at rest or during exercise test related to the target vessel or (3) an abnormal invasive functional diagnostic test (including Doppler flow velocity reserve or fractional flow reserve). A TLR/TVR with a diameter stenosis of over 70% was always considered clinically-driven. Secondary efficacy endpoints included QCA-derived vessel parameters of the in-stent segment and 5 mm proximal and 5 mm distal from the edge of the stent: including acute gain, MLD, mean diameter, percent diameter stenosis, QCA derived percent volume obstruction, and binary restenosis rate, angiographic and procedural success, clinically justified TLR free rate at 6 months. Stent thrombosis was defined as an angiographically documented complete occlusion or a flow limiting thrombus (TIMI flow 1 or 2) of a previously successfully treated artery. An independent Clinical Events Committee adjudicated all major adverse cardiac events. A data safety monitoring board reviewed safety data on a regular basis.

Quantification of circulating CD34+/KDR+ endothelial progenitor cells titer

To quantify circulating EPCs by flow cytometric analysis in the patients, whole blood was incubated with 7AAD viability dye, APC-labeled anti-hCD45, FITC-labeled anti-hCD34 (Pharmingen) and PE-labeled anti-hKDR (R&D systems) according to the manufacturer

protocol (and ISHAGE guidelines) for 20 minutes at room temperature using Stem-Kit™ Reagent; (Beckman Coulter Comp, Cedex,F). After addition of counting fluorospheres (Beckman Coulter Comp, Cedex,F), the red cell fraction was lysed and analyzed on an automated flow cytometer (FACSCanto®, Becton&Dickinson). Corresponding isotypic IgG1 controls were used to set proper gating for each antibody.

Statistical analysis

The primary analysis was performed according to the intention to treat principle and included all patients initially enrolled in the study. Continuous variables are summarized by mean \pm standard deviation. Post-procedural and 6- and 18-month FU angiographic changes were compared using a 2-tailed paired t-test. $P < 0.05$ was considered to be statistically significant. Only events that have been adjudicated by the Clinical Event Committee have been taken into account for the analysis of MACE.

RESULTS

Baseline characteristics and procedural outcome

One hundred patients were included in the HEALING IIB study. Four patients were per protocol excluded from post-procedural analysis; two patients did not meet the in- and exclusion criteria, one patient was not on Atorvastatin during two weeks pre-procedure as required per protocol and one patient had a post-procedural diameter stenosis of 32% despite post dilatation (see figure 1 for flow chart). The baseline patient demographics, lesion characteristics and clinical outcomes of the current HEALING IIB and earlier HEALING II study are summarized in tables 1-3. The study population had an average age of 64 years, whereas 20% of the patients suffered from diabetes mellitus. Compared to the HEALING II study, patients in the HEALING IIB study had significantly more hypertension, hypercholesterolemia and stable angina and there were more current smokers. On the other hand, there were significantly less previous smokers and patients with unstable angina. At the index procedure, 100% of the patients were initiated on high dose Atorvastatin therapy (80 mg qd) for at least 2 weeks according to the protocol outline. At one month FU, 91% of the patients were still being treated with Atorvastatin 80 mg qd. In 82 patients, one single index lesion was treated, whereas in 14 patients, 2 lesions in 2 independent coronary arteries received a study stent (total 110 lesions treated). The average lesion length comprised 12.64 ± 5.69 mm in length, with a diameter stenosis of $57.9\% \pm 9.9\%$, as assessed by QCA. Angiographic and overall procedural success were respectively 97.3% (107 out of 110 lesions treated) and 93% (89/96 patients; table 4). A second overlapping EPC capture stent was implanted in three patients to treat a dissection

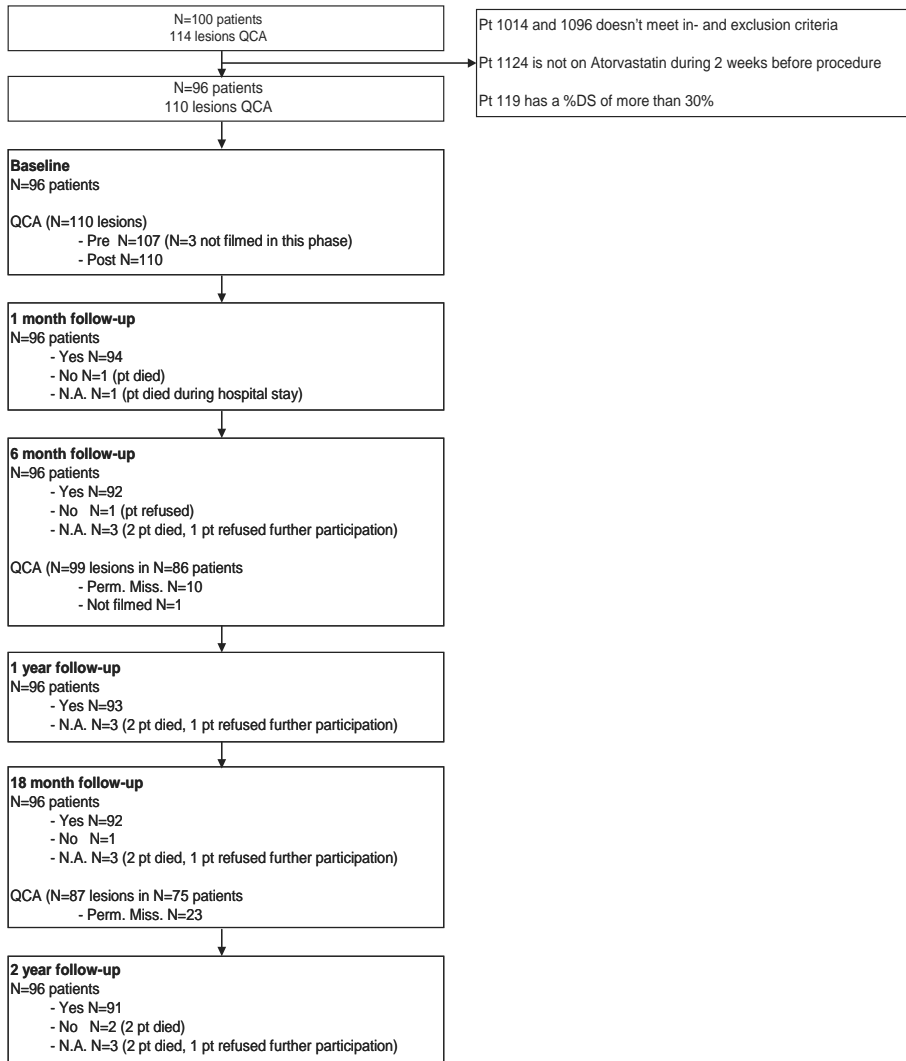


Figure 1
Flow chart showing enrollment and follow-up of 100 patients

following implantation of the first stent, in three patients due to a type A/B dissection, and in eight patients due to incomplete coverage of the target lesion by the first stent. Two patients displayed a transient TIMI II coronary flow following stent deployment. None of the patients received GIIb/IIIa inhibitors during or after the index procedure.

Table 1. Patient demographics and clinical characteristics

Patient parameter	HEALING II (N=63)	HEALING IIB (N=96)
Age (years)		
Mean \pm SD	60.8 \pm 10.2	63.7 \pm 9.8
Min-max	43-78	43-78
Body Mass Index (kg/m ²)		
Mean \pm SD	26.8 \pm 3.7	27.3 \pm 4.5
Min-max	18.7-38.1	17.1-41.9
Male	66.7% (42/63)	73.7% (71/96)
Diabetes mellitus	12.7% (8/63)	19.8% (19/96)
Hypertension	46.0% (29/63)	66.7% (64/96) ^a
Hypercholesterolemia	66.7% (42/63)	84.4% (81/96) ^a
Previous stroke	3.2% (2/63)	3.1% (3/96)
Congestive heart failure	0.0% (0/63)	3.0% (3/96)
Family history of MI	52.4% (33/63)	55.2% (53/96)
Peripheral vascular disease	3.2% (2/63)	9.4% (9/96)
Previous MI	23.8% (15/63)	26.0% (25/96)
Previous CABG	3.2% (2/63)	2.0% (2/96)
Previous PTCA	9.5% (6/63)	18.8% (18/96)
Smoking history		
Previous	2.2% (14/63)	42.7% (41/96) ^b
Current	41.3% (26/63)	20.8% (20/96) ^b
Unstable angina	27.0% (17/63)	8.3% (8/96) ^b
Braunwald I	9.5% (6/63)	1.0% (1/96)
Braunwald II	19.2% (12/63)	5.2% (5/96)
Braunwald III	4.8% (3/63)	2.1% (2/96)
Stable angina	60.3% (38/63)	80.2% (77/96) ^b
CCS I	7.9% (5/63)	11.5% (11/96)
CCS II	28.6% (18/63)	56.3% (54/96)
CCS III	20.6% (13/63)	10.4% (10/96)
CCS IV	3.2% (2/63)	2.1% (2/96)
Silent ischemia	12.7% (8/63)	11.5% (11/96)

Numbers are % (counts/available field sample size) or mean \pm 1 Standard deviation

SD Standard deviation

MI Myocardial Infarction

CABG Coronary Artery Bypass Graft

PTCA Percutaneous Transluminal Coronary Angioplasty

Braunwald Braunwald Classification

CCS Canadian Cardiovascular Society Classification

^a $P < 0.05$

^b $P < 0.01$

Table 2. Lesion characteristics

Parameter	HEALING II		HEALING IIB	
	#	SD or %	#	SD or %
Study stents per patient	1.1	0.4	1.3	0.5 ^b
Treated segments	63		110	
RCA	24	38.1%	40	36.5%
LM	0	0.0%	0	0.0%
LAD	25	39.7%	43	39.1%
LCX	14	22.2%	27	24.5%
Total stent length (mm)	17.0	2.9	21.4	8.5 ^b
Lesion type ^a	63		107	
A	0	0.0%	1	0.9%
B1	27	42.9%	49	45.8%
B2	36	57.2%	53	49.5%
C	0	0.0%	4	3.7%

LAD *Left Anterior Descending*

LCX *Left Circumflex Artery*

LM *Left Main*

RCA *Right Coronary Artery*

^a According to ACC/AHA classification

^b $P < 0.0001$

Clinical outcomes

Compliance to clinical FU at 6, 12 and 24 months was 96%, 96% and 95% respectively. Table 3 provides an overview of the major adverse cardiac events (MACE) at 1, 6, 12, 18 and 24 months. Clinical outcomes were comparable with the HEALING II study, as there was only a significant difference in TVR at 18 months. Acute in-stent thrombosis was verified in two patients within the 30 days FU. One patient suffered from an angiographically verified in-stent thrombosis at day one post-implantation and died. Another patient suffered from an angiographically verified acute in-stent thrombosis at day 9 post-implantation and the patient died. This patient received stents in a bifurcation with residual dissection following stent implantation, whereas a second stent could not be implanted. The procedure was assumed not to be a procedural success with suboptimal stent implantation. Both of these events have been adjudicated as cardiac deaths due to a definite in-stent thrombosis by the independent CEC. Finally, one patient had a clinically driven target lesion revascularization (TLR) at 181 days following the index procedure, and 4 days after the re-intervention due to a clinically-driven TLR, designated as a secondary, definite in-stent thrombosis. During the re-intervention the interventionist reported a left main dissection and thrombus in situ in LAD and left circumflex with normal coronary flow.

Table 3. Clinical outcomes in HEALING II and HEALING IIB studies

	At discharge		1 Month FU		6 Month FU		9 Month FU		12 Month FU		18 Month FU		24 Month FU	
	HEALING II	HEALING IIB	HEALING II	HEALING IIB	HEALING II	HEALING IIB	HEALING II	HEALING IIB	HEALING II	HEALING IIB	HEALING II	HEALING IIB	HEALING II	HEALING IIB
	63	96	63	96	63	96	63	96	63	96	63	96	63	96
N	63	96	63	96	63	96	63	96	63	96	63	96	63	96
MACE	0.0%	5.2%	0.0%	5.2%	NA	9.4%	7.9%	7.9%	NA	15.6%	7.9%	15.6%	NA	16.6%
Cardiac death	0.0%	1.0%	0.0%	2.1%	NA	2.1%	1.6%	1.6%	NA	2.1%	1.6%	2.1%	NA	2.1%
MI	0.0%	4.2%	0.0%	5.2%	NA	5.2%	0.0%	0.0%	NA	5.2%	0.0%	5.2%	NA	5.2%
Q-wave	0.0%	1.0%	0.0%	2.1%	NA	2.1%	0.0%	0.0%	NA	2.1%	0.0%	2.1%	NA	2.1%
Non Q-wave	0.0%	3.1%	0.0%	3.1%	NA	3.1%	0.0%	0.0%	NA	3.1%	0.0%	3.1%	NA	3.1%
TLR clinically driven	0.0%	1.0%	0.0%	2.1%	NA	6.3%	6.3%	6.3%	NA	11.5%	6.3%	11.5%	NA	11.5%
CABG	0.0%	0.0%	0.0%	0.0%	NA	0.0%	0.0%	0.0%	NA	2.1%	0.0%	2.1%	NA	2.1%
Re-PCI	0.0%	1.0%	0.0%	2.1%	NA	6.3%	6.3%	6.3%	NA	9.4%	6.3%	9.4%	NA	9.4%
TVR	0.0%	1.0%	0.0%	2.1%	NA	6.3%	20.6%	20.6%	NA	15.6%	25.4%	15.6%	NA	16.6%
TVF	0.0%	2.1%	0.0%	3.1%	NA	7.3%	11.2%	11.2%	NA	14.6%	11.2%	14.6%	NA	14.6%
Stent thrombosis	0.0%	1.0%	0.0%	2.1%	NA	2.1%	0.0%	0.0%	NA	3.1%	0.0%	3.1%	NA	3.1%
Definite/probable	0.0%	1.0%	0.0%	2.1%	NA	2.1%	0.0%	0.0%	NA	3.1%	0.0%	3.1%	NA	3.1%
Definite	0.0%	1.0%	0.0%	2.1%	NA	2.1%	0.0%	0.0%	NA	3.1%	0.0%	3.1%	NA	3.1%
Probable	0.0%	1.0%	0.0%	2.1%	NA	2.1%	0.0%	0.0%	NA	3.1%	0.0%	3.1%	NA	3.1%
Possible	0.0%	1.0%	0.0%	1.0%	NA	1.0%	0.0%	0.0%	NA	0.0%	0.0%	0.0%	NA	0.0%

CABG Coronary Artery Bypass Graft

MACE Major Adverse Cardiac Events: Cardiac Death, Myocardial Infarction (Q-wave, non Q-wave, emergent CABG or Clinically driven TLR as determined by the CEC

TLR Target Lesion Revascularization

TVR Target Vessel Revascularization, clinically and non-clinically driven

TVF Target Vessel Failure: clinically driven target vessel revascularization, Q-wave or non Q-wave MI, or cardiac death that could be clearly attributed to a vessel other than the target vessel

Table 4. *Principal effectiveness and safety (results n=96 patients, n=110 lesions)*

Effectiveness measures	Post procedure		6 Months FU		18 Months FU	
Angiographic success	97.3%	(107/110)				
Procedural success	93.0%	(89/96)				
In-stent binary restenosis rate			23%	(23/99)		
RVD	2.95±0.50	(n=110)	2.79±0.61	(n=96)	2.72±0.60	(n=84)
MLD	0.57±0.41	(n=110)	1.81±0.68	(n=99)	1.68±0.68	(n=87)
% DS in-stent	12.73±6.20	(n=110)	35.2±18.74	(n=99)	31.75±19.96	(n=87)
Stent thrombosis			3.1%	(3/96)	3.1%	(3/96)
Late loss in-stent (mm)			0.76±0.50	(n=99)	0.67±0.54	(n=86)
Acute gain in-stent (mm)	1.42±0.38	(n=107)				
In-stent malapposition	0.0%	(0/62)				
QCA in-stent volume obstruction			32.68±25.2	(n=96)	22.5±28.33	(n=84)

MACE Major Adverse Cardiac Events: Cardiac Death, Myocardial Infarction (Q-wave, non Q-wave, emergent CABG or clinically driven TLR as determined by the CEC

RVD Reference vessel diameter (mm)

MLD Minimal luminal diameter (mm)

%DS Percent diameter stenosis

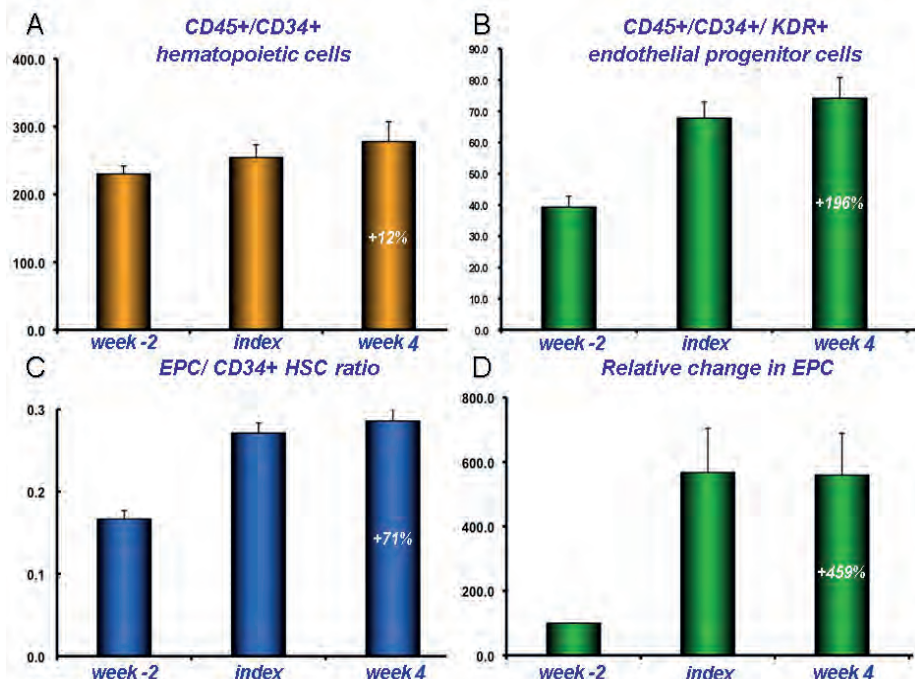
Numbers are % (counts/available field sample size) or mean ± standard deviation

Clinically driven TLR by repeat PCI occurred in 6.3% at 6 month FU and increased to 9.4% at 12 month FU. After 12 month FU, no further TLRs were reported and the TLR rate remained stable at 9.4%. Total MACE rate of the patients treated with the EPC capture device was 9.4%, 15.6% and 16.6% at 6,12 and 24 months respectively (see figure 3 for Kaplan-Meier curve). Target vessel failure (clinically-driven TVR, recurrent infarction or cardiac death that cannot be attributed to a vessel other than the target vessel) was 7.3% at 6 month FU and 14.6% at 12 and 24 month FU (table 3).

Angiographic FU occurred in 89.9% (86/96 patients; 99 lesions) at 6 months and in 78.1% (75/96 patients; 87 lesions) at 18 months. The mean in-stent luminal diameter (MLD) in the Genous Stent at 6 months was 1.81±0.68 mm (post-procedural in-stent MLD 2.57±0.41 mm), whereas late luminal loss was 0.76±0.50 mm by QCA (table 4). At 18 month angiographic FU, mean MLD increased to 1.86±0.68, whereas late luminal loss significantly decreased to 0.67±0.54 (12% reduction as compared to 6 month FU; 10% reduction using serial matched analysis, P=0.001). There was no difference in late luminal loss between diabetics and non diabetics (0.76±0.56 mm vs. 0.76±0.50 mm).

Circulating EPC levels in patients receiving the Genous Stent

EPC titer was analyzed before initiation of Atorvastatin 80 qd at screening, at the index procedure (at 2 weeks statin treatment) and at 1 month FU. Blood samples were quantified

**Figure 2**

Effect of high dose Atorvastatin on circulating CD34+ haematopoietic cells and EPC levels. High dose Atorvastatin leads to a mild increase in CD34+ haematopoietic cells (A), whereas absolute and relative EPC count were markedly increased (B and D). There was a subsequent increase in EPC/CD34+ haematopoietic stem cell (HSC).

in a blinded fashion in all 100 patients. At screening, 49% of patients were maintained on some statin therapy at conventional doses. Two weeks following conversion to high dose Atorvastatin, relative EPC levels were increased by 5.6-fold \pm 1.30 to 63.4 EPCs/100 μ l whole blood, as compared to baseline values (fig. 2D), whereas CD34+ circulating haematopoietic cells remained largely unaffected by statin therapy with an increase of only 12% (fig. 2A). These data suggest that high dose statin therapy facilitates commitment of the CD34/CD45 haematopoietic cell lineage into the committed endothelial (progenitor) cell fate, rather than recruitment of endothelial progenitor cells and haematopoietic stem cells from the primary niche. EPC levels remained elevated until the 30 day FU after stent implantation.

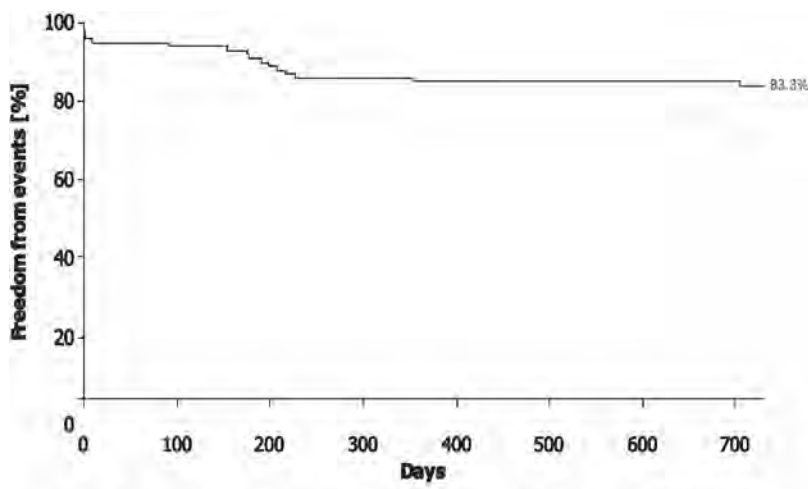


Figure 3

Kaplan-Meier curve showing the event free survival for Major Adverse Cardiac Events (MACE). Mace are defined as the incidence of cardiac death, Q-wave or non Q-wave myocardial infarction, emergency cardiac surgery and clinically justified target lesion revascularization

DISCUSSION

The HEALING IIB clinical trial was a multi-centered, open-label, prospective study to evaluate the safety and efficacy of a stent bioengineered to capture circulating EPCs to promote stent re-endothelialization and initiate vascular healing in combination with optimized statin therapy. Previously, post-hoc stratification of study patients in the HEALING II study suggested that in particular patients with low EPC titers responded poorly to the EPC capture stent technology with a late loss and TLR events equivalent to bare metal stents ⁷. Moreover, several studies have suggested that cardiovascular risk factors, including hypertension, aging, hypercholesterolemia, and diabetes mellitus, are associated with low EPC titers and EPC dysfunction ⁹. Low EPC titer in the HEALING II study was also associated with a lack of statin therapy in these CAD patients (statin use in patients with low vs. normal EPC levels: 41% vs. 92%) ⁷. Indeed, statin therapy has been shown to augment EPC levels in-vivo, and improve EPC survival, clonal capacity and adhesion in in-vitro assays by improved eNOS bioavailability, as well as via activation of the PI3-Akt dependent eNOS pathway ⁹⁻¹¹. Therefore, we hypothesized that combined treatment of high-dose statin therapy with the EPC capture stent technology may improve the response of the patient population with low EPC titers, and the overall response to this pro-healing concept of percutaneous coronary intervention.

At enrollment, 79% of CAD patients were already maintained on statin therapy (34% Atorvastatin, 45% other statin therapy). Within two weeks after initiation of high dose Atorvastatin pharmacotherapy, relative EPC levels increased by 5.6-fold at the time of the index procedure and maintained elevated during a 30 day FU. Despite effective EPC recruitment,

treatment of elective patients with de-novo coronary artery disease with the EPC capture Genous Stent resulted at 6 month angiographic FU in a late luminal loss of 0.76 ± 0.50 , and a QCA-derived percent volume obstruction of $34\pm 26\%$ (table 4). The overall ischemia-driven and non-ischemia-driven revascularization rate at 6 month FU comprised 6.3%, whereas all MACE were 9.4%. These data are not significantly different from the results of the HEALING II study, although MACE seems somewhat increased in the HEALING IIB study. This difference may be explained by the fact that in the Healing II study patients with only one vessel disease were included, whereas in the HEALING IIB study, patients with multivessel disease were also included, making them more complex patients and more susceptible to MACE. Consequently, the number of study stents per patient and total stent length was significantly higher in the HEALING IIB study (see Table 2). Remarkably, comparable with the HEALING II study, angiographic late loss was significantly reduced by 0.10 mm (by matched serial analysis, $P=0.001$) between 6 and 18 months. This finding contrasts with findings in DES treated patients, where a progression of late loss is generally observed¹². Furthermore, one could speculate whether this regression in late luminal loss was reflected in clinical outcome, as MACE and TLR stabilized between 12 and 24 month FU. The question can therefore be raised whether the apparent advantage of DES in comparison with the EPC capture stent is only a temporal advantage, or whether longer-term clinical outcomes will prove otherwise. To address this question, randomized studies comparing DES and the Genous Stent, with clinical and angiographic FU after 24 months are required.

Re-endothelialization to inhibit in-stent restenosis formation

The assumption that regrowth of endothelium may limit neo-intimal accumulation has raised inconsistent results in pre-clinical and clinical studies. In gently denudated rat aortas, smooth muscle cell proliferation is not increased subjacent to the areas of endothelial loss¹³. In rat carotid arteries, neo-intimal accumulation after arterial injury is more related to medial injury than endothelial loss¹⁴. In balloon-injured rabbit iliofemoral arteries, early restoration of endothelium by autologous endothelial seeding did not decrease neo-intimal accumulation¹⁵. Human atherosclerotic plaques have been shown to develop under morphologically intact endothelium¹⁶, whereas endothelialized human coronary stents also contained substantial neo-intimal hyperplasia¹⁷. This suggests that the presence of endothelium and a resistance to intimal growth hence is not inextricably linked. In contrast, in a rabbit arterial balloon injury model, local delivery of VEGF accelerated stent endothelialization and reduced neo-intimal hyperplasia at 28 days FU¹⁸.

Various studies have shown that circulating EPCs are up-regulated following arterial injury and incorporated at the site of balloon or stent injury to form a new endothelial lining and initiate the vascular repair response¹⁹. Also, low circulating EPC levels or dysfunctional EPCs in CAD patients were associated with an increased risk of restenosis formation²⁰. Stents

bearing coatings of antibodies that specifically capture EPCs and immobilize these to the strut surface have been shown to accelerate endothelialization of the stent within 24 hours following stent implantation in rabbit aortic and porcine iliofemoral and coronary arteries (RGD coating ²¹, anti-CD105 coating [Active Endothelial Cell Capture by Stents Coated with Antibody against CD105, Song et al. TCT Asia Pacific 2009], and anti-CD34 coating).

However, the role of circulating EPCs on progression of atherosclerosis and neo-intimal hyperplasia is poorly understood and various lines of research have yielded conflicting results. Whereas Rausher and co-workers demonstrated that bone marrow-derived mononuclear cells attenuated the atherosclerotic burden in ApoE-deficient mice, others have shown that in the ApoE-deficient mice intravenous infusion of bone marrow derived mononuclear cells promoted atherosclerosis formation and in some studies was also associated with a more vulnerable composition of the atherosclerotic lesions with enhanced vascularization, larger lipid cores, thinner fibrous caps and higher numbers of infiltrating CD3 cells ²². Also, the effect of CD34+ circulating endothelial and smooth muscle progenitor cells on post-injury neo-intimal hyperplasia is poorly understood. Whereas some studies indicated a benefit on in-stent neo-intimal hyperplasia in stented pig arterial segments explanted at different time points ²³, others have failed to demonstrate a benefit in in-stent neo-intimal hyperplasia in porcine coronary arteries, despite a benefit on EPC capture and accelerated endothelialization (EPC capture in stented porcine coronary arteries increases endothelialization, but does not affect intimal thickening, HM van Beusekom et al., accepted in CCI, 2011). Also, accelerated coverage of PTFE prosthetic vascular in a porcine AV shunt graft model failed to prevent neo-intimal hyperplasia at the venous anastomosis, and actually, stimulated cellular proliferation led to prominent neo-intima formation ²⁴. The current study suggests that despite stimulation of EPC titer in all elective CAD patients, accelerated coverage of the EPC capture stent did not seem to impede restenosis formation and clinical MACE at 6 month FU and questions the paradigm that early re-endothelialization is a prerequisite for appropriate attenuation of neo-intimal hyperplasia. Even though we were unable to find an early effect on restenosis, there was a significant long term effect in terms of a reduction in late luminal loss between 6 and 18 months. This regression was accompanied by a stabilization of MACE and TLR rates between 12 and 24 months FU.

Re-endothelialization to inhibit in-stent thrombosis

Alternatively, accelerated re-endothelialization by an EPC capture stent technology may provide a non-thrombogenic coating of the exposed stent struts, thereby reducing the risk of in-stent thrombosis and potentially decreasing or eliminating the need for anti-thrombotic therapy. Recently, we showed in an ex-vivo human and baboon shunt model that in-stent thrombosis is decreased in the Genous Stent when compared to BMS ²⁵. Together with a decrease in mural thrombi, we showed a significant decrease in expression of tissue factor

pathway inhibitor (TFPI) and plasminogen activator inhibitor-1 (PAI-1), markers of thrombosis and coagulation, in the Genous Stent compared to BMS. On the contrary, some animal studies of arterial injury have previously suggested that thrombogenicity following arterial injury decreases in the absence of endothelialization. For instance, in balloon-injured rabbit aortas platelet deposition occurred within minutes, but did not increase over the subsequent 24 hours²⁶. Despite the absence of endothelialization, over the course of a week, the number of vessel-adhered platelets actually decreased, indicating that thrombogenicity decrease preceded endothelial regrowth. Moreover, exposed smooth muscle cells in balloon-injured rat carotid arteries were able to maintain a relatively non-thrombogenic surface²⁷. Local delivery of VEGF in stented iliac arteries of non-atherosclerotic rabbits resulted in a near complete re-endothelialization by day 7 following stent implantation versus placebo delivery with an associated reduction of mural thrombus formation. Even though the strength of the inverse correlation between stent endothelialization and the development of organized thrombus was relatively low ($r^2=.52$), these results suggest that next to endothelialization, other factors play an important role in thrombus suppression²⁸.

Recent autopsy and angiography studies suggested that following implantation of sirolimus eluting stents (SES) and paclitaxel eluting stents (PES), reendothelialization and arterial healing was incomplete for up to 6-12 months, therefore rendering the vessel more prone to late in-stent thrombosis²⁹. More extensive endothelial dysfunction and impeded arterial repair following implantation of SES/PES in remote vascular segments have been suggested by a persistent aberrant coronary vasomotor response to exercise and acetylcholine stimulation of the vascular segments adjacent to the implanted stent. The secondary end points of the HEALING IIB study therefore included in-stent thrombosis at 30 days and incidence of MACE at 6-month FU. 3 Patients suffered from a definite in-stent thrombosis at day 1, 9 and 181 days following the index procedure (by ARC definitions). The overall 3% incidence of definite in-stent thrombosis does not suggest an anti-thrombotic capacity of the EPC capture stent technology in the current study; however, all three events had documented significant procedural complications, which might have facilitated the in-stent thrombosis. For example, in the HEALING II study 0% stent thrombosis was reported and in the e-HEALING clinical registry of a real-world population (n=4939) treated with the Genous Stent, the 12 month definite and probable stent thrombosis rate was 1.1%³⁰. Moreover, it should be noted that the current study was largely underpowered to obtain a reliable estimate of the stent thrombosis rate with the Genous Stent. The stent thrombosis rate reported in the e-HEALING registry seems to confirm the favorable real world results with the Genous Stent, even in the absence of prolonged dual anti-platelet therapy.

A limitation of the study is the low compliance to 18 month angiographic follow up (78.1%, 75/96), which may have resulted in loss-to-follow up bias and underestimation of the stent thrombosis rate or late luminal loss.

In conclusion, in the HEALING IIB study, 100 elective patients with de novo coronary artery lesions received a Genous Stent in conjunction with HmG-CoA-reductase inhibitors (statins) to stimulate EPC recruitment. Although high dose statin therapy adequately enhanced EPC titers at the index procedure, the EPC capture stent technology did not sufficiently impede clinical restenosis rates and late luminal loss at 6 month angiographic FU. However, a significant reduction in late luminal loss was observed between 6 and 18 month angiographic FU which was accompanied by a stabilization of MACE and TLR rates between 12 and 24 months FU.

REFERENCES

1. Serruys PW, Morice MC, Kappetein AP, Colombo A, Holmes DR, Mack MJ, Stahle E, Feldman TE, van den Brand M, Bass EJ, Van Dyck N, Leadley K, Dawkins KD, Mohr FW. Percutaneous coronary intervention versus coronary-artery bypass grafting for severe coronary artery disease. *N Engl J Med* 2009;360:961-72.
2. Nakazawa G, Finn AV, Joner M, Ladich E, Kutys R, Mont EK, Gold HK, Burke AP, Kolodgie FD, Virmani R. Delayed arterial healing and increased late stent thrombosis at culprit sites after drug-eluting stent placement for acute myocardial infarction patients: an autopsy study. *Circulation* 2008;118:1138-45.
3. Hofma SH, van der Giessen WJ, van Dalen BM, Lemos PA, McFadden EP, Sianos G, Ligthart JM, van Essen D, de Feyter PJ, Serruys PW. Indication of long-term endothelial dysfunction after sirolimus-eluting stent implantation. *Eur Heart J* 2006;27:166-70.
4. Walter DH, Cejna M, Diaz-Sandoval L, Willis S, Kirkwood L, Stratford PW, Tietz AB, Kirchmair R, Silver M, Curry C, Wecker A, Yoon YS, Heidenreich R, Hanley A, Kearney M, Tio FO, Kuenzler P, Isner JM, Losordo DW. Local gene transfer of phVEGF-2 plasmid by gene-eluting stents: an alternative strategy for inhibition of restenosis. *Circulation* 2004;110:36-45.
5. Nakazawa G, Granada JF, Alviar CL, Tellez A, Kaluza GL, Guilhermier MY, Parker S, Rowland SM, Kolodgie FD, Leon MB, Virmani R. Anti-CD34 antibodies immobilized on the surface of sirolimus-eluting stents enhance stent endothelialization. *JACC Cardiovasc Interv*;3:68-75.
6. Aoki J, Serruys PW, van Beusekom H, Ong AT, McFadden EP, Sianos G, van der Giessen WJ, Regar E, de Feyter PJ, Davis HR, Rowland S, Kutryk MJ. Endothelial progenitor cell capture by stents coated with antibody against CD34: the HEALING-FIM (Healthy Endothelial Accelerated Lining Inhibits Neointimal Growth-First In Man) Registry. *J Am Coll Cardiol* 2005;45:1574-9.
7. Duckers HJ, Silber S, de Winter R, den Heijer P, Rensing B, Rau M, Mudra H, Benit E, Verheye S, Wijns W, Serruys PW. Circulating endothelial progenitor cells predict angiographic and intravascular ultrasound outcome following percutaneous coronary interventions in the HEALING-II trial: evaluation of an endothelial progenitor cell capturing stent. *EuroIntervention* 2007;3:67-75.
8. Duckers HJ, Soullie T, den Heijer P, Rensing B, de Winter RJ, Rau M, Mudra H, Silber S, Benit E, Verheye S, Wijns W, Serruys PW. Accelerated vascular repair following percutaneous coronary intervention by capture of endothelial progenitor cells promotes regression of neointimal growth at long term follow-up: final results of the Healing II trial using an endothelial progenitor cell capturing stent (Genous R stent). *EuroIntervention* 2007;3:350-8.
9. Vasa M, Fichtlscherer S, Aicher A, Adler K, Urbich C, Martin H, Zeiher AM, Dimmeler S. Number and migratory activity of circulating endothelial progenitor cells inversely correlate with risk factors for coronary artery disease. *Circ Res* 2001;89:E1-7.
10. Dimmeler S, Aicher A, Vasa M, Mildner-Rihm C, Adler K, Tiemann M, Rutten H, Fichtlscherer S, Martin H, Zeiher AM. HMG-CoA reductase inhibitors (statins) increase endothelial progenitor cells via the PI 3-kinase/Akt pathway. *J Clin Invest* 2001;108:391-7.
11. Spyridopoulos I, Haendeler J, Urbich C, Brummendorf TH, Oh H, Schneider MD, Zeiher AM, Dimmeler S. Statins enhance migratory capacity by upregulation of the telomere repeat-binding factor TRF2 in endothelial progenitor cells. *Circulation* 2004;110:3136-42.

12. Aoki J, Abizaid AC, Serruys PW, Ong AT, Boersma E, Sousa JE, Bruining N. Evaluation of four-year coronary artery response after sirolimus-eluting stent implantation using serial quantitative intravascular ultrasound and computer-assisted grayscale value analysis for plaque composition in event-free patients. *J Am Coll Cardiol* 2005;46:1670-6.
13. Reidy MA, Silver M. Endothelial regeneration. VII. Lack of intimal proliferation after defined injury to rat aorta. *Am J Pathol* 1985;118:173-7.
14. Fingerle J, Au YP, Clowes AW, Reidy MA. Intimal lesion formation in rat carotid arteries after endothelial denudation in absence of medial injury. *Arteriosclerosis* 1990;10:1082-7.
15. Conte MS, Choudhury RP, Shirakawa M, Fallon JT, Birinyi LK, Choudhry RP. Endothelial cell seeding fails to attenuate intimal thickening in balloon-injured rabbit arteries. *J Vasc Surg* 1995;21:413-21.
16. Ross R. The pathogenesis of atherosclerosis: a perspective for the 1990s. *Nature* 1993;362:801-9.
17. Anderson PG, Bajaj RK, Baxley WA, Roubin GS. Vascular pathology of balloon-expandable flexible coil stents in humans. *J Am Coll Cardiol* 1992;19:372-81.
18. Van Belle E, Maillard L, Tio FO, Isner JM. Accelerated endothelialization by local delivery of recombinant human vascular endothelial growth factor reduces in-stent intimal formation. *Biochem Biophys Res Commun* 1997;235:311-6.
19. Rauscher FM, Goldschmidt-Clermont PJ, Davis BH, Wang T, Gregg D, Ramaswami P, Phippen AM, Annex BH, Dong C, Taylor DA. Aging, progenitor cell exhaustion, and atherosclerosis. *Circulation* 2003;108:457-63.
20. George J, Herz I, Goldstein E, Abashidze S, Deutch V, Finkelstein A, Michowitz Y, Miller H, Keren G. Number and adhesive properties of circulating endothelial progenitor cells in patients with in-stent restenosis. *Arterioscler Thromb Vasc Biol* 2003;23:e57-60.
21. Blindt R, Vogt F, Astafieva I, Fach C, Hristov M, Krott N, Seitz B, Kapurniotu A, Kwok C, Dewor M, Bosserhoff AK, Bernhagen J, Hanrath P, Hoffmann R, Weber C. A novel drug-eluting stent coated with an integrin-binding cyclic Arg-Gly-Asp peptide inhibits neointimal hyperplasia by recruiting endothelial progenitor cells. *J Am Coll Cardiol* 2006;47:1786-95.
22. George J, Afek A, Abashidze A, Shmilovich H, Deutsch V, Kopolovich J, Miller H, Keren G. Transfer of endothelial progenitor and bone marrow cells influences atherosclerotic plaque size and composition in apolipoprotein E knockout mice. *Arterioscler Thromb Vasc Biol* 2005;25:2636-41.
23. Granada JF, Inami S, Aboodi MS, Tellez A, Milewski K, Wallace-Bradley D, Parker S, Rowland S, Nakazawa G, Vorpahl M, Kolodgie FD, Kaluza GL, Leon MB, Virmani R. Development of a novel prohealing stent designed to deliver sirolimus from a biodegradable abluminal matrix. *Circ Cardiovasc Interv*;3:257-66.
24. Rotmans JI, Heyligers JM, Verhagen HJ, Velema E, Nagtegaal MM, de Kleijn DP, de Groot FG, Stroes ES, Pasterkamp G. In vivo cell seeding with anti-CD34 antibodies successfully accelerates endothelialization but stimulates intimal hyperplasia in porcine arteriovenous expanded polytetrafluoroethylene grafts. *Circulation* 2005;112:12-8.
25. Larsen K, Cheng C, Tempel D, Parker S, Yazdani S, den Dekker WK, Houtgraaf JH, de Jong R, Swager-ten Hoor S, Ligtenberg E, Hansen S, Rowland S, Kolodgie F, Serruys PW, Virmani R, Duckers HJ. Capture of circulatory endothelial progenitor cells and accelerated re-endothelialization of a bio-engineered stent in human ex-vivo shunt and rabbit model. *Eur Heart J* in press
26. Groves HM, Kinlough-Rathbone RL, Richardson M, Moore S, Mustard JF. Platelet interaction with damaged rabbit aorta. *Lab Invest* 1979;40:194-200.

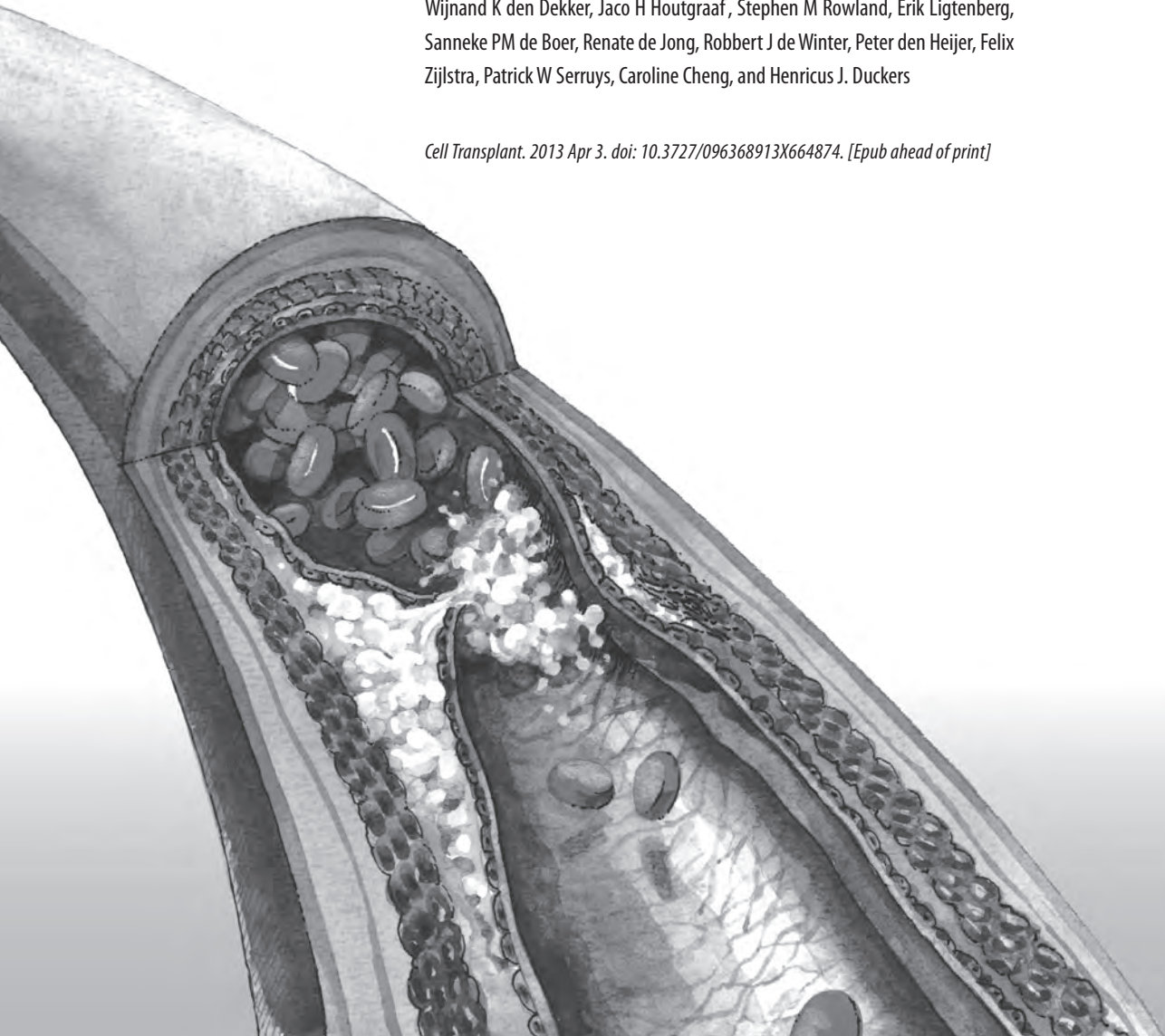
27. Clowes AW, Clowes MM, Reidy MA. Kinetics of cellular proliferation after arterial injury. III. Endothelial and smooth muscle growth in chronically denuded vessels. *Lab Invest* 1986;54:295-303.
28. Van Belle E, Tio FO, Couffinhal T, Maillard L, Passeri J, Isner JM. Stent endothelialization. Time course, impact of local catheter delivery, feasibility of recombinant protein administration, and response to cytokine expedition. *Circulation* 1997;95:438-48.
29. Nakazawa G, Ladich E, Finn AV, Virmani R. Pathophysiology of vascular healing and stent mediated arterial injury. *EuroIntervention* 2008;4 Suppl C:C7-10.
30. Silber S, Damman P, Klomp M, Beijk MA, Grisold M, Ribeiro EE, Suryapranata H, Wojcik J, Hian Sim K, Tijssen JG, de Winter RJ. Clinical results after coronary stenting with the Genous Bio-engineered R stent: 12-month outcomes of the e-HEALING (Healthy Endothelial Accelerated Lining Inhibits Neointimal Growth) worldwide registry. *EuroIntervention*;6:819-25.

Chapter 7

Efficiency of statin treatment on EPC recruitment depends on baseline EPC titer, and does not improve angiographic outcome in coronary artery disease patients treated with the Genous™ stent

Wijnand K den Dekker, Jaco H Houtgraaf, Stephen M Rowland, Erik Ligtenberg, Sanneke PM de Boer, Renate de Jong, Robbert J de Winter, Peter den Heijer, Felix Zijlstra, Patrick W Serruys, Caroline Cheng, and Henricus J. Duckers

Cell Transplant. 2013 Apr 3. doi: 10.3727/096368913X664874. [Epub ahead of print]



ABSTRACT

Objective To assess the effect of high dose Atorvastatin treatment on endothelial progenitor cell (EPC) recruitment and angiographic and clinical outcome in coronary artery disease (CAD) patients treated with the Genous™ EPC capturing stent.

Methods The HEALING IIB study was a multi-center, open-label, prospective trial that enrolled 100 patients. Patients were started on 80mg Atorvastatin qd, at least two weeks before index procedure and continued for at least four weeks after the index procedure.

Results 87 Patients were included in this analysis. EPC levels significantly increased as early as 2 weeks after start of statin. Remarkably, among this group, 31 patients proved to be non-responder to Atorvastatin treatment (i.e. no increase in EPC levels) while 56 patients were responders (i.e. rise in EPC count between week -2 and 0). Compared to responders, non-responders had a significantly higher baseline EPC count (76 ± 10 vs. 41 ± 5 , $p < 0.01$) with a lower LLL at 6 and 18 month FU (0.61 ± 0.07 vs. 0.88 ± 0.08 $p < 0.05$ and 0.50 ± 0.08 vs. 0.82 ± 0.08 $p < 0.01$ respectively). Furthermore, baseline EPC count inversely correlated with LLL at 6 month follow-up (FU) ($R = -0.42$, $p < 0.001$).

Conclusion Patients with higher EPC count at baseline showed no increase in EPC recruitment in response to statin treatment but had favorable LLL at 6 and 18 month FU, whereas patients with lower EPC count were responsive to statin therapy but EPCs might be less functional as they had higher LLL at 6 and 18 month FU. These data imply that, although statin treatment can enhance EPC titer in these patients with low baseline levels, there is no indication for a possible beneficial clinical effect with EPC capture stents.

INTRODUCTION

In recent years there has been a tremendous development in the treatment of coronary artery disease (CAD), from balloon angioplasty to bare metal stent placement to stents with active coatings. The introduction of bare metal improved the outcome of percutaneous coronary intervention (PCI), but on the long-term, restenosis of the stent can occur due to vascular smooth muscle cell (VSMC) proliferation. Nowadays, more advanced stents bearing cytostatic compounds have been developed. These so-called drug eluting stents (DES) have largely overcome the problem of restenosis as they inhibit the proliferation of VSMCs. However, DES have been associated with stent thrombosis as they also inhibit the regrowth of the endothelium. The endothelium plays a pivotal role in maintaining vascular integrity and function and injury or dysfunction can trigger the onset of cardiovascular disease. It is therefore important to maintain vascular integrity by rapid restoration of any damage to the endothelium. Vascular repair can be ensured by proliferation and migration of adjacent mature endothelial cells or incorporation of circulating endothelial progenitor cells (EPCs). EPCs were first described by Asahara et al in 1997 and were defined as CD34+ or KDR+ cells with the ability to differentiate into endothelial cells *in vitro* (2). Furthermore, they showed *in vivo* that those cells contributed to neoangiogenesis in a murine and a rabbit hindlimb ischemia model. Since this initial study, many researchers have reported a beneficial effect of EPCs on neovascularization, reendothelialization and reduction of neo-intima formation in animal studies (11,12,13,21). Observational clinical studies showed that circulating EPC levels were correlated with cardiovascular risk factors and outcome (5,19,22).

As EPCs can enhance the arterial repair, an anti-human antibody coated stent (Genous™ Bio-engineered R stent, OrbusNeich) was designed to bind circulating CD34+ hematopoietic cells and facilitate accelerated vascular repair and decrease neo-intima formation after stent placement (1,15). The HEALING II study showed that use of the Genous stent for the treatment of de novo coronary artery disease is safe and feasible with an in stent late luminal loss (LLL) after 6 months of 0.78 ± 0.39 mm (6,7). Remarkably, patients with low circulating EPC levels responded relatively poorly to the Genous stent with worse clinical and angiographic outcome. We therefore hypothesized that an increase in the number of circulating EPCs would improve the response to the Genous stent and subsequently improve clinical and angiographic outcome. As statins can increase circulating EPCs (16,20,22), we designed the HEALING IIB study in which we evaluated the efficacy of the Genous stent in conjunction with high dose statin (Atorvastatin 80mg qd) therapy. We previously reported the clinical and angiographic outcome of the HEALING IIB study (4). Here, we present the in depth-analysis of the effect of Atorvastatin treatment on circulating EPC levels and correlate these findings with patient clinical outcome of the HEALING IIB trial.

MATERIAL AND METHODS

Study population and protocol

The design and clinical results of the HEALING IIB trial were recently published¹⁶. Briefly, 100 patients, from 13 sites in 7 European countries were enrolled, with a diagnosis of de novo stable or unstable angina or silent ischemia with a maximum of two de novo lesions in two independent native coronary arteries eligible for coronary stenting. Patients were started on 80mg atorvastatin qd at two weeks before index procedure and continued for at least four weeks after index procedure. Patients already on statin therapy were switched to 80 mg atorvastatin qd. Aspirin treatment was initiated 12 hours before the procedure (75 mg qd), whereas a loading dose of 300 mg of clopidogrel was administered prior to the procedure, proceeded by 75 mg qd for the period of 4 weeks. Administration of GPIIb/IIIa was left at the investigator's discretion.

Anginal status (according to the Canadian Cardiovascular Society Classification of Angina and the Braunwald Classification for Unstable Angina) and the documentation of Major Adverse Cardiac Events (MACE) were assessed at 1, 6, 12, 18 and 24 month follow-up (FU). Circulating CD34+ EPC titers were quantified by flow cytometric analysis at screening (baseline), 2 weeks after initiation of high dose Atorvastatin and at 30 days FU of the index procedure.

Quantitative angiographic analysis was performed at 6- and 18-month FU. Coronary angiograms were obtained in perpendicular views following an intracoronary injection of nitrates. Off-line quantitative analyses of pre-procedural, post-procedural, 6- and 18-month FU angiographic data were performed at an independent imaging core laboratory (Cardialysis, Rotterdam, the Netherlands).

The trial was reviewed and approved by the local Medical Ethics Review Committees, and written informed consent was obtained from all patients.

Genous™ R stent - Endothelial progenitor cell capture technology

The Genous™ Bio-engineered R stent is based on a 316L stainless steel stent platform with study devices available in diameters of 2.5, 3.0, and 3.5mm and lengths of 9, 18, 23, and 33mm (OrbusNeich Medical, Fort Lauderdale, FL) with a polysaccharide matrix coating covalently coupled with murine anti-human CD34 antibodies which specifically target the CD34-positive circulating endothelial cell progenitor population.

Blood sample preparation

Venous blood was drawn under sterile conditions and collected in EDTA collection tubes. Whole blood was used to measure circulating EPC levels.

Quantification of circulating endothelial progenitor cells

EPCs were measured using the Stem Cell Kit (Beckman Coulter Comp, Cedex, F) and a modified ISHAGE protocol. Whole blood was incubated with complete antibody mix, i.e. APC-labeled anti-hCD45, FITC-labeled anti-hCD34 (Pharmingen) and PE-labeled anti-hKDR (R&D systems). As negative control we used PE labeled anti-hIgG (Pharmingen). Blood was incubated for twenty minutes at room temperature. Dead cells were excluded using 7-AAD viability dye. Samples were lysed for ten minutes at room temperature using two ml of lysis buffer. Hundred microliter counting beads were added to correlate cell amounts to blood volume. Duplicate samples and one isotypic control were analyzed on an automated flow cytometer (FACSCanto®, Becton&Dickinson). Final data analysis was done with Flowjo software (Tree Star, Inc., USA, see figure 1). We first excluded dead cells by gating on a 7-AAD vs. side scatter (SSC) dot plot. The remaining viable cells were displayed on a CD45 vs. SSC dot plot. We gated the CD45 positive and dim population to select lymphocytes and exclude red blood cells and debris. On the third plot, showing the CD34 vs. SSC dot plot, we gated the bright CD34 cell population and further excluded irrelevant cells by a lymphogate. EPCs were characterized as 7-AAD-, CD45 dim/+, CD34+, FSC/SSC_{low} and VegfR2+. The EPC gate is set according to the IgG1-PE isotypic control.

Statistical analysis

Continuous data are presented as mean \pm standard deviation (SD) and categorical variables are expressed as numbers and percentages. The Kolmogorov-Smirnov test was used to analyze whether continuous data were normally distributed. Differences in baseline characteristics between responders and non-responders were analyzed by student's t-tests, the Mann-Whitney-U test, chi-square tests, and Fisher's Exact test as appropriate. EPC counts at different time points were compared using repeated measurements ANOVA for normally distributed variables, with Newman-Keuls as post-hoc test and Friedman test for non-normally distributed variables, with Dunn's multiple comparison test as post-hoc test. Spearman correlation coefficient was used to correlate circulating EPC counts with clinical outcome.

We applied a univariable logistic regression (LR) analysis to detect clinical characteristics that influenced the risk of being a non-responder to Atorvastatin treatment. To determine independent risk factor of being a non-responder, we applied a multivariable LR analysis. Non-responder was considered the dependent variable and the following independent

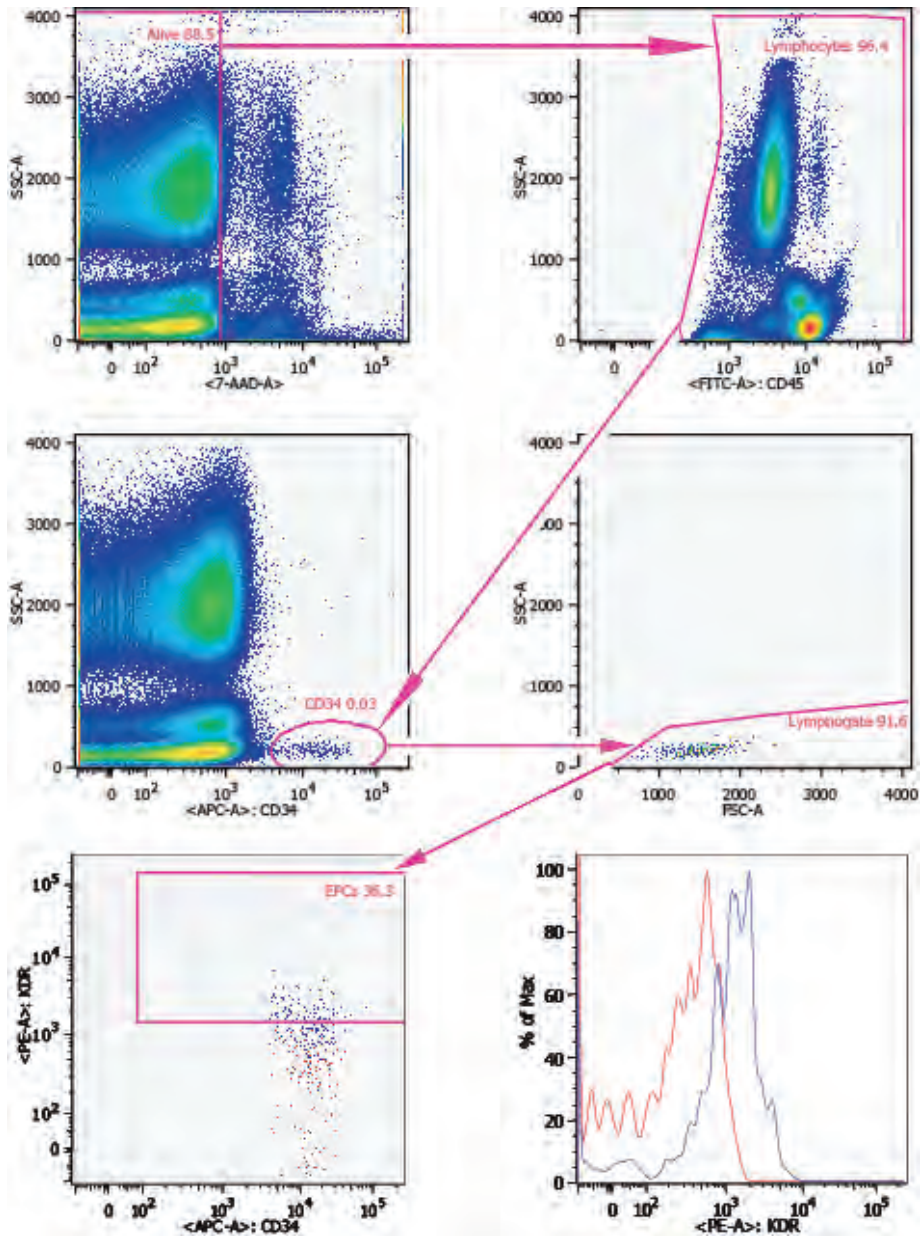


Figure 1

We used a novel method to measure EPCs in whole blood using a modified ISHAGE protocol. Dead cells are excluded with a 7-AAD viability dye. Lymphocytes are selected as CD45 dim and positive cells. The bright CD34 cell population is selected and a lymphogate excludes irrelevant cells. EPCs are characterized as 7-AAD-, CD45dim/+, CD34+, FSC/SSC low and KDR+. The gate is always set according to the IgG1-PE isotypic control

variables: baseline EPC count, age, sex, hypertension, diabetes mellitus, hypercholesterolemia, previous statin use, BMI and smoking history were considered potential determinants. Because of the relatively small sample size, we performed multivariable LR with backward deletion and all variables with a *P*-value <0.15 were maintained in the model.

We report crude and adjusted odds ratios (ORs) along with their 95% confidence intervals (CIs). For all tests, a two-sided *P*-value of less than 0.05 was considered significant. All statistical analyses were performed using SPSS 17.0 for Windows (SPSS, Inc., Chicago, IL) and GraphPad Prism 4.

RESULTS

Baseline characteristics

We included one hundred patients in the HEALING IIB study. Four patients were per protocol excluded from post-procedural analysis; two patients did not meet the in- and exclusion criteria, one patient was not on Atorvastatin during two weeks pre-procedure as required per protocol and one patient had a post-procedural diameter stenosis of 32% despite post dilatation. Another 9 patients were excluded from this analysis because of missing values in EPC count on baseline or two weeks FU.

Among the final 87 patients, 31 patients were non-responders to Atorvastatin treatment (i.e. no rise in EPC count between week -2 and week 0) and 56 patients were responders (i.e. rise in EPC count between week -2 and 0). Baseline characteristics for the non-responder and responder groups are summarized in table 1. Baseline characteristics between non-responders and responders were relatively similar, except for baseline EPC count, sex and smoking status. There was no difference in medication use between the two groups (data not shown). Seventy-one percent of the patients in the responders group and 74 percent of the patients in the non-responders group were already on statin therapy before start of the study ($p=0.78$) and switched to 80 mg of Atorvastatin treatment. At the index procedure, 100% of the patients were initiated on high dose Atorvastatin therapy (80 mg qd) for at least 2 weeks according to the protocol outline. At one month FU, 91% of the patients were still being treated with Atorvastatin 80 mg qd.

Effect of Atorvastatin treatment on serum lipid profile in responders and non-responders

As shown in table 2, Atorvastatin treatment resulted in a significant decrease in total cholesterol, LDL-cholesterol and triglyceride level in the responders group, while there was no effect on HDL-cholesterol. Likewise, the non-responders showed a significant decrease in total cholesterol and LDL-cholesterol and a trend towards a decrease in triglyceride level. HDL cholesterol was not affected by Atorvastatin in the non-responders.

Table 1. Patient demographics and clinical characteristics

Patient parameter	Responders (N=56)	Non responders (N=31)	P value
Age (years)			
Mean \pm SD	62.110.5	64.9 \pm 8.3	>0.05
Min-max	37-80	49-82	
Body Mass Index (kg/m ²)			
Mean \pm SD	27.2 \pm 3.5	27.9 \pm 6.0	>0.05
Min-max	21.5-40.4	17.1-41.9	
Male	82.1% (46/56)	54.8% (17/31)	<0.05
Diabetes mellitus	17.9% (10/56)	25.8% (8/31)	>0.05
Hypertension	62.5% (35/56)	77.4% (24/31)	>0.05
Hypercholesterolemia	87.5% (49/56)	77.4% (24/31)	>0.05
Previous stroke	3.6% (2/56)	0.0% (0/31)	>0.05
Congestive heart failure	5.4% (3/56)	0.0% (0/31)	>0.05
Family history of MI	48.2% (27/56)	58.1% (18/31)	>0.05
Previous MI	32.1% (18/56)	16.1% (5/31)	>0.05
Previous CABG	3.2% (2/56)	0.0% (0/31)	>0.05
Previous PTCA	14.3% (8/56)	19.4% (6/31)	>0.05
Smoking history			
Never	29,8% (17/56)	51.6% (16/31)	
Previous	50.9% (29/56)	22.6% (7/31)	
Current	17.5% (10/56)	25.8% (10/31)	
Ischemic status			
Unstable angina	3.5% (2/56)	16.1% (5/31)	>0.05
Stable angina	86.0% (49/56)	71.0% (22/31)	>0.05
Silent ischemia	10.5% (6/56)	12.9% (4/31)	>0.05

Numbers are % (counts/available field sample size) or mean \pm 1 Standard deviation

SD Standard deviation

MI Myocardial Infarction

CABG Coronary Artery Bypass Graft

PTCA Percutaneous Transluminal Coronary Angioplasty

Table 2. Serum lipid levels before and after start of 80 mg Atorvastatin treatment

		T=-2 weeks	T=+4 weeks	p value
Non responder	Total cholesterol	178,2±6,8	136,2±5,9	p<0,01
	LDL cholesterol	48,2±2,4	44,7±2,7	p=0,3
	HDL cholesterol	99,5±6,6	69,5±5,2	p<0,01
	Triglycerides	124,9±16,8	90,2±13,3	p=0,13
Responder	Total cholesterol	186,2±6,4	127,9±17,1	p<0,01
	LDL cholesterol	45,0±1,8	42,9±5,7	p=0,39
	HDL cholesterol	112,7±5,8	67,1±9,0	p<0,01
	Triglycerides	125,5±10,2	82,3±11,0	p<0,01

Effect of Atorvastatin on circulating endothelial progenitor cell levels

First, we assessed the effect of Atorvastatin treatment on circulating EPC levels for the complete HIIB cohort. As shown in figure 2A, baseline EPC levels were 53.7 ± 5.4 cells/100 μ l. Two weeks of Atorvastatin treatment resulted in a significant increase in EPC levels to 74.9 ± 6.3 cells/100 μ l ($p < 0.05$ by repeated measurements ANOVA) and this was maintained until six weeks after start of treatment (85.2 cells ± 8.5 cells/100 μ l, $p < 0.05$ by repeated measurements ANOVA and compared to baseline). When we divided the patients into responders to Atorvastatin treatment and non-responders, the responders had a significant increase in EPC levels from 41.1 ± 5.2 cells/100 μ l to 89.4 ± 7.9 cells/100 μ l at two weeks ($p < 0.001$) and 96.4 ± 11.8 cells/100 μ l at six weeks ($p < 0.001$, see figure 2B), while the non-responders showed a significant decrease upon Atorvastatin treatment from 76.4 ± 10.9 cells/100 μ l to 48.6 ± 8.3 cells/100 μ l at two weeks ($p < 0.001$) and 65.7 ± 9.9 cells/100 μ l at six weeks ($p < 0.05$, see figure 2C). At baseline, there were significantly higher numbers of circulating EPCs in the non-responder group compared to the responder group (76.4 ± 10.9 cells/100 μ l vs. 41.1 ± 5.2 cells/100 μ l, $p < 0.01$). Two weeks of Atorvastatin treatment reversed this and the non-responders had a significantly lower number of circulating EPCs (48.6 ± 8.3 cells/100 μ l vs. to 89.4 ± 7.9 cells/100, for non-responders and responders respectively, $p < 0.001$, see figure 2D).

Determinants of response to atorvastatin treatment

Baseline EPC count and the number of patients that never smoked were significantly higher in non-responders, whereas there were less men. When we applied our LR model, only baseline EPC count (aOR: 1.02 and 95% CI: 1.007-1.031) and having never smoked (aOR 0.27 and 95% CI: .082-.913) were independent risk factors for being a non-responder (see table 3).

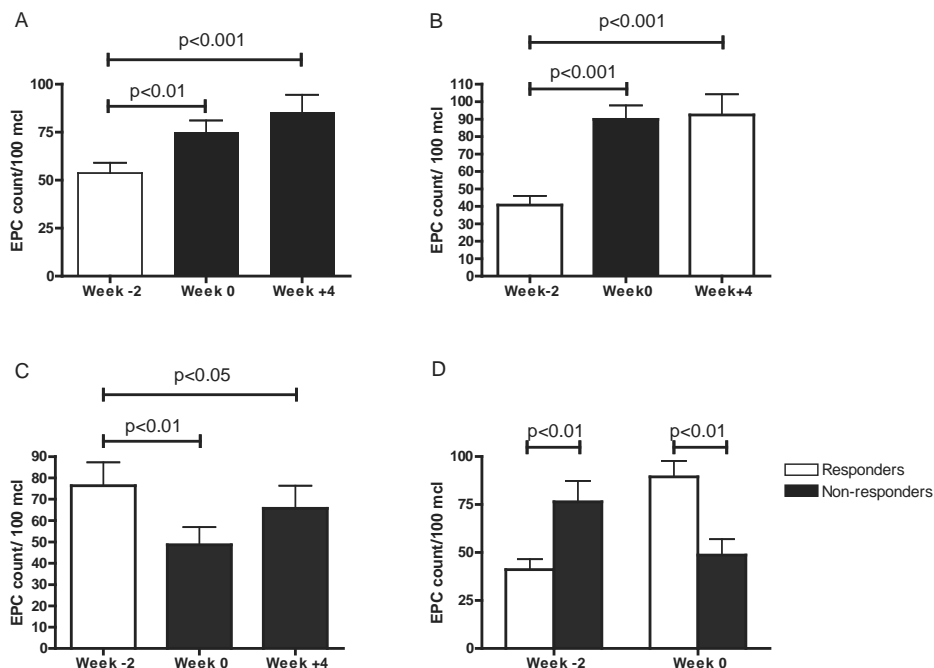


Figure 2

Statin increased circulating EPC levels for the complete HEALING IIB cohort as early as two weeks and was maintained until six weeks. Responders to statin therapy had a significant increase in circulating EPC levels, two and six weeks after start of treatment. Non-responders showed even a significant decrease in circulating EPC levels upon statin treatment. Non-responders had a significant higher baseline EPC count compared to responders. Two weeks after start of treatment, this was reversed and responders had a significant higher EPC count.

Circulating endothelial progenitor cell levels and clinical and angiographic outcome

Complete H2B cohort

Baseline EPC count inversely correlated with late luminal loss (LLL) at six months (see figure 3A, Spearman $r = -0.41$, $p < 0.001$). EPC levels at baseline did not correlate with major adverse cardiac events (MACE) or target lesion revascularization (TLR) at six months. Although statin significantly increased circulating EPC levels for the complete HEALING IIB cohort, this was not accompanied by an improvement in LLL as LLL was comparable with the HEALING II study.

Non-responders vs. responders

Baseline EPC count of non-responders inversely correlated with LLL (Spearman $r = -0.38$, $p < 0.05$ and Spearman $r = -0.26$, $p > 0.05$, see figure 3B and 3C). Responders did not show such a

correlation. LLL at six and eighteen months were significantly lower in non-responders compared to responders (0.61 ± 0.07 vs. 0.88 ± 0.08 , $p < 0.05$ and 0.50 ± 0.08 vs. 0.82 ± 0.08 , $p < 0.01$, see figure 4). There were no target lesion revascularizations (TLRs) in the non-responders group and six in the responders group ($p = 0.09$).

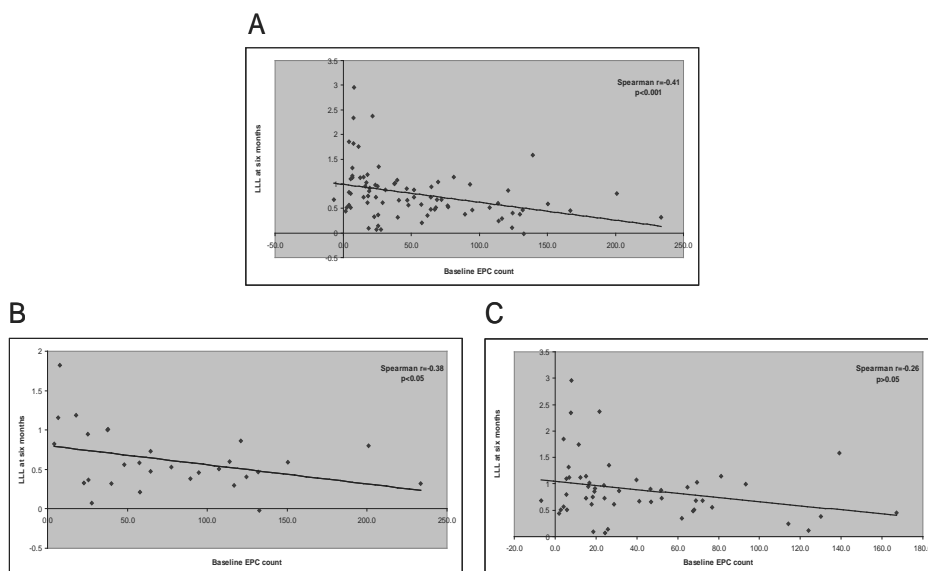


Figure 3
A. Baseline EPC count significantly correlates with LLL in the complete HEALING IIB cohort. B. Baseline EPC also significantly correlates with LLL in the non-responders group but not in the responders group (C).

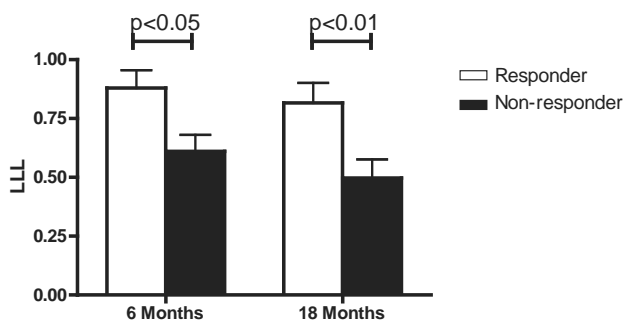


Figure 4
Non-responders group has a significantly lower LLL at six and eighteen month FU.

DISCUSSION

In this subanalysis of the HEALING IIB study we evaluated the effect of high dose Atorvastatin treatment on circulating EPC levels and correlation with angiographic and clinical follow-up. Prati and co-workers already showed that high dose Atorvastatin treatment could reduce in stent restenosis and late luminal loss (18). However, in contrast to the RESTART study, we specifically looked at the effect of high dose Atorvastatin treatment on EPC levels and its effect on late luminal loss. Our study supplies data on the possible role of EPCs in LLL and demonstrate that statin treatment in patients might contribute to vascular healing via EPC recruitment.

In line with earlier studies (16,20,22), statin treatment significantly increased circulating EPC levels for the complete HEALING IIB cohort, as early as two weeks after start of statin treatment. When we evaluated EPC levels for each individual patient at every time point, we could divide the cohort in patients responding to statin treatment with a rise in EPC level (responder group) and patients who did not respond to statin treatment with an increase in EPC level (non-responder group). Interestingly, the non-responder group had a significantly higher baseline EPC count in comparison to the responders group, suggesting that the response to statin treatment on EPC level depends on baseline EPC count and that patients with a high baseline EPC count are unable to recruit or produce more EPCs despite high dose statin treatment. An alternative, and maybe more logical explanation would be that non-responders react to vascular disease with a more efficient vascular repair response. That would explain the high basal level of EPC count in blood in non-responders versus responders (76.4 ± 10.9 cells/100 μ l vs. 41.1 ± 5.2 cells/100 μ l, $p < 0.01$), which indicates that the non-responders are more capable of recruiting EPCs from the bone marrow into the blood stream. Likewise, the blood circulatory pool of EPCs of non-responders may be more efficient in homing to the affected vascular area, an intrinsic capacity that was further amplified by statin treatment (3,14). For the responders, the data might imply that although recruitment of EPCs from bone marrow by statin treatment is successful, the recruited EPCs in the bloodstream remain inefficient in homing capacity to the target vessel wall. Further research is required to assess this hypothesis on the complex effect of statins on EPC recruitment and homing.

EPC levels and cardiovascular risk factors

Earlier publications showed that several cardiovascular risk factors, for example hypertension, diabetes, age, smoking status or increased body mass index could affect EPC titer. Vasa and coworkers reported that patients with coronary artery disease had lower EPC levels compared to healthy volunteers. Moreover, the number of risk factors was significantly correlated with lower EPC levels and multivariate analysis showed that smoking status was an independent predictor of reduced EPC levels. Later, Hill and coworkers showed in a relative small group of

healthy volunteers that the number of EPC colony forming units was significantly reduced in patients with diabetes, hypercholesterolemia or hypertension. When they adjusted for age, only hypercholesterolemia remained significant. Multivariate analysis revealed that only flow mediated brachial reactivity, a composite measure of endothelial integrity, was an independent predictor of reduced EPC colonies. Here we assessed whether cardiovascular risk factors could affect being a non-responder or responder. We found a significant difference between responders and non-responders in baseline EPC count, smoking status and sex. However, when we applied our LR model, only baseline EPC count and smoking status remained significant predictors for being a non-responder, i.e higher baseline EPC count.

EPC levels and cardiovascular outcomes

Baseline EPC count inversely correlated with late luminal loss (LLL) for the complete HEALING IIB cohort. Furthermore, patients from the non-responders group had a lower LLL at six months FU compared to patients from the responders group. This difference in LLL was even more pronounced at eighteen months FU. As Ellis and coworkers showed that LLL can serve as surrogate clinical endpoint (8), we evaluated the occurrence of target lesion revascularization (TLR). Indeed, we found a trend towards more TLRs in the responders group. These results suggest that baseline EPC count can predict the response to the GENOUS stent in terms of LLL and perhaps clinical benefit. There is much debate about the significance of baseline EPC count in the pathophysiology of cardiovascular disease. It was already shown that low circulating EPC levels are associated with less favorable cardiovascular outcomes (5,9,19). As circulating EPCs play an important role in maintaining integrity of the endothelial layer by accelerating re-endothelialization in injured arteries, low levels of EPCs could result in delayed re-endothelialization and increased cardiovascular risk. Our study confirmed these results, but furthermore showed that baseline EPC count is correlated with angiographic outcome, not only at six months FU but also at 18 months FU. Pelliccia and coworkers were the first to prospectively assess circulating EPC levels and the occurrence of in-stent restenosis or progression of coronary artery disease in patients treated with a bare metal stent (17). In contrast to our findings, they showed that high circulating EPC count correlated with the occurrence of in-stent restenosis and high late LLL, possibly due to engraftment of EPCs in the neo-intima and subsequently differentiation into vascular smooth muscle cells. There was no correlation between EPC count and progression of atherosclerosis, stable coronary artery disease or healthy controls. There are some differences between our work and the work of Pelliccia. First of all, as with many papers on EPCs, there is a difference in characterization of EPCs, as there is no standardized way to measure EPCs. Originally, EPCs were described as CD34+ or KDR+ cells and now different combination of cell surface markers have been advocated to define EPCs, most commonly CD133+/CD34+/KDR+, CD34+KDR+, CD34+/KDR+/CD45- or CD14+/CD34^{low}. We measured EPCs using a modified ISHAGE protocol using whole blood in which

the EPC population was defined as CD45+/CD34+/KDR+, whereas Pelliccia and coworkers used mononuclear cells, defining EPCs as CD45-/CD34+/KDR+. Secondly, Pelliccia included only stable angina patients, whereas we also included patients with unstable angina and silent ischemia. Thirdly, our patients were treated with the GENOUS stent and Pelliccia used the bare metal stent. However, it seems unlikely that this influenced baseline EPC count, as blood was drawn at least one day before PCI. More recently, in contrast to our work and the work of Pelliccia, Haine et al. reported that they found no correlation between circulating EPC levels and angiographic and clinical restenosis (*Blood endothelial progenitor cells as predictive markers for coronary in-stent restenosis*, moderated poster session, ESC, Paris 2011), making it even more complex to understand the role of EPCs in cardiovascular disease and outcome. We believe that, at least for the clinical outcome after GENOUS stent placement, baseline EPC count is a valid biomarker for and reflects the regenerative potency of the vascular bed.

Interestingly, although statin treatment significantly increased circulating EPC count in the responders group, this increase was not reflected in a favorable LLL. One explanation could be that the responders group not only had lower baseline EPC count but also less functional EPCs and that statin therapy can increase EPC count but can not improve the angiogenic capacities of these cells. However, we can only speculate on this as we only performed a quantitative analysis of the EPCs, but no functional analysis. Future studies to elucidate the angiogenic potential of EPCs of this specific subset of non-responder patients will help to understand the complex biology behind these clinical findings.

Conclusion

To our best knowledge, this is the first prospective study to show that there is a significant difference in baseline EPC count between responders and non-responders to Atorvastatin 80 mg treatment for EPC recruitment in coronary artery disease patients treated with the GENOUS stent. Furthermore, higher baseline EPC count correlated with favorable angiographic outcome with less LLL at six and eighteen months FU compared to lower baseline EPC count. Although statin treatment significantly increased circulating EPC levels in the responders group, this was not reflected in improved angiographic outcome, suggesting that low EPC count reflects less functional EPCs. EPCs might be used as predictor for angiographic outcome for patients treated with the GENOUS stent.

REFERENCES

1. Aoki, J.; Serruys, P.W.; van Beusekom, H.; Ong, A.T.; McFadden, E.P.; Sianos, G.; van der Giessen, W.J.; Regar, E.; de Feyter, P.J.; Davis, H.R.; Rowland, S.; Kutryk, M.J. Endothelial progenitor cell capture by stents coated with antibody against CD34: the HEALING-FIM (Healthy Endothelial Accelerated Lining Inhibits Neointimal Growth-First In Man) Registry. *J. Am. Coll. Cardiol.* 45(10):1574-1579; 2005.
2. Asahara, T.; Murohara, T.; Sullivan, A.; Silver, M.; van der Zee, R.; Li, T.; Witztzenbichler, B.; Schatteman, G.; Isner, J.M. Isolation of putative progenitor endothelial cells for angiogenesis. *Science* 275(5302):964-967; 1997.
3. Asahara, T.; Masuda, H.; Takahashi, T.; Kalka, C.; Pastore, C.; Silver, M.; Kearne, M.; Magner, M.; Isner, J.M. Bone marrow origin of endothelial progenitor cells responsible for postnatal vasculogenesis in physiological and pathological neovascularization. *Circ Res.* 85(3):221-228; 1999.
4. den Dekker, W.K.; Houtgraaf, J.H.; Onuma, Y.; Benit, E.; de Winter, R.J.; Wijns, W.; Grisold, M.; Verheye, S.; Silber, S.; Teiger, E.; Rowland, S.M.; Ligtenberg, E.; Hill, J.; Wiemer, M.; den Heijer, P.; Rensing, B.J.; Channon, K.M.; Serruys, P.W.; Duckers, H.J. Final results of the HEALING IIB trial to evaluate a bio-engineered CD34 antibody coated stent (GenousStent) designed to promote vascular healing by capture of circulating endothelial progenitor cells in CAD patients. *Atherosclerosis* 219(1):245-52; 2011.
5. Dimmeler, S.; Aicher, A.; Vasa, M.; Mildner-Rihm, C.; Adler, K.; Tiemann, M.; Rutten, H.; Fichtlscherer, S.; Martin, H.; Zeiher, A.M. HMG-CoA reductase inhibitors (statins) increase endothelial progenitor cells via the PI 3-kinase/Akt pathway. *J. Clin. Invest.* 108(3):391-397; 2001.
6. Duckers, H.J.; Silber, S.; de Winter, R.; den Heijer, P.; Rensing, B.; Rau, M.; Mudra, H.; Benit, E.; Verheye, S.; Wijns, W.; Serruys, P.W. Circulating endothelial progenitor cells predict angiographic and intravascular ultrasound outcome following percutaneous coronary interventions in the HEALING-II trial: evaluation of an endothelial progenitor cell capturing stent. *EuroIntervention* 3(1):67-75; 2007.
7. Duckers, H.J.; Soullie, T.; den Heijer, P.; Rensing, B.; de Winter, R.J.; Rau, M.; Mudra, H.; Silber, S.; Benit, E.; Verheye, S.; Wijns, W.; Serruys, P.W. Accelerated vascular repair following percutaneous coronary intervention by capture of endothelial progenitor cells promotes regression of neointimal growth at long term follow-up: final results of the Healing II trial using an endothelial progenitor cell capturing stent (Genous R stent). *EuroIntervention* 3(3):350-358; 2007.
8. Ellis, S.G.; Popma, J.J.; Lasala, J.M.; Koglin, J.J.; Cox, D.A.; Hermiller, J.; O'Shaughnessy, C.; Mann, J.T.; Turco, M.; Caputo, R.; Bergin, P.; Greenberg, J.; Stone, G.W. Relationship between angiographic late loss and target lesion revascularization after coronary stent implantation: analysis from the TAXUS-IV trial. *J. Am. Coll. Cardiol.* 45(8):1193-1200; 2005.
9. Fadini, G.P.; Maruyama, S.; Ozaki, T.; Taguchi, A.; Meigs, J.; Dimmeler, S.; Zeiher, A.M.; de Kreutzenberg, S.; Avogaro, A.; Nickenig, G.; Schmidt-Lucke, C.; Werner, N.; Circulating progenitor cell count for cardiovascular risk stratification: a pooled analysis. *PLoS one* 5(7):e11488; 2010.
10. Hill, J.M.; Zalos, G.; Halcox, J.P.; Schenke, W.H.; Waclawiw, M.A.; Quyyumi, A.A.; Finkel, T. Circulating endothelial progenitor cells, vascular function, and cardiovascular risk. *N. Engl. J. Med.* 348(7):593-600; 2003.

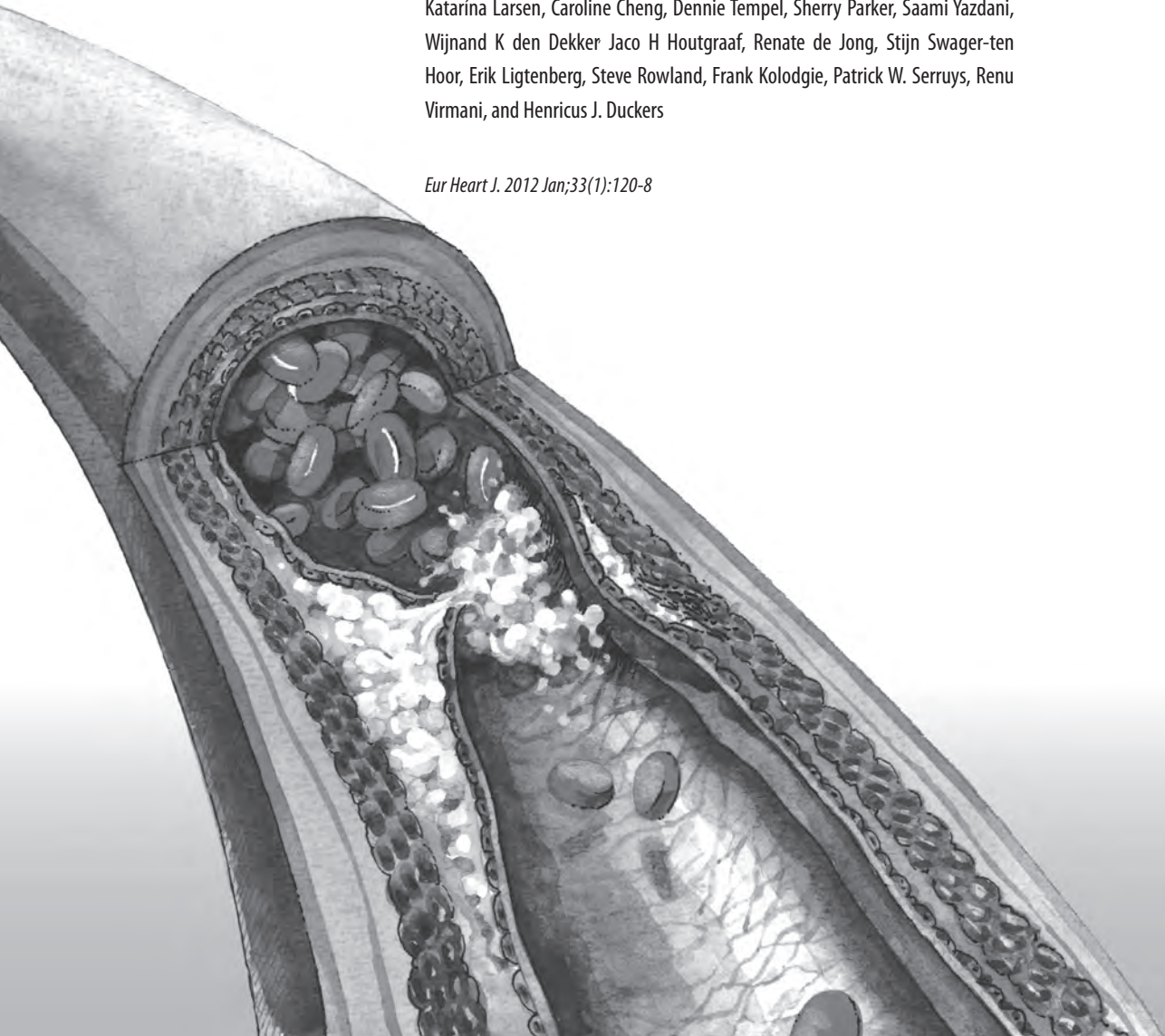
11. Kalka, C.; Masuda, H.; Takahashi, T.; Kalka-Moll, W.M.; Silver, M.; Kearney, M.; Li, T.; Isner, J.M.; Asahara, T. Transplantation of ex vivo expanded endothelial progenitor cells for therapeutic neovascularization. *Proc. Natl. Acad. Sci. USA.* 7(7):3422-3427; 2009.
12. Kong, D.; Melo, L.G.; Gneccchi, M.; Zhang, L.; Mostoslavsky, G.; Liew, C.C.; Pratt, R.E.; Dzau, V.J. Cytokine-induced mobilization of circulating endothelial progenitor cells enhances repair of injured arteries. *Circulation* 110(14):2039-2046; 2004.
13. Kong, D.; Melo, L.G.; Mangi, A.A.; Zhang, L.; Lopez-Illasaca, M.; Perrella, M.A.; Liew, C.C.; Pratt, R.E.; Dzau, V.J. Enhanced inhibition of neointimal hyperplasia by genetically engineered endothelial progenitor cells. *Circulation* 109(14):1769-1775; 2004.
14. Landmesser, U.; Engberding, N.; Bahlmann, F.H.; Schaefer, A.; Wiencke, A.; Heineke, A.; Spiekermann, S.; Hilfiker-Kleiner, D.; Templin, C.; Kotlarz, D.; Mueller, M.; Fuchs, M.; Hornig, B.; Haller, H.; Drexler, H. Statin-induced improvement of endothelial progenitor cell mobilization, myocardial neovascularization, left ventricular function, and survival after experimental myocardial infarction requires endothelial nitric oxide synthase. *Circulation* 110(14):1933-1939; 2004
15. Larsen, K.; Cheng, C.; Tempel, D.; Parker, S.; Yazdani, S.; den Dekker, W.K.; Houtgraaf, J.H.; de Jong, R.; Swager-ten Hoor, S.; Ligtenberg, E.; Hanson, S.R.; Rowland, S.; Kolodgie, F.; Serruys, P.W.; Virmani, R.; Duckers, H.J. Capture of circulatory endothelial progenitor cells and accelerated re-endothelialization of a bio-engineered stent in human ex vivo shunt and rabbit denudation model. *Eur. Heart J.* 33(1):120-128; 2012.
16. Llevadot, J.; Murasawa, S.; Kureishi, Y.; Uchida, S.; Masuda, H.; Kawamoto, A.; Walsh, K.; Isner, J.M.; Asahara, T. HMG-CoA reductase inhibitor mobilizes bone marrow—derived endothelial progenitor cells. *J. Clin. Invest.* 108(3):399-405; 2001.
17. Pelliccia, F.; Cianfrocca, C.; Rosano, G.; Mercurio, G.; Speciale, G.; Pasceri, V. Role of endothelial progenitor cells in restenosis and progression of coronary atherosclerosis after percutaneous coronary intervention: a prospective study. *Jacc. Cardiovasc. Interv.* 3(1):78-86; 2010.
18. Prati, F.; Imola, F.; Corvo, P.; Cernigliaro, C.; Fouadi, T.; Ramazzotti, V.; Manzoli, A.; Pappalardo, A.; Cera, M. The RESTART project: high-dose atorvastatin helps control RESTenosis After sTenting procedures at high risk for restenosis. Results from a prospective study and a matched control group comparison. *EuroIntervention* 3(1):89-94; 2007.
19. Schmidt-Lucke, C.; Rossig, L.; Fichtlscherer, S.; Vasa, M.; Britten, M.; Kamper, U.; Dimmeler, S.; Zeiher, A.M. Reduced number of circulating endothelial progenitor cells predicts future cardiovascular events: proof of concept for the clinical importance of endogenous vascular repair. *Circulation* 111(22):2981-2987; 2005.
20. Vasa, M.; Fichtlscherer, S.; Adler, K.; Aicher, A.; Martin, H.; Zeiher, A.M.; Dimmeler, S. Increase in circulating endothelial progenitor cells by statin therapy in patients with stable coronary artery disease. *Circulation* 103(24):2885-2890; 2001.
21. Walter, D.; Rittig, K.; Bahlmann, F.H.; Kirchmair, R.; Silver, M.; Murayama, T.; Nishimura, H.; Losordo, D.W.; Asahara, T.; Isner, J.M. Statin therapy accelerates reendothelialization: a novel effect involving mobilization and incorporation of bone marrow-derived endothelial progenitor cells. *Circulation* 105(25):3017-3024; 2002.
22. Werner, N.; Kosiol, S.; Schiegl, T.; Ahlers, P.; Walenta, K.; Link, A.; Bohm, M.; Nickenig, G. Circulating endothelial progenitor cells and cardiovascular outcomes. *N. Engl. J. Med.* 353(10):999-1007; 2005.

Chapter 8

Capture of circulatory endothelial progenitor cells and accelerated re-endothelialization of a bioengineered stent in human *ex vivo* shunt and rabbit denudation model

Katarína Larsen, Caroline Cheng, Dennie Tempel, Sherry Parker, Saami Yazdani, Wijnand K den Dekker, Jaco H Houtgraaf, Renate de Jong, Stijn Swager-ten Hoor, Erik Ligtenberg, Steve Rowland, Frank Kolodgie, Patrick W. Serruys, Renu Virmani, and Henricus J. Duckers

Eur Heart J. 2012 Jan;33(1):120-8



ABSTRACT

Aims: The Genous™ Bio-engineered R™ stent (GS) aims to promote vascular healing by capture of circulatory endothelial progenitor cells (EPCs) to the surface of the stent struts, resulting in accelerated re-endothelialization. Here, we assessed the function of the GS in comparison to bare metal stent (BMS), when exposed to the human and animal circulation.

Methods and Results:

First, Fifteen patients undergoing coronary angiography received an extracorporeal femoral AV shunt containing BMS and GS. Macroscopical mural thrombi were observed in BMS, whereas GS remained visibly clean. Confocal and scanning electron microscope (SEM) analysis of GS showed increase in strut coverage. qPCR analysis of captured cells on the GS demonstrated increased expression of endothelial markers KDR/VEGFR2 and E-Selectin, and decrease of pro-thrombogenic markers TFPI and PAI-1 compared to BMS.

Secondly, a similar primate AV shunt-model was used to validate these findings, and occlusion of BMS was observed, while GS remained patent, as demonstrated by live-imaging of Indium-labelled platelets.

Thirdly, in an *in vitro* cell-capture assay, GS struts showed increased coverage by EPCs whereas monocyte-coverage remained similar to BMS.

Finally, assessment of re-endothelialization was studied in a rabbit denudation model. 20 animals received BMS and GS in the aorta and iliac arteries for 7 days. SEM analysis showed a trend towards increased strut coverage, confirmed by qPCR analysis revealing increased levels of endothelial markers (Tie2, CD34, PCD31 and P-selectin) in GS.

Conclusions: In this proof of concept study, we have demonstrated that the bio-engineered EPC capture stent, Genous™ R™ stent, is effective in EPC-capture, resulting in accelerated re-endothelialization and reduced thrombogenicity.

INTRODUCTION

Vascular homeostasis is maintained by the endothelial cell (EC) layer that is involved in the regulation of platelet adhesion, vasomotor function and cell cycle quiescence of the cellular constituents of the vascular wall(1). Bone-marrow derived circulating endothelial progenitor cells (EPC) aid in the regeneration of damaged and dysfunctional endothelium and therefore play a central role in the vascular repair response(2-4). Recruitment of EPC to the site of vascular injury has been proposed to promote vascular healing, and has been shown to inhibit neo-intimal proliferation and restenosis associated with percutaneous coronary intervention (PCI)(5). The GENOUS™ Bio-engineered R™ stent (Genous stent) (OrbusNeich Medical BV, Hovevelaken, the Netherlands) has been developed to enhance the capture of circulating EPCs to the stent surface using an immobilized antihuman-CD34 monoclonal antibody. CD34 was previously shown to be expressed in circulating haematopoietic cells in humans(4, 6). The sequestered EPC are thought to enhance endothelial healing and thus protect the stented vascular segment against acute thrombosis with minimized neo-intimal hyperplasia.

The safety, feasibility and efficacy of the Genous stent in human coronary artery disease (CAD) have been the subject of multiple clinical studies(7-11). Although the long-term effect of the Genous stent on clinical outcome has been investigated, the efficacy of the bio-engineered stent to promote initial endothelial recovery has never been shown in humans before. Here, we studied early cellular interactions of the Genous stent within the circulation of CAD patients.

In the first part of the study, a temporary *ex vivo* arteriovenous (AV) shunt was established by canulation of the femoral artery and vein and connection of the two via a synthetic tube comprising the BMS and the Genous stent. The stents were exposed to the human circulation under continuous flow. EPC capture and subsequent EPC differentiation was analyzed using conventional ultrastructural analysis as well as by quantifying surrogate endothelial markers on the captured stent by qPCR analysis. In the second part of the study, the validation of accelerated endothelialization was further conducted in a well-established primate model for stent-related thrombogenicity. In the third part, CD34+ cells capture specificity was evaluated in an *in vitro* capture model. In the final part of the study, long term effects of the Genous stent on the vascular endothelium was evaluated in a rabbit model of arterial balloon injury and vascular repair.

MATERIAL AND METHODS

Study population

The study was performed in 15 patients undergoing elective heart catheterization, followed in 11 cases by PCI. Informed written consent was obtained prior to the procedure for all patients. The study was reviewed and approved by the institution's ethics review committee. The baseline characteristics of included patients are shown in the Table 1.

Table 1. *Patient clinical characteristics*

Patient characteristics	N	%
Male	10	66,67
Age	69,4	
PCI	11	73,33
Hypertension	8	53,33
Diabetes	0	0
Dyslipidemia	5	33,33
Smoking	6	40
Clinical pattern		
Stable angina pectoris	10	66,67
Unstable angina pectoris	4	26,67
Syncope	1	6,667
Periferal vascular disease	3	20
Stroke	2	13,33
Heart failure	3	20
Previous myocardial infarction	4	26,67
Previous PCI	7	46,67
Previous CABG	2	13,33
Use of:		
Statin	14	93,33
Aspirin	13	86,67
Clopidogrel	13	86,67
Warfarin	2	13,33
Beta blocker	3	20

Ex vivo human AV shunt

The Genous stent (OrbusNeich, Hoevelaken, The Netherlands) is coated with an immobilized murine monoclonal antibodies directed against human CD34, a known antigen expressed on EPCs. It is designed to capture circulating EPCs to promote vascular healing. Patients received an extracorporeal A-V shunt containing one Genous stent and one BMS stent (non-coated, stainless steel R-stent).

mRNA processing and qPCR analysis

The captured cells were harvested from the stents by directly retrieving the RNA using a lysis buffer provided by a commercial RNAeasy isolation kit, followed by cleanup using RNA isolation columns (Qiagen, The Netherlands) according to the manufacturer's protocol as conducted previously (12-14). Briefly; 20 ng carrier RNA was added to the cell lysate. 1 volume of 70% ethanol was added to the homogenized lysate and the sample was mixed and isolated by a commercial RNAeasy column. RNA was reverse transcribed using iScript reagents according to the manufacturer's protocol (Bio-Rad, The Netherlands). Gene expression was quantified using qPCR by the SensiMix™ SYBR & Fluorescein Kit (Bioline, The Netherlands), followed by signal detection on a MyiQ Single-Color Real-Time PCR Detection System (BioRad, the Netherlands). Negative were included, whereas GAPDH and beta actin served as housekeeping genes. Primers for the analysis were designed using the sequences available on GenBank (<http://www.ncbi.nlm.nih.gov/>) and Primer3 software to generate up to 3 primer pairs for each target sequence. All primers were tested and the optimal primer pair was ultimately used for sample analysis.

Rabbit model of arterial balloon injury

The early effects of Genous in accelerated reendothelialization were further assessed in a rabbit endothelial denudation model(15). Stents were implanted in 20 New Zealand white adult male rabbits. One BMS and one Genous stent were implanted per rabbit in the aorta (for qPCR analysis, N=11) and iliac artery (for SEM analysis, N=9). For the aorta, the stents were alternated in order. All stents were deployed at nominal pressure (9 atm) for 30 seconds. Angiography was performed to confirm appropriate stent placement and vessel diameter post-deployment. At 7 days post stenting, follow-up angiography was performed. To obtain stent samples for SEM analysis, the rabbits were perfusion fixed in 10% formalin and the stented arteries were harvested. For qPCR analysis, the vessels were isolated without *in situ* fixation, the stents were removed and incubated in RNA isolation buffer (RLT buffer, Qiagen, The Netherlands) and stored at -80°C until qPCR analysis.

RESULTS

Part 1: Human AV shunt study reveals evidence of accelerated capture of endothelial progenitor cells and protection against in stent thrombosis and inflammation in Genous versus BM stent.

The Genous stent has been tested extensively in animal models(16), but direct evidence of the *in vivo* EPC capture capability of this stent in the human circulation has not been presented.

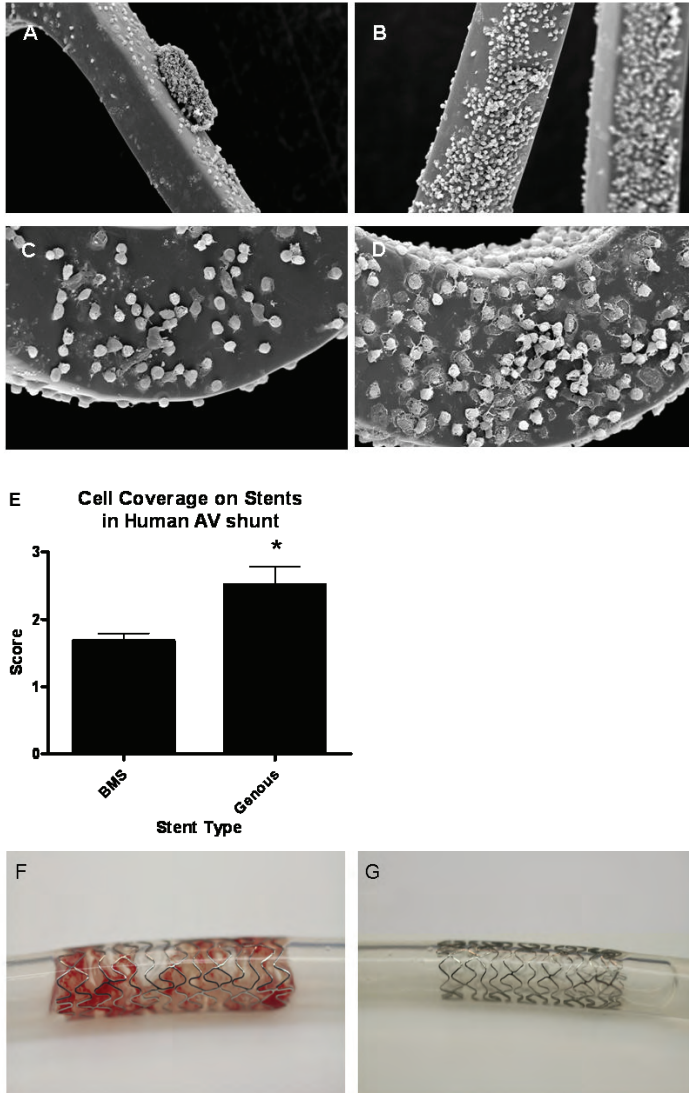


Figure 1

SEM analysis of the EPC capturing stent and BMS in the human AV shunt model revealed marked increase in cell strut coverage compared to BMS. SEM inspection of the study stents showed less strut coverage, and the presence of thrombus-like structures on BMS (A) as compared to Genous stent (B). High magnification SEM revealed more adhesion of cells with a flattened polygonal morphology on the struts of the stent (D) versus BMS (C). Average stent strut coverage was visually rated by blinded (core lab) technicians (CV-Path Institute, USA) on a 0-3 virtual scale (corresponding to 0-25, 25-50, 50-75 and 75-100% stent coverage). Bar graph indicates the level of strut coverage as assessed by SEM in the two stent study groups. * $p < 0.05$, $N = 9$ (E). Macroscopic appearance of BMS (F) and Genous (G) stents in the human ex vivo shunt model shows mural thrombi in the BMS, whereas the Genous stent remained free of thrombogenic material.

In the first part of the study, we investigated the acute effect of the Genous stent in patients undergoing coronary angiography. In addition, assessment of the Genous stent in a CAD patient setting provides relevant evaluation of bioactivity of the CD34 capture antibody that was raised specifically against human CD34 antigen. In this study, the EPC capture capacity of the Genous stent was compared to that of uncoated, stainless steel R-stents (BM stents).

The Genous and the BMS that were tested in the human AV shunt model were exposed to the circulation for up to 120 minutes. Stents selected for SEM analysis revealed marked increase in strut cell coverage in the Genous stent as compared to BMS (Figure 1A and C: BMS, Figure 1B and D: Genous stent). Average stent-strut coverage was visually rated by a blinded (core lab) technician on a 0-4 scale (corresponding to 0-25, 25-50, 50-75 and 75-100% stent coverage). Cell deposition on the struts was enhanced by 32.5% ($p=0.006$, $N=9$) in Genous stents as compared to BMS in paired analysis (Figure 1E). High resolution assessment of the SEM data revealed cellular deposits present on both stents that could be distinguished into a population of cells with a rounded and flattened morphology, cells with a more monocyte-like appearance, and blood platelets. To further elucidate the identity of this mixed population, we performed by qPCR of the cellular substrate. Macroscopical comparison of Genous and BM stents also revealed the substantial presence of mural thrombi in the 2 BMS stents, whereas all of the Genous stents remained free of thrombogenic material (Figure 1F and G). This observation led us to further examine markers of thrombogenicity and coagulation by qPCR.

For qPCR analysis, cells were directly lysed from the stents and subsequently analyzed by qPCR using the housekeeping genes GAPDH and beta actin to normalize for cell content and quality of total RNA. qPCR analysis of the attached cells showed no significant difference in CD34 expression between the Genous and BMS groups (data not shown). However, evaluation of endothelial markers revealed a marked increase of KDR/VEGFR2 ($p<0.001$), and E-Selectin RNA expression ($p<0.045$) with the Genous stents, as compared to BMS (Figure 2A). Expression of another endothelial specific marker Plvap (Figure 2A) showed a tendency to increase expression in Genous stent, although it was not statistically significant ($p=0.21$). An equivalent CD34 transcript content, with enhanced expression of endothelial markers would suggest accelerated ongoing differentiation into the endothelial lineage concomitant with downregulation of CD34 expression.

qPCR evaluation of markers of thrombosis and coagulation (Figure 2B) revealed a significant decrease in expression of tissue factor pathway inhibitor (TFPI) and plasminogen activator inhibitor-1 (PAI-1) in Genous compared to BMS ($p=0.04$, and $p=0.02$, for TFPI and TF respectively), suggestive of a less pro-thrombotic state of the cells attached to the Genous stent, and thus a reduced risk for stent thrombogenicity.

To assess the potency of the Genous stent to protect the vascular wall against inflammation, inflammatory markers were also included in the study. CD16 is an established neutrophil expression marker. Cells sequestered to the Genous stent, presented lower expression levels

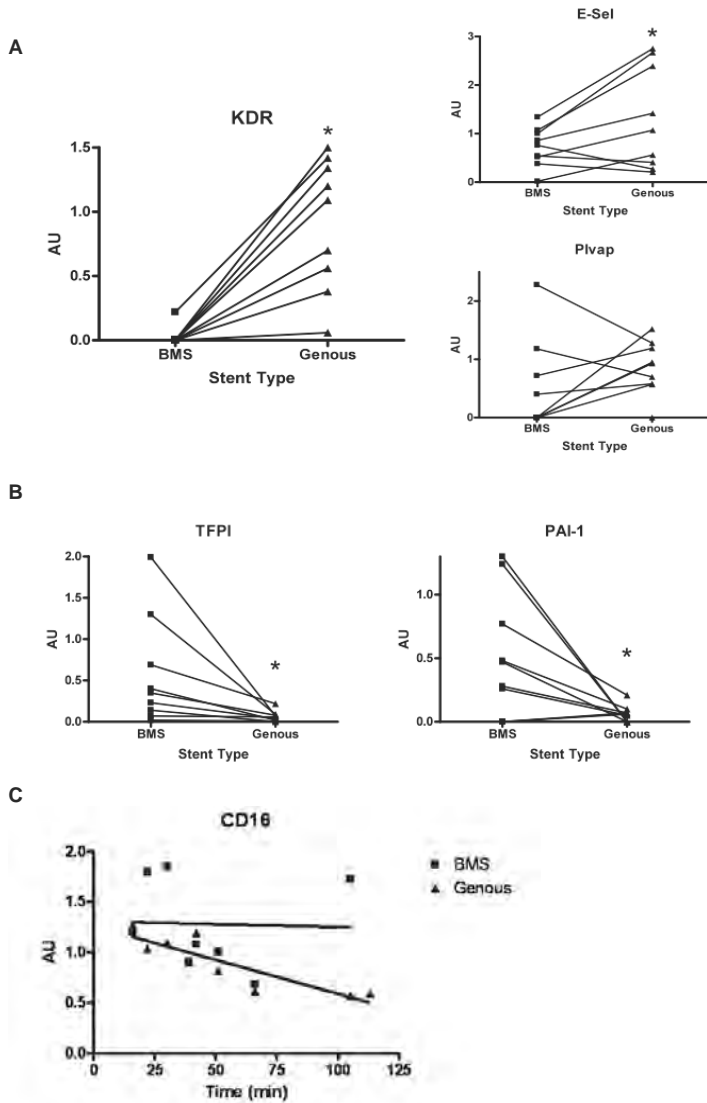


Figure 2

qPCR evaluation of cellular markers in cell lysates of captured cells in the human AV shunt stent model. Paired comparison of the expression levels of the individual genes revealed a marked increase in endothelial markers, including KDR/VEGFR2 ($p < 0.001$) and E-Selectin ($p < 0.045$) mRNA expression in the stents compared to BMS (A). Expression of another endothelial specific marker PLVAP (A) showed no significant increased expression in the stent ($p = 0.21$). qPCR analysis of markers of thrombosis, coagulation, and inflammation: Paired comparison of the expression levels of the individual genes revealed a marked decrease in tissue factor pathway inhibitor (TFPI) and plasminogen activator inhibitor-1 (PAI-1) in the Genous compared to the BM stent (B) ($p = 0.04$ and $p = 0.02$). qPCR showed a significant decrease in CD16 marker expression in the cells captured by the Genous stent over time, whereas the CD16 mRNA levels on BMS were maintained (C) (* $p < 0.05$, $p < 0.1$, $N = 9$).

of CD16 over time ($p < 0.002$), whereas the BMS showed persistent CD16+ expression in attached cells ($p < 0.932$), suggesting that adhesion of CD16+ inflammatory cells was prevented by accelerated capture of CD34+ endothelial progenitors and subsequent coverage of the stent struts (Figure 2C). Moreover, the inflammatory markers for immune cell subpopulations were not significantly different between the stents, including CD68, CD14, monocyte chemoattractant protein-1, CXCR-1 and VCAM1 (data not shown).

Combined, these qPCR analysis corroborate and extend the ultrastructural analysis by SEM, and confirm enhanced attachment of circulating EPCs to the Genous stent surface. In addition, these data suggest that the attached cells could undergo rapid endothelial commitment and differentiation (loss of CD34, increased expression of KDR1/ E-selectin), with reduced thrombogenicity and inflammatory response of the injured vascular wall.

Part 2: Genous inhibits in-stent thrombosis in a baboon AV shunt model.

Based on the differences on thrombogenicity by qPCR, and the lack of mural thrombi in the Genous stent as observed in the clinical study, we further assessed thrombogenicity of the Genous stent in an established primate model using a similar AV shunt setup with exclusion of anti-platelet treatment in the protocol. Live deposition of platelets and fibrinogen was studied in the AV shunt set up by measuring the accumulation of Indium labeled platelets with a gamma camera for up to 2 hours. In line with the human data, the Genous stent had a lower thrombogenic potential than BMS in the baboon shunt model. Within 65 minutes after initiation of the experiment, the BMS were occluded with a flow-limiting thrombus, while the Genous stents remained patent for at least 2 hours. (Figure 3A). Further SEM analysis revealed increased platelet deposition and in stent thrombus formation in BMS versus Genous stents (Figure 3B). Platelet deposition was significantly higher in BMS compared to Genous stents after flow exposure as quantified by gamma camera ($1.13 \pm 0.57 \times 10^9$ as compared to $0.50 \pm 0.22 \times 10^9$ platelets, in BMS versus Genous respectively, $p = 0.04$; Figure 3C). Although fibrinogen accumulation seemed less prominent on the Genous as compared to BM stents, no statistical difference was found between the groups. The values were 0.05 ± 0.02 mg/stent and 0.18 ± 0.10 mg/stent for the Genous and BM stents respectively.

Part 3: In vitro cell capture assay demonstrates specific adhesion of human peripheral blood derived CD34+ cells on Genous CD34 capture stents.

To examine whether the CD34 antibody on the Genous stent is also able to bind the more abundant circulatory inflammatory cells such as monocytes, an *in vitro* assay was performed to test the CD34+ cell capture specificity of the Genous stent. Genous and BM stents were deployed in silicon tubing and were exposed to a cell mixture of PKH26 red fluorescent labeled human monocytes (1×10^6 cells/ml) and PKH2 green fluorescent labeled human CD34+ cells

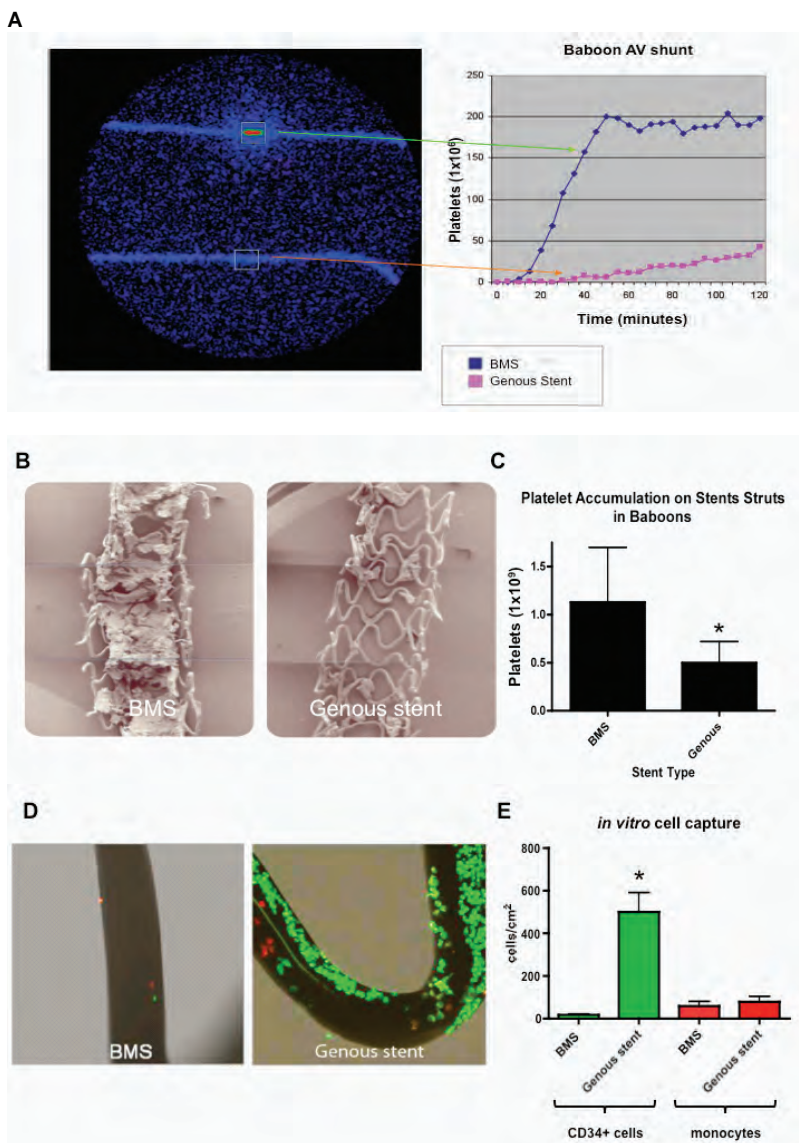


Figure 3

Live imaging of AV shunt set up using a gamma camera to measure deposition of Indium labeled platelets on the study stents (A). Line graph shows a typical example of accumulating platelet signal over time. Low magnification SEM images of the BMS and the EPC capture stent in the baboon AV shunt model revealed a decrease in mural thrombus in the Genous versus BMS (B). Bar graph showing the quantified number of platelets accumulated on the BMS and Genous stent after 2 hours of flow exposure (C). Data was acquired from the live imaging AV shunt set up * $p < 0.05$, $N = 3$.

In vitro assay to test the CD34+ cell capture specificity of the Genous stent: Genous and BM stents were deployed in silicon tubing and were exposed to a cell mixture of PKH26 red fluorescent labeled human monocytes (1×10^6 cells/ml) and PKH2 green fluorescent labeled human CD34+ cells (2×10^5 cells/ml), under a constant rotation speed of 0,3 RPM for 2 hours. Micrographs show confocal images of strut coverage of BMS and Genous stent (D). Bar graph shows the quantified number of CD34+ cells and monocytes per cm² strut area. * $p < 0.05$, $N = 3$ (E).

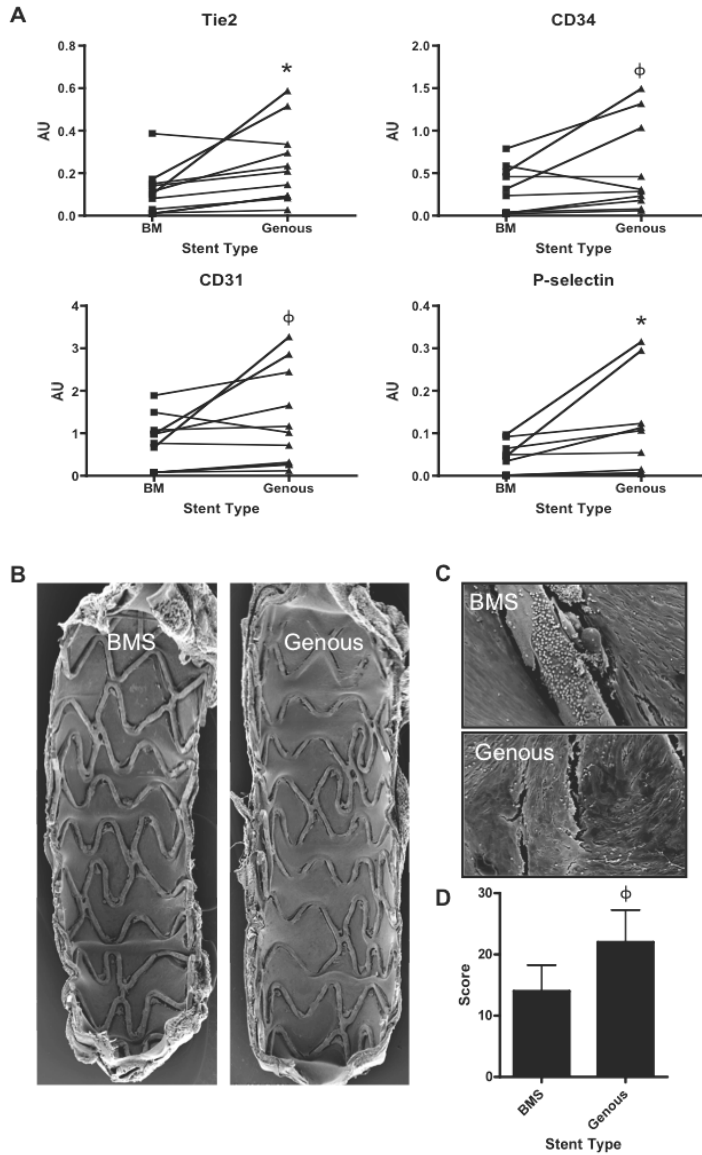


Figure 4

qPCR analysis of the study stents of 11 New Zealand white rabbits was performed to evaluate capture of cells and subsequent expression of EC markers. Paired qPCR analysis showed increased levels of endothelial markers by the cells captured on the Genous versus BMS stent treated arteries, including Tie2 ($p=0.02$), CD34 ($p=0.07$), CD31 ($p=0.08$) and P-Selectin ($p=0.05$). $*p<0.05$, $p<0.01$, $N=11$ (A).

SEM analysis of the stents implanted iliac vessels of 9 New Zealand white rabbits: Low (B) and high (C) magnification assessment revealed improved cell coverage between and above struts in the Genous stent versus BMS. Bargraph show the level of strut coverage as analyzed by SEM in the two stent groups. $p<0.01$, $N=9$ (D).

(2×10^5 cells/ml), under a constant rotation speed of 0,3 RPM for 2 hours. Confocal assessment of the stent struts showed a greater number of CD34+ cells to adhere to the Genous stent strut surface as compared to BMS; cell density for CD34+ cells was 500 ± 158 cells/cm² strut area on the Genous versus 17 ± 8 cells/cm² on the BM stent ($p=0.0009$; Figure 3D,E). In contrast, monocyte adherence was not significantly different between the two stent types (79 ± 44 cells/cm² as compared to 58 ± 39 cells/cm², Genous versus BMS respectively, $p=0.07$; Figure 3D,E). Therefore, the specificity of the Genous stent to capture CD34+ cells was significantly higher as compared to BMS, as 86% of the attached cells were CD34+ as compared to only 26% on the BMS.

Part 4: Genous stent promotes reendothelialization at 7 days in rabbit endothelial denudation model.

20 New Zealand white rabbits received stent placement after endothelial denudation in the aorta $N=11$ and iliac artery $n=9$ (left Genous, right BMS). From 11 animals, the aortic stents were harvested after 7 days and the cell lysates were evaluated for EC markers. qPCR analysis showed increased levels of endothelial markers in the Genous versus BM stent treated artery, including Tie2 ($p=0.02$), CD34 ($p=0.08$), CD31 ($p=0.07$), and P-selectin ($p=0.05$), indicating that the Genous stent promoted long term endothelialization (Figure 4A). These data support our finding of the AV shunt study in CAD patients where we propose earlier endothelialization in Genous stent compare to BMS. In line with these findings, SEM analysis of 9 rabbits that received the Genous (left) or BM (right) in bilateral denudated iliac arteries showed a trend of increased strut coverage at 7 days post implantation (Figure 4B-D). Together, these data indicate that the Genous stent efficiently promotes reendothelialization in a denudated vessel wall environment as shortly as 7 days after placement.

DISCUSSION

Endothelialization is a critical step in the initiation of vascular repair following stent implantation. Re-endothelialization of the damaged area involves activation and migration of resident EC adjacent to the stent area or by recruitment of blood-derived EPC. Early presence of a functional endothelial lining after vascular injury could improve the process of vascular healing and reduce the risk of restenosis and acute thrombosis.

The stent struts of the bio-engineered R stent (GENOUS®) incorporate an immuno-affinity surface, consisting of covalently bound monoclonal antibodies directed against the human CD34 antigen, a cell surface marker found on circulating EPC. The efficacy of EPC capture and re-endothelialization of the Genous stent has been extensively evaluated in porcine models⁽¹⁶⁾ relying on the cross-reactivity of the monoclonal CD34 antibody against porcine CD34. Although these studies gave a clear indication of stent performance, optimal capture

efficacy by the human CD34-directed antibody can only be truly tested under circumstances when the stent is exposed to the human circulation. Here, the performance of the BMS and the bio-engineered Genous stent was studied in an *ex vivo* AV shunt construction in which stents were exposed to the human circulation for up to 2 hours. The data of this study provide for the first time, direct evidence of the capture efficiency of a bio-engineered capture stent in the human circulation.

The efficacy of EPC capture was first assessed by conventional scanning electron microscope (SEM) analysis, which revealed the presence of blood-derived cells with a rounded or flat polygonal morphology indicative of EPC, and platelet aggregation on the stent struts. Semi-quantitative analysis of the Genous stent revealed increase in cellular density (platelets were excluded) on the stent surface as compared to BMS. To elucidate the identity of the captured cells, surrogate biomarkers for EPC, EC, and immunocompetent cells and thrombogenicity were assessed by qPCR analysis. Endothelial cell surface markers KDR, E-selectin, and PLVAP mRNA were expressed in the attached cells in the Genous samples, as compared to the BMS samples. However, only low expression levels of the CD34 marker were observed in the lysates obtained from both stents. Limited CD34 expression in the EPC capture stent sample could be due to active downregulation of CD34 in response to shear stress after cell immobilization on the struts and exposure to blood flow leading into EC differentiation(17). It is known that upregulation of EC markers and adaptation of the cultured EC morphology into a more *in vivo*-like phenotype could be induced within minutes after exposure to mechanical flow(18). In addition, loss of CD34 cell surface expression on circulating EPC is associated with commitment to the endothelial lineage. Furthermore, de Boer et al. has demonstrated that *in vivo* platelet activation could rapidly induce differentiation of CD34+ cells into more matured KDR+ ECs(19). Therefore, the low level of CD34 expression on the captured cells could be explained by rapid differentiation of the progenitor cells towards a mature EC type. In line with this hypothesis, expression of more mature EC markers, including E-selectin were indeed upregulated in the Genous stent samples as compared to BMS. For an extended discussion of the qPCR data, see supplemented data.

Previous studies have shown that, at least in the porcine models, the efficacy of EPC capture stent coverage was similar to that of BMS, with a optimal endothelial coverage of total stented area of 99% in both groups(16). However, it has to be taken into account that the lack of difference in response could be due to a low cross-reactivity of the human CD34 antibody on the Genous stent against porcine CD34 antigen, resulting in a suboptimal EPC capture. The *ex vivo* AV shunt data in the patients and primates in the current study, showed that the Genous stent was capable of rapid capture of circulating progenitor cells within the first hours of exposure. SEM and qPCR analysis have subsequently validated the endothelial phenotype of the adherent population. Taken together, our data indicate that the EPC capture stent is capable of accelerating the re-endothelialization process in exposure to the human

circulation and therefore aid the vascular healing after vascular injury as compared to the BMS stent.

The combination of the EPC-capture and drug-elution technology has shown thus far to be a promising strategy in the pre-clinical setting(16). In contrast to that type of study, which focuses on late stent outcome, this study was predominantly designed to provide first-time proof of efficient EPC capture in human patients. Therefore, we have chosen to focus on capture efficiency alone and compare the Genous to the BM stent. Although we have provided adequate proof for this cell-capture technology, drug-elution may compromise the cell capture efficiency and should be investigated for each of the new generation of combo-devices that are currently being developed.

A second important finding reported in this study is the effect of the Genous stent on thrombogenesis. The rapid coverage of the Genous stent by a protective endothelial lining was hypothesized to protect the stented area from thrombogenesis and inflammation, thereby promoting a more efficient healing of the vascular wall. Indeed, macroscopic comparison of the Genous and BMS revealed the clear presence of mural thrombi in the BMS stent of one of the patients, whereas all the EPC capture stent remained free of visible thrombi. It should be mentioned that this particular patient only received ASA (no Clopidogrel therapy) before PCI. Although the patient's blood was exposed to both Genous and BM stents and the Genous stents showed no signs of thrombi, the striking difference in thrombogenic response between the two stent types could be related to the absence of anti-platelet aggregation surface markers. To further elucidate this, biomarkers of coagulation and thrombosis were further examined in the human shunt material. We observed significant downregulation in PAI and TFPI expression in the lysates of EPC capture stent as compared to BMS, pointing to platelet aggregation on the stent struts(20). Similarly, TFPI mRNA enrichment in the attached cells indicates in the BMS a rich platelet environment promoted by recruited inflammatory cells(21)(22). Summarized, these data point to active EPC recruitment as playing a putative role in vascular protection against stent thrombosis. These findings were further validated in the baboon shunt experiments.

The early EC lining on the stent could protect against active accumulation of inflammatory cells involved in the innate immune response. However, in line with the *in vitro* findings, there was no difference in other inflammatory markers or innate immunity markers such as CD68, CD14, MCP1 and CXCR-1. This could be due to the short exposure time, but more importantly, paracrine stimulation by the injured vessel wall is lacking in the human AV shunt setup. In the absence of cytokine and chemokine release to trigger inflammatory cell activation, the protective effect of the stent reendothelializing by circulating EPC on the inflammatory response, may only be limited. Previously, Granada et al. performed a comparison study of stents (combining CD34 capture with the Sirolimus-eluting strategy) with conventional drug eluting stents including Xience and Cypher in a porcine experimental model. It was demon-

strated that the EPC capture technology further diminished overall intimal inflammation and giant cell accumulation after 28 days of implantation in the coronary arteries as compared to the Cypher and Xience stents(16). This was associated with a decrease in neo-intimal growth. This suggests that active re-endothelialization of drug eluting stents could indeed protect the injured vascular wall from further inflammatory activation, thereby protecting the stented area from further platelet adhesion and restenosis(16). Based on these findings, the Genous stent should provide vascular protection against thrombosis in the patients in short and long term follow-up. Recently, supporting data was presented by the e-HEALING (Healthy, Endothelial Accelerated Lining inhibits Neointimal Growth) multi-center registry in which the long-term effect of the Genous bio-engineered R stent was followed in 5000 patients. Indeed, low levels of in-stent thrombosis and repeat revascularization of 1.1% and 5.7% respectively was observed at 12-month post intervention (26). New clinical trials are currently under evaluation in which the CD34 capture technology will be combined with Sirolimus-elution to assess novel combination strategies (REMEDEE: NCT00967902).

In conclusion, we showed in an AV shunt construction in human CAD patients and baboons that the CD34+ EPC recruitment promotes re-endothelialization and inhibited platelet adhesion. This specific aspect of the biological behavior of the Genous stent is especially promising as it could, combined with a drug-eluting strategy(16), yield safe and efficient therapy against restenosis, while diminishing the need for dual antiplatelet therapy after stent implantation.

SOURCE OF FUNDING

This work was supported by Orbusneich medical, Fort Lauderdale, Fla.

ACKNOWLEDGEMENT

Dedicated to Katarina Larsen, a hardworking and talented colleague, a loving and caring friend, and a kind and wonderful person who will be greatly missed by us all.

REFERENCES

1. Urbich C, Dimmeler S. Endothelial progenitor cells: characterization and role in vascular biology. *Circ Res* 2004; 95(4):343-353.
2. Asahara T, Murohara T, Sullivan A. Isolation of putative progenitor endothelial cells for angiogenesis. *Science* 1997; 275(5302):964-967.
3. Gulati R, Simari RD. Cell therapy for acute myocardial infarction. *Med Clin North Am* 2007; 91(4):769-785; xiii.
4. Hristov M, Erl W, Weber PC. Endothelial progenitor cells: mobilization, differentiation, and homing. *Arterioscler Thromb Vasc Biol* 2003; 23(7):1185-1189.
5. Kipshidze N, Dangas G, Tsapenko M. Role of the endothelium in modulating neointimal formation: vasculoprotective approaches to attenuate restenosis after percutaneous coronary interventions. *J Am Coll Cardiol* 2004; 44(4):733-739.
6. Hristov M, Weber C. Endothelial progenitor cells: characterization, pathophysiology, and possible clinical relevance. *J Cell Mol Med* 2004; 8(4):498-508.
7. Co M, Tay E, Lee CH. Use of endothelial progenitor cell capture stent (Genous Bio-Engineered R Stent) during primary percutaneous coronary intervention in acute myocardial infarction: intermediate- to long-term clinical follow-up. *Am Heart J* 2008; 155(1):128-132.
8. Klomp M, Beijk MA, de Winter RJ. Genous endothelial progenitor cell-capturing stent system: a novel stent technology. *Expert Rev Med Devices* 2009; 6(4):365-375.
9. Beijk MA, Klomp M, Verouden NJ. Genous endothelial progenitor cell capturing stent vs. the Taxus Liberte stent in patients with de novo coronary lesions with a high-risk of coronary restenosis: a randomized, single-centre, pilot study. *Eur Heart J*; 31(9):1055-1064.
10. Duckers HJ, Soullie T, den Heijer P. Accelerated vascular repair following percutaneous coronary intervention by capture of endothelial progenitor cells promotes regression of neointimal growth at long term follow-up: final results of the Healing II trial using an endothelial progenitor cell capturing stent (Genous R stent). *EuroIntervention* 2007; 3(3):350-358.
11. Duckers HJ, Silber S, de Winter R. Circulating endothelial progenitor cells predict angiographic and intravascular ultrasound outcome following percutaneous coronary interventions in the HEALING-II trial: evaluation of an endothelial progenitor cell capturing stent. *EuroIntervention* 2007; 3(1):67-75.
12. Cheng C, Noorderloos AM, Jeney V. Heme oxygenase 1 determines atherosclerotic lesion progression into a vulnerable plaque. *Circulation* 2009; 119(23):3017-3027.
13. Cheng C, Tempel D, Oostlander A. Rapamycin modulates the eNOS vs. shear stress relationship. *Cardiovasc Res* 2008; 78(1):123-129.
14. Cheng C, Noorderloos M, van Deel ED. Dendritic cell function in transplantation arteriosclerosis is regulated by heme oxygenase 1. *Circ Res*; 106(10):1656-1666.
15. Segers D, Helderma F, Cheng C. Gelatinolytic activity in atherosclerotic plaques is highly localized and is associated with both macrophages and smooth muscle cells in vivo. *Circulation* 2007; 115(5):609-616.
16. Granada JF, Inami S, Aboodi MS. Development of a Novel Prohealing Stent Designed to Deliver Sirolimus From a Biodegradable Abluminal Matrix. *Circ Cardiovasc Interv* 2010.

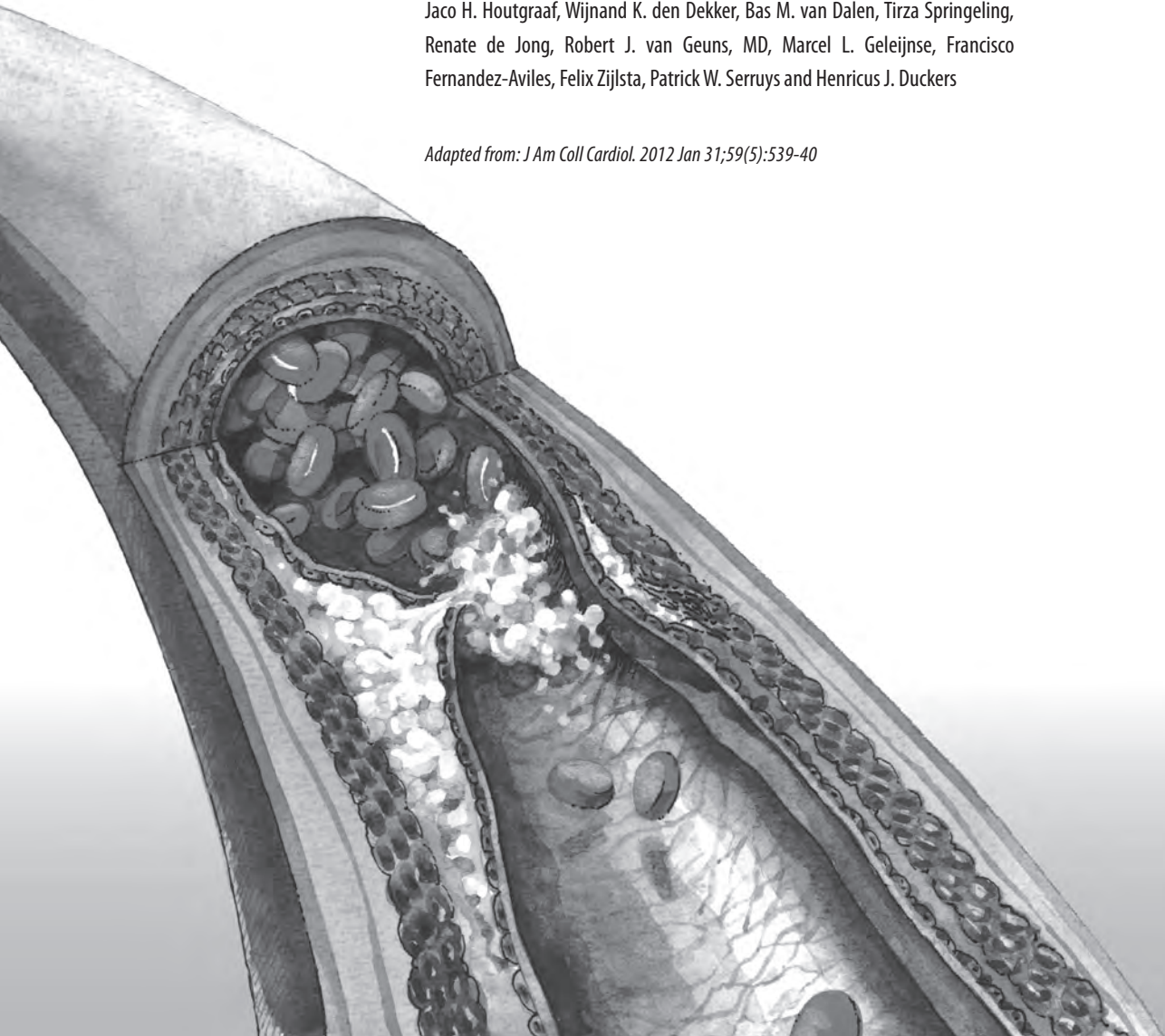
17. Ye C, Bai L, Yan ZQ. Shear stress and vascular smooth muscle cells promote endothelial differentiation of endothelial progenitor cells via activation of Akt. *Clin Biomech (Bristol, Avon)* 2008; 23 Suppl 1:S118-124.
18. Obi S, Yamamoto K, Shimizu N. Fluid shear stress induces arterial differentiation of endothelial progenitor cells. *J Appl Physiol* 2009; 106(1):203-211.
19. de Boer HC, Hovens MM, van Oeveren-Rietdijk AM. Human CD34+/KDR+ cells are generated from circulating CD34+ cells after immobilization on activated platelets. *Arterioscler Thromb Vasc Biol*; 31(2):408-415.
20. Harrison P, Goodall AH. "Message in the platelet"—more than just vestigial mRNA! *Platelets* 2008; 19(6):395-404.
21. Donahue BS, Gailani D, Mast AE. Disposition of tissue factor pathway inhibitor during cardiopulmonary bypass. *J Thromb Haemost* 2006; 4(5):1011-1016.
22. Osterud B, Bajaj MS, Bajaj SP. Sites of tissue factor pathway inhibitor (TFPI) and tissue factor expression under physiologic and pathologic conditions. On behalf of the Subcommittee on Tissue factor Pathway Inhibitor (TFPI) of the Scientific and Standardization Committee of the ISTH. *Thromb Haemost* 1995; 73(5):873-875.
23. Joner M, Finn AV, Farb A. Pathology of drug-eluting stents in humans: delayed healing and late thrombotic risk. *J Am Coll Cardiol* 2006; 48(1):193-202.
24. Kong D, Melo LG, Mangi AA. Enhanced inhibition of neointimal hyperplasia by genetically engineered endothelial progenitor cells. *Circulation* 2004; 109(14):1769-1775.
25. Eriksson EE. Leukocyte recruitment to atherosclerotic lesions, a complex web of dynamic cellular and molecular interactions. *Curr Drug Targets Cardiovasc Haematol Disord* 2003; 3(4):309-325.
26. Silber S, Damman P, Klomp M. Clinical results after coronary stenting with the Genous Bio-engineered R stent: 12-month outcomes of the e-HEALING (Healthy Endothelial Accelerated Lining Inhibits Neointimal Growth) worldwide registry. *EuroIntervention*; 6(7):819-825.

Chapter 9

Safety and Feasibility of Intracoronary Infusion of Adipose Tissue-Derived Regenerative Cells in Patients with ST-Elevation Myocardial Infarction

Jaco H. Houtgraaf, Wijnand K. den Dekker, Bas M. van Dalen, Tirza Springeling, Renate de Jong, Robert J. van Geuns, MD, Marcel L. Geleijnse, Francisco Fernandez-Aviles, Felix Zijlsta, Patrick W. Serruys and Henricus J. Duckers

Adapted from: J Am Coll Cardiol. 2012 Jan 31;59(5):539-40



ABSTRACT

Objectives: The APOLLO trial evaluated the safety and feasibility of intracoronary adipose tissue-derived regenerative cell (ADRC) infusion in the treatment of ST-elevation acute myocardial infarction (AMI) patients.

Background: Cell therapy holds great promise for the adjunctive treatment of AMI patients. ADRCs comprise among others mesenchymal-like stem cells that are similar to bone marrow-derived mesenchymal stem cells (MSC). However, the frequency of these cells in adipose tissue is higher than in bone-marrow, abolishing the need for cell culture expansion. ADRC isolation from adipose tissue requires 90 minutes, which makes the treatment of AMI patients possible within hours after the onset of AMI.

Methods: Fourteen patients were randomized to receive intracoronary infusion of 20 million ADRCs (n=10) or placebo (n=4) within 24 hours following the primary PCI.

Results: The liposuction procedure was well tolerated in all patients and intracoronary infusion of ADRC did not result in adverse effects. Though not powered for evaluation of efficacy end-points, the study results were encouraging with 50% reduction in infarct size as measured by delayed enhancement CMR ($p=0.002$), as well as improved perfusion defect ($p=0.004$), coronary flow reserve ($p=0.001$) and a trend towards improved ejection fraction (as measured by CMR and SPECT). Further, *post hoc* analysis demonstrated statistically significant reduction in arrhythmia.

Conclusions: Treatment of patients with an AMI by intracoronary delivery of ADRCs is safe and feasible, with indications of efficacy that are consistent with the presumed working mechanism in pre-clinical studies.

ABBREVIATIONS:

AMI	acute myocardial infarction
PCI	percutaneous coronary intervention
CMR	cardiac magnetic resonance imaging
MIBI-SPECT	sestamibi single photon-emission computed tomography
LV	left ventricular
LVEF	left ventricular ejection fraction
TIMI	thrombolysis in myocardial infarction
TTE	transthoracic echocardiography
MACCE	major adverse cardiac or cerebral events
(S)AE	(serious) adverse event

INTRODUCTION

Transplantation of bone-marrow (BM) derived mononuclear cells has shown promise in the treatment of AMI patients (1,2). However, it is the paracrine and immunomodulatory capabilities of rare mesenchymal stem cells (MSC) in BM-aspirates that are hypothesized to account for a large part of the beneficial effect (3). In order to obtain therapeutically relevant numbers of MSC from a BM-aspirate, extensive *in vitro* expansion in a good-manufacturing-practice facility is required. This excludes the use of these cells in the acute phase of an AMI. In addition, cell culture expansion of MSC leads to a significant increase in cell size, which has been shown to cause vascular obstruction and micro-infarctions following intracoronary infusion (4,5).

Adipose tissue was first identified as an alternative source of abundant numbers of multipotent mesenchymal-like stem cells in 2002 (6). Like BM-derived MSC, these cells stimulate neo-angiogenesis and cardiomyocyte survival both *in vitro* and *in vivo* by release of various angiogenic, anti-apoptotic and immunomodulatory factors (7-10). In animal models of AMI, administration of freshly isolated adipose tissue-derived regenerative cells (ADRCs) consistently improved left ventricular (LV) function and myocardial perfusion by cardiomyocyte salvage and stimulated neo-angiogenesis in the infarct border zone, resulting in reduced infarct scar formation (11-13). The frequency of ADRCs in freshly isolated adipose tissue digestates is ~ 2,500 fold greater than that of freshly aspirated BM, suggesting that culture may not be required to generate sufficient therapeutic cells (14,15). On average, 20-40 million cells can be isolated within two hours after a liposuction from as little as 200 grams of lipo-aspirate.

The consistent therapeutic effect in small and large animal models was the basis for the APOLLO trial as the first-in-man experience with ADRCs in the treatment of patients with an ST-elevation AMI. Primary objectives of this study were to determine the safety and feasibility of harvest and intracoronary infusion of ADRCs in the acute phase of an AMI, as well as to explore the potential efficacy of this cell therapy.

METHODS

Study Design and Patient Population

The APOLLO trial was a prospective, double-blind, randomized, placebo-controlled phase I/IIa study, conducted at the Thoraxcenter of the Erasmus MC in Rotterdam, The Netherlands, and at Hospital General Universitario Gregorio Marañón, Madrid, Spain, and designed to evaluate the safety and feasibility of intracoronary delivery of autologous ADRCs in the treatment of patients with an ST-elevation AMI.

Patients were eligible for enrolment after successful interventional treatment for their first AMI, had no history of heart disease and presented with clinical symptoms and electrocar-

diographic criteria consistent with an AMI for a minimum of 2 and a maximum of 12 hours from onset of symptoms. The area of LV hypo- or akinesia was required to correspond to the culprit lesion, and the residual LVEF needed to be between 30% and 50% as measured by left ventricular angiography or echocardiography following the primary PCI. Procedural success of the primary intervention was defined as restoration of TIMI 3 flow in the culprit vessel with a residual diameter stenosis of $\leq 20\%$ by quantitative coronary angiography analysis. The main exclusion criteria were defined as: hemodynamic instability, need of mechanical ventilation, the necessity of staged treatment of coronary artery disease, the occurrence of ventricular arrhythmias, or the inability to undergo liposuction.

After written informed consent, patients were 3:1 randomized to receive either 20 million ADRCs (n=10) or placebo solution (n=4). The study protocol was reviewed and approved by the Dutch Central Committee on Research involving Human Subjects (CCMO) and the institutional ethics committees of each center. All patients provided written informed consent after their eligibility was confirmed.

Liposuction Procedure and Preparation of ADRCs and Placebo

All patients underwent a standard liposuction procedure of the peri-umbilical region. Briefly, tumescent fluid (1 mg epinephrine/0,2% w/v lidocaine in 500 mL Ringer's lactate solution (RL)) was injected subcutaneously in the abdominal area by a blunt needle. After 30 minutes, adipose tissue was aspirated using a standard 4-mm blunt liposuction cannula connected to a Toomey syringe.

The lipoaspirate was processed using the automated Cytori Celution[®] 800 device (Cytori Therapeutics, San Diego, CA, USA) in order to separate the ADRCs from adipocytes. In short, enzymatic digestion into a single-cell suspension, and subsequent centrifugation, washing and concentration steps separate the non-buoyant ADRCs from the buoyant adipocytes and liquid fat. After the final washing step, the ADRCs were resuspended in RL to 20 million ADRCs per 8 mL. The placebo solution was generated by mixing 0.1 mL autologous whole blood in RL, which rendered the placebo solution visually indistinguishable from the ADRC suspension. The hospital pharmacist verified correct dosing and sufficient cell viability of the graft, and finally randomized patients to their treatment allocation using an interactive voice-response system

ADRC and Placebo Infusion Procedure

Within 24 hours of the primary PCI, the assigned treatment was slowly infused into the culprit vessel via a micro-infusion catheter connected to a proprietary cell strainer (Cytori Therapeutics, San Diego, CA, USA). Coronary flow reserve (CFR) was measured before and immediately after infusion of ADRCs or placebo to detect potential micro-vascular obstruction, whereas

TIMI flow was assessed every 3 minutes during infusion. CFR was determined by measuring flow using a Doppler flow wire (Combwire, Volcano, San Diego, CA, USA) at baseline and at maximal vasodilatation by adenosine infusion. Following infusion, patients were monitored for 24 hours in the intensive coronary care unit with routine ECG and blood analyses for the first 72 hours.

Six-month Clinical Follow-up

Clinical follow-up will be monitored for 36 months in all patients. Here we report the six-month clinical and angiographic follow-up of the patient cohorts. Telemetric electrocardiographic monitoring was maintained for the first 6 days following the index procedure. Routine 24-hour holter recordings were scheduled weekly for the first 4 weeks and monthly from months two to six, and finally every six months for the remainder of the 36 months clinical follow-up period. All patients underwent a physical examination and routine blood laboratory analysis at each scheduled visit to the outpatient clinic. CMR, MIBI-SPECT, and two-dimensional TTE were performed 2-4 days after the index procedure and at six-month follow-up. Holter and imaging data were analyzed by blinded, independent core laboratories (CMR: Cardiovascular Core Labs, Boston, MA, USA; MIBI-SPECT: Cardiovascular Core Labs, Boston, MA, USA; TTE: MedStar Research, Washington, DC, USA; Holter Monitoring: Agility Centralized Research, Banockburn, IL, USA).

Study end-points

The main safety end-points were defined as the change in TIMI flow pre- versus post-infusion, occurrence of MACCE (cardiac death, myocardial infarction, target lesion revascularization or stroke), or hospitalization due to congestive heart failure during the six-month clinical follow-up. Other safety end-points included: all SAE, including the occurrence of ventricular arrhythmias on holter monitoring, and reduction of coronary flow reserve (CFR) in the culprit vessel post-ADRC infusion. An independent, international Data Safety Monitoring Board (DSMB) and critical event committee (CEC) reviewed and adjudicated all MACCE and SAE events.

Feasibility end-points were defined as the change in LVEF and dimensions at six-month follow-up as assessed by CMR and MIBI-SPECT, infarct size as measured by delayed-enhancement CMR (DE-CMR), and the visual rest score (VRS; size of the perfusion defect) as quantified by MIBI-SPECT.

Statistical Analysis

The APOLLO trial was primarily designed as a safety and feasibility study. Therefore, all statistical tests were performed post-hoc and were considered exploratory, whereas no formal prior power calculations were performed. Unless otherwise specified, all statistical tests were two-sided unpaired Student's-*t*-tests. All values are presented as mean \pm SEM and statistical significance was assessed with respect to a nominal p-value \leq 0.05. All analyses were performed by an independent clinical research organization (Synteract, Carlsbad, CA, USA) using SAS[®] software (version 8.2 or higher).

RESULTS

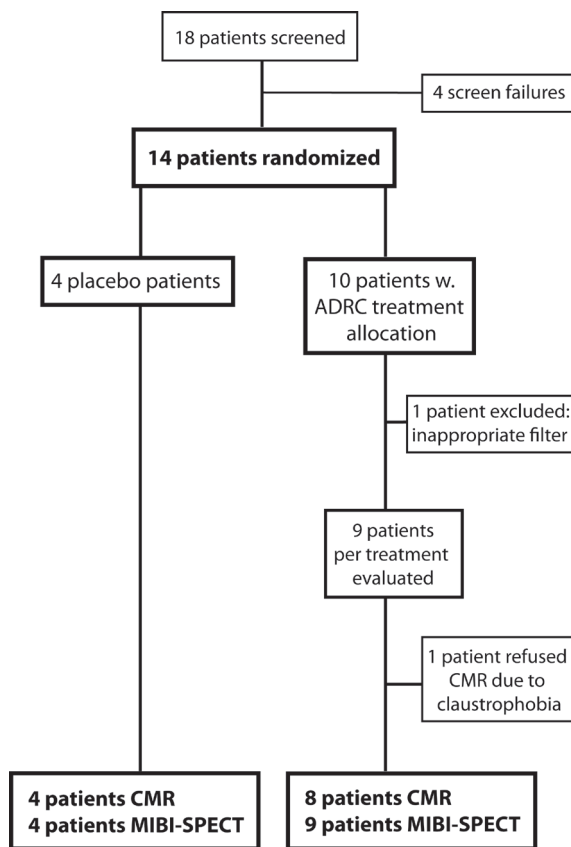
Study population

Between January 2008 and May 2009, 14 patients presenting with AMI were enrolled in the trial and randomized to receive either an intracoronary infusion of 20 million ADRCs (n=10) or placebo solution (n=4) in the culprit artery. In one patient in the ADRC group an inappropriate cell strainer was used during the infusion procedure. Whether this patient received cells and at what exact dose could not be determined afterwards, wherefore this patient was excluded from analysis. Thus, nine patients treated with ADRCs were included in the current per treatment evaluable analysis. Of these, one patient allocated to the treatment arm refused CMR analysis due to claustrophobia, resulting in eight analyzable patients with CMR follow-up (see Figure 1 for study flow chart).

Patients in the placebo group were 55 ± 7.5 years of age with a body mass index of 27.6 ± 3.3 and a baseline LVEF of $47.9 \pm 5.4\%$ (as assessed by CMR) and $52.0 \pm 10.0\%$ (as assessed by MIBI-SPECT). Patients in the treatment group were 61 ± 2.1 years of age with a body mass index of 27.5 ± 3.0 and a baseline LVEF of $52.4 \pm 4.8\%$ (by CMR) and $52.1 \pm 2.5\%$ (by MIBI-SPECT). The left anterior descending artery (LAD) was the culprit artery in all 14 patients and all patients were successfully treated using an everolimus drug-eluting stent (Xience V[®] stent; Abbott Vascular, Illinois, USA) with restoration of TIMI 3 flow. Demographics and baseline clinical characteristics are summarized in Table 1.

Liposuction procedure and cell isolation

The liposuction procedure was performed under local anesthesia and was well tolerated in all patients. On average, 196 ± 12 g of adipose tissue was harvested, which resulted in $164 \times 10^3 \pm 30 \times 10^3$ ADRCs per gram of fat tissue. Although the liposuction procedure was well tolerated in all patients, a procedure-related serious bleeding event occurred in two patients.

**Figure 1**

Flow chart of the APOLLO trial. ADRC: adipose tissue-derived regenerative cells; CMR: cardiac magnetic resonance imaging; MIBI-SPECT: sestamibi single photon-emission computed tomography.

In the first patient, the bleeding event was precipitated by pre-enrolment administration of a glycoprotein-IIb/IIIa inhibitor. In the second patient, blood loss was considered to be associated with an increased activated partial thromboplastin time (aPTT) due to heparin treatment during the primary PCI. The independent DSMB considered none of the bleeding episodes to be related to the ADRC infusion procedure. Modification of the study protocol to exclude patients previously treated with glycoprotein-IIb/IIIa inhibitors and those with an aPTT-ratio exceeding 1.8, prevented serious bleeding events in the remaining study patients.

Intracoronary infusion, TIMI flow and coronary flow reserve

Patients randomized to the treatment arm received an average dose of 17.4 ± 4.1 million ADRCs in 8 mL of RL. Intracoronary infusion of ADRCs was successful and well tolerated in all patients, and did not result in any coronary flow impediment, as assessed by TIMI flow rate or

Table 1. Demographics and Baseline Characteristics.*

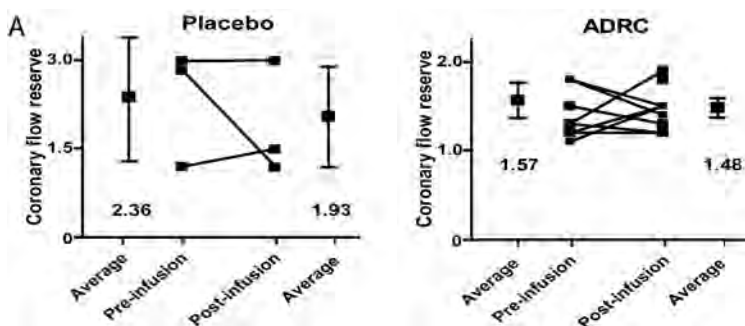
	Placebo (n=4)	ADRC (n=9)
Age (years)	55 ± 7.5	61 ± 2.1
Male (%)	100	78
Caucasian (%)	100	100
Body Mass Index	27.6 ± 3.3	27.5 ± 3.0
Smoking (%)	50.0	66.7
Hypertension (%)	50.0	66.7
Creatine Kinase MB (μmol/L)	92.0 ± 5.7	78.0 ± 3.9
NT-proBNP [†] (pmol/l)	225 ± 116	250 ± 86
Left Ventricular Ejection Fraction (%)		
2D Echocardiography (at screening)	43.5 ± 3.3	46.1 ± 2.5
Cardiac Magnetic Resonance Imaging	47.9 ± 5.4	52.4 ± 4.8
MIBI-SPECT [‡]	52.0 ± 10.0	52.1 ± 2.5
Infarct Size (% of Left Ventricle)	24.7 ± 9.2	31.6 ± 5.3
Perfusion Defect (VRS [§])	15.0 ± 4.9	16.9 ± 2.1

*Only includes per treatment evaluable (PTE) patients

[†]NT-proBNP: n-type brain-natriuretic peptide; [‡]MIBI-SPECT: sestamibi single photon-emission computed tomography; [§]VRS: visual rest score

quantified by coronary flow reserve (CFR). In both ADRC-treated patients, as well as controls, CFR remained unchanged before and after cell infusion (Figure 2).

Interestingly, at six-month follow-up, the CFR had increased significantly by 60% in ADRC-treated patients from 1.57 ± 0.39 to 2.51 ± 0.74 ($p=0.031$), as opposed to a non-significant increase of only 4% (from 2.37 ± 0.85 to 2.47 ± 0.72 ; $p=0.93$; Figure 3A) in the placebo group.

**Figure 2**

Coronary flow reserve following ADRC or placebo infusion. Individual and mean coronary flow reserve values before and after ADRC (bottom panel) or placebo infusion (top panel). CFR was unaffected in all ADRC-treated patients, suggestive of no micro-vascular obstruction due to the ADRC infusion. ADRC: adipose tissue-derived regenerative cells; CFR: coronary flow reserve.

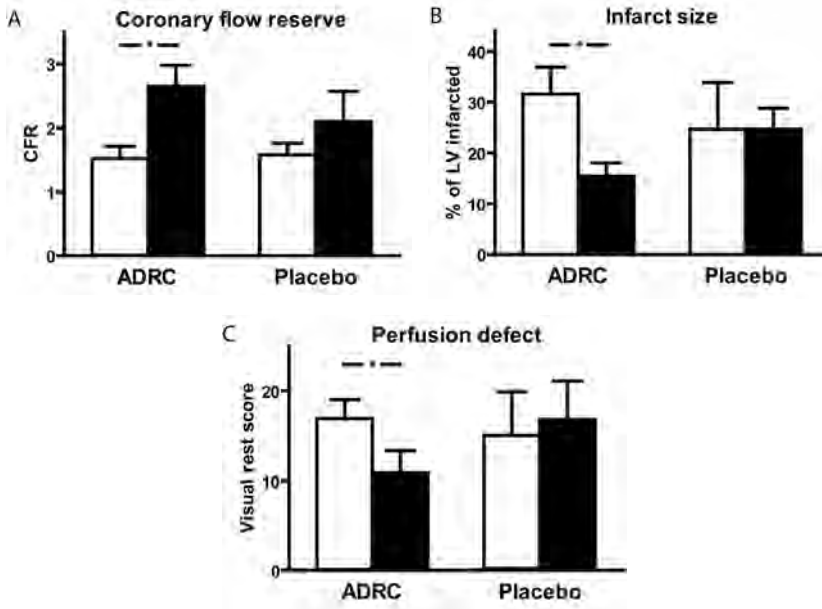


Figure 3

Change in coronary flow reserve (CFR), infarct size (DE-CMR), and perfusion defect (MIBI-SPECT) from baseline (white bars) to the six months follow-up (black bars) time-point. 3A; Coronary flow reserve was significantly enhanced by 72% in ADRC-treated patients, whereas the CFR in placebo patients did not improve in a significant manner. 3B; Percentage of LV infarcted improved by 50% in ADRC-treated patients as opposed to no change in placebo patients. 3C; The rest perfusion defect as determined by MIBI-SPECT and expressed as visual rest score (VRS) improved 4-fold in ADRC-treated patients as compared to a deterioration in placebo patients. ADRC: adipose tissue-derived regenerative cells; DE-CMR: delayed enhancement cardiac magnetic resonance imaging; MIBI-SPECT: sestamibi single photon-emission computed tomography.

MACCE / SAE

At six-month follow-up, no MACCE events were reported in the control group versus one in the treatment group (1/9, 11%). This patient presented with symptoms of unstable angina pectoris two months after the primary PCI based on thrombus formation just proximal to the stent in the culprit vessel. IVUS analysis ruled out the possibility of residual dissection or stent malapposition, and the patient was subsequently successfully treated by thrombectomy and stent placement, without a rise of cardiac enzymes. The patient was later diagnosed with an underlying anti-phospholipid syndrome that might have precipitated the target lesion revascularization (TLR).

SAE occurred in 2 out of 4 patients (50%) in the placebo group and 3 out of 9 (33%) patients in the ADRC group. The SAE in the placebo group consisted of a hospital admission for atypical, non-cardiac chest pain (n=1) and bleeding at the liposuction site (n=1). In the ADRC group, one patient experienced significant hematoma formation at both the liposuction site and in the groin (n=1), one TLR event (n=1; as previously described) and a hospital admission

due to paroxysmal atrial fibrillation (n=1). The patient that experienced an episode of atrial fibrillation had a medical history of paroxysmal atrial fibrillation before inclusion in the study. No unanticipated adverse effects related to the ADRC therapy were reported. All MACCE, SAE and AE are summarized in table 2.

Table 2

	Placebo (n=4)	ADRCs (n=9)	p value
Adverse Events (AE)			
Total AE	15	33	
AE per patient	3.8	3.7	
Patients with at least 1AE	4	9	1.000
Cardiac disorders	2	4	0.911
Gastro-intestinal	1	4	0.645
General disorders	4	14	0.592
Infectious disease	1	1	0.591
Post-procedural			
Aneurysm spurium femoral artery	1	0	0.164
Hematoma femoral puncture site	1	2	0.931
Hematoma abdominal wall	2	5	0.919
Metabolism	0	2	0.360
Nervous system	2	1	0.247
Serious Adverse Events (SAE)			
Patients with at least 1 SAE	2	3	0.710
Cardiac disorders			
Unstable angina pectoris	0	1	0.512
Atrial fibrillation	0	1	0.512
Post-procedural			
Bleeding post-liposuction	1	1	0.591
General disorders			
Non-cardiac chest pain	1	0	0.164
MACCE*			
Patients with at least 1 MACCE	0	1	0.512
Cardiac disorders			
Target lesion revascularization	0	1	0.512
Ventricular arrhythmia			
At least 1 arrhythmic event	2	3	0.710
Ventricular tachycardia episodes	10	3	0.018

Values are presented as n.; P-values are determined using two-tailed Chi-square tests.

*MACCE = major adverse cardiac or cerebral event.

Holter monitoring for arrhythmia

Following discharge, ambulatory 24 hour holter recordings were performed weekly for the first four weeks after the index procedure, and subsequently every month afterwards. Holter data were collected by an independent holter core-lab. Post-hoc analysis of the core-lab data revealed that ADRC therapy was associated with a significant reduction of the number of episodes of ventricular arrhythmias. A total of three episodes of non-sustained ventricular tachycardia (NSVT) were detected in the ADRC-treated group, as compared to 10 episodes in the placebo group ($p=0.018$). On average, each patient in the control group experienced 2.5 episodes of NSVT as opposed to only 0.3 episode of NSVT per ADRC-treated patient ($p=0.048$).

Moreover, a marked reduction in the number of premature ventricular contractions (PVC) per 24 hour holter recording was noted in ADRC-treated patients as compared to control patients (46 PVC/9 patients vs. 286 PVC/4 patients, $p<0.001$). Thus, each placebo patient had an average of 72 PVC per 24 hours as compared to 5 PVC in treated patients ($p=0.014$). Also, 3/4 (75%) placebo patients experienced >10 PVC/hour as opposed to none of the patients in the treatment group ($p=0.029$). Holter data are summarized in table 3.

Table 3. Ventricular arrhythmia and premature ventricular contractions.

	Placebo (n=4)	ADRCs (n=9)	p value
Ventricular tachycardia			
At least one episode of VT	2	3	0.710
Total episodes	10	3	0.018
Episodes/patient	2.5	0.33	0.048
Premature ventricular contractions (PVC)			
Patients with >10 PVC/hour	3	0	0.029
Total PVC/24 hours	286	46	<0.0001
PVC/patient/24 hours	72	5	0.014

Values are presented as n.; P-values are determined using two-tailed Chi-square tests when applicable.

Global left ventricular function

LV volumes and LVEF were determined by CMR and MIBI-SPECT. The analyses of ventricular volumes and global LVEF by the different imaging modalities are summarized in Table 4.

MIBI-SPECT analysis demonstrated a +4% improvement in global LVEF in ADRC-treated patients from 52.1% to 56.1%, whereas the placebo group deteriorated by -1.7% (52.0% to 50.3%), rendering an absolute difference between the treatment groups of +5.7% ($p=0.114$). A similar positive trend of improved cardiac function was found by CMR analysis, which

Table 4. Quantitative Measures of Left Ventricular Function and Volumes.

	Placebo (n=9)		ARDC (n=4)		p value
	Baseline	6 Months	Baseline	6 Months	
	LV ejection fraction				
CMR	48.0 ± 5.4	48.0 ± 2.1	52.4 ± 4.8	57.0 ± 3.8	0.091
SPECT	52.0 ± 10.0	50.3 ± 4.8	52.1 ± 2.5	56.1 ± 3.9	0.114
End-diastolic volume (ml)					
CMR	177 ± 6	199 ± 26	166 ± 15	193 ± 15	0.763
SPECT	155 ± 4	163 ± 14	165 ± 17	169 ± 19	0.729
End-systolic volume (ml)					
CMR	88.5 ± 7.6	105.0 ± 18.1	80.1 ± 12.8	83.2 ± 10.6	0.422
SPECT	74.0 ± 14.0	80.3 ± 7.5	81.4 ± 12.9	78.5 ± 15.1	0.536

Values are presented as mean ± standard error of the means

*CMR: cardiac magnetic resonance imaging; †SPECT: single photon emission computed tomography.

demonstrated a +4.6% improvement of global LVEF in the ADRC-treated group from baseline to six-month follow-up ($p=0.091$).

LV dimensions

At baseline, LV end-diastolic and end-systolic volumes were comparable between the treatment groups and imaging modalities (Table 4). Although the absolute end-diastolic volumes as analyzed by CMR and SPECT at six-month follow-up differed, the relative difference between the ADRC-treated and control group at six months follow-up was negligible.

The end-systolic volume in the placebo control group deteriorated by +16.5 mL as assessed by CMR, as compared to a +3.1 mL increase in the cell-treated group (relative difference -13.4 mL, $p=0.422$). A similar, non-significant reduction of end-systolic volumes was observed using MIBI-SPECT analysis, where the relative difference volume was -9.2 mL (-12.1%, $p=0.536$).

Myocardial infarct size analysis by DE-CMR

Treatment with ADRCs led to a substantial and significant reduction of both total infarct mass and the percentage of LV infarcted over time. Absolute infarct mass was decreased by -50% (47.0 ± 11.6 to 23.5 ± 4.2 g, $p < 0.001$), whereas the percentage of LV infarcted was reduced by -52% (31.6 ± 5.3 % to 15.3 ± 2.6 %, $p=0.002$; Figure 3B) in the ADRC-treated patients, as opposed to no change in the placebo-treated AMI patients (24.7 ± 9.2 % vs. 24.7 ± 4.1 %). However, the difference between the ADRC-treated group and placebo group was not statis-

tically significant for both absolute infarct mass ($p=0.313$) and the percentage of LV infarcted ($p=0.481$).

Myocardial perfusion analysis by MIBI-SPECT

Perfusion defects were assessed by MIBI-SPECT and expressed as the Visual Rest Score (VRS). The VRS is defined as the uptake of sestamibi into non-ischemic myocardium using a semi-quantitative, 17-segment scoring system in three short-axis slices. In the placebo group, the perfusion defect deteriorated by +11.6% (15.0 ± 4.9 to 16.8 ± 4.3 , $P=0.728$; Figure 3C). In contrast, treatment with ADRC resulted in a significant -36% reduction of the residual perfusion defect from 16.9 ± 2.1 to 10.9 ± 2.4 (change of -6.0, $p=0.004$). This represents a four-fold reduction of the rest perfusion defect of the left ventricle in cell-treated patients at six months post index-procedure as compared to control patients ($p=0.238$), suggestive of improved myocardial perfusion with sustained myocardial viability.

DISCUSSION

The APOLLO trial is the first-in-man experience of intracoronary infusion of ADRCs in the treatment of patients with ST-elevation AMI. The main findings at the six-months clinical and angiographic follow-up time-point are: 1) performing a liposuction to harvest ADRCs in the acute phase of a myocardial infarction is safe and feasible; 2) intracoronary infusion of freshly isolated ADRCs was safe and did not result in an alteration of coronary flow or micro-vascular obstruction; 3) ADRC therapy had no apparent pro-arrhythmogenic effects, but rather appeared to reduce the occurrence of ventricular arrhythmias and ectopy; 4) no serious adverse events were related to the ADRC therapy and 5) ADRC infusion resulted in a significant improvement of the perfusion defect and coronary flow reserve in the culprit vessel and a 50% reduction of myocardial scar formation. The latter might have resulted in trends to improved cardiac function.

In the APOLLO study, limited liposuction in the acute phase of the myocardial infarction appeared to be well tolerated. Although two patients experienced significant bleeding, this is likely to be associated with a severely prolonged aPTT and concomitant use of glycoprotein-IIb/IIIa-inhibitors in these particular patients. After modification of the protocol to monitor for normalization of the aPTT prior to the liposuction procedure and the exclusion of patients with prior treatment with glycoprotein-IIb/IIIa-inhibitors, the remaining 10 patients were uneventful. However, post-liposuction bleeding may still represent a concern in the following studies and needs to be carefully monitored.

During cell infusion, coronary flow was monitored by regular assessment of TIMI flow and by CFR analysis. Although intracoronary infusion of BM-derived and cell culture-expanded

MSC has raised concerns in pre-clinical studies with respect to micro-vascular obstruction and myocardial infarction (4,5), the intracoronary infusion of freshly isolated ADRCs did not result in any detectable effect on coronary flow. The observed lack of vascular obstruction in the APOLLO patients corroborates the concept that direct isolation and infusion of ADRCs may circumvent these issues.

No difference was observed between the occurrence of SAE in the ADRC-treated and placebo control group. Importantly, the independent DSMB considered no causal relationship between the MACCE and SAE events and ADRC therapy. Furthermore, ADRC therapy did not have any pro-arrhythmogenic effect. On the contrary, ADRC therapy was associated with a marked and significant reduction of ventricular arrhythmias and ventricular ectopy. This is in line with other clinical and pre-clinical observations in cell therapy studies, and might be correlated with the reduction of scar size and improved myocardial perfusion in ADRC-treated subjects (16-18).

In the APOLLO trial, ADRC therapy was initiated within 24 hours following the primary PCI. This is unlike many previous clinical studies in which cell therapy was only initiated in the sub-acute phase of the AMI due to logistic considerations and observations in pilot studies (1,2). However, one of the presumed working mechanisms underlying the beneficial effect of cellular therapy is the prevention of cardiomyocyte loss by paracrine release of anti-apoptotic, pro-survival and immunomodulatory factors (9,10,19). In line with this concept, cell therapy should be initiated as early as possible, when cardiomyocytes are at the highest risk of ischemia/reperfusion-induced apoptosis or necrosis, and the inflammatory response in the infarct area is most pronounced. The feasibility of ADRC therapy directly following reperfusion was demonstrated in various large animal models of AMI (12,13).

ADRCs are also known to secrete multiple pro-angiogenic factors (7,8,11). As a result, ADRC transplantation in pre-clinical AMI studies consistently led to increased capillary density with improved perfusion in the infarct border zone, resulting in preserved cardiac function (11-13). In our clinical study, significant improvement in both coronary flow reserve (+72%) and perfusion defect (-36%) were found at six-months follow-up, as opposed to no change in the control patient group. Interestingly, in the landmark REPAIR-AMI trial, CFR was also profoundly enhanced (20), which seems to confirm the pro-angiogenic and reparative potential of infused regenerative cells in AMI patients. The observations in the current study indicate that ADRCs may promote (neo-)angiogenesis in the peri-infarct region resulting in improved myocardial perfusion, thereby possibly limiting myocardial damage and improving function.

The major limitation of this phase I/IIa trial is the small sample size. However, the study was performed in a randomized, double-blind fashion with the analysis of imaging and holter end-points by independent core laboratories.

In conclusion, ADRC therapy appears to be safe and feasible in the acute phase of an AMI. Although no statistically significant effect on global LV function was found, significant improvements in infarct size, perfusion defect, coronary flow reserve, and arrhythmia suggest

a beneficial effect. Importantly, this beneficial effect is consistent with the findings in pre-clinical AMI studies, and concordant with the presumed pro-angiogenic, anti-apoptotic, and immunomodulatory working mechanism of ADRC therapy. ADRCs may thus represent an attractive adjunctive therapy to primary intervention of patients with a large AMI. However, further randomized, controlled trials are needed to confirm these promising results.

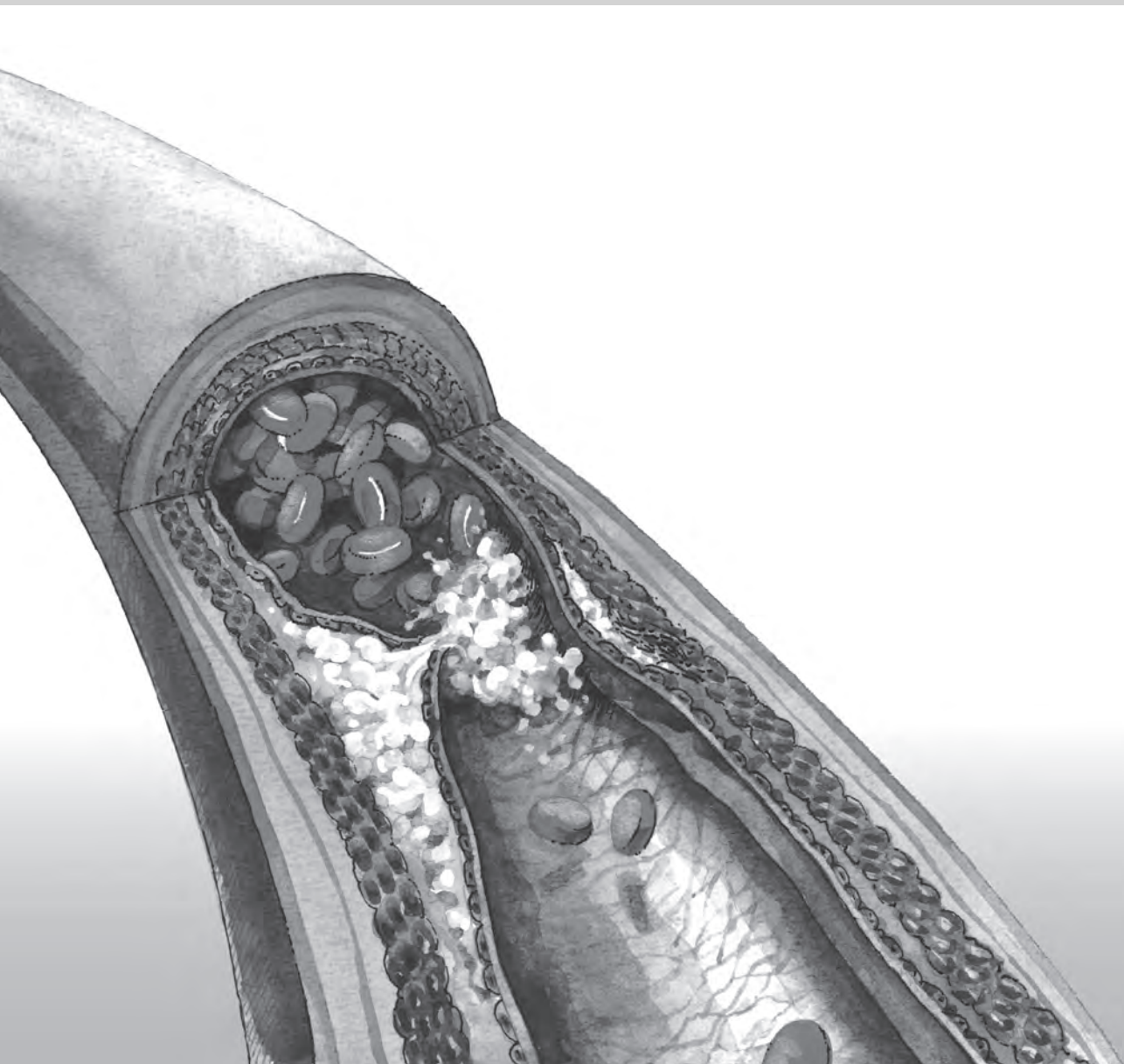
The forthcoming ADVANCE study is a multi-center, prospective, 2:1 randomized, placebo-controlled phase IIb/III trial in 375 patients, which will assess the safety and efficacy of intra-coronary infusion of ADRCs in patients with an ST-elevation AMI. This study will be initiated in the first half of 2011.

REFERENCES

1. Abdel-Latif A, Bolli R, Tleyjeh IM, et al. Adult bone marrow-derived cells for cardiac repair: a systematic review and meta-analysis. *Arch Intern Med* 2007;167:989-97.
2. Lipinski MJ, Biondi-Zoccai GG, Abbate A, et al. Impact of intracoronary cell therapy on left ventricular function in the setting of acute myocardial infarction: a collaborative systematic review and meta-analysis of controlled clinical trials. *J Am Coll Cardiol* 2007;50:1761-7.
3. Choi YH, Kurtz A, Stamm C. Mesenchymal stem cells for cardiac cell therapy. *Hum Gene Ther* 2011;Jan:3-17.
4. Perin EC, Silva GV, Assad JA, et al. Comparison of intracoronary and transendocardial delivery of allogeneic mesenchymal cells in a canine model of acute myocardial infarction. *J Mol Cell Cardiol* 2008;44:486-95.
5. Vulliet PR, Greeley M, Halloran SM, MacDonald KA, Kittleson MD. Intra-coronary arterial injection of mesenchymal stromal cells and microinfarction in dogs. *Lancet* 2004;363:783-4.
6. Zuk PA, Zhu M, Ashjian P, et al. Human adipose tissue is a source of multipotent stem cells. *Mol Biol Cell* 2002;13:4279-95.
7. Traktuev DO, Merfeld-Clauss S, Li J, et al. A population of multipotent CD34-positive adipose stromal cells share pericyte and mesenchymal surface markers, reside in a periendothelial location, and stabilize endothelial networks. *Circ Res* 2008;102:77-85.
8. Rubina K, Kalinina N, Efimenko A, et al. Adipose stromal cells stimulate angiogenesis via promoting progenitor cell differentiation, secretion of angiogenic factors, and enhancing vessel maturation. *Tissue Eng Part A* 2009;15:2039-50.
9. Madonna R, Geng YJ, De Caterina R. Adipose tissue-derived stem cells: characterization and potential for cardiovascular repair. *Arterioscler Thromb Vasc Biol* 2009;29:1723-9.
10. Meliga E, Strem BM, Duckers HJ, Serruys PW. Adipose-derived cells. *Cell Transplant* 2007;16:963-70.
11. Cai L, Johnstone BH, Cook TG, et al. IFATS collection: Human adipose tissue-derived stem cells induce angiogenesis and nerve sprouting following myocardial infarction, in conjunction with potent preservation of cardiac function. *Stem Cells* 2009;27:230-7.
12. Valina C, Pinkernell K, Song YH, et al. Intracoronary administration of autologous adipose tissue-derived stem cells improves left ventricular function, perfusion, and remodelling after acute myocardial infarction. *Eur Heart J* 2007;28:2667-77.
13. Alt E, Pinkernell K, Scharlau M, et al. Effect of freshly isolated autologous tissue resident stromal cells on cardiac function and perfusion following acute myocardial infarction. *Int J Cardiol*;144:26-35.
14. Fraser JK, Schreiber R, Strem B, et al. Plasticity of human adipose stem cells toward endothelial cells and cardiomyocytes. *Nat Clin Pract Cardiovasc Med* 2006;3 Suppl 1:S33-7.
15. Caplan AI. Why are MSCs therapeutic? New data: new insight. *J Pathol* 2009;217:318-24.
16. Hare JM, Traverse JH, Henry TD, et al. A randomized, double-blind, placebo-controlled, dose-escalation study of intravenous adult human mesenchymal stem cells (prochymal) after acute myocardial infarction. *J Am Coll Cardiol* 2009;54:2277-86.

17. Fotuhi P, Song YH, Alt E. Electrophysiological consequence of adipose-derived stem cell transplantation in infarcted porcine myocardium. *Europace* 2007;9:1218-21.
18. Bello D, Fieno DS, Kim RJ, et al. Infarct morphology identifies patients with substrate for sustained ventricular tachycardia. *J Am Coll Cardiol* 2005;45:1104-8.
19. Ruvinov E, Dvir T, Leor J, Cohen S. Myocardial repair: from salvage to tissue reconstruction. *Expert Rev Cardiovasc Ther* 2008;6:669-86.
20. Erbs S, Linke A, Schachinger V, et al. Restoration of microvascular function in the infarct-related artery by intracoronary transplantation of bone marrow progenitor cells in patients with acute myocardial infarction: the Doppler Substudy of the Reinfusion of Enriched Progenitor Cells and Infarct Remodeling in Acute Myocardial Infarction (REPAIR-AMI) trial. *Circulation* 2007;116:366-74.

Chapter 10 Summarizing discussion



Atherosclerosis is a complex disease which already starts in childhood, but usually does not reveal itself until (late) adolescence, and constitutes a major burden on health care, not only now, but also in the future. It is therefore of great interest to better understand the pathophysiology of atherosclerotic disease, for the development of novel therapeutic and diagnostic tools. This thesis is divided into two sections. The first section studies the molecular and cellular basis of plaque destabilization, including immune regulation and neovascularization. The second section describes the clinical studies in which we evaluated novel therapies for the treatment of coronary artery disease. We describe the results of the HEALING IIB trial, which evaluated the use of a novel bioengineered stent that captures circulating endothelial progenitor cells and we show that this novel stent indeed captures endothelial progenitor cells and accelerates re-endothelialization and reduces thrombogenicity. Furthermore, we show the results of the APOLLO trial, in which we evaluated the use of adipose tissue-derived regenerative cells in the treatment of ST segment elevation myocardial infarction.

THE IMMUNE SYSTEM AND ATHEROSCLEROSIS

It is nowadays widely accepted that atherosclerosis is an inflammatory disease and therefore modulation of the immune system as treatment for atherosclerosis has gained much interest. In order to do this, one must understand the role of innate and adaptive immunity in atherosclerosis. In **chapter two** we provide a general overview of one part of the innate immune system in atherosclerosis, namely the Toll like receptor 4 (TLR4). Activation of this receptor leads to a signaling cascade that ultimately ends in nuclear translocation of NF κ B and transcription of pro-inflammatory cytokines. TLR4 is expressed on many celltypes of the innate immune system that are present in the atherosclerotic plaque. Furthermore, different pro-atherogenic ligands have been shown to activate TLR4, although it remains unclear how the TLR4 signaling cascade in the pathophysiology of atherosclerosis is exactly regulated. TLR4/apolipoprotein E (ApoE) double knock out mice developed significantly fewer aortic atherosclerotic lesions compared to ApoE knock out mice, suggesting involvement of TLR4 in atherogenesis. They also showed a reduction in macrophage and lipid content in plaques in the aortic sinus of TLR4/ApoE double knock out mice, independent of the plasma lipid levels. In addition, double knock out mice also had reduced numbers of circulating pro-inflammatory cytokines suggesting that a decreased systemic inflammation plays a role in the atheroprotective effects of TLR4 deficiency¹. Interestingly, Ding and coworkers did find a significant reduction in cholesterol and triglycerides levels in TLR4/low density lipid receptor receptor double knock out mice compared to low density lipid receptor single knock out mice². Moreover, reduced hypercholesterolemia did not affect intra-abdominal macrophage accumulation, hinting that systemic inflammation plays a less prominent role in this low density lipid receptor knock out atherosclerosis model. It appears that there is enough evidence

for the involvement of TLR4 in atherogenesis, although there is still much uncertainty about how TLR4 is activated in the setting of atherosclerosis or how TLR4 would exactly implement its atherogenic properties.

In **chapter three** we studied the role of TLR4 in the murine vulnerable plaque model and especially the effect on the fibrous cap. The cap of the atherosclerotic plaque consists of vascular smooth muscle cells and a proteoglycan-collagen network. Thinning of this cap in the setting of vulnerable plaque formation occurs due to a number of factors. For example, matrix metalloproteinases, released by inflammatory cells, weaken the proteoglycan-collagen network. Furthermore, local apoptosis of vascular smooth muscle cells (VSMCs) can occur due to pro-inflammatory cytokines produced by macrophages or mast cells. Eventually, this thinning of the cap can, in conjunction with expansion of the lipid-rich necrotic core, lead to rupture of the cap. As the highly thrombogenic content of the plaque comes in contact with circulating blood, a thrombus is formed leading to an acute coronary syndrome. There is accumulating evidence that mast cells are important mediators in determining plaque stability³⁻⁶. For example, activated mast cells are mainly located in the shoulder region of coronary plaques, which is the region with the highest chance of rupture⁷. Activated mast cells may contribute to vulnerable plaque formation by inducing VSMC apoptosis⁸. Leskinen and coworkers showed that mast cell induced VSMC apoptosis is regulated via chymase in a dose- and time-dependent manner⁸. However, the mechanism by which mast cells release chymase in atherosclerosis, thus inducing VSMC apoptosis and plaque destabilization, remains to be elucidated. Activation of TLR4 leads to activation of a downstream signalling pathway, facilitating nuclear translocation of NF κ B and subsequent transcription of pro-inflammatory cytokines, including IL-6⁹. Because it has been shown that IL-6 can upregulate chymase expression in human mast cells, TLR4 might be involved in chymase release in mast cells. Therefore, we investigated the role of TLR4 signalling in mast cells during mast cell induced VSMC apoptosis, in a validated murine model for the vulnerable plaque as well as in co-culture experiments. We were able to show that antagonizing or silencing TLR4 can prevent mast cell induced cap thinning and VSMC apoptosis *in vivo*. *In vitro* studies showed that TLR4 induced cell death was regulated via IL-6 and chymase in a TLR4 dependent manner. Our study was one of the first studies to show a role for TLR4 signalling in vulnerable plaque formation *in vivo*. Recently, Blich and coworkers showed another role for TLR4 in plaque progression¹⁰. They showed that macrophages, which are abundantly present in vulnerable plaques, were activated via TLR4 by heparanase and that heparanase staining was increased in vulnerable plaques compared to stable plaques.

THE RABBIT ATHEROSCLEROSIS MODEL

Different animal models for atherosclerosis and vulnerable plaque formation exist to date. The rabbit is widely used as it is relatively small and easy to handle. When rabbits are fed a high cholesterol diet, they become hyperlipidemic and develop fatty streaks¹¹⁻¹³. To create more advanced lesions, a number of additional interventions have been developed, including endothelial balloon denudation or cuff implantation. In **chapter four** we tried to develop a shear stress-induced vulnerable plaque model in the rabbit, based on the vulnerable plaque model in the ApoE^{-/-} mouse. We have previously shown that shear stress alteration by a flow altering device can induce atherosclerotic plaque development in ApoE^{-/-} mice. In low shear stress conditions in particular, NO-dependent atheroprotection is impaired due to decreased eNOS production^{14,15}, increased reactive oxygen species production, and down regulation of intracellular reactive oxygen species scavengers^{14,16}. In addition, low shear stress increases LDL accumulation and enhances endothelial cell permeability, facilitating trans-endothelial LDL migration and sub-endothelial LDL accumulation^{17,18} and promotes inflammation by increasing recruitment of inflammatory cells. Finally, nuclear translocation of NFκB and subsequent transcription of pro-inflammatory cytokines, due to low shear stress, promotes VSMC differentiation, proliferation and migration^{19,20} and a pro-inflammatory environment, promoting atherosclerotic plaque development. Indeed, in our murine model, we could create vulnerable plaque like-lesions upstream of the tapered cast, where low shear stress conditions prevail. Conversely, downstream of the cast, where oscillatory shear stress is induced, a more stable plaque developed. In conjunction with the murine model, we were able to create the same hemodynamic conditions with the tapered cast in the carotid position in our rabbit model. Furthermore, a high cholesterol diet indeed led to hyperlipidemia in the rabbits. To our knowledge, this is the first study to show that shear stress alteration in rabbit carotid arteries in combination with a high cholesterol diet, leads to atherosclerotic plaque formation. However, when we evaluated plaque phenotype, they seemed less vulnerable than in our murine model, even when we combined the tapered cast with endothelial damage by perivascular manipulation. We did find a high percentage of macrophages and lipids and some degree of neovascularization, but a distinct necrotic core was lacking. It remains speculative why we were unable to reproduce the findings from our murine model in the rabbits. It might be that lipoprotein profile of ApoE^{-/-} mice is more atherogenic than New Zealand white rabbits. It is known that ApoE deficiency causes a pro-inflammatory state in mice, leading to a pro-atherogenic environment. In this light, it would be interesting to see what the effect of the tapered cast would be in the Watanabe Heritable Hyperlipidemic (WHHL) rabbit. These rabbits are transgenic and have a mutation in the LDL receptor, leading to accumulation of LDL and VLDL in blood. We are currently performing these studies.

NEOVASCULARIZATION IN ATHEROSCLEROSIS AND VULNERABLE PLAQUE

The vulnerable plaque has a number of key features including a lipid-rich necrotic core, a thin cap with few vascular smooth muscle cells and the presence of inflammatory cells. More recently, neovascularization has also been identified as an important feature of a vulnerable plaque.

In a recently performed genome-wide screen, we identified Thrombospondin, type 1, domain containing 1 (Thsd-1) as a new potent angiogenic regulatory factor. During murine embryogenesis, we compared the RNA expression of Flk1 positive angioblasts with Flk1 negative cells. Thsd1 was specifically up-regulated in Flk1 positive angioblasts at day 10 and 11, which mark the timeframe of developmental angiogenesis. The Thsd-1 gene was first described by Takayanagi and coworkers in 2006²¹. They concluded that Thsd-1 was a novel marker for primitive haematopoietic stem cells and endothelial cells but a clear definition on any functional properties of Thsd-1 was lacking. In **chapter five** we were able to show from gain-and-loss of function studies, performed in a number of well-validated angiogenesis assays *in vitro* and *in vivo*, that Thsd-1 was vital for establishing endothelial barrier function during new vessel formation. Therefore, we hypothesized that Thsd-1 is involved in plaque destabilization by influencing the vascular integrity of intimal neovessels. We first investigated whether Thsd-1 is expressed in carotid endarterectomy specimens with a vulnerable plaque phenotype. Secondly, we elucidated the role of Thsd-1 *in vivo* in our well-validated murine vulnerable plaque model. Lastly, we studied the mechanism by which atherogenic factors could influence Thsd-1 expression in endothelial cells *in vitro*. These studies identify Thsd-1 as a vital factor in the formation and conservation of intimal neovessel stability, as it determines the integrity of the vascular endothelium in advanced atherosclerotic lesions. Loss of Thsd-1 function results in extensive intraplaque haemorrhaging and amplifies the inflamed state of the plaque lesion, ultimately resulting in further decline of vulnerable plaque stability.

Neovascularization in atherosclerosis is the result of intraplaque hypoxia and inflammation, leading to up-regulation of pro-angiogenic regulatory growth factors including VEGFA^{22, 23}. Newly formed vessels are phenotypically immature, defined by lack of vascular integrity and increased fragility to rupture. They are prone to extravasation of leucocytes and erythrocytes, which leads to intraplaque haemorrhaging. Accumulated red blood cells are phagocytosed by macrophages, which ultimately leads to expansion of the necrotic core at the expense of the fibrous cap and thus atherosclerotic lesion stability^{24, 25}. Pathological studies of human lesions have identified a remarkable correlation between intraplaque haemorrhaging and extensive necrotic core size with plaque rupture and clinical events²⁶⁻²⁸. These recent findings identify neovessels in advanced lesions as a potential mechanism of vulnerable plaque progression, and marks intimal neoangiogenesis as a potent target for pharmaceutical intervention to benefit treatment with the aim of stabilization of culprit lesion in patients^{29, 30}. The results from our *in vivo* data suggest that Thsd-1 might be a novel therapeutic option

to prevent vulnerable plaque formation by preventing vascular leakage from newly formed vessels. For example, one could use gene therapy or local delivery of the Thsd-1 protein.

THE GENOUS™ R STENT FOR TREATMENT OF CORONARY ARTERY DISEASE

We have previously conducted the HEALING II study in which we evaluated the efficacy of the Genous™ R stent in 63 patients with coronary artery disease. The Genous stent is an anti-human CD34 antibody coated stent to bind circulating CD34+ haematopoietic stem cells, thereby facilitating vascular repair. This accelerated endothelial healing would reduce the risk of stent thrombosis and shorten the required period of dual antiplatelet therapy. The HEALING II trial was the successor of the HEALING-FIM trial, where we evaluated the safety and feasibility of the Genous stent in sixteen patients with de novo coronary artery disease. This novel technique seemed safe with a major adverse cardiac and cerebrovascular events (MACCE) rate of 6.3% (one symptom-driven target revascularization in a single patient) and a late luminal loss of 0.63 ± 0.21 mm at six months angiographic follow-up (FU). Indeed, patients used only one month of dual antiplatelet therapy and there was no in stent thrombosis reported. In the HEALING II trial late luminal loss at six months FU was 0.78 ± 0.39 mm, while the MACCE rate at eighteen months FU was 7.9%. Again, no stent thrombosis was observed, despite only one month of dual antiplatelet therapy. Surprisingly, eighteen months angiographic FU showed a significant regression in late luminal loss to 0.59 ± 0.31 mm, a phenomenon which is in contrast with the drug eluting stents where generally an increase in late luminal loss is observed³¹. Furthermore, sub-analysis showed a positive correlation of circulating CD34+ endothelial progenitor cells (EPCs) and angiographic outcome, i.e. patients with low circulating EPCs had a relatively high late luminal loss and higher incidence of revascularizations at six months FU. More interestingly, patients with low levels of circulating EPCs did not receive HMG-CoA-reductase inhibitors (statins) therapy. As statins have been shown to increase circulating EPC levels³²⁻³⁴, we designed the HEALING IIB study in which we evaluated the efficacy of the Genous stent in conjunction with high dose statin (Atorvastatin 80 mg once daily) therapy. Patients were started on 80 mg atorvastatin once daily two weeks prior to the index procedure and continued for at least four weeks after the index procedure. Patients already on statin therapy were switched to 80 mg atorvastatin once daily.

In **chapter six** we report the results of the HEALING IIB study. The patient population of the HEALING IIB study was comparable with the HEALING II study. Statin therapy significantly increased circulating CD34+ EPC levels. Despite this increase in circulating EPC levels, late luminal loss at six months FU remained 0.76 ± 0.50 mm, comparable to the HEALING II trial. Major adverse cardiac events at six months FU seemed somewhat increased in the HEALING IIB trial compared to the HEALING II trial (9.4% at six months FU compared to 7.9% at nine months FU). This could be partially explained by study design, as the HEALING II trial

included only single vessel disease whereas the HEALING IIB trial also included multi-vessel disease. Likewise, we also found a significant reduction in late luminal loss at long term FU, from 0.76 ± 50 mm at six months to 0.67 ± 0.54 mm at eighteen months. This reduction in late luminal loss was accompanied by a low rate of major adverse cardiac events and target lesion revascularization between twelve and 24 months FU. Late luminal loss of the Genous stent are higher than most drug-eluting stents (DES) to date. However, late luminal loss seems to increase in DES over time, while we have consistently shown that late luminal loss in the Genous stent declines. Therefore, one could speculate whether DES and Genous stent would yield comparable results beyond 24 months FU. To address this question, randomized studies comparing DES and the Genous Stent, with clinical and angiographic FU beyond 24 months are required. Disappointingly, in the HEALING IIB trial there was a 3% incidence of stent thrombosis. In three patient stent thrombosis occurred at day 1, 9 and 181 post-procedure. However, all three events had documented significant procedural complications, which might have facilitated the in-stent thrombosis. The low stent thrombosis rate of 1.1% reported in the e-HEALING registry seems to confirm the favourable real world experience with the Genous Stent, even in the absence of prolonged dual anti-platelet therapy³⁵.

In **chapter seven** we performed a sub-analysis of the HEALING IIB trial to characterize the patients that had an increase in EPC levels upon statin treatment. Furthermore, we evaluated whether baseline EPC levels could predict angiographic and clinical FU. We divided the patients into a group that did not respond to Atorvastatin treatment with an increase in EPC levels, and a group that did respond to Atorvastatin treatment. Independent risk factors for being a non-responder were baseline EPC levels and having never smoked. In other words, non-responders had a higher baseline EPC level and had more often never smoked compared to responders. It is already known that endothelial dysfunction and different cardiovascular risk factors negatively influence the number of circulating EPCs. In this study we were also able to show that smoking was associated with a low baseline level of circulating EPCs. However, we were unable to show a correlation between other cardiovascular risk factors or risk factor for endothelial dysfunction, including diabetes, hypertension or hypercholesterolemia. Interestingly, non-responders had a higher baseline EPC count than responders, suggesting that non-responders were unable to recruit more EPCs from the bone marrow despite efficient treatment with Atorvastatin. Alternatively, non-responders might have an increase in EPCs, but may be more efficient in homing of the recruited EPCs to the affected vascular area, an intrinsic capacity that was further amplified by statin treatment^{36,37}. Therefore, no real increase in circulating EPCs may be found. Vice versa, for the responders, the data might imply that although recruitment of EPCs from bone marrow by statin treatment is successful, the recruited EPCs in the bloodstream remain inefficient in homing to the target stented vessel wall. The fact that precisely the non-responders had a more favourable late luminal loss at six months may hint that the latter mechanism indeed plays a role. This difference was even more pronounced at eighteen months FU. This observation seemed clinically

relevant as there was a trend towards a decrease in target lesion revascularizations in the non-responders group.

Consequently, in our study baseline EPC count was negatively correlated with late luminal loss at six and eighteen months FU for patients treated with the Genous stent and high dose Atorvastatin. These findings were in contrast with the findings from Pelliccia and co-workers who showed that higher levels of circulating EPCs correlated with a higher percentage of in-stent restenosis and late luminal loss³⁸, an observation that was still valid at five years FU³⁹. Although the original EPC was described as CD34+ or KDR+, no universal definition has been formulated for EPCs. Therefore, the most important difference between our work and the work of Pelliccia is the definition of the EPC. We defined EPCs as CD45+/CD34+/KDR+, whereas Pelliccia defined them as CD45-/CD34+/KDR+. Furthermore, we included a broader category of patients with coronary artery disease and we used a different type of stent. In conclusion we have shown that, higher baseline EPC count correlated with favourable angiographic outcome with less late luminal loss at six and eighteen months FU compared to lower baseline EPC count. Furthermore, EPCs might be used as predictor for angiographic outcome for patients treated with the GENOUS stent. However, the exact role of the level of circulating EPCs in the regenerative potency of the vascular bed needs to be determined.

Interestingly, although we have proven the safety and feasibility of the Genous stent in different clinical studies, it was never shown in humans that the Genous stent actually enhances capturing of CD34 positive EPCs. Therefore, in **chapter eight**, we performed a proof of principle study to show that the Genous stent indeed enhances EPC capturing. We showed in an *ex vivo* human arteriovenous shunt model that the Genous stent had a higher stent-strut coverage. Further evaluation of these cells by qPCR showed that the Genous stent had a higher percentage of endothelial cell coverage compared to the bare metal stent. This increased number in endothelial cells was accompanied by decreased thrombogenicity, not only macroscopic but also by qPCR analysis. These *ex vivo* human results were confirmed by subsequent studies in a baboon arteriovenous shunt model and a rabbit endothelial denudation model. Furthermore, we showed *in vitro* that the Genous stent indeed captures more CD34 positive cells, but not monocytes. Although we proved that the Genous stent indeed promotes re-endothelialization, this was not accompanied by less late luminal loss in the HEALING IIB trial, questioning the paradigm that early re-endothelialization is necessary to prevent neo-intima hyperplasia. The decreased thrombogenicity was also not observed in the HEALING IIB trial but we did find less in-stent thrombosis in the HEALING II trial and the e-HEALING registry. Furthermore, one must bear in mind that patients only used one month of dual antiplatelet therapy, making the GENOUS stent suitable for patients that have a (relative) contra-indication for dual antiplatelet therapy.

To combine the two benefits of drug eluting stents and CD34 antibody coated stents, the Combo stent (OrbusNeich Medical, Ft. Lauderdale, Florida) was developed. The Combo stent is a combined sirolimus-eluting CD34 antibody coated stent. Recently, the results of

the first-in-man randomized, controlled multicenter REMEDEE trial (Randomized study to Evaluate the safety and effectiveness of an abluMinal sirolimus coatED bio-Engineered StEnt) was published⁴⁰. The Combo stent was non-inferior to the paclitaxel eluting stent in terms of late luminal loss at nine months or the incidence of MACE at twelve months FU. Also, no stent thrombosis was observed. This reduction in late luminal loss compared to the Genous stent was at the expense of a longer duration of dual antiplatelet therapy compared to the Genous stent. It is interesting to see whether long term follow up also shows a reduction in late luminal loss and stabilization in clinical events, as we have shown with the Genous stent.

ADIPOSE TISSUE- DERIVED REGENERATIVE CELLS FOR THE TREATMENT OF ACUTE MYOCARDIAL INFARCTION

Skeletal myoblasts and bone marrow-derived mononuclear cells were the first regenerative cells used for treatment of ischemic heart disease. The results of the skeletal myoblasts were rather disappointing with an absence of improvement in regional or global left ventricular function in the MAGIC trial⁴¹ and only an improvement in six minute walking test in the SEISMIC and MARVEL study^{42, 43}. More concerning, skeletal myoblast injections were associated with ventricular tachyarrhythmia, making them unattractive for clinical use. More clinical experience has been gained with bone marrow-derived mononuclear cells. Recently, a number of meta analyses were published that evaluated the effect of intracoronary delivery of bone marrow derived mononuclear cells for the treatment of acute myocardial infarction⁴⁴⁻⁴⁶. Although the papers differed somewhat in the number of randomized controlled trials that were included, they all reported a modest beneficial effect on left ventricular ejection fraction ranging from 2.6% to 4.0%. However, the main disadvantage of bone marrow-derived mononuclear cell therapy is the heterogeneity of the infused cell population. Furthermore, if one would transplant solely the mesenchymal stem cell fraction, subculturing is mandatory to select and expand a sufficient number of stem cells. In this light, adipose tissue-derived regenerative cells (ADRCs) are very interesting as they can be easily harvested in large amounts from adult patients by lipoaspiration. Furthermore, ADRCs have been shown to have the same properties as the bone marrow derived mesenchymal stem cell⁴⁷. We therefore performed a randomized, double-blind, placebo-controlled phase I/IIa trial to evaluate the safety and efficacy of ADRCs for the treatment of ST segment elevation myocardial infarction. ADRCs were harvested and processed from a lipoaspirate from patients admitted for an acute myocardial infarction. As more than 20 million cells could be harvested from as little as 200 gram of lipoaspirate, intracoronary infusion of ADRCs could be performed within hours after the primary percutaneous coronary intervention. A total of 14 patients were included, of whom ten were treated with ADRCs and four with placebo. We were able to show that intracoronary infusion of ADRCs is safe and feasible for the treatment of ST segment eleva-

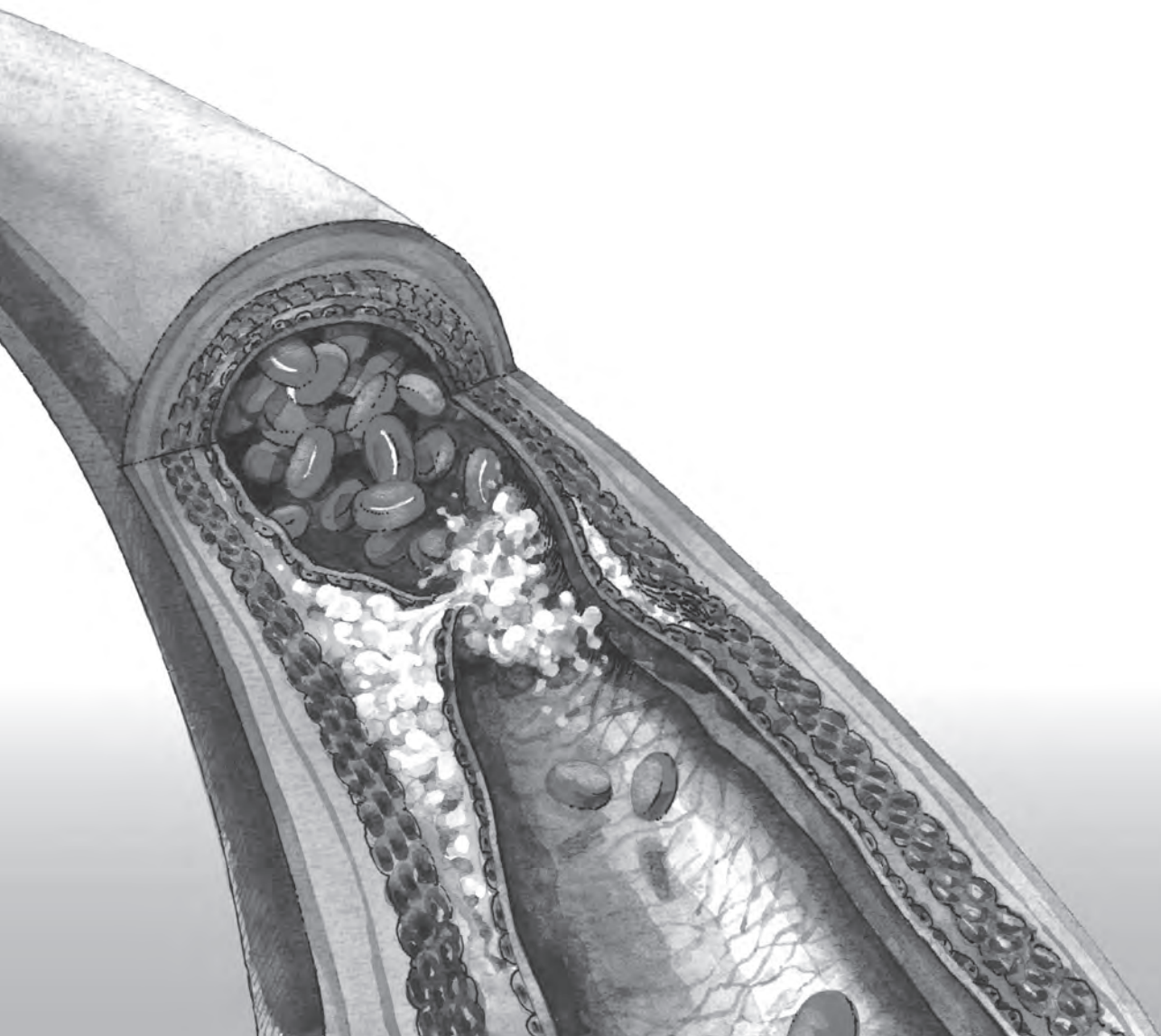
tion myocardial infarction. There was a trend towards improvement in global left ventricular ejection fraction, measured by transthoracic echocardiography, MIBI-SPECT or cardiac MRI. Furthermore, there was a significant improvement of the perfusion defect and a fifty percent reduction in left ventricular infarction. Larger randomized controlled trials are warranted to further evaluate and expand the results from the APOLLO trial. The ADVANCE trial has been initiated as a multicenter, prospective, randomized, placebo-controlled phase IIb/III trial to evaluate the use of up to two doses of ADRCs in the treatment of ST segment elevated myocardial infarction.

GENERAL CONCLUSION

In conclusion, we have shown in the first part of this thesis the importance of a) TLR4 signaling in mast cells in the prevention of VSMC apoptosis and b) neovessel stabilization in the prevention of intraplaque haemorrhage in the pathogenesis of vulnerable plaque formation. Both VSMC apoptosis and intraplaque haemorrhage are associated with plaque destabilization and progression towards a vulnerable plaque. Our findings contribute to a better understanding of the pathophysiology of the vulnerable plaque in order to prevent vulnerable plaque formation and reduce the risk of plaque rupture and the occurrence of an acute coronary syndrome. Indeed, research in atherosclerotic disease shifts more and more towards prevention, diagnosing, and treatment of the vulnerable plaque in order to adequately prevent a clinical event. The immune system likewise plays an essential role as it seems involved in nearly all processes involved in vulnerable plaque formation. For example, use of the immune system as biomarker or modulation of the immune system by gene therapy or vaccination are currently investigated and might be available in the near future.

In the second part of this thesis, we evaluated some novel therapies for the treatment of coronary artery disease. The Genous stent seems safe and feasible, but not as effective as the newest generation of drug eluting stents, although head to head comparisons are lacking. It would be especially interesting to see whether the Genous stent can compete with drug eluting stents in long term FU. For now, the use of a bioabsorbable anti-CD34 antibody coated stents is currently investigated in preclinical studies and already a combined sirolimus-eluting and anti-CD34 antibody coated stent is evaluated in clinical studies. It would be interesting to assess whether it is possible to combine the Genous stent with a compound that specifically inhibits VSMC proliferation. In the APOLLO trial, we showed for the first time that ADRCs are safe and feasible for the treatment of ST segment elevated acute myocardial infarction. Larger randomized controlled trials are needed to evaluate the efficacy of the ADRCs in this setting.

Chapter 11 Nederlandse samenvatting



NEDERLANDSE SAMENVATTING

Hart- en vaatziekten blijven een belangrijke doodsoorzaak in de Westerse wereld ondanks continue ontwikkelingen in diagnostische mogelijkheden en behandeling. Atherosclerose of aderverkalking speelt hierbij een zeer belangrijke rol. Atherosclerose ontstaat doordat de binnenste laag van een bloedvat, het endotheel, niet meer goed functioneert. Hierdoor kunnen low density lipoproteïne (LDL) partikels het sub-endotheel in migreren. In het sub-endotheel oxideert het LDL tot geoxideerd LDL. Naast LDL kunnen ook monocyt en lymfocyt en aan het disfunctionerende endotheel binden en door het endotheel migreren. De monocyt en differentiëren tot macrofagen en nemen het geoxideerde LDL op zodat er schuimcellen gevormd worden. Er heeft zich nu een zogenaamde fatty streak gevormd, de vroegste vorm van atherosclerose. De fatty streak kan uitgroeien tot een stabiele of instabiele plaque. Stabiele plaques hebben een dikke kap waardoor ze niet ruptureren. Deze plaques zijn meestal klinisch symptomeloos of leiden tot stabiele angina pectoris. De instabiele plaque echter heeft een dunne kap die weinig gladde spiercellen bevat, een grote lipiden rijke necrotische kern en veel ontstekingscellen. Vanwege de dunne kap kan deze plaque makkelijk ruptureren. Als de plaque ruptureert komt de trombogene inhoud in contact met het bloed waardoor een trombus gevormd kan worden. Deze trombus kan een coronair arterie geheel of gedeeltelijk afsluiten en zo een acuut coronair syndroom veroorzaken. Voor de ontwikkeling van nieuwe behandelmethodes is het zeer belangrijk om de pathofysiologie van atherosclerose en de vorming van een instabiele plaque zo goed mogelijk te begrijpen. Dit proefschrift is verdeeld in twee gedeeltes. Het eerste gedeelte omvat de pre-klinische en basaal wetenschappelijke studies en onderzoekt in het bijzonder de pathofysiologie van atherosclerose. Het tweede gedeelte bevat voornamelijk klinische studies en bespreekt de resultaten van nieuwe behandelingen voor coronairlijden.

Het immuunsysteem speelt een zeer belangrijke rol in het ontstaan en de vooruitgang van atherosclerose. Het immuunsysteem bestaat uit een aangeboren gedeelte en een adaptief gedeelte. Toll like receptor 4 (TLR4) is een belangrijk onderdeel van het aangeboren immuun systeem. In **hoofdstuk twee** geven we een overzicht van de rol van TLR4 in het ontstaan van atherosclerose en progressie tot instabiele plaque. TLR4 blijkt op veel celtypen voor te komen die een rol spelen bij atherosclerose en lijkt dan ook zeker betrokken bij de vorming van atherosclerose. Het precieze mechanisme van activatie en werking blijft echter tot nog toe onduidelijk. In **hoofdstuk drie** hebben we naar een specifieke rol van TLR4 gekeken in een muizenmodel met een instabiele plaque. Als we *in vivo* TLR4 signalering blokkeren op mestcellen worden er stabielere plaques met een dikkere kap gevormd. De kap bestaat voornamelijk uit gladde spiercellen en collageen, en blokkering van TLR4 signalering in mestcellen voorkomt gladde spiercel apoptose en leidt zo tot een stevigere kap. Verdere *in*

vitro studies hebben aangetoond dat deze blokkering van gladde spiercel apoptose werkt via IL-6 en chymase.

Een belangrijke manier om atherosclerose te onderzoeken is met proefdiermodellen. Er bestaat een grote verscheidenheid aan proefdiermodellen voor atherosclerose, elk met zijn eigen voor- en nadelen. Binnen onze afdeling hebben we een gevalideerd muizenmodel om atherosclerose en met name vorming van de instabiele plaque te bestuderen. Dit model is gebaseerd op shear stress, welke gecreëerd wordt door gebruik te maken van een cylinder, waarvan de binnenkant taps toeloopt (een zogenaamde cast). Wanneer deze cast om de rechter carotis arterie wordt geplaatst ontstaat er oscillatoire shear stress stroomopwaarts van de cast, terwijl een lage shear stress stroomafwaarts van de cast ontstaat. Als gevolg hiervan ontwikkelt zich stroomopwaarts een instabiele plaque, terwijl stroomafwaarts een stabiele plaque wordt gevormd. Het nadeel van dit model is de grootte van het proefdier wat het moeilijk maakt om het bijvoorbeeld te gebruiken voor de ontwikkeling van nieuwe intravasculaire behandelmethodes. We hebben daarom in **hoofdstuk vier** dit model toegepast op het konijn. Konijnen kregen een cholesterolrijk dieet en de cast werd vergroot zodat hij om de carotis arterie van het konijn past. We waren in staat om bij het konijn hyperlipidemie te veroorzaken met het hoog cholesterol dieet. Daarnaast konden we met de cast dezelfde hemodynamische veranderingen als in de muis creëren. Net zoals bij de muis ontstonden zowel stroomopwaarts als stroomafwaarts plaques, echter deze waren veel stabielier dan bij de muis. Stroomopwaarts bevatten de plaques wel veel macrofagen en wat vaatnieuwvorming, maar een necrotische kern ontbrak. Het is niet geheel duidelijk waarom we tot op heden in het konijn geen instabiele plaque kunnen creëren. Mogelijk dat de genetische achtergrond van de muis hierin een rol speelt.

In **hoofdstuk vijf** hebben we een ander aspect van instabiele plaque vorming onderzocht, namelijk vaatnieuwvorming. Het blijkt dat dit een belangrijke rol speelt in het ontstaan van een instabiele plaque, omdat de nieuw gevormde vaten niet goed aangelegd worden en permeabel zijn voor bijvoorbeeld rode en witte bloedcellen. Hierdoor kunnen zich makkelijk bloedingen in de plaque voordoen en wordt de necrotische kern steeds groter. Dit blijkt klinisch ook relevant aangezien er een relatie is aangetoond tussen intraplaque bloedingen en plaque ruptuur en klinische events. In dit hoofdstuk hebben we aangetoond dat Thsd-1, wat we eerder in een genoom wijde screening als mogelijk agiogenetische factor hebben ontdekt, een belangrijke rol speelt in het behouden van integriteit van het bloedvat en het voorkomen van extravasatie van rode en witte bloedcellen. Thsd-1 zou in de toekomst een nieuwe therapeutische optie kunnen zijn om instabiele plaque vorming te voorkomen door vasculaire lekkage van nieuw gevormde vaten te verhinderen.

Patiënten met coronair lijden kunnen medicamenteus behandeld worden of percutaan of chirurgisch gerevasculariseerd worden. In de afgelopen jaren is er een enorme ontwikkeling geweest in percutane behandelopties, van ballon angioplastie tot bare metal stents en van drug eluting stents tot bio-absorbeerbare stents. In hoofdstuk zes tot en met

acht worden de resultaten beschreven van een nieuwe stent, de Genous™ R stent. Deze stent is gecoat met anti-humane CD34 antilichamen zodat CD34+ endotheel voorloper cellen aan de stent kunnen binden. De gedachte is dat deze endotheel voorloper cellen uitgroeien tot nieuwe endotheelcellen zodat het vasculaire herstel na stentplaatsing wordt versneld. Dit vermindert het risico op stent trombose en verkort de duur van duale antiplaatjes therapie. Het is gebleken dat statines het aantal CD34+ endotheel voorloper cellen verhoogt. In **hoofdstuk zes** beschrijven we de resultaten van de HEALING IIB studie waarin we de effectiviteit van de Genous stent in combinatie met hoge dosering Atorvastatine hebben bekeken. Hoge dosering Atorvastatine leidt niet tot verbeterde effectiviteit van de Genous stent, ondanks toename van de CD34+ endotheel voorloper cellen. Wel zien we dat de Genous stent in de loop van de tijd een afname van intima hyperplasie laat zien, iets wat we bij de drug eluting stent niet zien. Mogelijk dat langere follow up nodig is om aan te tonen dat de Genous stent uiteindelijk net zo effectief is als de drug eluting stent.

In **hoofdstuk zeven** hebben we een sub-analyse van de HEALING IIB studie verricht waarin we gekeken hebben of we kunnen voorspellen welke patiënt inderdaad een verhoging van endotheel voorloper cellen kreeg bij statine behandeling en of dit correleerde met angiografische en klinische follow up. Patiënten waarbij statine behandeling leidde tot verhoging van endotheel voorloper cellen hadden een lagere baseline waarde van endotheel voorloper cellen dan patiënten zonder verhoging. Ondanks toename in endotheel voorloper cellen bleek dat de angiografische en klinische follow up in deze patiënten slechter was dan in patiënten zonder toename in endotheel voorloper cellen. Anderzijds kan men stellen dat patiënten met een lage baseline waarde van endotheel voorloper cellen een slechte angiografische en klinische follow up hadden vergeleken met patiënten met een hogere baseline waarde. Mogelijk dat deze endotheel voorloper cellen zouden kunnen dienen als voorspeller voor de effectiviteit van de Genous stent.

Als laatste hebben we in **hoofdstuk acht** een proof-of-principle studie gedaan om aan te tonen dat de Genous stent inderdaad CD34+ endotheel voorloper cellen bindt en dat dit leidt tot lagere trombogeniciteit. Inderdaad is de Genous stent meer bedekt met endotheelcellen dan de bare metal stent, wat ook geassocieerd was met minder trombogeniciteit. Ondanks dat we hebben aangetoond dat gebruik van de Genous stent leidt tot snellere re-endothelialisatie in vergelijking met de bare metal stent, was dit in de HEALING IIB niet geassocieerd met betere angiografische of klinische follow up. Ook hebben we niet aan kunnen tonen dat dit leidt tot minder stent trombose.

In **hoofdstuk negen** beschrijven we de resultaten van de APOLLO studie, waarin we de eerste resultaten van de veiligheid en effectiviteit van uit vetcellen verkregen regeneratieve cellen voor behandeling van een acuut myocard infarct beschrijven. We hebben aangetoond dat het veilig is om deze regeneratieve cellen uit vet te verkrijgen door middel van liposuctie ondanks het gebruik van antistolling en antiplaatjes therapie bij deze patiënten. Verder is het veilig om deze cellen intracoronair te injecteren na een acuut myocard infarct. Ondanks

de kleine aantallen leek er een vermindering van infarctgrootte te zijn en een verbetering in linker ventrikel functie.

Samengevat toont dit proefschrift in het eerste gedeelte het belang van a) TLR4 signalering in het voorkomen van gladde spiercel apoptose en b) stabilisatie van nieuw gevormde vaten in het voorkomen van intraplaque bloedingen in de pathogenese van instabiele plaque vorming. Zowel gladde spiercel apoptose als intraplaque bloedingen zijn geassocieerd met plaque destabilisatie en progressie tot instabiele plaque. Onze resultaten dragen bij tot een beter begrip van de pathofysiologie van de instabiele plaque zodat we beter de vorming van een instabiele plaque kunnen voorkomen en het risico op plaque ruptuur en het optreden van een acuut coronair syndroom kunnen reduceren. Onderzoek in atherosclerose richt zich ook meer en meer op het voorkomen, opsporen en behandelen van de instabiele plaque, om een klinisch event te voorkomen. Het immuunsysteem speelt een essentiële rol omdat het betrokken is bij bijna alle processen van instabiele plaque vorming. Bijvoorbeeld, het gebruik van het immuunsysteem als biomarker of modulatie van het immuunsysteem door genterapie wordt op dit moment onderzocht en is wellicht in de toekomst bruikbaar .

In het tweede gedeelte van dit proefschrift hebben we nieuwe behandelingen voor coronairlijden onderzocht. De Genous stent lijkt veilig en toepasbaar, maar niet zo effectief als de nieuwste drug eluting stents alhoewel direct vergelijkende studies ontbreken. Het zou met name interessant zijn om te bestuderen of de Genous stent vergelijkbaar effectief is als de drug eluting stent op de langere termijn. Op dit moment wordt een bio-absorbeerbare anti-CD34 antilichaam gecoate stent onderzocht in pre-klinische studies en een gecombineerde sirolimus eluting en anti-CD34 gecoate stent is al onderzocht in klinische studies. Het zou interessant zijn om te zien of de Genous stent gecombineerd kan worden met een stof die specifiek de gladde spiercel proliferatie remt. In de APOLLO studie hebben we voor het eerst aangetoond dat het gebruik van uit vetcel verkregen regeneratieve cellen veilig en toepasbaar is voor de behandeling na een acuut myocardinfarct. Grotere studies zijn nodig om de effectiviteit te beoordelen.

REFERENCES

1. Michelsen KS, Wong MH, Shah PK, Zhang W, Yano J, Doherty TM, Akira S, Rajavashisth TB, Arditi M. Lack of Toll-like receptor 4 or myeloid differentiation factor 88 reduces atherosclerosis and alters plaque phenotype in mice deficient in apolipoprotein E. *Proc Natl Acad Sci U S A*. 2004;101:10679-10684.
2. Ding Y, Subramanian S, Montes VN, Goodspeed L, Wang S, Han C, Teresa AS, 3rd, Kim J, O'Brien KD, Chait A. Toll-like receptor 4 deficiency decreases atherosclerosis but does not protect against inflammation in obese low-density lipoprotein receptor-deficient mice. *Arterioscler Thromb Vasc Biol*. 2012;32:1596-1604.
3. Lindstedt KA, Kovanen PT. Mast cells in vulnerable coronary plaques: potential mechanisms linking mast cell activation to plaque erosion and rupture. *Curr Opin Lipidol*. 2004;15:567-573.
4. Lindstedt KA, Mayranpaa MI, Kovanen PT. Mast cells in vulnerable atherosclerotic plaques—a view to a kill. *J Cell Mol Med*. 2007;11:739-758.
5. Bot I, de Jager SC, Zerneck A, Lindstedt KA, van Berkel TJ, Weber C, Biessen EA. Perivascular mast cells promote atherogenesis and induce plaque destabilization in apolipoprotein E-deficient mice. *Circulation*. 2007;115:2516-2525.
6. Sun J, Sukhova GK, Wolters PJ, Yang M, Kitamoto S, Libby P, MacFarlane LA, Mallen-St Clair J, Shi GP. Mast cells promote atherosclerosis by releasing proinflammatory cytokines. *Nat Med*. 2007;13:719-724.
7. Kaartinen M, Penttila A, Kovanen PT. Accumulation of activated mast cells in the shoulder region of human coronary atheroma, the predilection site of atheromatous rupture. *Circulation*. 1994;90:1669-1678.
8. Leskinen M, Wang Y, Leszczynski D, Lindstedt KA, Kovanen PT. Mast cell chymase induces apoptosis of vascular smooth muscle cells. *Arteriosclerosis, thrombosis, and vascular biology*. 2001;21:516-522.
9. Palsson-McDermott EM, O'Neill LA. Signal transduction by the lipopolysaccharide receptor, Toll-like receptor-4. *Immunology*. 2004;113:153-162.
10. Blich M, Golan A, Arvatz G, Sebbag A, Shafat I, Sabo E, Cohen-Kaplan V, Petcherski S, Avniel-Polak S, Eitan A, Hammerman H, Aronson D, Axelman E, Ilan N, Nussbaum G, Vlodavsky I. Macrophage activation by heparanase is mediated by TLR-2 and TLR-4 and associates with plaque progression. *Arterioscler Thromb Vasc Biol*. 2013;33:e56-65.
11. Bocan TM, Mueller SB, Mazur MJ, Uhlendorf PD, Brown EQ, Kieft KA. The relationship between the degree of dietary-induced hypercholesterolemia in the rabbit and atherosclerotic lesion formation. *Atherosclerosis*. 1993;102:9-22.
12. Clarkson S, Newburgh LH. The Relation between Atherosclerosis and Ingested Cholesterol in the Rabbit. *J Exp Med*. 1926;43:595-612.
13. Kolodgie FD, Katocs AS, Jr., Largis EE, Wrenn SM, Cornhill JF, Herderick EE, Lee SJ, Virmani R. Hypercholesterolemia in the rabbit induced by feeding graded amounts of low-level cholesterol. Methodological considerations regarding individual variability in response to dietary cholesterol and development of lesion type. *Arterioscler Thromb Vasc Biol*. 1996;16:1454-1464.

14. Cheng C, de Crom R, van Haperen R, Helderma F, Mousavi Gourabi B, van Damme LC, Kirschbaum SW, Slager CJ, van der Steen AF, Krams R. The role of shear stress in atherosclerosis: action through gene expression and inflammation? *Cell Biochem Biophys*. 2004;41:279-294.
15. Cheng C, van Haperen R, de Waard M, van Damme LC, Tempel D, Hanemaaijer L, van Cappellen GW, Bos J, Slager CJ, Duncker DJ, van der Steen AF, de Crom R, Krams R. Shear stress affects the intracellular distribution of eNOS: direct demonstration by a novel in vivo technique. *Blood*. 2005;106:3691-3698.
16. Inoue N, Ramasamy S, Fukai T, Nerem RM, Harrison DG. Shear stress modulates expression of Cu/Zn superoxide dismutase in human aortic endothelial cells. *Circ Res*. 1996;79:32-37.
17. Deng X, Marois Y, How T, Merhi Y, King M, Guidoin R, Karino T. Luminal surface concentration of lipoprotein (LDL) and its effect on the wall uptake of cholesterol by canine carotid arteries. *J Vasc Surg*. 1995;21:135-145.
18. Soulis JV, Fytanidis DK, Papaioannou VC, Giannoglou GD. Wall shear stress on LDL accumulation in human RCAs. *Med Eng Phys*. 2010;32:867-877.
19. Cunningham KS, Gotlieb AI. The role of shear stress in the pathogenesis of atherosclerosis. *Lab Invest*. 2005;85:9-23.
20. Passerini AG, Polacek DC, Shi C, Francesco NM, Manduchi E, Grant GR, Pritchard WF, Powell S, Chang GY, Stoeckert CJ, Jr, Davies PF. Coexisting proinflammatory and antioxidative endothelial transcription profiles in a disturbed flow region of the adult porcine aorta. *Proc Natl Acad Sci U S A*. 2004;101:2482-2487.
21. Takayanagi S, Hiroshima T, Yamazaki S, Nakajima T, Morita Y, Usui J, Eto K, Motohashi T, Shiomi K, Keino-Masu K, Masu M, Oike Y, Mori S, Yoshida N, Iwama A, Nakauchi H. Genetic marking of hematopoietic stem and endothelial cells: identification of the Tmtsp gene encoding a novel cell surface protein with the thrombospondin-1 domain. *Blood*. 2006;107:4317-4325.
22. Moreno PR, Purushothaman KR, Sirol M, Levy AP, Fuster V. Neovascularization in human atherosclerosis. *Circulation*. 2006;113:2245-2252.
23. Sluimer JC, Daemen MJ. Novel concepts in atherogenesis: angiogenesis and hypoxia in atherosclerosis. *J Pathol*. 2009;218:7-29.
24. Kolodgie FD, Gold HK, Burke AP, Fowler DR, Kruth HS, Weber DK, Farb A, Guerrero LJ, Hayase M, Kutys R, Narula J, Finn AV, Virmani R. Intraplaque hemorrhage and progression of coronary atheroma. *N Engl J Med*. 2003;349:2316-2325.
25. Virmani R, Kolodgie FD, Burke AP, Finn AV, Gold HK, Tulenko TN, Wrenn SP, Narula J. Atherosclerotic plaque progression and vulnerability to rupture: angiogenesis as a source of intraplaque hemorrhage. *Arterioscler Thromb Vasc Biol*. 2005;25:2054-2061.
26. Altaf N, MacSweeney ST, Gladman J, Auer DP. Carotid intraplaque hemorrhage predicts recurrent symptoms in patients with high-grade carotid stenosis. *Stroke*. 2007;38:1633-1635.
27. Hellings WE, Peeters W, Moll FL, Piers SR, van Setten J, Van der Spek PJ, de Vries JP, Seldenrijk KA, De Bruin PC, Vink A, Velema E, de Kleijn DP, Pasterkamp G. Composition of carotid atherosclerotic plaque is associated with cardiovascular outcome: a prognostic study. *Circulation*. 2010;121:1941-1950.
28. Koole D, Heyligers J, Moll FL, Pasterkamp G. Intraplaque neovascularization and hemorrhage: markers for cardiovascular risk stratification and therapeutic monitoring. *J Cardiovasc Med (Hagerstown)*. 2012;13:635-639.

29. Doyle B, Caplice N. Plaque neovascularization and antiangiogenic therapy for atherosclerosis. *J Am Coll Cardiol.* 2007;49:2073-2080.
30. Jain RK, Finn AV, Kolodgie FD, Gold HK, Virmani R. Antiangiogenic therapy for normalization of atherosclerotic plaque vasculature: a potential strategy for plaque stabilization. *Nat Clin Pract Cardiovasc Med.* 2007;4:491-502.
31. Aoki J, Abizaid AC, Serruys PW, Ong AT, Boersma E, Sousa JE, Bruining N. Evaluation of four-year coronary artery response after sirolimus-eluting stent implantation using serial quantitative intravascular ultrasound and computer-assisted grayscale value analysis for plaque composition in event-free patients. *J Am Coll Cardiol.* 2005;46:1670-1676.
32. Dimmeler S, Aicher A, Vasa M, Mildner-Rihm C, Adler K, Tiemann M, Rutten H, Fichtlscherer S, Martin H, Zeiher AM. HMG-CoA reductase inhibitors (statins) increase endothelial progenitor cells via the PI 3-kinase/Akt pathway. *J Clin Invest.* 2001;108:391-397.
33. Llevadot J, Murasawa S, Kureishi Y, Uchida S, Masuda H, Kawamoto A, Walsh K, Isner JM, Asahara T. HMG-CoA reductase inhibitor mobilizes bone marrow—derived endothelial progenitor cells. *J Clin Invest.* 2001;108:399-405.
34. Vasa M, Fichtlscherer S, Adler K, Aicher A, Martin H, Zeiher AM, Dimmeler S. Increase in circulating endothelial progenitor cells by statin therapy in patients with stable coronary artery disease. *Circulation.* 2001;103:2885-2890.
35. Silber S, Damman P, Klomp M, Beijk MA, Grisold M, Ribeiro EE, Suryapranata H, Wojcik J, Hian Sim K, Tijssen JG, de Winter RJ. Clinical results after coronary stenting with the Genous Bio-engineered R stent: 12-month outcomes of the e-HEALING (Healthy Endothelial Accelerated Lining Inhibits Neointimal Growth) worldwide registry. *EuroIntervention.* 2011;6:819-825.
36. Asahara T, Masuda H, Takahashi T, Kalka C, Pastore C, Silver M, Kearne M, Magner M, Isner JM. Bone marrow origin of endothelial progenitor cells responsible for postnatal vasculogenesis in physiological and pathological neovascularization. *Circ Res.* 1999;85:221-228.
37. Landmesser U, Engberding N, Bahlmann FH, Schaefer A, Wiencke A, Heineke A, Spiekermann S, Hilfiker-Kleiner D, Templin C, Kotlarz D, Mueller M, Fuchs M, Hornig B, Haller H, Drexler H. Statin-induced improvement of endothelial progenitor cell mobilization, myocardial neovascularization, left ventricular function, and survival after experimental myocardial infarction requires endothelial nitric oxide synthase. *Circulation.* 2004;110:1933-1939.
38. Pelliccia F, Cianfrocca C, Rosano G, Mercurio G, Speciale G, Pasceri V. Role of endothelial progenitor cells in restenosis and progression of coronary atherosclerosis after percutaneous coronary intervention: a prospective study. *JACC Cardiovasc Interv.* 2010;3:78-86.
39. Pelliccia F, Pasceri V, Rosano G, Pristipino C, Roncella A, Speciale G, Pannarale G, Schiariti M, Greco C, Gaudio C. Endothelial progenitor cells predict long-term prognosis in patients with stable angina treated with percutaneous coronary intervention: five-year follow-up of the PROCREATION study. *Circ J.* 2013;77:1728-1735.
40. Haude M, Lee SW, Worthley SG, Silber S, Verheye S, Erbs S, Rosli MA, Botelho R, Meredith I, Sim KH, Stella PR, Tan HC, Whitbourn R, Thambar S, Abizaid A, Koh TH, Den Heijer P, Parise H, Cristea E, Maehara A, Mehran R. The REMEDEE trial: a randomized comparison of a combination sirolimus-eluting endothelial progenitor cell capture stent with a paclitaxel-eluting stent. *JACC Cardiovasc Interv.* 2013;6:334-343.

41. Menasche P, Alfieri O, Janssens S, McKenna W, Reichenspurner H, Trinquart L, Vilquin JT, Marolleau JP, Seymour B, Larghero J, Lake S, Chatellier G, Solomon S, Desnos M, Hagege AA. The Myoblast Autologous Grafting in Ischemic Cardiomyopathy (MAGIC) trial: first randomized placebo-controlled study of myoblast transplantation. *Circulation*. 2008;117:1189-1200.
42. Duckers HJ, Houtgraaf J, Hehrlein C, Schofer J, Waltenberger J, Gershlick A, Bartunek J, Nienaber C, Macaya C, Peters N, Smits P, Siminiak T, van Mieghem W, Legrand V, Serruys PW. Final results of a phase IIa, randomised, open-label trial to evaluate the percutaneous intramyocardial transplantation of autologous skeletal myoblasts in congestive heart failure patients: the SEISMIC trial. *EuroIntervention*. 2011;6:805-812.
43. Povsic TJ, O'Connor CM, Henry T, Taussig A, Kereiakes DJ, Fortuin FD, Niederman A, Schatz R, Spencer Rt, Owens D, Banks M, Joseph D, Roberts R, Alexander JH, Sherman W. A double-blind, randomized, controlled, multicenter study to assess the safety and cardiovascular effects of skeletal myoblast implantation by catheter delivery in patients with chronic heart failure after myocardial infarction. *Am Heart J*. 2011;162:654-662 e651.
44. Delewi R, Hirsch A, Tijssen JG, Schachinger V, Wojakowski W, Roncalli J, Aakhus S, Erbs S, Assmus B, Tendera M, Goekmen Turan R, Corti R, Henry T, Lemarchand P, Lunde K, Cao F, Huikuri HV, Surder D, Simari RD, Janssens S, Wollert KC, Plewka M, Grajek S, Traverse JH, Zijlstra F, Piek JJ. Impact of intracoronary bone marrow cell therapy on left ventricular function in the setting of ST-segment elevation myocardial infarction: a collaborative meta-analysis. *Eur Heart J*. 2013.
45. Jeevanantham V, Butler M, Saad A, Abdel-Latif A, Zuba-Surma EK, Dawn B. Adult bone marrow cell therapy improves survival and induces long-term improvement in cardiac parameters: a systematic review and meta-analysis. *Circulation*. 2012;126:551-568.
46. Zimmet H, Porapakkhram P, Porapakkhram P, Sata Y, Haas SJ, Itescu S, Forbes A, Krum H. Short- and long-term outcomes of intracoronary and endogenously mobilized bone marrow stem cells in the treatment of ST-segment elevation myocardial infarction: a meta-analysis of randomized control trials. *Eur J Heart Fail*. 2012;14:91-105.
47. Gimble JM, Katz AJ, Bunnell BA. Adipose-derived stem cells for regenerative medicine. *Circ Res*. 2007;100:1249-1260.

PHD PORTFOLIO SUMMARY

Summary of PhD training and teaching activities



Name PhD student: Wijnand den Dekker
Erasmus MC Department: Experimental Cardiology
Research School: COEUR

PhD period: 2008-2014
Promotor: Professor dr. F.J. Zijlstra
Supervisors: dr. H.J. Duckers and dr. C. Cheng

1. PhD training

	Year	Workload (Hours/ECTS)
General academic skills		
- Biomedical English Writing and Communication	2010	3
- Research Integrity	2010	1
- Laboratory animal science	1999	3
Courses		
- Basic science summer school ESC	2009	2
- Vascular Biology NHS	2009	2
- Molecular Biology in atherosclerosis and cardiovascular research	2009	1,5
- Cardiovascular imaging and diagnostics	2008	1,5
- Heart failure research	2008	1,5
- Vascular medicine	2007	1,5
- Course in radiation, level 4	2000	2
International conferences		
- ESC congress	2012, 2011	4
- AHA congress	2011, 2010, 2009	6
- Vulnerable plaque meeting	2010	1
- Keystone meeting atherosclerosis	2010	2
- Dutch German cardiology meeting	2010, 2009	2
- Cardiology & Vascular medicine	2009, 2008	2
Seminars and workshops		
- COEUR research seminars	2008-2014	4,8

2. Teaching activities

	Year	Workload (Hours/ECTS)
Supervising bachelor theses		
- Higher laboratory education (3x)	2011, 2010, 2009	6
- Middle laboratory education (2X)	2011, 2010	4

AWARDS

Presentation award Dutch Atherosclerosis Society (DAS) 2009, best oral presentation:
"Evaluation of auto-antibody patterns in cardiovascular disease; implications for diagnosis."

ORAL PRESENTATIONS

Wijnand K. den Dekker *Efficiency of statin treatment on EPC recruitment depends on baseline EPC titer, and does not improve angiographic outcome in coronary artery disease patients treated with the Genous™ stent* **European Society of Cardiology congress 2012**

Wijnand K. den Dekker *Auto-antibodies as novel biomarker for acute myocardial infarction* **COEUR Research Seminar 21-09-2012**

Wijnand K. den Dekker, Caroline Cheng, Dennie Tempel, Leo AB Joosten, Mihai Netea, Jos van der Meer, Henricus J Duckers *Mast Cells Induce Vascular Smooth Muscle Cell Apoptosis via a Toll Like Receptor 4 Pathway* **COEUR Research Seminar 29-10-2011**

Wijnand K. den Dekker, Jaco H Houtgraaf, Yoshinobu Onuma, Robbert J de Winter, Stephen M Rowland, Erik Ligtenberg, Pieter den Heijer, Benno J Rensing, Patrick W Serruys, Henricus J Duckers *Final Results of the HEALING IIB Trial to Evaluate a Bioengineered CD34 Antibody Coated Stent (Genous™ Stent) Designed to Promote Vascular Healing by Capture of Circulating Endothelial Progenitor Cells in CAD Patients* **NVVC Najaarscongres 2011**

Wijnand K. den Dekker, Caroline Cheng, Dennie Tempel, Remco Haasdijk, Robert Herpers, Frank Bos, Esther H. van de Kamp, Lau Blonden, Stefan Schulte-Merker, Henricus J. Duckers *Neovascularization in Atherosclerosis: The Role of ETS2 in Intraplaque Haemorrhaging* **COEUR Research Seminar 04-02-2011**

Wijnand K. den Dekker, Caroline Cheng, Dennie Tempel, Mihai Netea, Jos van der Meer, Henricus J Duckers *Mast Cells Induce Vascular Smooth Muscle Cell Apoptosis in Atherosclerotic Plaques via a Toll-Like Receptor 4 Activation Pathway* **Cardio Vasculaire Conferentie 2011**

Wijnand K. den Dekker, Moniek de Maat, Frank Leebeek, Eli Sahar, Irun Cohen, Henricus J. Duckers *Evaluation of auto-antibody patterns in cardiovascular disease; implications for diagnosis.* **Dutch Atherosclerosis Society (DAS) 2009**

POSTER PRESENTATIONS

Wijnand K. den Dekker, Remco Haasdijk, Dennie Tempel, Jaco H Houtgraaf, Renate de Jong, Caroline Cheng, Henricus J Duckers *Thsd-1 Determines Plaque Phenotype by Regulating Vascular Permeability and Intraplaque Haemorrhaging* **American Heart Association congress 2011**

Wijnand K. den Dekker, Caroline Cheng, Dennie Tempel, Leo AB Joosten, Mihai Netea, Jos van der Meer, Henricus J Duckers *Mast Cells Induce Vascular Smooth Muscle Cell Apoptosis via a Toll Like Receptor 4 Pathway* **European Society of Cardiology congress 2011**

Wijnand K. den Dekker, Moniek de Maat, Frank Leebeek, Eli Sahar, Irun Cohen, Henricus J. Duckers *Auto-Antibody Serum Profile as Novel Biomarker for Acute Myocardial Infarction* **European Society of Cardiology congress 2011**

Wijnand K. den Dekker, Caroline Cheng, Mihai Netea, Jos van der Meer, Henricus J Duckers *Mast Cells Induce Vascular Smooth Muscle Cell Apoptosis via a Toll Like Receptor 4 Pathway* **American heart Association congress 2010**

Wijnand K. den Dekker, Caroline Cheng, Mihai Netea, Jos van der Meer, Henricus J Duckers *Mast Cells Induce Plaque Destabilization via Toll Like Receptor 4 Activation Pathway* **Dutch-German meeting 2010**

Wijnand K. den Dekker, Caroline Cheng, Mihai Netea, Jos van der Meer, Henricus J Duckers *Mast Cells Induce Plaque Destabilization via Toll Like Receptor 4 Activation Pathway* **Keystone congress february 2010**

Wijnand K. den Dekker, Moniek de Maat, Frank Leebeek, Eli Sahar, Irun Cohen, Henricus J. Duckers *Auto-Antibody Serum Profile as Novel Biomarker for Acute Myocardial Infarction* **American Heart Association congress 2009**

Wijnand K. den Dekker, Moniek de Maat, Frank Leebeek, Eli Sahar, Irun Cohen, Henricus J. Duckers *Evaluation of auto-antibody patterns in cardiovascular disease; implications for diagnosis.* **NVVC voorjaarscongres 2009**

Wijnand K. den Dekker, Moniek de Maat, Frank Leebeek, Eli Sahar, Irun Cohen, Henricus J. Duckers *Evaluation of auto-antibody patterns in cardiovascular disease; implications for diagnosis.* **Dutch-German Meeting 2009**

Wijnand K. den Dekker, D. Tempel, C. Cheng, H.J. Duckers *The development of a shear stress induced vulnerable plaque model in the rabbit* **Vascular biology, Papendal 2008**

LIST OF PUBLICATIONS

Wijnand K. den Dekker, Jaco H Houtgraaf, Stephen M Rowland, Erik Ligtenberg, Sanneke PM de Boer, Renate de Jong, Robbert J de Winter, Peter den Heijer, Felix Zijlstra, Patrick W Serruys, Caroline Cheng, and Henricus J. Duckers *Efficiency of statin treatment on EPC recruitment depends on baseline EPC titer, and does not improve angiographic outcome in coronary artery disease patients treated with the Genous™ stent* **Cell Transplantation 2013 april 3 Epub ahead of print**

Jaco H. Houtgraaf, Renate de Jong, Kim Monkhorst, Dennie Tempel, Esther H.M. van de Kamp, **Wijnand K. den Dekker**, Imo Hoefler, Gerard Pasterkamp, Andrew L. Lewis, Peter W. Stratford, Christine Wallrapp, Felix Zijlstra and Henricus J Duckers *Feasibility of intracoronary GLP-1 eluting Cellbead infusion in acute myocardial infarction* **Cell Transplantation 2013;22(3):535-43**

den Dekker WK, Tempel D, Bot I, Biessen EA, Joosten LA, Netea MG, van der Meer JW, Cheng C, Duckers HJ *Mast cells induce vascular smooth muscle cell apoptosis via a toll-like receptor 4 activation pathway.* **Arterioscler Thromb Vasc Biol. 2012 Aug;32(8):1960-9**

Cheng C, Haasdijk RA, Tempel D, **den Dekker WK**, Chrifi I, Blonden LA, van de Kamp EH, de Boer M, Bürgisser PE, Noorderloos A, Rens JA, Ten Hagen TL, Duckers HJ. *PDGF-Induced Migration of Vascular Smooth Muscle Cells Is Inhibited by Heme Oxygenase-1 via VEGFR2 Upregulation and Subsequent Assembly of Inactive VEGFR2/PDGFR β Heterodimers.* **Arterioscler Thromb Vasc Biol. 2012 Aug;32(8):1960-9**

Cheng C, Haasdijk R, Tempel D, van de Kamp EH, Herpers R, Bos F, **Den Dekker WK**, Blonden LA, de Jong R, Bürgisser PE, Chrifi I, Biessen EA, Dimmeler S, Schulte-Merker S, Duckers HJ *Endothelial cell-specific FGD5 involvement in vascular pruning defines neovessel fate in mice.* **Circulation. 2012 Jun 26;125(25):3142-58**

Jaco H. Houtgraaf, **Wijnand K. den Dekker**, Bas M. van Dalen, Tirza Springeling, Renate de Jong, MD, S. Swager-ten Hoor, Marcel Geleijnse, Paco Sanchez, Francisco Fernandez-Aviles, Patrick W. Serruys and Henricus J. Duckers *First-in-Man Results of Adipose Tissue-Derived Regenerative Cells in the Treatment of Patients with ST-Elevation Myocardial Infarction* **J Am Coll Cardiol. 2012 Jan 31;59(5):539-40.**

Katarína Larsen, Caroline Cheng, Dennie Tempel, Sherry Parker, Saami Yazdani, **Wijnand K. den Dekker**, Jaco H Houtgraaf, Renate de Jong, Stijn Swager-ten Hoor, Erik Ligtenberg, Steve Rowland, Frank Kolodgie, Patrick W. Serruys, Renu Virmani, and Henricus J. Duckers

Capture of circulatory endothelial progenitor cells and accelerated re-endothelialization of a bioengineered stent in human ex vivo shunt and rabbit denudation model **Eur Heart J. 2012 Jan;33(1):120-8.**

Wijnand K. den Dekker, Jaco H Houtgraaf, Yoshinobu Onuma, Edouard Benit, Robbert J de Winter, William Wijns, Manfred Grisold, Stephan Verheye, Sigmund Silber, Emmanuel Teiger, Jonathan Hill, Marcus Wiemer, Peter den Heijer, Benno J Rensing, Keith M Channon, Patrick WJC Serruys and Henricus J Duckers *Final Results of the HEALING IIB Trial to Evaluate a Bioengineered CD34 Antibody Coated Stent (Genous™Stent) Designed to Promote Vascular Healing by Capture of Circulating Endothelial Progenitor Cells in CAD Patients* **Atherosclerosis. 2011 Nov;219(1):245-52**

Caroline Cheng, Dennie Tempel, **Wijnand K. den Dekker**, Remco Haasdijk, Robert Herpers, Frank Bos, Esther H. van de Kamp, Lau Blonden, Stefan Schulte-Merker, Henricus J. Duckers *Ets2 Determines the Inflammatory State of Endothelial Cells in Advanced Atherosclerotic Lesions* **Circ Res. 2011 Aug 5;109(4):382-95.**

Caroline Cheng, Annemarie Noordeloos, Elza van Deel, Dennie Tempel, **Wijnand K. den Dekker**, Kim Wagtmans, Dirk-Jan Duncker, Miguel Soares, John Laman, Henricus J Duckers *Dendritic Cell function in transplantation arteriosclerosis is regulated by heme oxygenase 1* **Circulation Research 2010 May 18; 106 (10); 1656-66**

Wijnand K. den Dekker, Caroline Cheng, Gerard Pasterkamp, Henricus J. Duckers *Toll Like Receptor 4 in atherosclerosis and plaque destabilization* **Atherosclerosis 2010 Apr; 209 (2): 314-320**

Julia Oosterom, Keith M. Garner, **Wijnand K. den Dekker**, Wouter A. Nijenhuis, Willem H. Gispen, Peter Burbach, Gregory S. Barsh, Roger A. Adan. *Common requirements for melanocortin-4 receptor selectivity of structurally unrelated melanocortin agonist and endogenous antagonist, Agouti protein.* **J Biol Chem. 2001 Jan 12;276(2):931-6**

ABSTRACTS

Wijnand K. den Dekker, Jaco H Houtgraaf, Stephen M Rowland, Erik Ligtenberg, Sanneke PM de Boer, Renate de Jong, Robbert J de Winter, Peter den Heijer, Felix Zijlstra, Patrick W Serruys, Caroline Cheng, and Henricus J. Duckers Efficiency of statin treatment on EPC recruitment depends on baseline EPC titer, and does not improve angiographic outcome in coronary artery disease patients treated with the Genous™ stent **Eur Heart J (2012) 33 (suppl 1): 1123-1196**

Wijnand K. den Dekker Remco Haasdijk, Dennie Tempel, Jaco H Houtgraaf, Renate de Jong, Caroline Cheng, Henricus J Duckers Thsd-1 Determines Plaque Phenotype by Regulating Vascular Permeability and Intraplaque Haemorrhaging **Circulation 2011;124:A14844**

Wijnand K. den Dekker, Caroline Cheng, Dennie Tempel, Mihai Netea, Jos van der Meer, Henricus Duckers Mast Cells Induce Vascular Smooth Muscle Cell Apoptosis in Atherosclerotic Plaques via a Toll-Like Receptor 4 Activation Pathway **Eur Heart J (2011) 32(suppl 1): 1119-1194**

Katarina Larsen, Caroline Cheng, Dennie Tempel, Jaco Houtgraaf, Sherry Parker, Renate de Jong, **Wijnand K. den Dekker**, Stephen M Rowland, Patrick Serruys, Henricus J Duckers Evaluation of a Bioengineered Stent Designed to Capture Circulating Endothelial Progenitor Cells in a Human Ex Vivo Shunt Model **Circulation 2010;122:A12533**

Wijnand K. den Dekker, Caroline Cheng, Dennie Tempel, Mihai Netea, Jos van der Meer, Henricus J Duckers Mast Cells Induce Vascular Smooth Muscle Cell Apoptosis in Atherosclerotic Plaques via a Toll-Like Receptor 4 Activation Pathway **Circulation 2010;122:A12533**

Jaco H Houtgraaf, Henricus J Duckers, **Wijnand K. den Dekker**, Stijn Swager, Robbert Jan van Geuns F Fernandez-Aviles, Patrick W Serruys First-in-man experience of adipose tissue-derived regenerative cell transplantation in the treatment of patients with an acute ST-elevation myocardial infarction (APOLLO trial) **Eur Heart J. 2010 Sept; 31(1); 494-494**

Wijnand K. den Dekker, Moniek M. de Maat, Frank W. Leebeek, Irun R. Cohen, Patrick W. Serruys, Henricus J. Duckers Auto-Antibody Serum Profile as Novel Biomarker for Acute Myocardial Infarction **Circulation Nov. 2009;120:S427**

Caroline Cheng, Dennie Tempel, **Wijnand K. den Dekker**, Remco Haasdijk, Robert Herpers, Frank Bos, Esther H. van de Kamp, Lau Blonden, Stefan Schulte-Merker, Henricus J. Duckers ETS2 promotes development of a pro-atherogenic endothelial phenotype causing plaque destabilization in advanced atherosclerotic lesions **Circulation Nov. 2009;120:S1127**

Wijnand K. den Dekker, Caroline Cheng, Jos van der Meer, Mihai Netea, Jos van der Meer, Henricus J. Duckers *Role of Toll Like Receptor 4 in mast cells in plaque destabilization*. **Vasculaire geneeskunde, 2009**

Wijnand K. den Dekker, Moniek de Maat, Frank Leebeek, Eli Sahar, Irun Cohen, Henricus J. Duckers *Evaluation of auto-antibody patterns in cardiovascular disease; implications for diagnosis*. **Vasculaire geneeskunde, 2009**

CURRICULUM VITAE

De auteur van dit proefschrift, Wijnand Khatulistono den Dekker, werd geboren op 19 maart 1979 te Pontianak, Indonesië. In 1996 behaalde hij zijn gymnasium diploma aan het Johan de Witt gymnasium in Dordrecht. In hetzelfde jaar begon hij aan de studie Medische Biologie in Utrecht. In 1999 stapte hij over naar de Geneeskunde studie, waar hij in 2005 zijn artsexamen behaalde. Hij werkte twee jaar als ANIOS, respectievelijk bij de interne geneeskunde in het Sint Elisabeth Hospitaal in Willemstad, Curaçao, en de cardiologie in het Erasmus MC in Rotterdam. In 2008 begon hij als promovendus op de afdeling experimentele cardiologie in het Erasmus MC met als promotor professor dr. F.J.Zijlstra, en als co-promotoren dr. H.J. Duckers en dr. C. Cheng. De resultaten uit dit onderzoek zijn beschreven in dit proefschrift. In 2012 is hij begonnen met de opleiding cardiologie. Hij heeft zijn twee jaren vooropleiding interne geneeskunde in het Albert Schweitzer ziekenhuis gedaan onder supervisie van dr. E.F.H. van Bommel. In 2014 is hij gestart in het Maasstad ziekenhuis onder supervisie van dr. P.C. Smits. Vanaf 2015 zal hij werkzaam zijn in het Erasmus MC onder supervisie van dr. J. W. Deckers. Hij is getrouwd met Hanneke Henny, zij hebben een dochter Eveline en een zoon Martijn.

DANKWOORD

Zes jaar geleden ben ik begonnen met dit promotie onderzoek en nu is het dan eindelijk klaar. Het heeft veel tijd en energie gekost, maar ik heb het altijd met veel plezier gedaan en kijk er dan ook met voldoening op terug. Nu het einde er dan toch is wil ik graag alle mensen bedanken die mij de afgelopen jaren geholpen en gesteund hebben in het volbrengen van dit proefschrift.

Allereerst wil ik mijn co-promotor, Eric Duckers, bedanken. In 2007 spraken we elkaar voor het eerst en jouw enthousiasme en de diversiteit aan onderzoeksmogelijkheden bij jou, werkelijk van bench tot bedside, werkten aanstekelijk. Ik ben blij dat ik toen besloten heb om bij jou onderzoek te gaan doen en eerst dit promotieonderzoek te beginnen alvorens aan de cardiologie opleiding te beginnen. Bedankt voor de vrijheid die je me hebt gegeven tijdens het onderzoek en hulp bij het schrijven van de verschillende artikelen. Helaas ben je nu verhuisd naar Utrecht, maar wie weet kunnen we in de toekomst samen onderzoek blijven doen.

Caroline Cheng, ik ben erg blij dat je mijn tweede co-promotor bent. Ik kan wel stellen dat zonder jou dit boekje nooit tot stand was gekomen. Niet alleen heb je me ontzettend veel geholpen bij het praktische gedeelte van het onderzoek, je was ook altijd bereid om mee te denken over interpretatie van resultaten en het bedenken van vervolgexperimenten. Als ik weer eens in de put zat omdat iets niet lukte, zag jij altijd wel weer iets positiefs. Stelling 9 is dan ook zeker op jou van toepassing.

Mijn promotor, professor dr. Zijlstra wil ik hartelijk danken voor de hulp bij het schrijven van dit proefschrift. Dankzij uw op- en aanmerkingen is dit proefschrift geworden tot wat het nu is.

De leescommissie bestaande uit professor dr. Duncker, professor dr. Laman en professor dr. Pasterkamp wil ik graag bedanken voor hun bereidheid om mijn manuscript te beoordelen en van commentaar te voorzien. Daarnaast wil ik natuurlijk professor dr. Boersma, professor dr. De Jaegere en professor dr. Sijbrands dank zeggen voor het opponeren tijdens mijn promotie.

Mijn beide paranimfen, Virgil en Martijn, wil ik natuurlijk ook bedanken. Virgil, ik ken je nu al 20 jaar en 'there has never been a dull moment'. Er is altijd wat te beleven met jou, ook al is het leven nu nog hectischer met een carrière en (nu nog) één kind. Ik hoop dat we binnenkort weer wat meer tijd hebben om te snookeren en dronken aan de bar bij Faab te zitten. Ook hoop ik dat we ooit toch nog samen wat onderzoek kunnen doen, atherosclerose is per slot van rekening een inflammatoire ziekte! Martijn, ook jij bent behoorlijk aan de weg aan het timmeren in onderzoeksland en ook jij combineert dat feilloos met een gezin. Respect hoe je dat allemaal voor elkaar krijgt. De lunches samen waren altijd ontspannen en een goed

moment om weer even bij te kletsen. Het cerebellum en atherosclerose valt wat moeilijker aan elkaar te rijmen, dus de kans dat wij samen onderzoek gaan doen acht ik niet zo groot.

Alle mensen van de experimentele cardiologie op de 23^e verdieping wil ik natuurlijk bedanken voor de vele gezellige jaren. Zonder jullie was het zeker niet gelukt. De vele borrels, bbq's en andere etentjes, sommige kan ik me niet eens meer herinneren, waren legendarisch en ontzettend gezellig. Die ga ik zeker missen!

Ik wil natuurlijk in het bijzonder de mensen op kamer Ee2389 bedanken. Allereerst wil ik bij Jaco beginnen. Jij was net begonnen toen ik als onderzoeker startte en hebt me in het begin wegwijs gemaakt op de afdeling. Jij hebt me ook aangespoord om achter de opleiding aan te gaan, wat er zeker toe heeft bijgedragen dat ik nu in opleiding ben. Daarvoor ben ik je erg dankbaar. Ik ben blij dat je een baan in het Maasstad ziekenhuis hebt gevonden en dat we elkaar daar dus nog regelmatig treffen.

Dennie! Jouw kennis en optimisme zijn ongeëvenaard. Jij hebt overal wel een antwoord op en altijd het laatste woord. Maar daarnaast ben je een harde werker en altijd bereid om te helpen. Jij hebt me dan ook veel geholpen met praktische dingen. De congresbezoeken samen waren erg gezellig, hopelijk kunnen we dat in de toekomst nog eens doen. Ik ben ontzettend blij dat jouw proefschrift ook af is en wens je veel succes in Utrecht.

Lieve Esther, zonder jou is/was er geen moleculaire cardiologie lab en was ik dus ook niet gepromoveerd. Jij was de spil van de afdeling. Elke keer liep het weer in het honderd als je (weer :-p) eens op vakantie was. Ik zal de gezellige lunches missen. Ik hoop dat je het naar je zin gaat hebben bij de experimentele cardiologie en ik kom graag bij je koffie drinken!

Renate, jij bent nu bezig met de laatste loodjes en gaat binnenkort in de kliniek beginnen. Je was veel in Utrecht, maar als je in Rotterdam, vond ik het altijd gezellig! Tot snel in de kliniek!

Remco, je gedrevenheid en doorzettingsvermogen om je proefschrift tot een goed einde te brengen is bewonderenswaardig. Gelukkig is het jou ook gelukt! Ik hoop dat je binnenkort een leuke baan in de kliniek vindt.

Petra, ook jij bent nu naar Utrecht verhuisd om daar je onderzoek voort te zetten. Ik hoop dat het daar net zo gezellig als in Rotterdam is. Tegenwoordig lunct niemand hier meer omdat jij altijd degene was om ons vanachter ons bureau mee te sleuren voor de lunch. Het is goed dat je tegenwoordig ook wijn drinkt en niet alleen maar Martini. Moeten zeker nog eens testen of je daar net zo slecht tegen kunt als Martini! Ben benieuwd waar jullie volgende reis naar toegaat!

Stijn, bedankt voor alle hulp bij de klinische studies. Je was altijd goed op de hoogte van alles en hebt ons veel werk uit handen genomen. Veel succes met je eigen bedrijf.

Lau, de onverstoorbare en onzichtbare motor van het lab. We zouden wat vaker bij de witte aap moeten gaan drinken!

Ihsan, de favoriet van Caroline en de sociale jongen van de afdeling, de ramadan was altijd een zware tijd voor je met alle grappen van ons, maar daar sloeg je je keurig doorheen. Nu je promotie nog!

Maarten, de andere favoriet van Caroline, en Lizanne, bedankt voor alle gezelligheid, humor en leuke foto's.

Mijn collega's aan de andere kant van de klapdeuren, Elza, Martine, Marc, Andre, Tuncay, Vincent, Liesbeth, Monique, Nienke, Oana, Richard, Ilona, Heleen, Rob wil ik allemaal bedanken voor de gezelligheid en de lunches samen.

Een speciaal woord van dank voor Hendrik Bouw. Ontzettend bedankt dat jij, in deze voor jou moeilijke tijd, mij hebt willen helpen. Zonder jou had ik niet zo'n mooie omslag gehad, terwijl ik je ook pas op het laatste moment gevraagd heb.

Zonder mijn familie was dit natuurlijk ook allemaal niet gelukt. Foekje, Terry, Denise, Maurice, Pytsje, Bareld, Vera, Ivan, Romy, Gideon, Margaretha, Steve, Catharina en Thomas, allemaal bedankt voor alle steun en toeverlaat en alle gezellige momenten. Ik hoop dat ik nu wat meer tijd heb om af te spreken. Papa en mama, ontzettend bedankt dat jullie me deze kans gegeven hebben. Ook al ben ik geadopteerd, ik denk dat ik stiekem best veel op jullie lijk. Nog twee jaar, dan wordt het voor jullie ook wat rustiger.

Lieve Eveline en Martijn, jullie hebben mijn leven wel op zijn kop gezet, maar ik zou me geen leven zonder jullie meer voor kunnen stellen. De slapeloze nachten zijn het meer dan waard. En Eveline, papa zal wat minder vaak gaan werken....

Lieve Hanneke, dushi, wat ben ik blij dat we ooit allebei besloten om in Curaçao te gaan werken en elkaar daar ontmoet hebben. Ontzettend bedankt voor alle steun en begrip tijdens het schrijven van dit proefschrift. Menig avondje en weekend was ik met dit proefschrift bezig zonder dat jij geklaagd hebt. Hopelijk wordt het nu wat rustiger. Ik kijk uit naar de toekomst met zijn vieren!

Wijnand K. den Dekker

ARTHEROSCLEROSIS

from bench to bedside and

from pathophysiology to treatment